



MR13-04

10-29 July 2013

Preliminary Cruise Report

doi : 10.17596/0002985

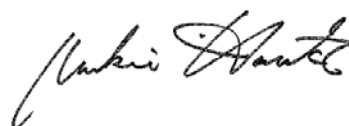
JAMSTEC

Note

This cruise report is a preliminary documentation published in approximately a month after the end of this cruise. It may not be corrected even if changes on contents are found after publication. It may also be changed without notice. Data on the cruise report may be raw or not processed. Please ask the principal investigator and persons in charge of respective observations for the latest information and permission before using. Users of data are requested to submit their results to JAMSTEC Data Integration and Analysis Group (DIAG).

September 2013

Principal Investigator of MR13-04

A handwritten signature in black ink, appearing to read 'Makio Honda', written in a cursive style.

Makio Honda
JAMSTEC

Cruise Report ERRATA of the Nutrients part

page	Error	Correction
52	potassium nitrate CAS No. 7757-91-1	potassium nitrate CAS No. 7757-79-1
50	1N H ₂ SO ₄	1M H ₂ SO ₄

Cruise Report ERRATA of the Photosynthetic Pigments part

page	Error	Correction
106	Ethyl-apo-8'-carotenoate	trans-β-Apo-8'-carotenal

Contents of MR13-04 Preliminary Cruise Report

A. Cruise summary

1. Cruise information (A1)

- (1) Cruise designation
- (2) Cruise title
- (3) Principal investigator
- (4) Science proposal of cruise
- (5) Cruise period (port call) (A2)
- (6) Cruise region (geographical boundary)
- (7) Cruise track and stations (GODI) (A3)

2. Outline of MR13-04

- 2.1 Objective of this cruise (A4)
- 2.2 Cruise summary (highlights)

B. Text

1. Outline of MR13-04

- 1.1 Cruise summary (1)
 - (1) Introduction of principal science proposal
 - (2) Objective of this cruise
 - (3) Cruise summary (2)
 - (4) Scientific gears (5)
- 1.2 Track and log (6)
- 1.3 Cruise participants (10)

2. General observation

- 2.1 Meteorological observations (12)
- 2.2 Surface meteorological observation
 - 2.2.1 Ceilometer observation (18)
 - 2.2.2 Lidar observations of clouds and aerosols (21)
 - 2.2.3 Maritime aerosol optical properties from measurements of Ship-borne Sky radiometer (23)
 - 2.2.4 Tropospheric aerosol and gas profile (24)
- 2.3 Physical oceanographic observation
 - 2.3.1 CTD cast and water sampling (26)
 - 2.3.2 Salinity measurement (31)
 - 2.3.3 Shipboard ADCP (35)
- 2.4 Sea surface water monitoring (38)
- 2.5 Dissolved oxygen (41)

2.6 Nutrients	(44)
2.7 pH	(61)
2.8 Dissolved inorganic carbon –DIC-	(64)
2.9 Total alkalinity	(67)
2.10 Underway pCO ₂	(70)

3. Special observation

3.1 BGC mooring	
3.1.1 Recovery and deployment	(72)
3.1.2 Instruments	(82)
3.1.3 Sampling schedule	(86)
3.1.4 Preliminary results	(87)
3.2 Underwater profiling buoy system (Primary productivity profiler)	
3.2.1 POPPS	(89)
3.2.2 RAS	(95)
3.3 Phytoplankton	
3.3.1 Chlorophyll a measurements by fluorometric determination	(100)
3.3.2 HPLC measurements of marine phytoplankton pigments	(105)
3.3.3 Phytoplankton abundance	(110)
3.3.4 Primary production and new production	(112)
3.3.5 P vs E curve	(117)
3.3.6 Oxygen evolution (gross primary production)	(120)
3.3.7 Absorption coefficients of phytoplankton and CDOM	(122)
3.3.8 Taxonomy and genome analysis of eukaryotic picophytoplankton originated from cryopreserved marine environmental specimens	(126)
3.4 Optical measurement	(140)
3.5 Biological study for phytoplankton and zooplankton	
3.5.1 Planktic foraminifera and radiolarian study in the western Pacific	(142)
3.5.2 Shell-bearing phytoplankton studies in the western North Pacific	(145)
3.5.3 Symbiotic algae studies in the western North Pacific	(147)
3.6 Community structures and metabolic activities of microbes	
(Studies on the microbial-geochemical processes that regulate the operation of the biological pump in the subarctic and subtropical regions of the western North Pacific)	(150)
3.7 Particles in the water column	
3.7.1 LISST	(152)
3.7.2 Suspended particles	(153)
3.8 Dissolved organic carbon	(154)
3.9 Chlorofluorocarbons and sulfur hexafluoride	(155)
3.10 Vertical distribution of isotopic composition of dissolved oxygen	(159)

- 3.11 Argo float (160)
- 3.12 Temporal changes in water properties of abyssal water in the western North Pacific (166)
- 3.13 Fukushima related observation
 - 3.13.1 The concentrations of radionuclides in the western North Pacific (172)
 - 3.13.2 Zooplankton (175)
 - 3.13.3 Sediment trap experiment at station F1 (177)
 - 3.13.4 Biogeochemical cycle and accumulation of anthropogenic radionuclides derived from the accident of Fukushima-Daiichi Nuclear Power Plant (183)
- 3.14 A study of the cycles of global warming related materials using their isotopomers in the western North Pacific (188)

4. Geophysical observation

- 4.1 Swath bathymetry (195)
- 4.2 Sea surface gravity (197)
- 4.3 Sea surface magnetic field (198)
- 4.4 Tectonic history of the mid-Cretaceous Pacific Plate (200)

5. Satellite image acquisition (MCSST from NOAA/HPRT) (202)

Cover sheet: the first prize of “MR13-04 CRUISE REPORT COVER SHEET CONTEST”. The winner is Haruka Takagi, graduate student from JAMSTEC.

A. Cruise summary

1. Cruise information

(1) Cruise designation (research vessel)

MR13-04 (R/V MIRAI)

(2) Cruise title (principal science proposal) and introduction

Change in material cycles and ecosystem by the climate change and its feedback

Some disturbing effects are progressively coming to the fore in the ocean by climate change, such as rising water temperature, intensification of upper ocean stratification and ocean acidification. It is supposed that these effects result in serious damage to the ocean ecosystems. Disturbed ocean ecosystems will change a material cycle through the change of biological pump efficiency, and it will be fed back into the climate. We are aimed at clarifying the mechanisms of changes in the ocean structure in ocean ecosystems derived from the climate change,

We arranged the time-series observation stations in the subarctic gyre (K2: 47°N 160°E) and the subtropical gyre (S1: 30°N, 145°E) in the western North Pacific. In general, biological pump is more efficient in the subarctic gyre than the subtropical gyre because large size phytoplankton (diatom) is abundant in the subarctic gyre by its eutrophic oceanic condition. It is suspected that the responses against climate change are different for respective gyres. To elucidate the oceanic structures in ocean ecosystems and material cycles at both gyres is important to understand the relationship between ecosystem, material cycle and climate change in the global ocean.

There are significant seasonal variations in the ocean environments in both gyres. The seasonal variability of oceanic structures will be estimated by the mooring systems and by the seasonally repetitive ship observations scheduled for next several years.

(3) Principal Investigator (PI)

Makio Honda

Research Institute for Global Change (RIGC)

Japan Agency for Marine-Earth Science and Technology (JAMSTEC)

(4) Science proposals of cruise

Affiliation	PI	Proposal titles
Japan Atomic Energy Agency	Shigeyoshi OTOSAKA	Biogeochemical cycle and accumulation of anthropogenic radionuclides derived from the accident of Fukushima-Daiichi Nuclear Power Plant
University of Tokyo	Koji HAMASAKI	Studies on the microbial-geochemical processes that regulate the operation of the biological pump in the subarctic and subtropical regions of the western North Pacific – IV
National Institute for Environmental Studies	Masanobu KAWACHI	Taxonomy and genome analysis of eukaryotic picophytoplankton originated from cryopreserved marine environmental specimens

Tokyo Institute of Technology	Naohiro YOSHIDA	A study of the cycles of global warming related materials using their isotopomers in the western North Pacific.
JAMSTEC	Hiroshi UCHIDA	Temporal changes in water properties of abyssal water in the western North Pacific
JAMSTEC	Toshio SUGA	Study of ocean circulation and heat and freshwater transport and their variability, and experimental comprehensive study of physical, chemical, and biochemical processes in the western North Pacific by the deployment of Argo floats and using Argo data
National Institute of Radiological Sciences	Tstuso AONO	The concentrations of radionuclides in the western North Pacific
Nagoya University	Osamu ABE	Estimation of Paleo-primary productivity by measurements of oxygen isotopes in the intermediate water
not onboard study		
Chiba Univ.	Masao NAKANISHI	Tectonics of the mid-Cretaceous Pacific Plate
National Institute for Environmental Sciences	Nobuo SUGIMOTO	Study of distribution and optical characteristics of ice/water clouds and marine aerosols
Ryukyu Univ.	Takeshi MATSUMOTO	Standardization of marine geophysical data and its application to the ocean floor geodynamics studies
Toyama Univ.	Kazuma AOKI	Maritime aerosol optical properties from measurements of Ship-borne sky radiometer

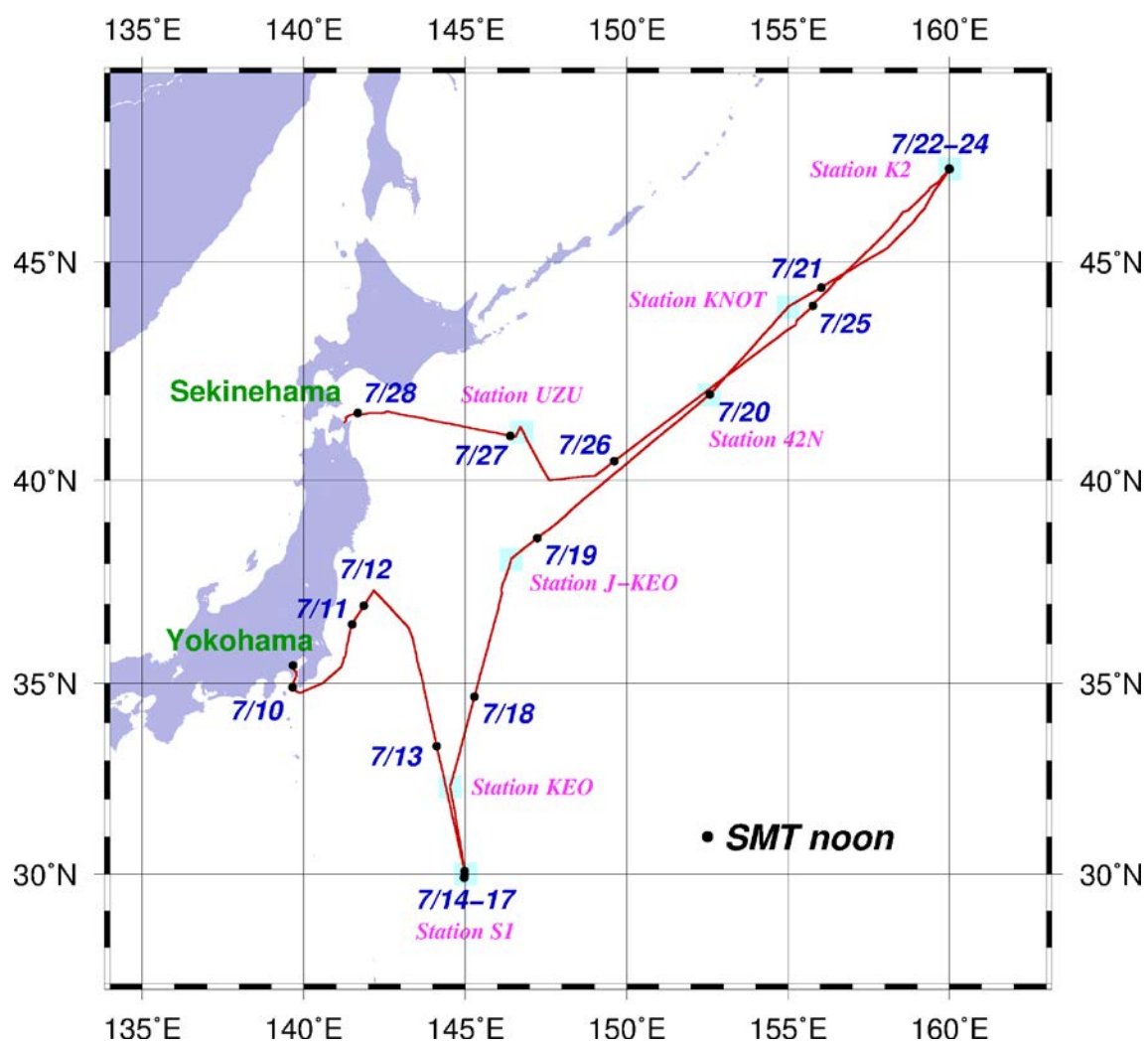
(5) Cruise period (port call)

10 July (Yokohama) – 29 July 2013 (Sekinehama)

(6) Cruise region (geographical boundary)

The western North Pacific (50°N – 30°N, 140°E – 160°W)

(7) Cruise track and stations



2. Outline of MR13-04

2.1 Objective of this cruise

Principal objective of this cruise is to observe early summer ecosystem and biogeochemical cycle at time-series stations in the sub-arctic and sub-tropical gyres. In addition, we conducted biogeochemical observation off Fukushima in order to investigate dispersion of radionuclides from the Fukushima Daiichi nuclear power plant.

2.2 Cruise summary (highlights)

The length of this cruise was $2/3 \sim 1/2$ of previous cruises for K2/S1 time-series observation for biogeochemistry. However, owing to good weather and sea condition, recovery and re-deployment of three mooring systems were successfully conducted at stations K2 and S1. In addition, we successfully recovered two sediment trap mooring systems off Fukushima and redeployed one sediment trap mooring system as scheduled. On the other hand, water sampling for various purposes were conducted at stations K2, S1, KEO, JKEO and KNOTS. At stations K2 and S1, phyto- / zoo-plankton sampling, measurement of primary productivity and collection of suspended substances by using in situ pumping were conducted successfully. Moreover, on the way back to Mutsu, water sampling and CTD observation was conducted inside and outside of meso-scale eddy located east of Hokkaido. A few cruise highlights are as follows.

(1) Time-series observation of vertical profile in chlorophyll-a

At station S1, a POPPS mooring system that consists of underwater winch, observation buoy, automatic water sampler (RAS) and ADCP was recovered. Time-series data of fluorometer was successfully obtained for about 8 months between July 2012 and March 2013. Fig. 1 shows seasonal variability in vertical profile of chlorophyll-a (chl-a). Between July 2012 and October 2013, relatively higher chl-a was observed in the subsurface layer (around bottom of euphotic layer) while surface chl-a was quite low. This data is very unique because subsurface chl-a maximum cannot be observed by satellite. Between November 2012 and January 2013, chl-a was very low upper 150 m. After January 2013, chl-a began to increase upper 150 m and higher chl-a was observed late March 2013. This seasonal variability qualitatively synchronized well with that of sinking particles observed by 200 m sediment trap (Fig.2).

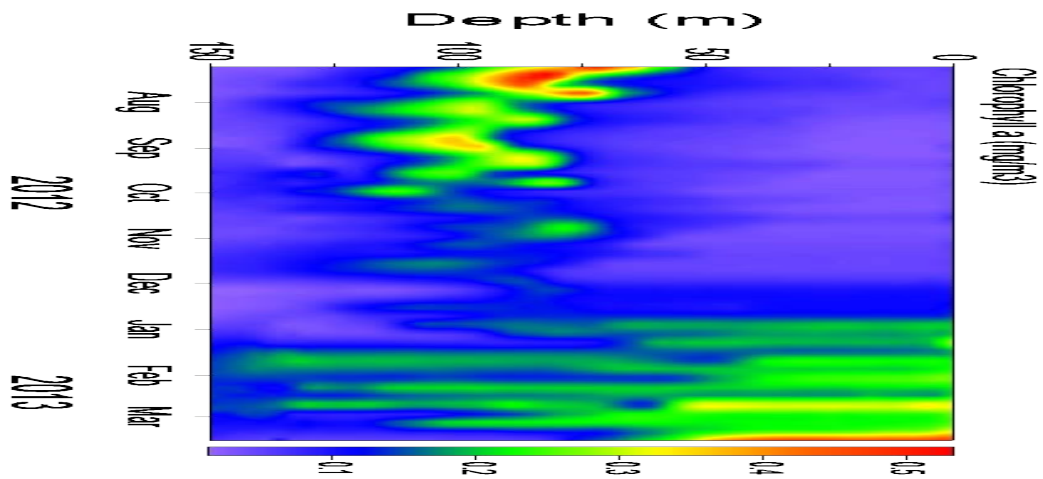


Fig. 1 Seasonal variability in vertical profile of chlorophyll-a upper 150 m between July 2012 and March 2013 observed by POPPS mooring system

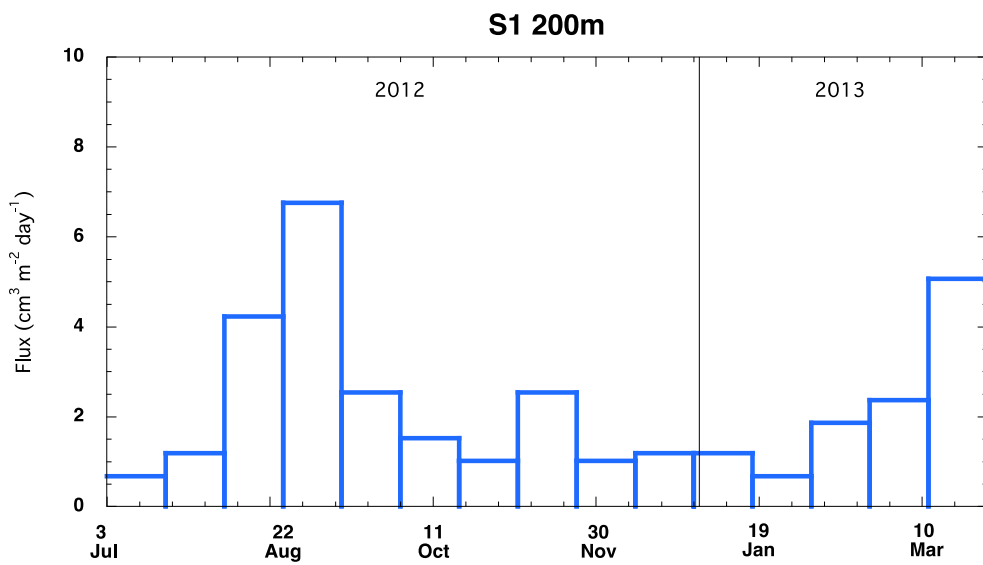


Fig.2 Seasonal variability in total mass flux observed by 200 m sediment trap between July 2012 and March 2013

(2) High primary productivity at S1

Integrated primary productivity (PP) at S1 was estimated to be $330 \pm 30 \text{ mg m}^{-2} \text{ day}^{-1}$ and higher than that observed previously in summer and comparable to that in early spring (Fig. 3). Why is PP relatively high in summer when nutrients are little or depleted? Based on vertical profile of NO_3 , relatively higher NO_3 was observed only near surface (Fig. 4). High nutrient near surface was also observed during last summer cruise (MR12-02: see MR12-02 Preliminary cruise report). It might be attributed to atmospheric input. On the other hand, nitrogen-fixing cyanobacteria that lives in a symbiotic relationship with diatom was detected at S1 (Photo 1). Nitrogen-fixation is another possibility to supply N

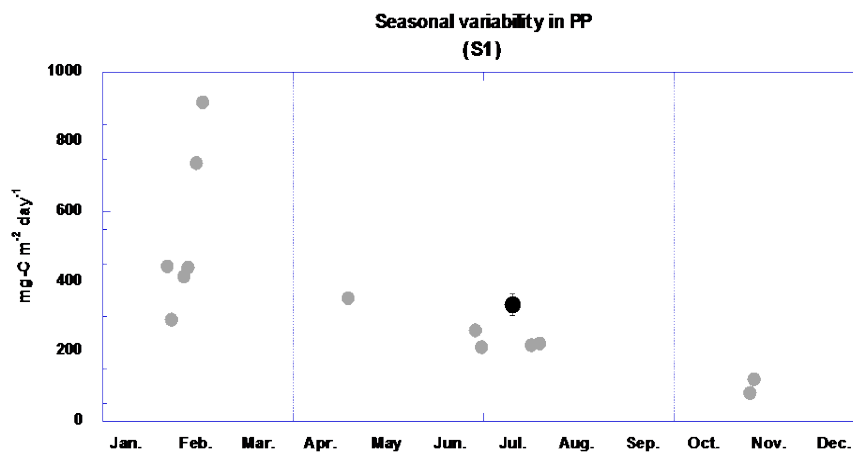


Fig.3 Seasonal variability of primary productivity. Black circle is observed value this cruise.

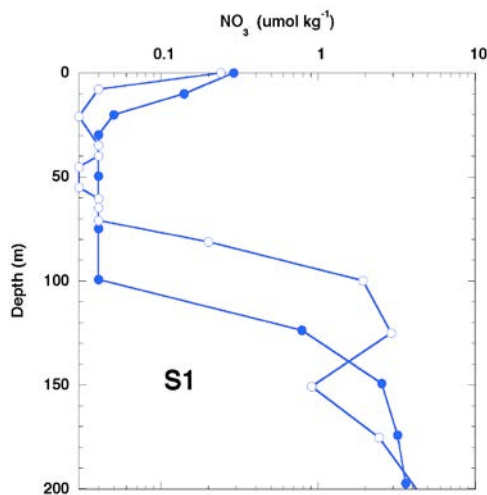


Fig.4 Vertical profile of NO_3 at S1

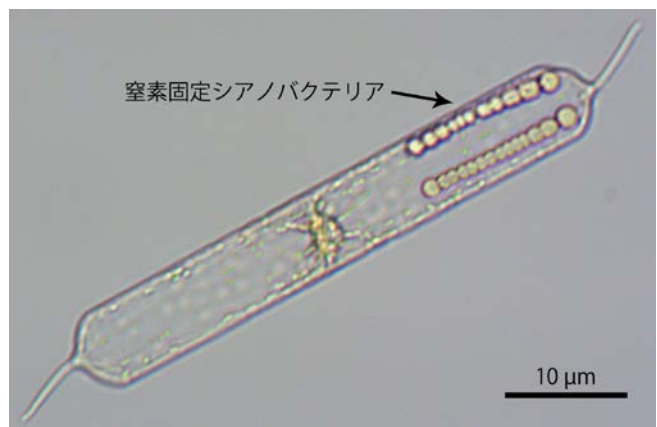


Photo 1 Cyanobacteria that lives in a symbiotic relationship with diatom

B. Text

1. Outline of MR13-04

1.1 Cruise summary

(1) Introduction of principle science proposal

Change in material cycles and ecosystem by the climate change and its feedback

Some disturbing effects are progressively coming to the fore in the ocean by climate change, such as rising water temperature, intensification of upper ocean stratification and ocean acidification. It is supposed that these effects result in serious damage to the ocean ecosystems. Disturbed ocean ecosystems will change a material cycle through the change of biological pump efficiency, and it will be fed back into the climate. We are aimed at clarifying the mechanisms of changes in the ocean structure in ocean ecosystems derived from the climate change,

We arranged the time-series observation stations in the subarctic gyre (K2: 47°N 160°E) and the subtropical gyre (S1: 30°N, 145°E) in the western North Pacific. In general, biological pump is more efficient in the subarctic gyre than the subtropical gyre because large size phytoplankton (diatom) is abundant in the subarctic gyre by its eutrophic oceanic condition. It is suspected that the responses against climate change are different for respective gyres. To elucidate the oceanic structures in ocean ecosystems and material cycles at both gyres is important to understand the relationship between ecosystem, material cycle and climate change in the global ocean.

There are significant seasonal variations in the ocean environments in both gyres. The seasonal variability of oceanic structures will be estimated by the mooring systems and by the seasonally repetitive ship observations scheduled for next several years.

(2) Objective of this cruise

Principal objective of this cruise is to observe early summer ecosystem and biogeochemical cycle at time-series stations in the sub-arctic and sub-tropical gyres. In addition, we conducted biogeochemical observation off Fukushima in order to investigate dispersion of radionuclides from the Fukushima Daiichi nuclear power plant.

(3) Cruise summary (highlights)

The length of this cruise was $2/3 \sim 1/2$ of previous cruises for K2/S1 time-series observation for biogeochemistry. However, owing to good weather and sea condition, recovery and re-deployment of three mooring systems were successfully conducted at stations K2 and S1. In addition, we successfully recovered two sediment trap mooring systems off Fukushima and redeployed one sediment trap mooring system as scheduled. On the other hand, water sampling for various purposes were conducted at stations K2, S1, KEO, JKEO and KNOTS. At stations K2 and S1, phyto- / zoo-plankton sampling, measurement of primary productivity and collection of suspended substances by using in situ pumping were conducted successfully. Moreover, on the way back to Mutsu, water sampling and CTD observation was conducted inside and outside of meso-scale eddy located east of Hokkaido. A few cruise highlights are as follows.

(1) Time-series observation of vertical profile in chlorophyll-a

At station S1, a POPPS mooring system that consists of underwater winch, observation buoy, automatic water sampler (RAS) and ADCP was recovered. Time-series data of fluorometer was successfully obtained for about 8 months between July 2012 and March 2013. Fig. 1 shows seasonal variability in vertical profile of chlorophyll-a (chl-a). Between July 2012 and October 2013, relatively higher chl-a was observed in the subsurface layer (around bottom of euphotic layer) while surface chl-a was quite low. This data is very unique because subsurface chl-a maximum cannot be observed by satellite. Between November 2012 and January 2013, chl-a was very low upper 150 m. After January 2013, chl-a began to increase upper 150 m and higher chl-a was observed late March 2013. This seasonal variability qualitatively synchronized well with that of sinking particles observed by 200 m sediment trap (Fig.2).

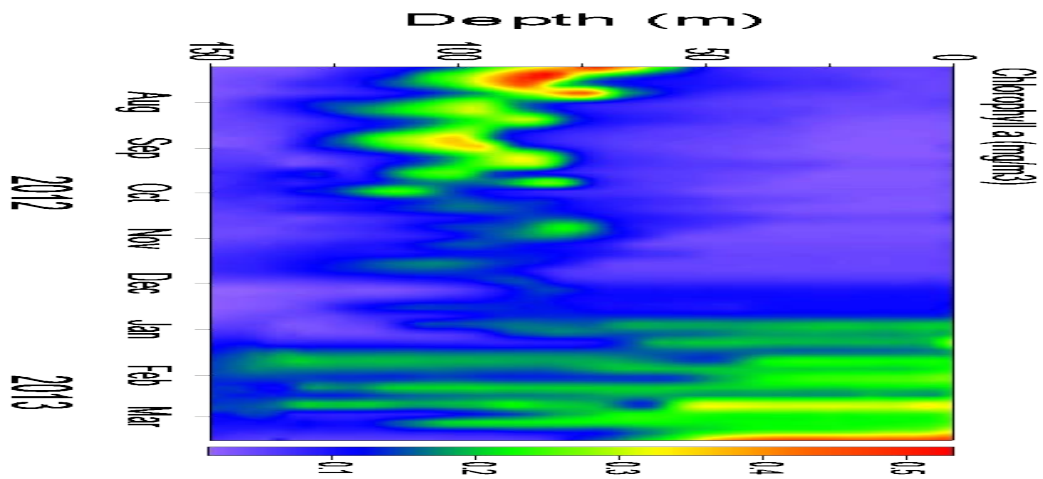


Fig. 1 Seasonal variability in vertical profile of chlorophyll-a upper 150 m between July 2012 and March 2013 observed by POPPS mooring system

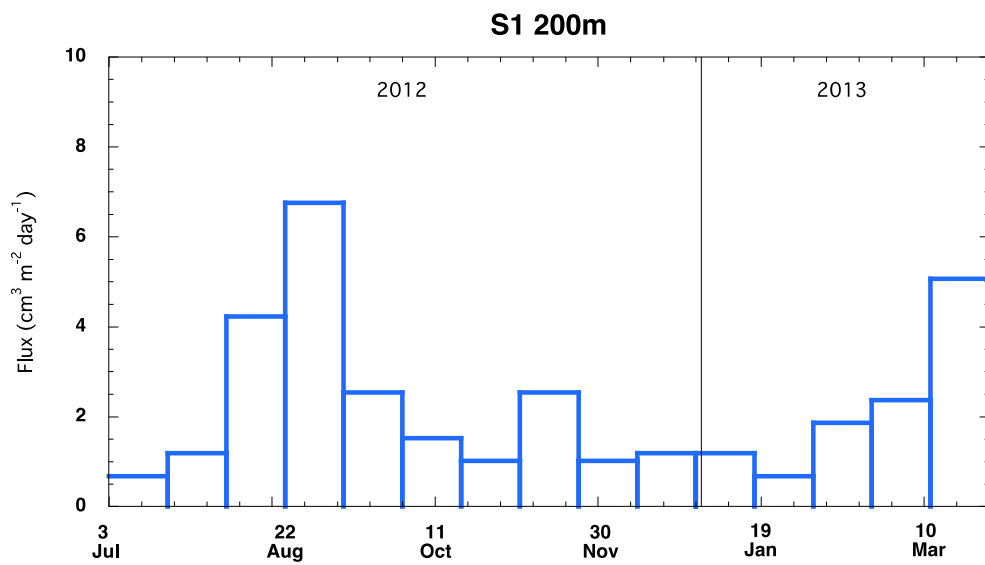


Fig.2 Seasonal variability in total mass flux observed by 200 m sediment trap between July 2012 and March 2013

(2) High primary productivity at S1

Integrated primary productivity (PP) at S1 was estimated to be $330 \pm 30 \text{ mg m}^{-2} \text{ day}^{-1}$ and higher than that observed previously in summer and comparable to that in early spring (Fig. 3). Why is PP relatively high in summer when nutrients are little or depleted? Based on vertical profile of NO_3 , relatively higher NO_3 was observed only near surface (Fig. 4). High nutrient near surface was also observed during last summer cruise (MR12-02: see MR12-02 Preliminary cruise report). It might be attributed to atmospheric input. On the other hand, nitrogen-fixing cyanobacteria that lives in a symbiotic relationship with diatom was detected at S1 (Photo 1). Nitrogen-fixation is another possibility to supply N

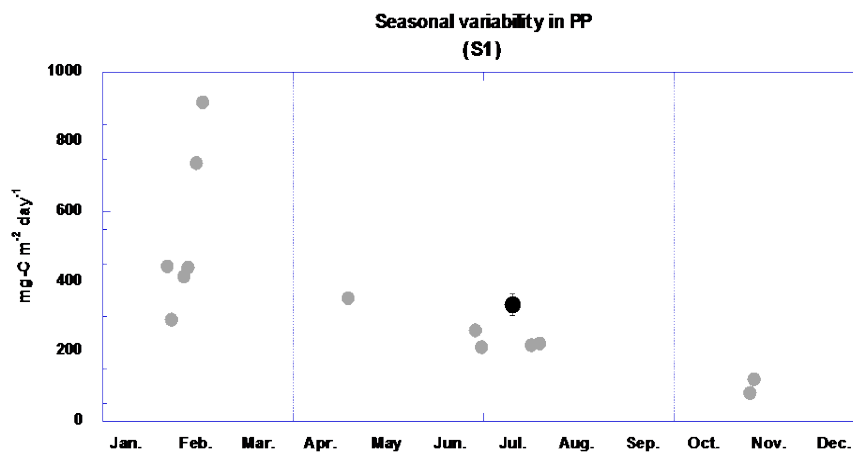


Fig.3 Seasonal variability of primary productivity. Black circle is observed value this cruise.

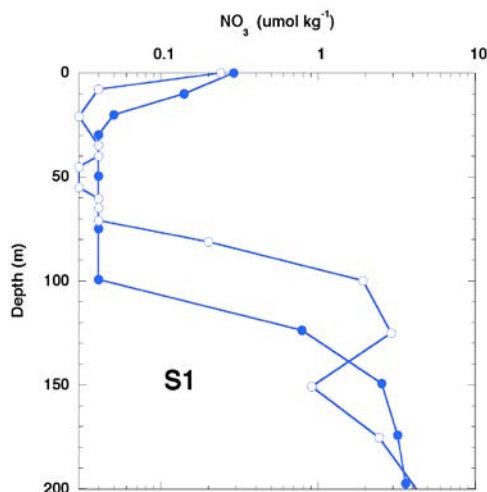


Fig.4 Vertical profile of NO_3 at S1

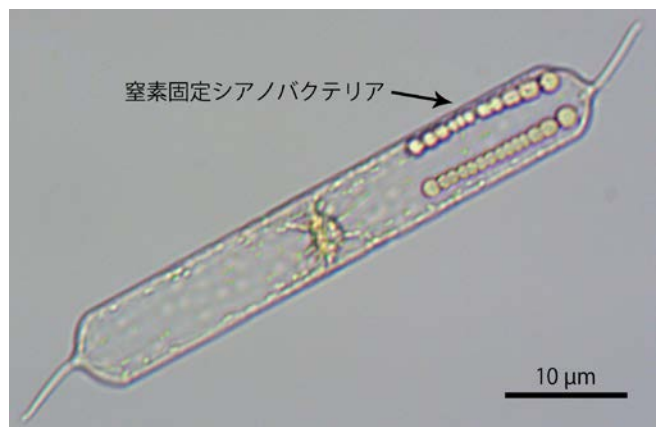


Photo 1 Cyanobacteria that lives in a symbiotic relationship with diatom

(4) Scientific gears

All hydrocasts were conducted at stations F1, S1, KEO, JKEO, KNOT and K2 using 36-position 12 liter Niskin bottles carousel system with SBE CTD-DO system, fluorescence and transmission sensors. JAMSTEC scientists and MWJ (Marine Work Japan Co. Ltd.) technician group were responsible for analyzing water sample for salinity, dissolved oxygen, nutrients, CFCs, total carbon contents, alkalinity and pH. Cruise participants from JAMSTEC, National Institute for Environmental Studies, Rakuno Gakuen University, National Institute of Radiological Sciences, University of Tokyo, National Institute of Polar Research, Nagoya University and National Institute for Radiological Sciences helped to divide seawater from Niskin bottles to sample bottles for analysis. Surface water was collected with bucket.

Optical measurement in air and underwater was conducted with PAR sensor (RAMSES-ACC) and PAR sensor on CTD, respectively.

For collecting suspended particles at stations F1, S1 and K2, Large Volume Pump (LVP) was deployed. For observing in situ particles, optical sensor called LISST (Laser In Situ Scattering and Transmissometer) was deployed by University of Tokyo.

GODI technicians group undertook responsibility for underway current direction and velocity measurements using an Acoustic Current Profiler (ADCP), geological measurements (topography, geo-magnetic field and gravity), and collecting meteorological data.

For collection of zooplankton, NORPAC plankton net, and IONESS were deployed.

Sediment trap mooring system was also recovered and redeployed at station F1 for observation of radionuclides from the Fukushima Daiichi nuclear power plant.

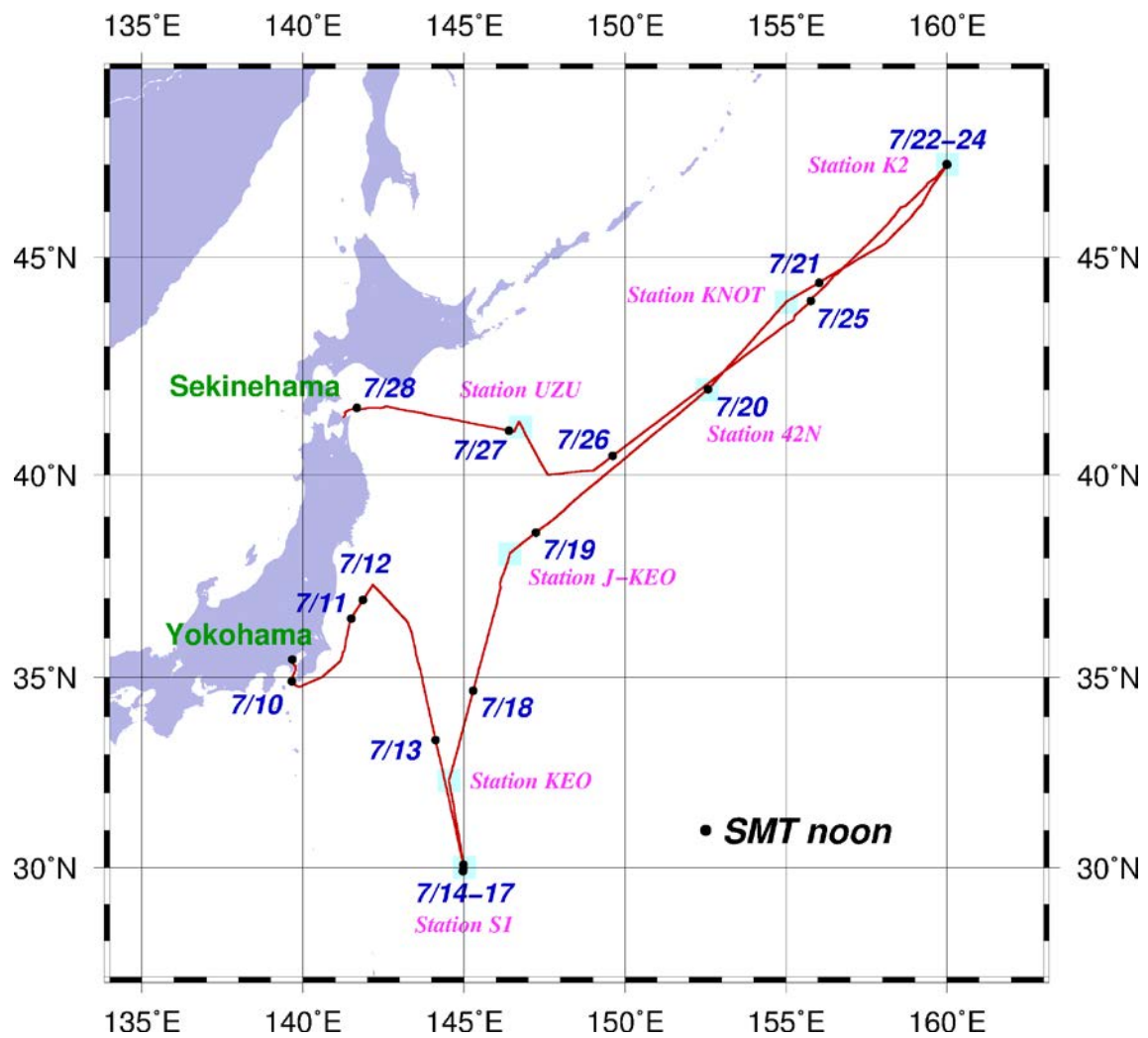
For observing vertical profile of primary productivity optically, FRRF was deployed.

In order to conduct time-series observation in biogeochemical cycle, JAMSTEC Sediment trap mooring system and POPPS mooring system were recovered and re-deployed at station K2 and S1 (POPPS mooring only for S1).

For observation of atmospheric chemistry (aerosol and gas), various instruments including “sky-radiometer” and ship-borne compact system for measuring atmospheric trace gas column densities were onboard and automatic measurement was conducted.

Please read text for more detail information and other instruments used for oceanographic and meteorological or atmospheric observation.

1.2 Track and log



Cruise log

U.T.C.		S.M.T.		Position		Event logs
Date	Time	Date	Time	Latitude	Longitude	
7.9	23:50	7.10	08:50	35-27N	139-40E	Departure from Yokohama
	05:00		14:00	-	-	Continuous observations start
7.10	15:48	7.11	00:48	36-29N	141-30E	Arrival at Station F1
	23:03		08:03	36-29.09N	141-29.77E	Large Volume Pump (LVP) #01 (200 m / 4 hours)
7.11	03:58		12:58	36-29.22N	141-29.63E	Laser In Situ Scattering and Transmissometer (LISST) #01 (200 m)
	06:07		15:07	36-28.42N	141-28.79E	WHOI mooring recovery
	07:31		16:31	36-28.67N	141-28.67E	CTD cast #01 (1280 m)
	09:10		18:10	36-28.11N	141-29.48E	Calibration for magnetometer #01
	10:57		19:57	36-28.41N	141-28.73E	Intelligent Operative Net Sampling System (IONESS) #01 (200 m)
	23:10	7.12	08:10	36-28.51N	141-28.38E	WHOI mooring deployment
				36-28.52N	141-28.54E	WHOI mooring fixed position (Depth : 1298 m)
7.12	00:54		09:54	-	-	Departure from Station F1
	04:54		13:54	37-20N	142-10E	Arrival at Station FS1
	05:05		14:05	37-19.43N	142-10.12E	JAEA mooring recovery
	06:30		15:30	-	-	Departure from Station FS1
7.13	19:00	7.14	04:00	30-00N	145-00E	Arrival at Station S1
	22:55		07:55	29-54.81N	144-57.90E	POPPS mooring recovery
	02:36		11:36	29-53.92N	144-58.21E	Optical measurements #01-1 (150 m)
	03:02		12:02	29-53.69N	144-57.81E	Optical measurements #01-2 (200 m)
	04:03		13:03	29-58.34N	144-58.86E	CTD cast #02 (5910 m)
7.14	08:27		17:27	29-58.06N	144-58.03E	Plankton net #01-1 (NORPAC: 20 m)
	08:37		17:37	29-57.97N	144-57.99E	Plankton net #01-2 (NORPAC: 50 m)
	08:48		17:48	29-57.84N	144-57.96E	Plankton net #01-3 (NORPAC: 100 m)
	08:59		17:59	29-57.75N	144-57.95E	Plankton net #01-4 (NORPAC: 150 m)
	09:14		18:14	29-57.60N	144-57.95E	Plankton net #01-5 (NORPAC: 200 m)
	09:30		18:30	29-57.43N	144-57.94E	Plankton net #01-6 (NORPAC: 300 m)
	09:56		18:56	29-57.27N	144-57.98E	Plankton net #01-7 (NORPAC: 100 m)
	10:02		19:02	29-57.07N	144-59.42E	IONESS #02 (200 m)
	16:58	7.15	01:58	29-59.74N	145-00.02E	CTD cast #03 (300 m)
	18:06		03:06	29-59.60N	144-59.69E	FRRF #01 (150 m)
	22:27		07:27	30-02.54N	144-59.52E	FRRF #02 (150 m)
	23:27		08:27	30-03.38N	144-59.94E	CTD cast #04 (500 m)
7.15	00:23		09:23	30-03.01N	144-59.95E	LISST #02 (200 m)
	02:12		11:12	30-04.58N	144-58.75E	Optical measurements #02-1 (200 m)
	02:27		11:27	30-04.47N	144-58.53E	Optical measurements #02-2 (200 m)
	03:14		12:14	30-04.37N	144-58.13E	FRRF #03 (150 m)
	04:10		13:10	30-03.06N	144-57.37E	BGC mooring recovery
	07:26		16:26	30-01.76N	144-56.49E	FRRF #04 (150 m)
	09:00		18:00	30-00.00N	144-59.96E	Plankton net #02-1 (NORPAC: 25 m)
	09:07		18:07	30-00.01N	144-59.88E	Plankton net #02-2 (NORPAC: 75 m)
	09:17		18:17	30-00.16N	144-59.83E	Plankton net #02-3 (NORPAC: 75 m)
	09:27		18:27	30-00.00N	144-59.76E	Plankton net #02-4 (NORPAC: 125 m)
	09:39		18:39	29-59.97N	144-59.70E	Plankton net #02-5 (NORPAC: 125 m)
	09:51		18:51	29-59.91N	144-59.60E	Plankton net #02-6 (NORPAC: 200 m)
	10:09		19:09	29-59.88N	144-59.57E	Plankton net #02-7 (NORPAC: 75 m)
	10:29		19:29	30-00.19N	144-59.48E	Calibration for magnetometer #02
	20:30	7.16	05:30	29-54.68N	144-57.33E	CTD cast #05 (2000 m)
	23:30		08:30	29-54.96N	144-52.43E	POPPS mooring deployment
				29-56.15N	144-58.45E	POPPS mooring fixed position (Depth : 5912 m)
7.16	05:17		14:17	29-58.23N	144-59.61E	LVP #02 (200 m / 4 hours)
	10:08		19:08	29-58.27N	144-59.59E	LISST #03
	19:59	7.17	04:59	30-04.16N	144-58.32E	CTD cast #06 (2000 m)
7.17	00:00		09:00	30-03.24N	144-53.92E	BGC mooring deployment

U.T.C.		S.M.T.		Position		Event logs
Date	Time	Date	Time	Latitude	Longitude	
	03:48		12:48	30-03.86N	144-57.81E	BGC mooring fixed position (Depth : 5927 m)
	03:50		12:50	30-04.05N	144-58.09E	ARGO float deployment #01
	04:00		13:00	-	-	ARGO float deployment #02
						Departure from Station S1
	13:00		22:00	32-19N	144-32E	Arrival at Station KEO
	13:06		22:06	32-18.82N	144-31.74E	CTD cast #07 (5667 m)
	17:00	7.18	02:00	-	-	Departure from Station KEO
7.18	13:00		22:00	-	-	Time adjustment +1 hour (SMT=UTC+10h)
	18:42	7.19	04:42	38-05N	146-25E	Arrival at Station JKEO
	19:00		05:00	38-05.57N	146-24.98E	CTD cast #08 (5380 m)
	22:48		08:48	-	-	Departure from Station JKEO
7.19	23:48	7.20	09:48	42-00N	152-33E	Arrival at Station 42N
	23:58		09:58	42-00.20N	152-33.29E	CTD cast #09 (2000 m)
7.20	01:53		11:53	42-00.44N	142-33.89E	ARGO float deployment #03
	02:00		12:00	-	-	Departure from Station 42N
	12:00		22:00	-	-	Time adjustment +1 hour (SMT=UTC+11h)
	15:48	7.21	02:48	44-00N	155-00E	Arrival at Station KNOT
	15:59		02:59	44-00.29N	155-00.18E	CTD cast #10 (5295 m)
	21:01		08:01	44-00.79N	155-01.01E	Cesium magnetometer towing start
	21:06		08:06	-	-	Departure from Station KNOT
7.21	18:54	7.22	05:54	47-00N	160-05E	Arrival at Station K2
	18:59		05:59	46-58.63N	159-58.61E	Cesium magnetometer towing finish
	21:01		08:01	47-02.08N	160-00.08E	BGC mooring recovery
7.22	02:02		13:02	47-00.12N	160-00.30E	CTD cast #11 (5170 m)
	06:32		17:32	47-00.02N	159-59.60E	Plankton net #03-1 (NORPAC: 20 m)
	06:39		17:39	46-59.99N	159-59.54E	Plankton net #03-3 (NORPAC: 50 m)
	06:50		17:50	46-59.97N	159-59.48E	Plankton net #03-4 (NORPAC: 100 m)
	07:02		18:02	46-59.94N	159-59.35E	Plankton net #03-5 (NORPAC: 150 m)
	07:15		18:15	46-59.93N	159-59.23E	Plankton net #03-6 (NORPAC: 200 m)
	07:30		18:30	46-59.93N	159-59.08E	Plankton net #03-7 (NORPAC: 300 m)
	07:48		18:48	46-59.92N	159-58.99E	Plankton net #03-8 (NORPAC: 50 m)
	10:02		21:02	46-58.56N	159-58.12E	IONESS #03 (200 m)
	15:03	7.23	02:03	47-00.15N	160-00.38E	CTD cast #12 (300 m)
	16:09		03:09	47-00.27N	160-00.24E	FRRF #05 (100 m)
	20:27		07:27	46-59.93N	159-59.95E	FRRF #06 (100 m)
	20:58		07:58	47-00.07N	159-59.64E	CTD cast #13 (2000 m)
7.23	00:54		11:54	47-00.08N	159-59.81E	FRRF #07 (100 m)
	01:58		12:58	47-00.23N	159-59.74E	CTD cast #14 (2000 m)
	03:50		14:50	47-00.79N	159-59.55E	Plankton net #04-1 (NORPAC: 20 m)
	03:58		14:58	47-00.86N	159-59.55E	Plankton net #04-2 (NORPAC: 50 m)
	04:08		15:08	47-00.94N	159-59.58E	Plankton net #04-3 (NORPAC: 100 m)
	04:20		15:20	47-01.06N	159-59.57E	Plankton net #04-4 (NORPAC: 150 m)
	04:34		15:34	47-01.21N	159-59.58E	Plankton net #04-5 (NORPAC: 200 m)
	04:50		15:50	47-01.36N	159-59.55E	Plankton net #04-6 (NORPAC: 300 m)
	05:10		16:10	47-01.48N	159-59.54E	Plankton net #04-7 (NORPAC: 50 m)
	05:14		16:14	47-01.51N	159-59.52E	Plankton net #04-8 (NORPAC: 50 m)
	05:18		16:18	47-01.54N	159-59.53E	Plankton net #04-9 (NORPAC: 50 m)
	05:34		16:34	47-01.68N	159-59.31E	CTD cast #15 (200 m)
	06:39		17:39	46-59.73N	160-00.09E	LISST #04 (200 m)
	07:34		18:34	46-59.71N	160-00.40E	FRRF #08 (100 m)
	08:10		19:10	46-59.16N	160-00.56E	Calibration for magnetometer #03
	21:07	7.24	08:07	47-01.09N	159-51.56E	BGC mooring deployment
7.24	00:34		11:34	47-00.47N	159-58.40E	BGC mooring fixed position (Depth : 5219 m)

U.T.C.		S.M.T.		Position		Event logs
Date	Time	Date	Time	Latitude	Longitude	
	01:56		12:56	47-00.20N	160-01.04E	LVP #03 (200m / 4 hours)
	06:54		17:54	-	-	Departure from Station K2
7.25	11:00	7.25	22:00	-	-	Time adjustment -1 hour (SMT=UTC+10h)
7.26	04:36	7.26	14:36	40-07N	149-02E	Arrival at Station E03
	04:40		14:40	40-07.02N	149-02.18E	CTD cast #16 (2000 m)
	06:42		16:42	-	-	Departure from Station E03
	18:48	7.27	04:48	41-15N	146-43E	Arrival at Station E01
	18:57		04:57	41-15.13N	146-42.73E	CTD cast #17 (2000 m)
	20:59		06:59	41-15.48N	146-42.21E	ARGO float deployment #04
	21:00		07:00	-	-	Departure from Station E01
	23:18		09:18	41-02N	146-33E	Arrival at Station E02
	23:28		09:28	41-01.87N	146-32.59E	CTD cast #18 (2000m)
7.27	01:12		11:12	-	-	Departure from Station E02
	12:00		22:00	-	-	Time adjustment -1 hour (SMT=UTC+9h)
7.28	04:04	7.28	13:04	-	-	Continuous observations finish
7.28	00:04	7.28	09:04	41-22N	141-14E	Arrival at Sckinchama

1.3 Cruise participants

Name	Affiliation	Appointment
Makio HONDA (Principal Investigator)	Japan Agency for Marine-Earth Science and Technology (JAMSTEC) Research Institute for Global Change (RIGC)	Team leader
Kazuhiko MATSUMOTO (Deputy PI)	JAMSTEC, RIGC	Research scientist
Minoru KITAMURA	JAMSTEC, Institute of Biogeoscience (BIOGEOS)	Research scientist
Hajime KAWAKAMI	JAMSTEC, Mutsu Institute of Oceanigraphy (MIO)	Research scientist
Masahide WAKITA	JAMSTEC, MIO	Research scientist
Tetsuichi FUJIKI	JAMSTEC, RIGC	Scientist
Kosei SASAOKA	JAMSTEC, RIGC	Technical support stuff
Katsunori KIMOTO	JAMSTEC, RIGC	Research scientist
Haruka TAKAGI	JAMSTEC, RIGC	Graduate student
Hiroshi UCHIDA	JAMSTEC, RIGC	Research scientist
Chisato YOSHIKAWA	JAMSTEC, RIGC	Postdoctoral researcher
Steven J. MANGANINI	Woods Hole Oceanographic Institution	Research Specialist
Hideki FUKUDA	University of Tokyo	Assistant professor
Naomi SATO	University of Tokyo	Graduate student
Mario UCHIMIYA	National Institute of Polar Research	Postdoctoral researcher
Osamu ABE	Nagoya University	Assistant professor
Habeeb R. KEEDAKKADAN	Nagoya University	Graduate student
Shigeyoshi OTOSAKA	Japan Atomic Energy Agency	Senior Scientist
Masanobu KAWACHI	National Institute for Environmental Studies	Senior researcher
Haruyo YAMAGUCHI	National Institute for Environmental Studies	Postdoctoral researcher
Miho FUKUDA	National Institute of Radiological Sciences	Postdoctoral researcher
Haruka TAMADA	Rakuno Gakuen University	Graduate student
Katsunori SAGISHIMA	Marine Works Japan Inc.	Marine Technician

(Principal Marine Tech.)		
Tomohide NOGUCHI	Same as above	Same as above
Naoko MIYAMAOTO	Same as above	Same as above
Tomoyuki TAKAMORI	Same as above	Same as above
Shungo OSHITANI	Same as above	Same as above
Tamami UENO	Same as above	Same as above
Masaki FURUHATA	Same as above	Same as above
Atsushi ONO	Same as above	Same as above
Tomonori WATAI	Same as above	Same as above
Shin TAKADA	Same as above	Same as above
Yasuhiro ARII	Same as above	Same as above
Elena HAYASHI	Same as above	Same as above
Emi DEGUCHI	Same as above	Same as above
Hideki YAMAMOTO	Same as above	Same as above
Shinichiro YOKOGAWA	Same as above	Same as above
Hironori SATO	Same as above	Same as above
Yuta IIBUCHI	Same as above	Same as above
Kanako YOSHIDA	Same as above	Same as above
Keitaro MATSUMOTO	Same as above	Same as above
Wataru TOKUNAGA (Principal Marine Tech.)	Global Ocean Development Inc. (GODI)	Marine Technician
Miki MORIOKA	Same as above	Same as above

2. General observation

2.1 Meteorological observations

Makio HONDA	(JAMSTEC: Principal Investigator)
Wataru TOKUNAGA	(Global Ocean Development Inc., GODI)
Miki MORIOKA	(GODI)
Ryo OYAMA	(MIRAI crew)

(1) Objectives

Surface meteorological parameters are observed as a basic dataset of the meteorology. These parameters bring us the information about the temporal variation of the meteorological condition surrounding the ship.

(2) Methods

Surface meteorological parameters were observed throughout the MR13-04 cruise. We used two systems for the observation, during this cruise.

i) MIRAI Surface Meteorological observation (SMet) system

Instruments of SMet system are listed in Table.2.1-1 and measured parameters are listed in Table.2.1-2. Data were collected and processed by KOAC-7800 weather data processor made by Koshin-Denki, Japan. The data set consists of 6-second averaged data.

ii) Shipboard Oceanographic and Atmospheric Radiation (SOAR) system

SOAR system designed by BNL (Brookhaven National Laboratory, USA) consists of major three parts.

- a) Portable Radiation Package (PRP) designed by BNL - short and long wave downward radiation.
- b) Zeno Meteorological (Zeno/Met) system designed by BNL - wind, air temperature, relative humidity, pressure, and rainfall measurement.
- c) Scientific Computer System (SCS) developed by NOAA (National Oceanic and Atmospheric Administration, USA) - centralized data acquisition and logging of all data sets.

SCS recorded PRP data every 6 seconds, while Zeno/Met data every 10 seconds. Instruments and their locations are listed in Table.2.1-3 and measured parameters are listed in Table.2.1.1-4.

For the quality control as post processing, we checked the following sensors, before and after the cruise.

i. Young Rain gauge (SMet and SOAR)

Inspect of the linearity of output value from the rain gauge sensor to change

- Input value by adding fixed quantity of test water.
 - ii. Barometer (SMet and SOAR)
 - Comparison with the portable barometer value, PTB220CASE, VAISALA.
 - iii. Thermometer (air temperature and relative humidity) (SMet and SOAR)
 - Comparison with the portable thermometer value, HMP41/45, VAISALA.
- (3) Preliminary results
- Figure 2.1-1 shows the time series of the following parameters;
- Wind (SMet)
 - Air temperature (SMet)
 - Relative humidity (SMet)
 - Precipitation (SOAR, rain gauge)
 - Short/long wave radiation (SOAR)
 - Pressure (SMet)
 - Sea surface temperature (SMet)
 - Significant wave height (SMet)
- (4) Data archives
- These meteorological data will be submitted to the Data Management Group (DMG) of JAMSTEC just after the cruise.
- (5) Remarks
- i. SST (Sea Surface Temperature) data were available in the following periods.
05:05UTC 10 June - 14:55UTC 28 July
 - ii. SMet Young rain gauge includes invalid data at the following time due to MF/HF transmit.
 - iii. SOAR (PRP) long wave radiation data were not available in following period due to sensor output error.

Table.2.1-1 Instruments and installations of
MIRAI Surface Meteorological observation system

Sensors	Type	Manufacturer	Location (altitude from surface)
Anemometer	KE-500	Koshin Denki, Japan	foremast (24 m)
Tair/RH	HMP155	Vaisala, Finland	compass deck (21 m) starboard and port side
	with 43408 Gill aspirated radiation shield	R.M. Young, USA	
Thermometer (SST)	RFN1-0	Koshin Denki, Japan	4th deck (-1m, inlet -5m)
Barometer	Model-370	Setra System, USA	captain deck (13 m) weather observation room
Rain gauge	50202	R. M. Young, USA	compass deck (19 m)
Optical rain gauge	ORG-815DR	Osi, USA	compass deck (19 m)
Radiometer (short wave)	MS-801	Eiko Seiki, Japan	radar mast (28 m)
Radiometer (long wave)	MS-200	Eiko Seiki, Japan	radar mast (28 m)
Wave height meter	MW-2	Tsurumi-seiki, Japan	bow (10 m) port side stern (8 m)

Table.2.1-2 Parameters of MIRAI Surface Meteorological observation system

Parameter	Units	Remarks
1 Latitude	degree	
2 Longitude	degree	
3 Ship's speed	knot	MIRAI log, DS-30 Furuno
4 Ship's heading	degree	MIRAI gyro, TG-6000, Tokimec
5 Relative wind speed	m/s	6sec./10min. averaged
6 Relative wind direction	degree	6sec./10min. averaged
7 True wind speed	m/s	6sec./10min. averaged
8 True wind direction	degree	6sec./10min. averaged
9 Barometric pressure	hPa	adjusted to sea surface level 6sec. averaged
10 Air temperature (starboard)	degC	6sec. averaged
11 Air temperature (port side)	degC	6sec. averaged
12 Dewpoint temperature (starboard)	degC	6sec. averaged
13 Dewpoint temperature (side)	degC	6sec. averaged
14 Relative humidity (starboard)	%	6sec. averaged
15 Relative humidity (port side)	%	6sec. averaged
16 Sea surface temperature	degC	6sec. averaged
17 Rain rate (optical rain gauge)	mm/hr	hourly accumulation
18 Rain rate (capacitive rain gauge)	mm/hr	hourly accumulation
19 Down welling shortwave radiation	W/m ²	6sec. averaged
20 Down welling infra-red radiation	W/m ²	6sec. averaged
21 Significant wave height (bow)	m	hourly
22 Significant wave height (aft)	m	hourly
23 Significant wave period (bow)	second	hourly

24 Significant wave period (aft) second hourly

Table.2.1-3 Instruments and installation locations of SOAR system

Sensors (Zeno/Met)	Type	Manufacturer	Location (altitude from surface)
Anemometer	05106	R.M. Young, USA	foremast (25 m)
Tair/RH	HMP45A	Vaisala, Finland	foremast (23 m)
	with 43408 Gill aspirated radiation shield	R.M. Young, USA	
Barometer	61202V	R.M. Young, USA	foremast (23 m)
	with 61002 Gill pressure port	R.M. Young, USA	
Rain gauge	50202	R.M. Young, USA	foremast (24 m)
Optical rain gauge	ORG-815DA	Osi, USA	foremast (24 m)
Sensors (PRP)	Type	Manufacturer	Location (altitude from surface)
Radiometer (short wave)	PSP	Epply Labs, USA	foremast (25 m)
Radiometer (long wave)	PIR	Epply Labs, USA	foremast (25 m)
Fast rotating shadowband radiometer		Yankee, USA	foremast (25 m)

Table.2.1-4 Parameters of SOAR system

Parameter	Units	Remarks
1 Latitude	degree	
2 Longitude	degree	
3 SOG	knot	
4 COG	degree	
5 Relative wind speed	m/s	
6 Relative wind direction	degree	
7 Barometric pressure	hPa	
8 Air temperature	degC	
9 Relative humidity	%	
10 Rain rate (optical rain gauge)	mm/hr	
11 Precipitation (capacitive rain gauge)	mm	reset at 50 mm
12 Down welling shortwave radiation	W/m ²	
13 Down welling infra-red radiation	W/m ²	
14 Defuse irradiance	W/m ²	

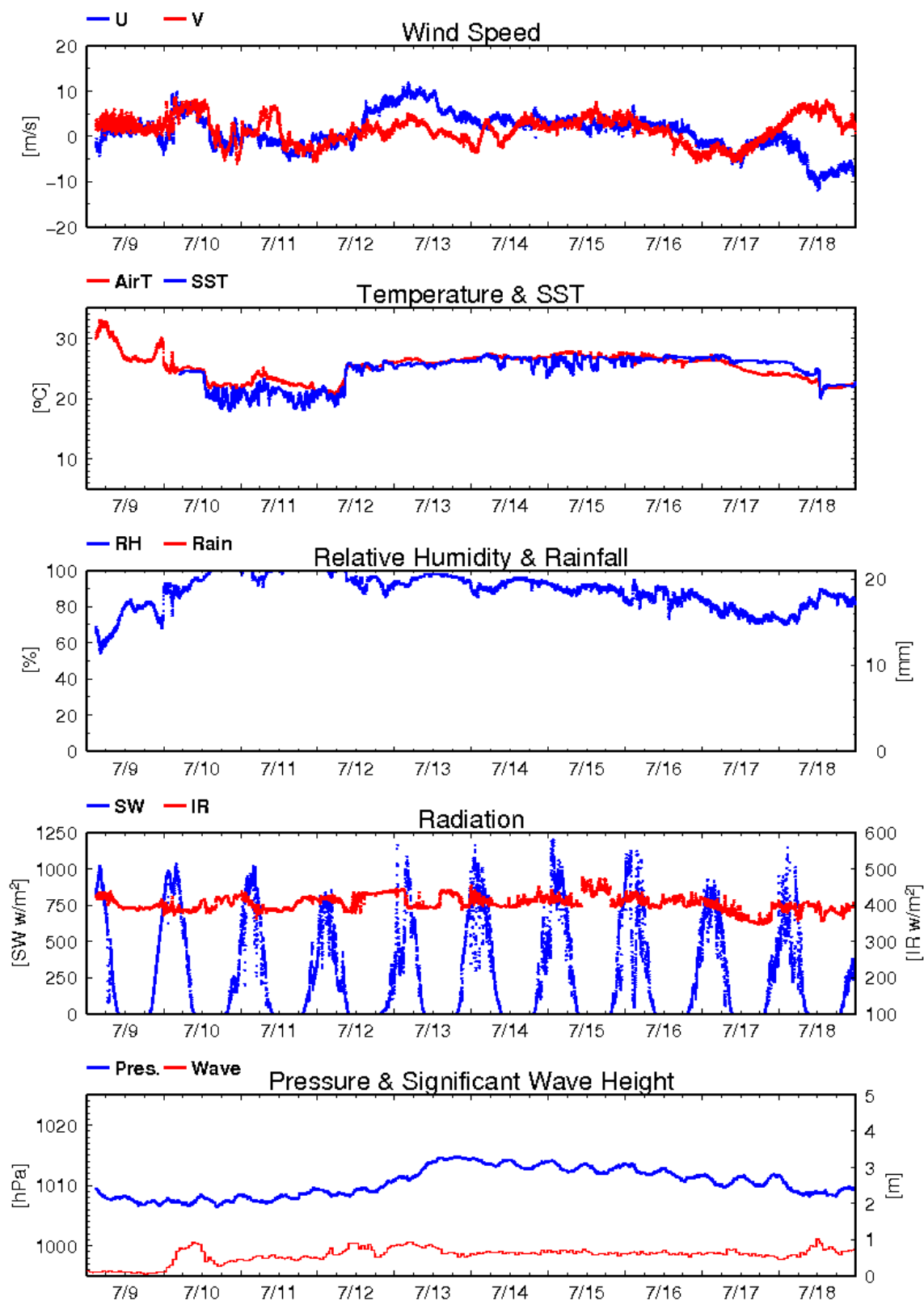


Fig.2.1-1 Time series of surface meteorological parameters during the MR13-04 cruise

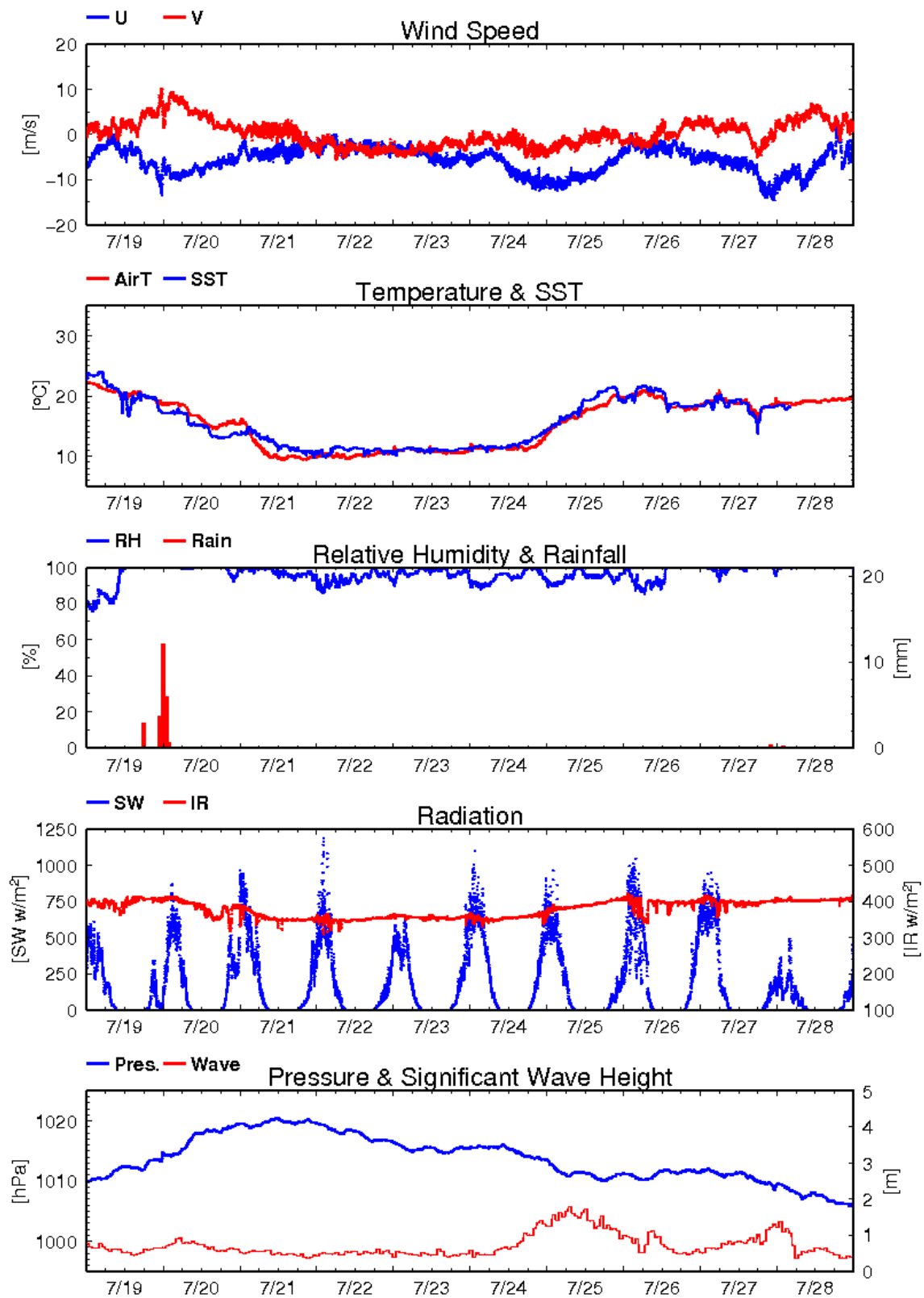


Fig.2.1-1 Continued

2.2 Surface meteorological observations

2.2.1 Ceilometer observation

Makio HONDA (JAMSTEC: Principal Investigator)

Wataru TOKUNAGA (Global Ocean Development Inc., GODI)

Miki MORIOKA (GODI)

Ryo OYAMA (MIRAI crew)

(1) Objectives

The information of cloud base height and the liquid water amount around cloud base is important to understand the process on formation of the cloud. As one of the methods to measure them, the ceilometer observation was carried out.

(2) Parameters

1. Cloud base height [m].
2. Backscatter profile, sensitivity and range normalized at 10 m resolution.
3. Estimated cloud amount [oktas] and height [m]; Sky Condition Algorithm.

(3) Methods

We measured cloud base height and backscatter profile using ceilometer (CL51, VAISALA, Finland) throughout the MR13-04 cruise from the departure of Yokohama on 10 July, 2013 to arrival of Sekinehama on 29 July, 2013.

Major parameters for the measurement configuration are as follows;

Laser source:	Indium Gallium Arsenide (InGaAs) Diode Laser
Transmitting center wavelength:	910±10 nm at 25 degC
Transmitting average power:	19.5 mW
Repetition rate:	6.5 kHz
Detector:	Silicon avalanche photodiode (APD)
Measurement range:	0 ~ 15 km 0 ~ 13 km (Cloud detection)
Resolution:	10 meter in full range
Sampling rate:	36 sec
Sky Condition	0, 1, 3, 5, 7, 8 oktas (9: Vertical Visibility) (0: Sky Clear, 1:Few, 3:Scattered, 5-7: Broken, 8: Overcast)

On the archive dataset, cloud base height and backscatter profile are recorded with the resolution of 10 m.

(4) Preliminary results

Figure 2.2.1-1 shows the time series of the lowest, second and third cloud base height.

(5) Data archives

The raw data obtained during this cruise will be submitted to the Data Management Group (DMG) in JAMSTEC.

(6) Remarks

1. Window cleaning;
09:42UTC 12 July

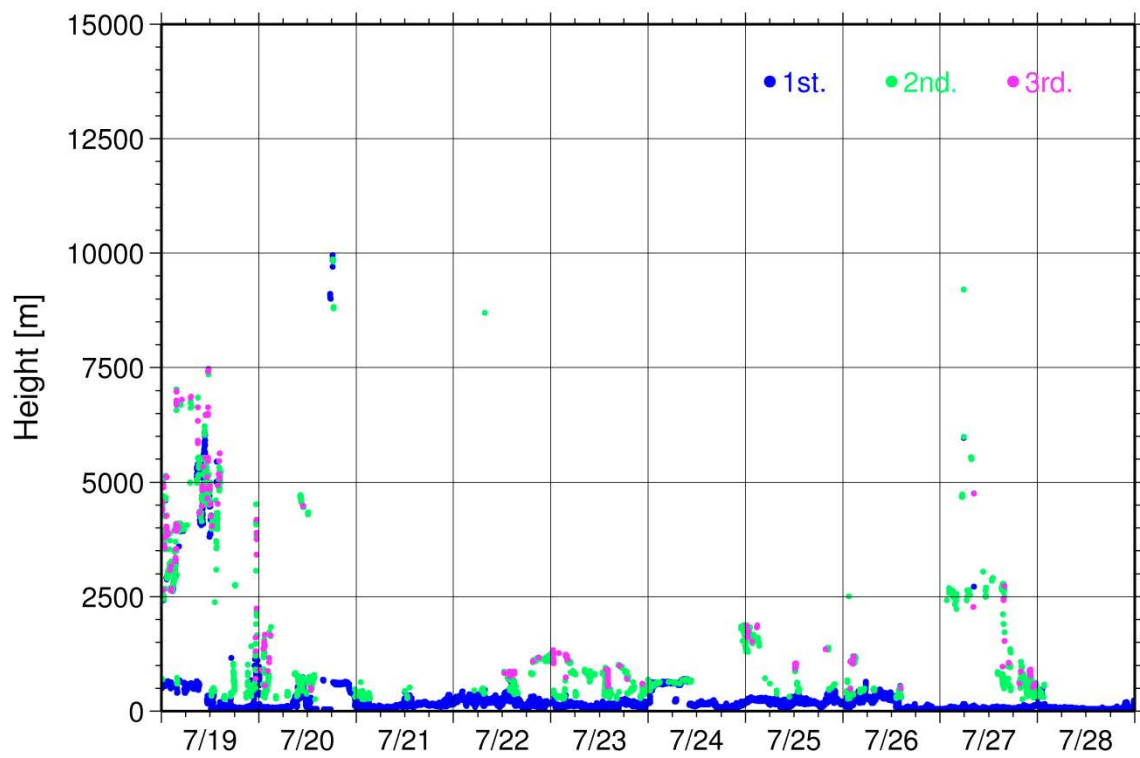
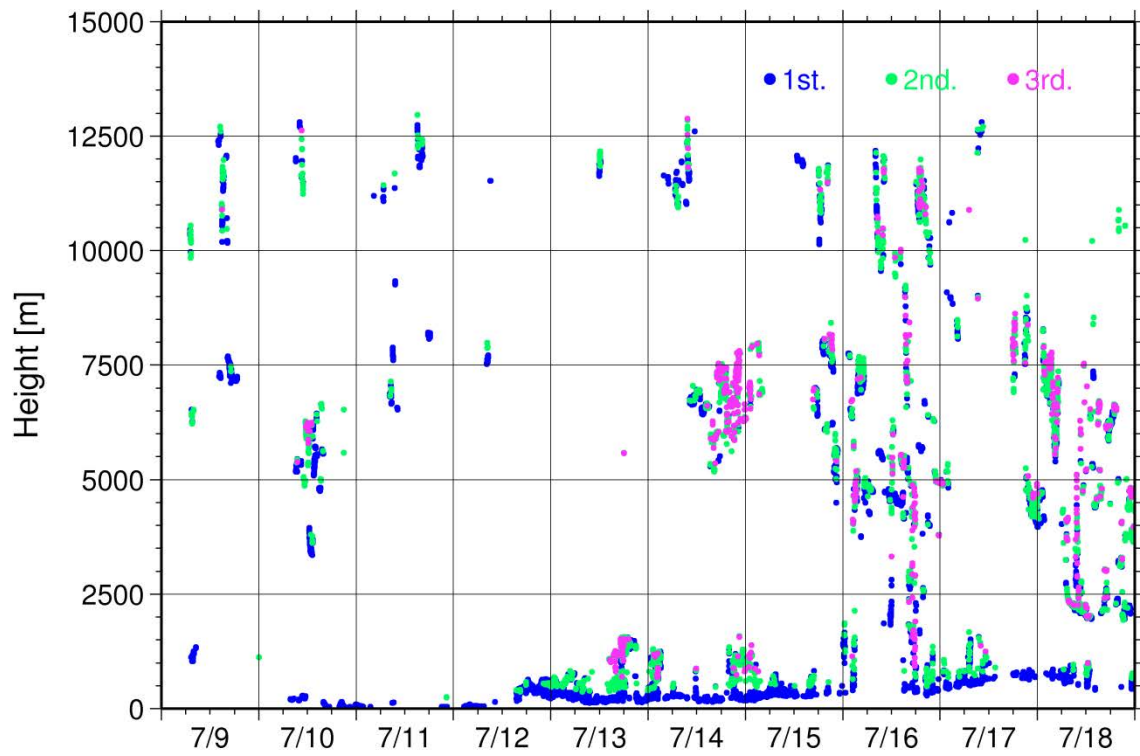


Fig.2.2.1-1 Lowest, 2nd and 3rd cloud base height during the cruise.

2.2.2 Lidar observations of clouds and aerosols

Nobuo SUGIMOTO (NIES)

Ichiro MATSUI (NIES)

Atsushi SHIMIZU (NIES)

Tomoaki NISHIZAWA (NIES)

(Lidar operation was supported by Global Ocean Development Inc. (GODI).)

(1) Objectives

Objectives of the observations in this cruise is to study distribution and optical characteristics of ice/water clouds and marine aerosols using a two-wavelength polarization Mie lidar.

(2) Description of instruments deployed

Vertical profiles of aerosols and clouds are measured with a two-wavelength polarization Mie lidar. The lidar employs a Nd:YAG laser as a light source which generates the fundamental output at 1064nm and the second harmonic at 532nm. Transmitted laser energy is typically 30mJ per pulse at both of 1064 and 532nm. The pulse repetition rate is 10Hz. The receiver telescope has a diameter of 20 cm. The receiver has three detection channels to receive the lidar signals at 1064 nm and the parallel and perpendicular polarization components at 532nm. An analog-mode avalanche photo diode (APD) is used as a detector for 1064nm, and photomultiplier tubes (PMTs) are used for 532 nm. The detected signals are recorded with a transient recorder and stored on a hard disk with a computer. The lidar system was installed in a container with a glass window on the roof, and the lidar was operated continuously regardless of weather. Every 10 minutes vertical profiles of four channels (532 parallel, 532 perpendicular, 1064, 532 near range) are recorded.

(3) Preliminary results

The two wavelength polarization Mie lidar worked well and succeeded in getting the lidar data during the observation period. Examples of the measured data are depicted in Fig. 1. The figure indicates that the lidar could detect water clouds formed at the top of the PBL formed at 1km and ice clouds in the upper layer (8km to 16km). In addition, you can find aerosols in the PBL (e.g., see the left figure (00UTC to 0600UTC on July 7 2013)), though the concentration was low during the observation period. In the latter half of the observation period, clouds or fogs formed in very low layers below 0.5km appeared (see the right figure). Thus, there were few cases that the lidar could observe aerosol layers since the lidar signals were attenuated due to optically thick clouds or fogs formed in lower layers.

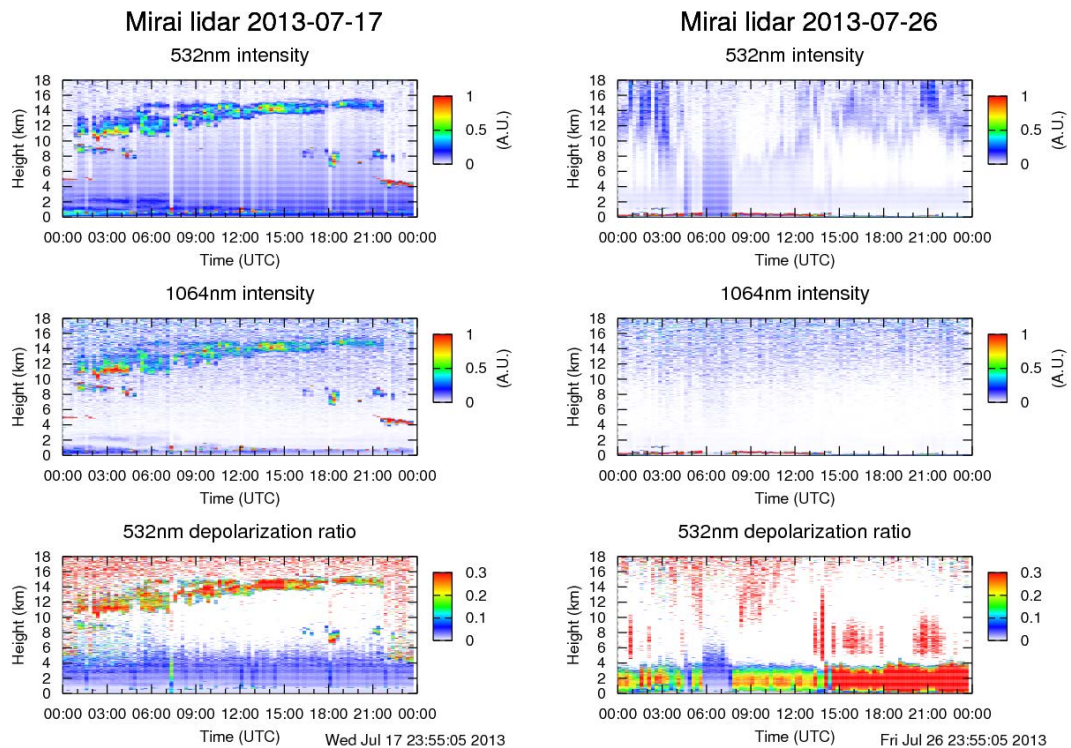


Figure 1: Time-height sections of backscatter intensities at 532nm and 1064nm and total depolarization ratios at 532nm measured on July 17 and July 26, 2013.

(4) Data archive

- Raw data

temporal resolution 10min / vertical resolution 6 m

data period (UTC): . July 17, 2013 ~ July 28, 2013

lidar signal at 532 nm, lidar signal at 1064 nm, depolarization ratio at 532 nm

- Processed data (plan)

cloud base height, apparent cloud top height, phase of clouds (ice/water), cloud fraction

boundary layer height (aerosol layer upper boundary height),

backscatter coefficient of aerosols, particle depolarization ratio of aerosols

* Data policy and Citation

Contact NIES lidar team (nsugimot/i-matsui/shimizua/nisizawa@nies.go.jp) to utilize lidar data for productive use.

2.2.3 Maritime aerosol optical properties from measurements of Ship-borne Sky radiometer

Kazuma AOKI (University of Toyama) Principal Investigator / not onboard
Tadahiro HAYASAKA (Tohoku University) Co-worker / not onboard
Sky radiometer operation was supported by Global Ocean Development Inc.

(1) Objectives

Objective of this observation is to study distribution and optical characteristics of marine aerosols by using a ship-borne sky radiometer (POM-01 MKII: PREDE Co. Ltd., Japan). Furthermore, collections of the data for calibration and validation to the remote sensing data were performed simultaneously.

(2) Methods and Instruments

The sky radiometer measures the direct solar irradiance and the solar aureole radiance distribution with seven interference filters (0.34, 0.4, 0.5, 0.675, 0.87, 0.94, and 1.02 μm). Analysis of these data was performed by SKYRAD.pack version 4.2 developed by Nakajima *et al.* 1996.

@ Measured parameters

- Aerosol optical thickness at five wavelengths (400, 500, 675, 870 and 1020 nm)
- Ångström exponent
- Single scattering albedo at five wavelengths
- Size distribution of volume (0.01 μm – 20 μm)

GPS provides the position with longitude and latitude and heading direction of the vessel, and azimuth and elevation angle of the sun. Horizon sensor provides rolling and pitching angles.

(3) Preliminary results

Only data collection were performed onboard. At the time of writing, the data obtained in this cruise are under post-cruise processing at University of Toyama.

(4) Data archives

Aerosol optical data are to be archived at University of Toyama (K.Aoki, SKYNET/SKY: <http://skyrad.sci.u-toyama.ac.jp/>) after the quality check and will be submitted to JAMSTEC.

2.2.4 Tropospheric aerosol and gas observations

Yugo KANAYA (JAMSTEC RIGC, not on board)

Makio HONDA (JAMSTEC RIGC)

Hisahiro TAKASHIMA (JAMSTEC RIGC, not on board)

Fumikazu TAKETANI (JAMSTEC RIGC, not on board)

Xiaole PAN (JAMSTEC RIGC, not on board)

Yuichi KOMAZAKI (JAMSTEC RIGC, not on board)

Takuma MIYAKAWA (JAMSTEC RIGC, not on board)

Shin NAGAI (JAMSTEC RIGC, not on board)

Operation was supported by Global Ocean Development Inc.

(1) Objective

- To clarify transport processes of atmospheric pollutants from the Asian continent to the ocean
- To investigate processes of biogeochemical cycles between the atmosphere and the ocean
- To advance validation of satellite observations of atmospheric composition
- To record atmospheric conditions and ocean color

(2) Description of instruments deployed

(2-1) MAX-DOAS

Multi-Axis Differential Optical Absorption Spectroscopy (MAX-DOAS), a passive remote sensing technique measuring spectra of scattered visible and ultraviolet (UV) solar radiation, was used for atmospheric aerosol and gas profile measurements. Our MAX-DOAS instrument consists of two main parts: an outdoor telescope unit and an indoor spectrometer (Acton SP-2358 with Princeton Instruments PIXIS-400B), connected to each other by a 14-m bundle cable that consists of 60 cores with 100- μm radii. On the roof top of the anti-rolling system of R/V Mirai, the telescope unit was installed on a gimbal mount, which compensates for the pitch and roll motion of the ship. The line of sight was in directions of the starboard and portside of the vessel. The integration time for UV and visible spectra recording (centered on 340 and 452 nm) was set to 0.20 and 0.08 s. Measurements were made every 30 min at elevation angles of 1.5, 3, 5, 10, 20, 30, 70, 110, 150, 160, 170, 175, and 177 degrees.

For the selected spectra recorded with elevation angles with good accuracy, DOAS spectral fitting was performed to quantify the slant column density (SCD) of NO_2 (and other gases) and O_4 ($\text{O}_2\text{-O}_2$, collision complex of oxygen) for each elevation angle. Then, the O_4 SCDs were converted to the aerosol optical depth (AOD) and the vertical profile of aerosol extinction coefficient (AEC) using an optimal estimation inversion method with a radiative transfer model. Using derived aerosol information, retrievals of the tropospheric vertical column/profile of NO_2 and other gases were made.

(2-2) CO and O_3

Carbon monoxide (CO) and ozone (O_3) measurements were also continuously conducted during the cruise. For CO and O_3 measurements, ambient air was continuously sampled on the compass

deck and drawn through ~20-m-long Teflon tubes connected to a gas filter correlation CO analyzer (Model 48C, Thermo Fisher Scientific) and a UV photometric ozone analyzer (Model 49C, Thermo Fisher Scientific) in the Research Information Center.

(2-3) Aerosol observations: size distribution, fluorescent properties, black carbon (BC), and samplings

Size distributions and fluorescent properties of aerosol particles present in the oceanic atmosphere were continuously measured using an airborne particle spectrometer (LAS-X II, Particle Measurement Systems) and a single particle fluorescence sensor, WIBS4 (Waveband Integrated bioaerosol sensor), respectively. BC was measured by an instrument based on laser-induced incandescence (SP2, Droplet Measurement Technologies). For LAS-X II and SP2, ambient air was commonly sampled from the flying bridge by a 3-m-long conductive tube, and then introduced to each instrument.

For the measurements of fluorescent properties by WIBS4 located on the flying bridge, two pulsed xenon lamps emitting UV light (280 nm and 370 nm) were used for excitation and fluorescence emitted from a single particle within 310–400 nm and 420–650 nm wavelength windows was recorded. Ambient aerosol particles were collected along cruise track using a high-volume air sampler (HV-525PM, SIBATA) located on the flying bridge operated at a flow rate of 500 L min⁻¹. To avoid collecting particles emitted from the funnel of the own vessel, the sampling period was controlled automatically by using a “wind-direction selection system”. Coarse and fine particles separated at the diameter of 2.5 μm were collected on quartz and Teflon filters, respectively. Twelve filter samples obtained during the cruise are subject to chemical analysis of aerosol composition, including water-soluble ions and trace metals.

(2-4) Cameras to observe atmospheric conditions and ocean color

To observe canopy atmospheric conditions and ocean color, we installed automatic digital fisheye camera systems composed of a Coolpix 4300 digital camera (Nikon, Tokyo, Japan), an FC-E8 fisheye lens (Nikon), and an SPC31A controller (Hayasaka Rikoh, Sapporo, Japan) at the deck of the ship. During the daytime, the cameras were pointed upwards and sideways to capture hemispherical images of the sky and sea surface every 15 min, respectively and store them in the JPEG format.

(3) Preliminary results

N/A (All the data analysis is to be conducted.)

(4) Data archive

The data files will be submitted to JAMSTEC Data Integration and Analyses Group (DIAG), after the full analysis is completed, which will be <2 years after the end of the cruise.

2.3 Physical oceanographic observation

2.3.1 CTD cast and water sampling

Masahide WAKITA (JAMSTEC MIO): Principal investigator

Hiroshi UCHIDA (JAMSTEC RIGC)

Naoko MIYAMOTO (MWJ): Operation leader

Shungo OSHITANI (MWJ)

Atsushi ONO (MWJ)

(1) Objective

Investigation of oceanic structure and water sampling.

(2) Parameters

Temperature (Primary and Secondary)

Conductivity (Primary and Secondary)

Pressure

Dissolved Oxygen

Dissolved Oxygen voltage

Transmission % and voltage

Fluorescence

Photosynthetically Active Radiation

Altimeter

(3) Instruments and Methods

CTD/Carousel Water Sampling System, which is a 36-position Carousel water sampler (CWS) with Sea-Bird Electronics, Inc. CTD (SBE9plus), was used during this cruise. 12-liter Niskin Bottles, which were washed by alkaline detergent and HCl, were used for sampling seawater. The sensors attached on the CTD were temperature (Primary and Secondary), conductivity (Primary and Secondary), pressure, dissolved oxygen, RINKO-III (dissolved oxygen sensor), transmission, fluorescence, PAR, altimeter and deep ocean standards thermometer. The Practical Salinity was calculated by measured values of pressure, conductivity and temperature. The CTD/CWS was deployed from starboard on working deck.

The CTD raw data were acquired on real time using the Seasave-Win32 (ver.7.22.5) provided by Sea-Bird Electronics, Inc. and stored on the hard disk of the personal computer. Seawater was sampled during the up cast by sending fire commands from the personal computer. We stayed for 1 minute at above 300 m layers before fire command to stabilize CTD. At deeper layer, we stayed for 30 seconds.

SBE43, dissolved oxygen sensor voltage has a big spike near 3500db. And it has a periodic noise in a place deeper than 5000db in downcast. This condition occurred in KEOM01, JKEOM01, KNTM01, and K02M01 casts

In S01M04, #20 trigger of CWS was not released normally

18 casts of CTD measurements were conducted (Table 2.3.1-1).

Data processing procedures and used utilities of SBE Data Processing-Win32 (ver.7.22.5) and SEASOFT were as follows:

(The process in order)

DATCNV: Convert the binary raw data to engineering unit data. DATCNV also extracts bottle information where scans were marked with the bottle confirm bit during acquisition. The duration was set to 4.4 seconds, and the offset was set to 0.0 seconds.

RINKOCOR (original module): Corrected of the hysteresis of RINK-III voltage.

RINKOCORROS (original module): Corrected of the hysteresis of RINKO-III voltage bottle data.

BOTTLESUM: Create a summary of the bottle data. The data were averaged over 4.4 seconds.

ALIGNCTD: Convert the time-sequence of sensor outputs into the pressure sequence to ensure that all calculations were made using measurements from the same parcel of water. Dissolved oxygen data are systematically delayed with respect to depth mainly because of the long time constant of the dissolved oxygen sensor and of an additional delay from the transit time of water in the pumped plumbing line. This delay was compensated by 6 seconds advancing dissolved oxygen sensor (SBE43) output (dissolved oxygen voltage) relative to the temperature data. RINKO-III voltage (User polyminal 0 – 2) were advanced 1second, transmission data and transmission voltage were advanced 2 seconds

WILDEDIT: Mark extreme outliers in the data files. The first pass of WILDEDIT obtained an accurate estimate of the true standard deviation of the data. The data were read in blocks of 1000 scans. Data greater than 10 standard deviations were flagged. The second pass computed a standard deviation over the same 1000 scans excluding the flagged values. Values greater than 20 standard deviations were marked bad. This process was applied to pressure, depth, temperature, conductivity and dissolved oxygen voltage (SBE43).

CELLTM: Remove conductivity cell thermal mass effects from the measured conductivity. Typical values used were thermal anomaly amplitude $\alpha = 0.03$ and the time constant $1/\beta = 7.0$.

FILTER: Perform a low pass filter on pressure with a time constant of 0.15 second. In order to produce zero phase lag (no time shift) the filter runs forward first then backward

WFILTER: Perform a median filter to remove spikes in the fluorescence data, transmission data and voltage data. A median value was determined by 49 scans of the window.

SECTIONU (original module of SECTION): Select a time span of data based on scan number in order to reduce a file size. The minimum number was set to be the starting time when the CTD package was beneath the sea-surface after activation of the pump. The maximum number of was set to be the end time when the package came up from the surface.

LOOPEDIT: Mark scans where the CTD was moving less than the minimum velocity of 0.0 m/s (traveling backwards due to ship roll).

DESPIKE (original module): Remove spikes of the data. A median and mean absolute deviation was calculated in 1-dbar pressure bins for both down and up cast, excluding the flagged values. Values greater than 4 mean absolute deviations from the median were marked bad for each bin. This process was performed 2 times for temperature, conductivity, dissolved oxygen voltage (SBE43), RINKO-III voltage.

DERIVE: Compute dissolved oxygen (SBE43).

BINAVG: Average the data into 1-dbar pressure bins.

DERIVE: Compute the Practical Salinity, sigma-theta and potential temperature.

SPLIT: Separate the data from an input .cnv file into down cast and up cast files.

Configuration file: MR1304A.xmlcon

Specifications of the sensors are listed below.

CTD: SBE911plus CTD system

Under water unit:

SBE9plus (S/N 09P54451-1027, Sea-Bird Electronics, Inc.)

Pressure sensor: Digiquartz pressure sensor (S/N 117457)

Calibrated Date: 10 May 2013

Temperature sensors:

Primary: SBE03-04/F (S/N 031524, Sea-Bird Electronics, Inc.)

Calibrated Date: 22 Jun. 2012

Secondary: SBE03-04/F (S/N 031525, Sea-Bird Electronics, Inc.)

Calibrated Date: 31 Aug. 2012

Conductivity sensors:

Primary: SBE04C (S/N 043036, Sea-Bird Electronics, Inc.)

Calibrated Date: 26 Jun. 2012

Secondary: SBE04C (S/N 041203, Sea-Bird Electronics, Inc.)

Calibrated Date: 18 Apr. 2012

Dissolved Oxygen sensor:

SBE43 (S/N 430394, Sea-Bird Electronics, Inc.)

Calibrated Date: 08 Dec. 2012

RINK-III (S/N 0024 (144002A), Alec Electronics Co. Ltd.)

Calibrated Date: 27 Jun 2013

RINK-III (S/N 0037 (1204), Alec Electronics Co. Ltd.)

Calibrated Date: 24 Jun 2013

RINK-III (S/N 0079 (1204), Alec Electronics Co. Ltd.)

Calibrated Date: 24 Jun 2013

Transmissometer:

C-Star (S/N CST-1363DR, WET Labs, Inc.)

Calibrated Date: 02 Feb. 2013

Fluorescence:

Chlorophyll Fluorometer (S/N 2936, Seapoint Sensors, Inc.)

Photosynthetically Active Radiation:

PAR sensor (S/N 0049, Satlantic Inc.)

Calibrated Date: 22 Jan. 2009

Altimeter:

Benthos PSA-916T (S/N 1157, Teledyne Benthos, Inc.)

Deep Ocean Standards Thermometer:

SBE35 (S/N 0022, Sea-Bird Electronics, Inc.)

Calibrated Date: 06 Mar. 2012

Carousel water sampler:

SBE32 (S/N 3227443-0391, Sea-Bird Electronics, Inc.)

Deck unit: SBE11plus (S/N 11P9833-0344, Sea-Bird Electronics, Inc.)

(4) Preliminary Results

During this cruise, 18 casts of CTD observation were carried out. Date, time and locations of the CTD casts are listed in Table 2.3.1-1.

(5) Data archive

All raw and processed data files will be submitted to the Data Management Office (DMO), JAMSTEC, and will be opened to public via “R/V MIRAI Data Web Page” in the JAMSTEC home page.

Table 2.3.1-1 MR13-04 CTD cast table

Stnnbr	Castno	Date(UTC)	Time(UTC)		BottomPosition		Depth (m)	Wire Out(m)	HT Above Bottom(m)	Max Depth(m)	Max Pressure(db)	CTD Filename	Remark
		(mmddyy)	Start	End	Latitude	Longitude							
F01	1	071113	07:35	08:51	36-28.67N	141-28.67E	1299.0	1284.4	8.7	1282.5	1296.0	F01M01	for Routine
S01	1	071413	04:08	08:09	29-58.34N	144-58.86E	5926.0	5913.0	8.3	5911.1	6035.0	S01M01	for Routine
S01	2	071413	17:04	17:52	29-59.73N	145-00.02E	5955.0	298.7	-	301.7	304.0	S01M02	for P.P.
S01	3	071413	23:29	00:12	30-03.38N	144-59.94E	5916.0	499.4	-	501.0	505.0	S01M03	for AORI, PALEO
S01	4	071513	20:34	21:59	29-54.68N	144-57.33E	5866.0	2000.0	-	2000.6	2024.0	S01M04	for P.E., Trap, Cs
S01	5	071613	20:05	21:56	30-04.16N	144-58.32E	5924.0	1987.3	-	1979.9	2003.0	S01M05	for ARGO
KEO	1	071713	13:12	16:53	32-18.82N	144-31.74E	5697.0	5670.1	9.5	5667.3	5784.0	KEOM01	for Routine
JKO	1	071813	19:06	22:38	38-05.56N	146-24.98E	5422.0	5386.0	9.7	5382.0	5492.0	JKOM01	for Routine
42N	1	072013	00:03	01:46	42-00.20N	152-33.29E	5265.0	1978.6	-	1976.8	2002.0	42NM01	for ARGO
KNT	1	072013	16:04	19:35	44-00.29N	155-00.17E	5318.0	5317.9	8.9	5295.8	5406.0	KNTM01	for Routine
K02	1	072213	02:07	05:37	47-00.12N	160-00.30E	5188.0	5174.3	8.9	5172.4	5280.0	K02M01	for Routine
K02	2	072213	15:08	15:58	47-00.15N	160-00.37E	5188.0	298.4	-	300.3	303.0	K02M02	for P.P., TIT, NIES
K02	3	072213	21:03	22:44	47-00.06N	159-59.64E	5185.0	2011.5	-	2002.5	2029.0	K02M03	for P.E., NU, TIT, JAEA
K02	4	072313	02:03	03:35	47-00.23N	159-59.74E	5186.0	2007.7	-	2002.5	2029.0	K02M04	for Trap, AORI, NIES, NIRS
K02	5	072313	05:38	06:08	47-01.67N	159-59.31E	5197.0	198.8	-	201.2	203.0	K02M05	for AORI, PALEO
E03	1	072613	04:45	06:35	40-07.02N	149-02.17E	5676.0	1986.2	-	1978.2	2003.0	E03M01	for ARGO
E01	1	072613	19:03	20:52	41-15.13N	146-42.73E	5380.0	1981.9	-	1977.0	2002.0	E01M01	for ARGO
E02	1	072613	23:34	01:03	41-01.86N	146-32.59E	5295.0	1979.2	-	1978.0	2003.0	E02M01	for ARGO

ARGO: ARGO float release point

P.P.: Primary Production

PALEO: archaeobacteria cast

P.E.: P vs. E curve cast

TIT: TITech. Nitrogen Oxide, N₂O isotopomerNU: P.E., ¹⁸O

NIRS: Cs

Routine: Routine sampling

Cs: cesium (Jamstec)

Trap: water for the Sediment trap

AORI: POM

NIES: pico plankton

JAEA: ¹²⁹I

2.3.2 Salinity measurement

Masahide WAKITA (JAMSTEC MIO)

Tamami UENO (MWJ)

Tomohide NOGUCHI (MWJ)

(1) Objective

To measure bottle salinity obtained by CTD casts, bucket sampling, and The Continuous Sea Surface Water Monitoring System (TSG).

(2) Methods

a. Salinity Sample Collection

Seawater samples were collected with 12 liter Niskin-X bottles, bucket, and TSG. The salinity sample bottles of the 250ml brown glass bottles with screw caps were used for collecting the sample water. Each bottle was rinsed three times with the sample water, and filled with sample water to the bottle shoulder. The salinity sample bottles for TSG were sealed with both plastic inner caps and screw caps because we took into consideration the possibility of long term storage (for about one month). These caps were rinsed three times with the sample water before use. The bottles were stored for more than 24 hours in the laboratory before the salinity measurement.

The number of samples is shown as follows;

Table 2.3.2-1 The number of samples

Sampling type	Number of samples
CTD and Bucket	401
TSG	16
Total	417

b. Instruments and Method

The salinity measurement on R/V MIRAI was carried out during the cruise of MR13-04 using the salinometer (Model 8400B “AUTOSAL”; Guildline Instruments Ltd.: S/N 62827) with an additional peristaltic-type intake pump (Ocean Scientific International, Ltd.). A pair of precision digital thermometers (Model 9540; Guildline Instruments Ltd.: S/N 66528 and 62521) were used. The thermometer monitored the ambient temperature and the bath temperature of the salinometer.

The specifications of AUTOSAL salinometer and thermometer are shown as follows;

Salinometer (Model 8400B “AUTOSAL”; Guildline Instruments Ltd.)

Measurement Range : 0.005 to 42 (PSU)

Accuracy : Better than ± 0.002 (PSU) over 24 hours
without re-standardization

Maximum Resolution : Better than ± 0.0002 (PSU) at 35 (PSU)

Thermometer (Model 9540: Guildline Instruments Ltd.)

Measurement Range : -40 to +180 deg C
Resolution : 0.001
Limits of error \pm deg C : 0.01 (24 hours @ 23 deg C \pm 1 deg C)
Repeatability : \pm 2 least significant digits

The measurement system was almost the same as Aoyama *et al.* (2002). The salinometer was operated in the air-conditioned ship's laboratory at a bath temperature of 24 deg C. The ambient temperature varied from approximately 22.5 deg C to 24 deg C, while the bath temperature was very stable and varied within \pm 0.001 deg C on rare occasion.

The measurement for each sample was carried out with the double conductivity ratio and defined as the median of 31 readings of the salinometer. Data collection was started 5 seconds after filling the cell with the sample and it took about 10 seconds to collect 31 readings by the personal computer. Data were taken for the sixth and seventh filling of the cell after rinsing five times. In the case of the difference between the double conductivity ratio of these two fillings being smaller than 0.00002, the average value of the double conductivity ratio was used to calculate the bottle salinity with the algorithm for practical salinity scale, 1978 (UNESCO, 1981). If the difference was greater than or equal to 0.00003, an eighth filling of the cell was done. In the case of the difference between the double conductivity ratio of these two fillings being smaller than 0.00002, the average value of the double conductivity ratio was used to calculate the bottle salinity. In the case of the double conductivity ratio of eighth filling did not satisfy the criteria above, we measured a ninth filling of the cell and calculated the bottle salinity. The measurement was conducted in about 6 hours per day and the cell was cleaned with soap after the measurement of the day.

(3) Preliminary Result

a. Standard Seawater

Standardization control of the salinometer was set to 503 and all measurements were carried out at this setting. The value of STANDBY was 24+5427 \pm 0001 and that of ZERO was 0.0-0000 \pm 0001. The conductivity ratio of IAPSO Standard Seawater batch P154 was 0.99990 (the double conductivity ratio was 1.99980) and was used as the standard for salinity. We measured 30 bottles of P154.

The specifications of SSW used in this cruise are shown as follows ;

Batch : P154
conductivity ratio : 0.99990
salinity : 34.996
Use by : 20th Oct 2014

Fig.2.3.2-1 shows the history of the double conductivity ratio for the Standard Seawater batch P154 before correction. The average of the double conductivity ratio was 1.99981 and the standard deviation was 0.00001, which is equivalent to 0.0002 in salinity.

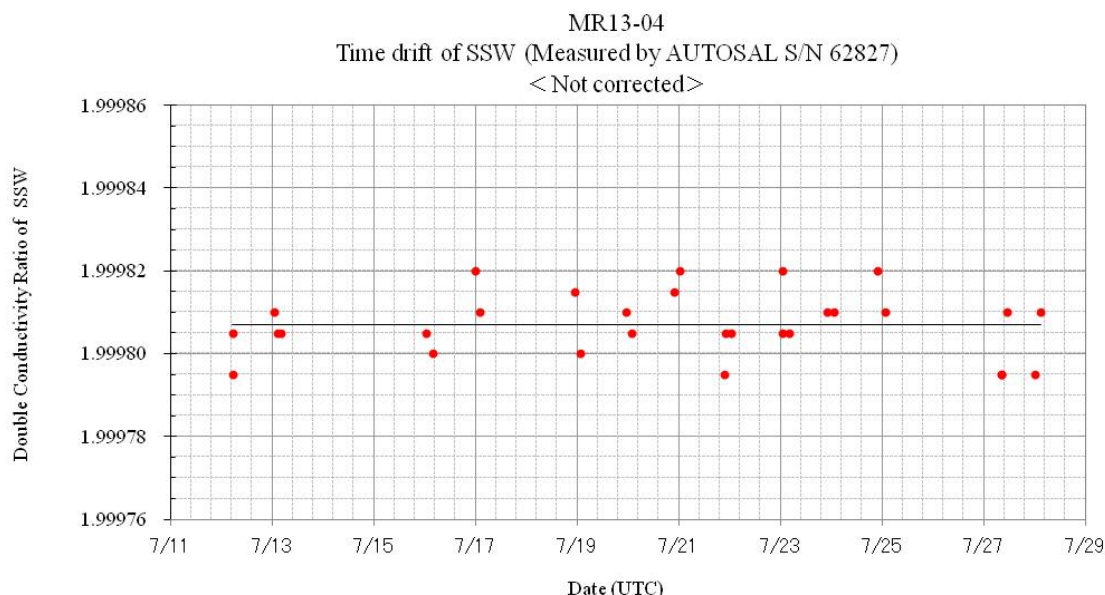


Fig. 2.3.2-1 The history of the double conductivity ratio for the Standard Seawater batch P154 (Before correction)

Fig.2.3.2-2 shows the history of the double conductivity ratio for the Standard Seawater batch P154 after correction. The average of the double conductivity ratio after correction was 1.99980 and the standard deviation was 0.00001, which is equivalent to 0.0001 in salinity.

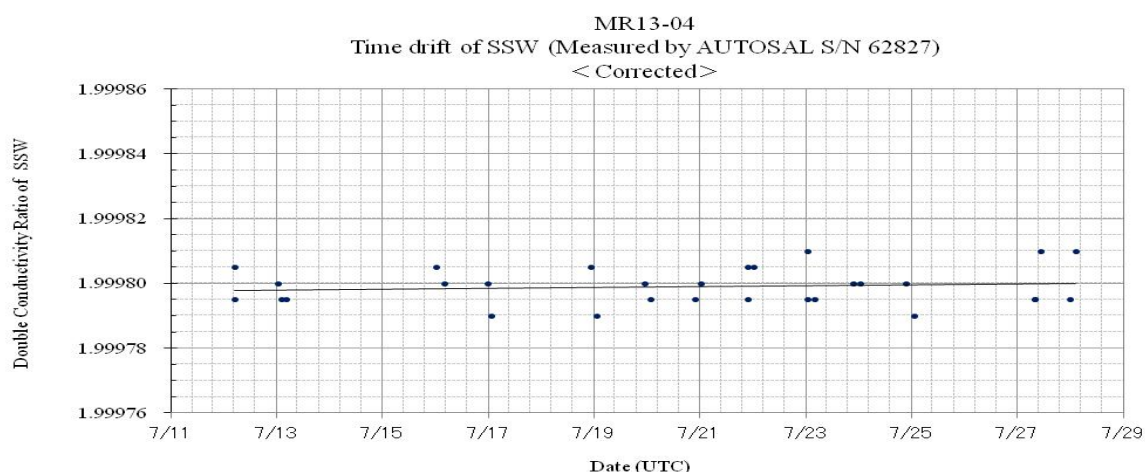


Fig. 2.3.2-2 The history of the double conductivity ratio for the Standard Seawater batch P154 (After correction)

b. Sub-Standard Seawater

Sub-standard seawater was made from sea water filtered by a pore size of

0.45 micrometer and stored in a 20-liter container made of polyethylene and stirred for at least 24 hours before start measuring. It was measured about every 6 samples in order to check for the possible sudden drifts of the salinometer.

c. Replicate Samples

We estimated the precision of this method using 39 pairs of replicate samples taken from the same Niskin bottle. Fig.2.3.2-3 shows the histogram of the absolute difference between each pair of the replicate samples. The average and the standard deviation of absolute difference among 39 pairs of replicate samples were 0.0002 and 0.0002 in salinity, respectively.

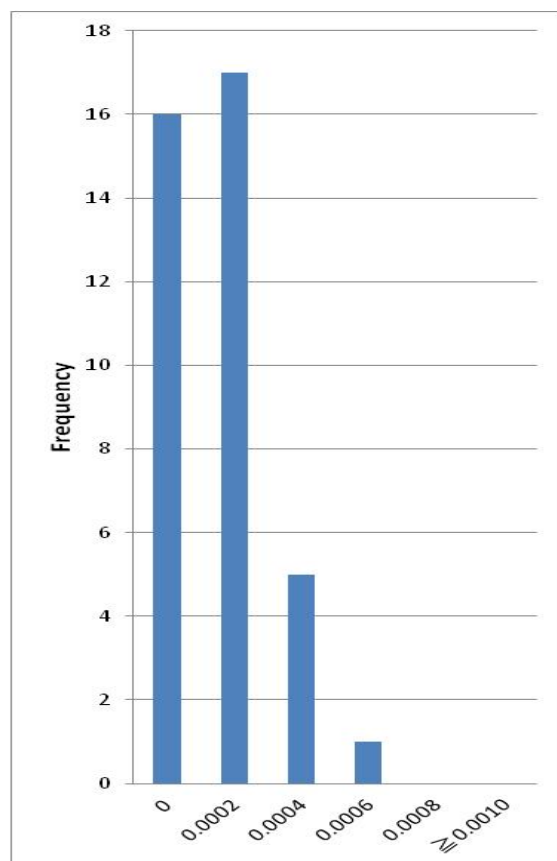


Fig. 2.3.2-3 The histogram of the double conductivity ratio for the absolute difference of replicate samples

(4) Data archive

These raw datasets will be submitted to JAMSTEC Data Management Office (DMO).

(5) Reference

- Aoyama, M. , T. Joyce, T. Kawano and Y. Takatsuki: Standard seawater comparison up to P129. Deep-Sea Research, I, Vol. 49, 1103~1114, 2002
- UNESCO : Tenth report of the Joint Panel on Oceanographic Tables and Standards. UNESCO Tech. Papers in Mar. Sci., 36, 25 pp., 1981

2.3.3 Shipboard ADCP

Makio HONDA (JAMSTEC: Principal Investigator)
Wataru TOKUNAGA (Global Ocean Development Inc., GODI)
Miki MORIOKA (GODI)
Ryo OYAMA (MIRAI crew)

(1) Objectives

To obtain continuous measurement of the current profile along the ship's track.

(2) Methods

Upper ocean current measurements were made in MR13-04 cruise, using the hull-mounted Acoustic Doppler Current Profiler (ADCP) system. For most of its operation the instrument was configured for water-tracking mode. Bottom-tracking mode, interleaved bottom-ping with water-ping, was made to get the calibration data for evaluating transducer misalignment angle in the shallow water. The system consists of following components;

1. R/V MIRAI has installed the Ocean Surveyor for vessel-mount ADCP (frequency 76.8 kHz; Teledyne RD Instruments, USA). It has a phased-array transducer with single ceramic assembly and creates 4 acoustic beams electronically. We mounted the transducer head rotated to a ship-relative angle of 45 degrees azimuth from the keel
2. For heading source, we use ship's gyro compass (Tokimec, Japan), continuously providing heading to the ADCP system directory. Additionally, we have Inertial Navigation System which provide high-precision heading, attitude information, pitch and roll, are stored in ".N2R" data files with a time stamp.
3. DGPS system (Trimble SPS751 & Fugro Multifix ver.6) providing precise ship's position.
4. We used VmDas software version 1.46.5 (TRDI) for data acquisition.
5. To synchronize time stamp of ping with GPS time, the clock of the logging computer is adjusted to GPS time every 1 minute.
6. Fresh water is charged in the sea chest to prevent biofouling at transducer face.
7. The sound speed at the transducer does affect the vertical bin mapping and vertical velocity measurement, is calculated from temperature, salinity (constant value; 35.0 PSU) and depth (6.5 m; transducer depth) by equation in Medwin (1975).

Data was configured for "8 m" intervals starting about 23 m below sea surface. Data was recorded every ping as raw ensemble data (.ENR). Also, 60 seconds and 300 seconds averaged data were recorded as short-term average (.STA) and long-term average (.LTA) data, respectively. Major parameters for the measurement, Direct Command, are shown in Table 2.3.3-1.

Table 2.3.3-1 Major parameters

<i>Bottom-Track Commands</i>	
BP = 001	Pings per Ensemble (almost less than 1,200m depth)
<i>Environmental Sensor Commands</i>	
EA = 04500	Heading Alignment (1/100 deg)
EB = +00000	Heading Bias (1/100 deg)
ED = 00065	Transducer Depth (0 - 65535 dm)
EF = +001	Pitch/Roll Divisor/Multiplier (pos/neg) [1/99 - 99]
EH = 00000	Heading (1/100 deg)
ES = 35	Salinity (0-40 pp thousand)
EX = 00000	Coord Transform (Xform:Type; Tilts; 3Bm; Map)
EZ = 10200010	Sensor Source (C; D; H; P; R; S; T; U)
C (1): Sound velocity calculates using ED, ES, ET (temp.)	
D (0): Manual ED	
H (2): External synchro	
P (0), R (0): Manual EP, ER (0 degree)	
S (0): Manual ES	
T (1): Internal transducer sensor	
U (0): Manual EU	
<i>Timing Commands</i>	
TE = 00:00:02.00	Time per Ensemble (hrs:min:sec.sec/100)
TP = 00:02.00	Time per Ping (min:sec.sec/100)
<i>Water-Track Commands</i>	
WA = 255	False Target Threshold (Max) (0-255 count)
WB = 1	Mode 1 Bandwidth Control (0=Wid, 1=Med, 2=Nar)
WC = 120	Low Correlation Threshold (0-255)
WD = 111 100 000	Data Out (V; C; A; PG; St; Vsum; Vsum^2; #G; P0)
WE = 1000	Error Velocity Threshold (0-5000 mm/s)
WF = 0800	Blank After Transmit (cm)
WG = 001	Percent Good Minimum (0-100%)
WI = 0	Clip Data Past Bottom (0 = OFF, 1 = ON)
WJ = 1	Rcvr Gain Select (0 = Low, 1 = High)
WM = 1	Profiling Mode (1-8)
WN = 100	Number of depth cells (1-128)
WP = 00001	Pings per Ensemble (0-16384)
WS = 800	Depth Cell Size (cm)
WT = 000	Transmit Length (cm) [0 = Bin Length]
WV = 0390	Mode 1 Ambiguity Velocity (cm/s radial)

(3) Preliminary results

Figure 2.3.3-1 shows the surface (about 100 ~ 200 m, 30-min averaged) current vector along the ship's track.

(4) Data archives

These data obtained in this cruise will be submitted to The Data Management Group (DMG) of JAMSTEC, and will be opened to the public via JAMSTEC home page.

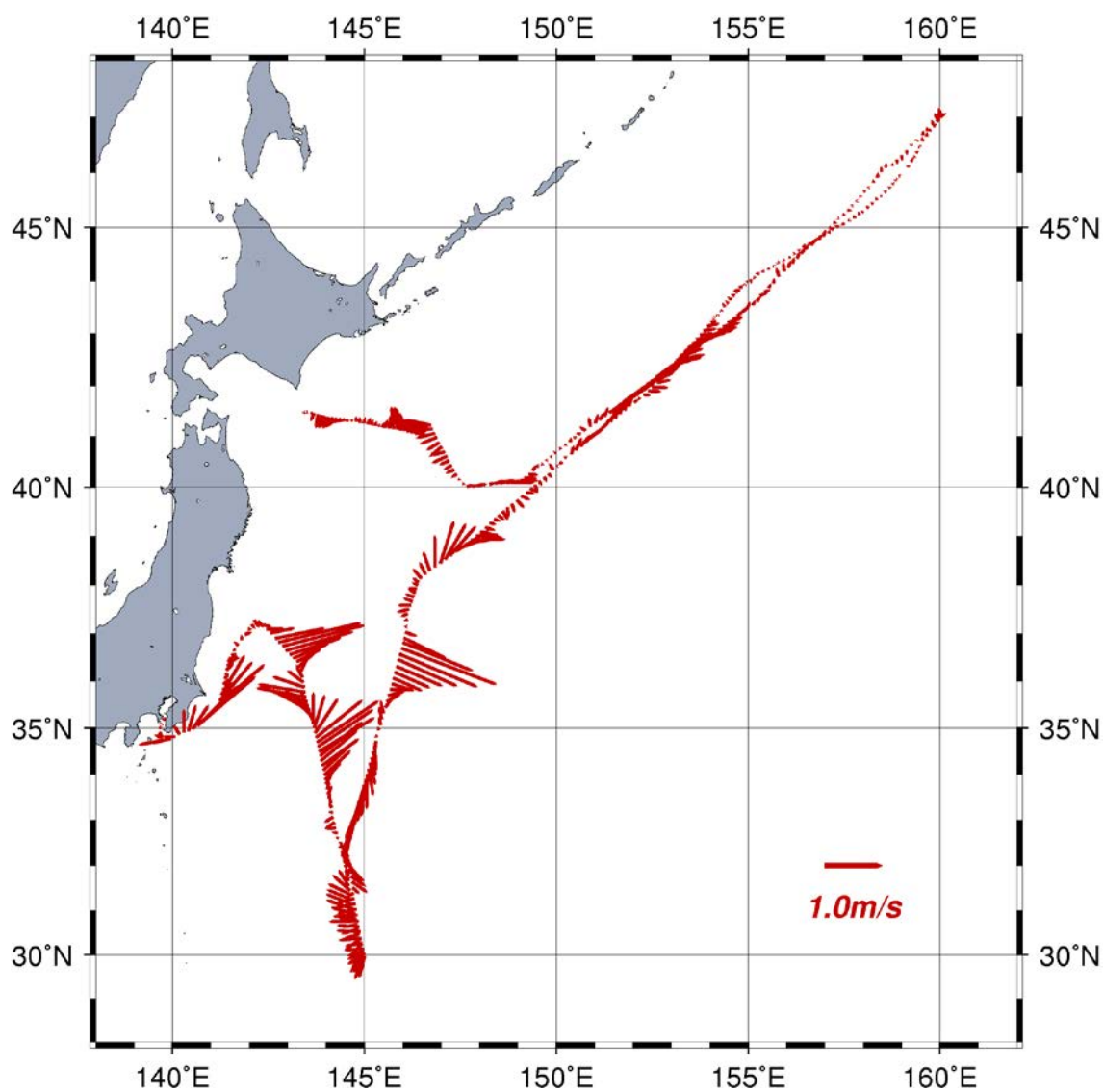


Figure 2.3.3-1 The surface current vector along the ship's track.

2.4 Sea surface water monitoring

Masahide WAKITA (JAMSTEC): Principal Investigator

Shinichiro YOKOGAWA (Marine Works Japan Co. Ltd): Operation Leader

Katsunori SAGISHIMA (Marine Works Japan Co. Ltd)

(1) Objective

Our purpose is to obtain temperature, salinity, dissolved oxygen, and fluorescence data continuously in near-sea surface water.

(2) Parameters

Temperature (surface water)

Salinity (surface water)

Dissolved oxygen (surface water)

Fluorescence (surface water)

(3) Instruments and Methods

The Continuous Sea Surface Water Monitoring System (Marine Works Japan Co. Ltd.) has five sensors and automatically measures temperature, conductivity, dissolved oxygen and fluorescence in near-sea surface water every one minute. This system is located in the “*sea surface monitoring laboratory*” and connected to shipboard LAN-system. Measured data, time, and location of the ship were stored in a data management PC. The near-surface water was continuously pumped up to the laboratory from about 4.5 m water depth and flowed into the system through a vinyl-chloride pipe. The flow rate of the surface seawater was adjusted to be $7\text{--}8\text{ dm}^3\text{ min}^{-1}$.

a. Instruments

Software

Seamoni-kun Ver.1.50

Sensors

Specifications of the each sensor in this system are listed below.

1) Temperature and Conductivity sensor

Model:	SBE-45, SEA-BIRD ELECTRONICS, INC.
Serial number:	4557820-0319
Measurement range:	Temperature -5 to $+35\text{ }^{\circ}\text{C}$ Conductivity 0 to 7 S m^{-1}
Initial accuracy:	Temperature $0.002\text{ }^{\circ}\text{C}$ Conductivity 0.0003 S m^{-1}
Typical stability (per month):	Temperature $0.0002\text{ }^{\circ}\text{C}$ Conductivity 0.0003 S m^{-1}
Resolution:	Temperatures $0.0001\text{ }^{\circ}\text{C}$

Conductivity 0.00001 S m⁻¹

2) Bottom of ship thermometer

Model: SBE 38, SEA-BIRD ELECTRONICS, INC.
Serial number: 3852788-0457
Measurement range: -5 to +35 °C
Initial accuracy: ±0.001 °C
Typical stability (per 6 month): 0.001 °C
Resolution: 0.00025 °C

3) Dissolved oxygen sensor

Model: OPTODE 3835, AANDERAA Instruments.
Serial number: 1519
Measuring range: 0 - 500 µmol dm⁻³
Resolution: <1 µmol dm⁻³
Accuracy: <8 µmol dm⁻³ or 5% whichever is greater
Settling time: <25 s

4) Dissolved oxygen sensor

Model: RINKO II, ARO-CAR/CAD
Serial number: 13
Measuring range: 0 - 540 µmol kg⁻¹
Resolution: 0.1 µmol kg⁻¹ or 0.1 % whichever is greater
Accuracy: 1 µmol kg⁻¹ or 0.1 % whichever is greater

5) Fluorometer

Model: C3, TURNER DESIGNS
Serial number: 2300384

b. Measurements

Periods of measurement during MR13-04 are listed in Table 2.4-1.

Table 2.4-1 Events list of the Sea surface water monitoring during MR13-04

System Date [UTC]	System Time [UTC]	Events	Remarks
2013/07/10	06:10	All the measurements were started and data was available.	Start
2013/07/28	00:00	All the measurements were stopped.	End

(4) Preliminary Result

We took the surface water samples to compare sensor data with bottle data of salinity, dissolved oxygen and fluorescence. The results are shown in Figs. 2.4-1 - 3. All the salinity samples were analyzed by the Guideline 8400B “AUTOSAL” (see 2.3.2), and dissolve oxygen samples were analyzed by Winkler method (see 2.5), and fluorescence were analyzed by Welschmeyer method (see 3.3.1).

(5) Data archive

These data obtained in this cruise will be submitted to the Data Management Office (DMO) of JAMSTEC, and will be opened to the public via “R/V Mirai Data Web Page” in JAMSTEC home page.

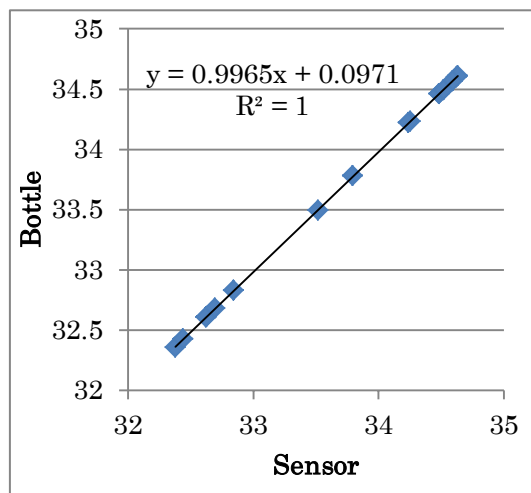


Fig. 2.4-1. Correlation of salinity between sensor and bottle data

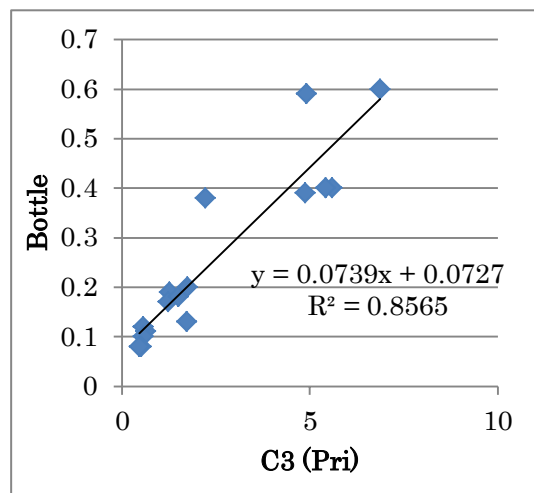


Fig. 2.4-2. Correlation of fluorescence between sensor and bottle chlorophyll data

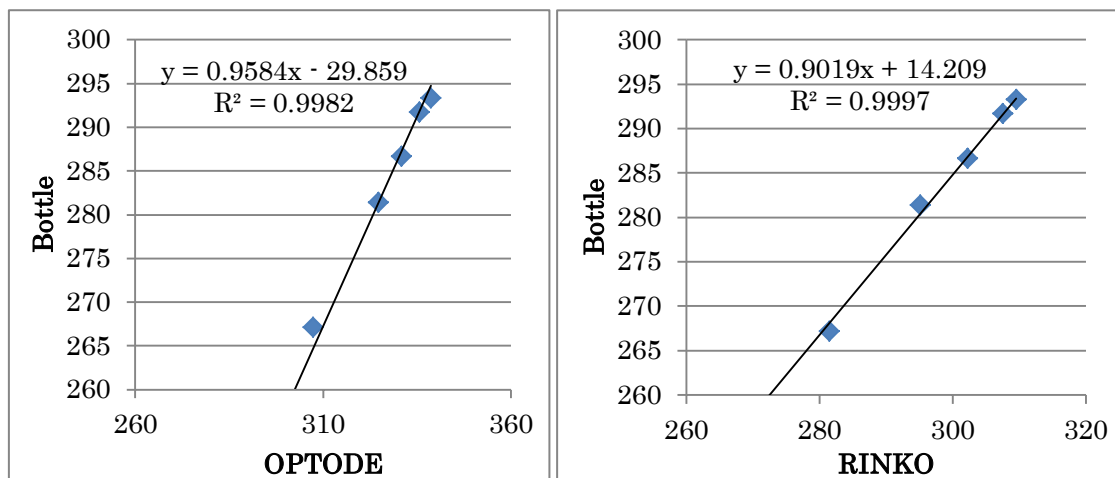


Fig. 2.4-3. Correlation of dissolved oxygen between sensor and bottle data

2.5 Dissolved oxygen

Masahide WAKITA (JAMSTEC): Principal Investigator

Shinichiro YOKOGAWA (Marine Works Japan Co. Ltd): Operation Leader

Katsunori SAGISHIMA (Marine Works Japan Co. Ltd)

(1) Objectives

Determination of dissolved oxygen in seawater by Winkler titration.

(2) Parameter

Dissolved Oxygen

(3) Instruments and Methods

Following procedure is based on an analytical method, entitled by “Determination of dissolved oxygen in sea water by Winkler titration”, in the WHP Operations and Methods (Dickson, 1996).

a. Instruments

Burette for sodium thiosulfate and potassium iodate;

APB-510 manufactured by Kyoto Electronic Co. Ltd. / 10 cm³ of titration vessel

APB-620 manufactured by Kyoto Electronic Co. Ltd. / 10 cm³ of titration vessel

Detector;

Automatic photometric titrator (DOT-01X) manufactured by Kimoto Electronic Co. Ltd.

Software;

DOT_Terminal Ver.1.2.0

b. Reagents

Pickling Reagent I: Manganese chloride solution (3 mol dm⁻³)

Pickling Reagent II: Sodium hydroxide (8 mol dm⁻³) / sodium iodide solution (4 mol dm⁻³)

Sulfuric acid solution (5 mol dm⁻³)

Sodium thiosulfate (0.025 mol dm⁻³)

Potassium iodide (0.001667 mol dm⁻³)

CSK standard of potassium iodide:

Lot DCE2131, Wako Pure Chemical Industries Ltd., 0.0100N

c. Sampling

Seawater samples were collected with Niskin bottle attached to the CTD-system and surface bucket sampler. Seawater for oxygen measurement was transferred from sampler to a volume calibrated flask (ca. 100 cm³). Three times volume of the flask of seawater was overflowed. Temperature was measured by digital thermometer during the overflowing. Then two reagent solutions (Reagent I and II) of 0.5 cm³ each were added immediately into the sample flask and the stopper was inserted carefully into the flask. The sample flask was then shaken vigorously to mix the contents and to disperse the precipitate finely throughout. After the

precipitate has settled at least halfway down the flask, the flask was shaken again vigorously to disperse the precipitate. The sample flasks containing pickled samples were stored in a laboratory until they were titrated.

d. Sample measurement

At least two hours after the re-shaking, the pickled samples were measured on board. 1 cm³ sulfuric acid solution and a magnetic stirrer bar were added into the sample flask and stirring began. Samples were titrated by sodium thiosulfate solution whose morality was determined by potassium iodate solution. Temperature of sodium thiosulfate during titration was recorded by a digital thermometer. During this cruise, we measured dissolved oxygen concentration using 2 sets of the titration apparatus. Dissolved oxygen concentration (μmol kg⁻¹) was calculated by sample temperature during seawater sampling, salinity, flask volume, and titrated volume of sodium thiosulfate solution without the blank. When we measured low concentration samples, titration procedure was adjusted manually.

e. Standardization and determination of the blank

Concentration of sodium thiosulfate titrant was determined by potassium iodate solution. Pure potassium iodate was dried in an oven at 130 °C. 1.7835 g potassium iodate weighed out accurately was dissolved in deionized water and diluted to final volume of 5 dm³ in a calibrated volumetric flask (0.001667 mol dm⁻³). 10 cm³ of the standard potassium iodate solution was added to a flask using a volume-calibrated dispenser. Then 90 cm³ of deionized water, 1 cm³ of sulfuric acid solution, and 0.5 cm³ of pickling reagent solution II and I were added into the flask in order. Amount of titrated volume of sodium thiosulfate (usually 5 times measurements average) gave the morality of sodium thiosulfate titrant.

The oxygen in the pickling reagents I (0.5 cm³) and II (0.5 cm³) was assumed to be 3.8 x 10⁻⁸ mol (Murray *et al.*, 1968). The blank due to other than oxygen was determined as follows. 1 and 2 cm³ of the standard potassium iodate solution were added to two flasks respectively using a calibrated dispenser. Then 100 cm³ of deionized water, 1 cm³ of sulfuric acid solution, and 0.5 cm³ of pickling reagent solution II and I each were added into the flask in order. The blank was determined by difference between the first (1 cm³ of KIO₃) titrated volume of the sodium thiosulfate and the second (2 cm³ of KIO₃) one. The results of 3 times blank determinations were averaged.

Table 2.3-1 shows results of the standardization and the blank determination during this cruise.

Date	KIO ₃ ID	Na ₂ S ₂ O ₃	DOT-01(No.1)		DOT-01(No.2)		Stations
			E.P.	Blank	E.P.	Blank	
2013/7/11	20130509-01-01	20130514-01	3.951	-0.003	3.951	-0.002	F01
2013/7/13	CSK EPJ3885	20130514-01	3.946	-	3.951	-	-
2013/7/13	20130509-01-02	20130514-01	3.948	-0.002	3.953	-0.002	S01, KEO, JKEO
2013/7/20	20130509-01-03	20130514-01	3.950	-0.003	3.953	-0.001	42N, KNOT, K02
2013/7/26	20130509-01-04	20130514-01	3.952	0.000	3.952	-0.001	E01, E03

f. Repeatability of sample measurement

Replicate samples were taken at every CTD casts. Total amount of the replicate sample pairs of good measurement was 42. The standard deviation of the replicate measurement was $0.11 \mu\text{mol kg}^{-1}$ that was calculated by a procedure in Guide to best practices for ocean CO_2 measurements Chapter4 SOP23 Ver.3.0 (2007). .

(4) Data archive

All data will be submitted to Chief Scientist.

(5) References

- Dickson, A.G., Determination of dissolved oxygen in sea water by Winkler titration. (1996)
Dickson, A.G., Sabine, C.L. and Christian, J.R. (Eds.), Guide to best practices for ocean CO_2 measurements. (2007)
Culberson, C.H., WHP Operations and Methods July-1991 “Dissolved Oxygen”, (1991)
Japan Meteorological Agency, Oceanographic research guidelines (Part 1). (1999)
KIMOTO electric CO. LTD., Automatic photometric titrator DOT-01X Instruction manual

2.6. Nutrients

Masahide WAKITA (JAMSTEC MIO) Principal investigator

Michio AOYAMA (Meteorological Research Institute)

Yasuhiro ARII (Department of Marine Science, Marine Works Japan Ltd.)

Elena HAYASHI (Department of Marine Science, Marine Works Japan Ltd.)

(1) Objectives

The objectives of nutrients analyses during the R/V MIRAI MR13-04 cruise in the Western North Pacific Ocean are as follows:

- Describe the present status of nutrients concentration with excellent comparability.
- Provide excellent nutrients data to biologist onboard MR13-04 to help their study.

(2) Parameters

The determinants are nitrate, nitrite, phosphate, silicate and ammonia in the western North Pacific Ocean.

(3) Summary of nutrients analysis

We made 11 runs for the samples at 7 stations (12 casts) in MR13-04. The total amount of layers of the seawater sample reached up to 306 for MR13-04. We made duplicate measurement at all layers. The station locations for nutrients measurement is shown in Figure 2.6.1

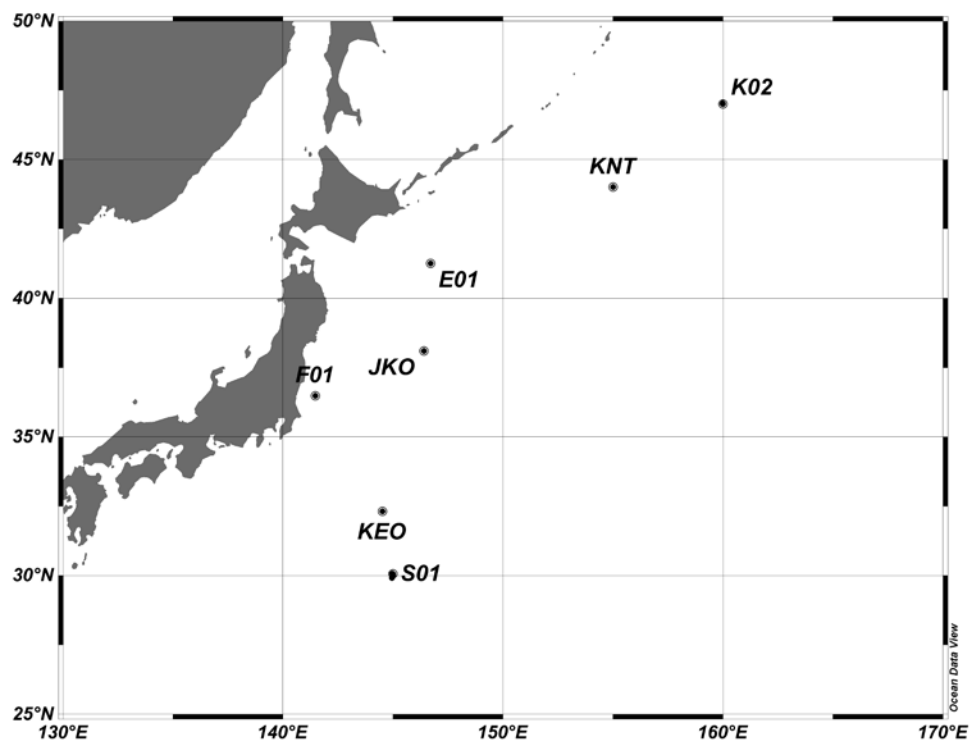


Figure 2.6.1 Sampling positions of nutrients sample.

(4) Instrument and methods

a). Analytical detail using QuAAtro system

Nitrate + nitrite and nitrite were analyzed according to the modification method of Grasshoff (1970). The sample nitrate was reduced to nitrite in a cadmium tube inside of which was coated with metallic copper. The sample stream with its equivalent nitrite was treated with an acidic, sulfanilamide reagent and the nitrite forms nitrous acid which reacted with the sulfanilamide to produce a diazonium ion. N-1-Naphthylethylene-diamine added to the sample stream then coupled with the diazonium ion to produce a red, azo dye. With reduction of the nitrate to nitrite, both nitrate and nitrite reacted and were measured; without reduction, only nitrite reacted. Thus, for the nitrite analysis, no reduction was performed and the alkaline buffer was not necessary. Nitrate was computed by difference.

The silicate method was analogous to that described for phosphate. The method used was essentially that of Grasshoff et al. (1983), wherein silicomolybdic acid was first formed from the silicate in the sample and added molybdic acid; then the silicomolybdic acid was reduced to silicomolybdous acid, or "molybdenum blue" using ascorbic acid as the reductant.

The phosphate analysis was a modification of the procedure of Murphy and Riley (1962). Molybdic acid was added to the seawater sample to form phosphomolybdic acid which was in turn reduced to phosphomolybdous acid using L-ascorbic acid as the reductant.

The analytical methods of the nutrients, nitrate, nitrite, and silicate during this cruise were same as the methods used in (Kawano et al. 2009) while the method of phosphate was modified as described later. The details of modification of analytical methods used in this cruise are also compatible with the methods described in nutrients section in GO-SHIP repeat hydrography manual (Hydes et al., 2010).

The ammonia in seawater was mixed with an alkaline containing EDTA, ammonia as gas state was formed from seawater. The ammonia (gas) was absorbed in sulfuric acid by way of 0.5 µm pore size membrane filter (ADVANTEC PTFE) at the dialyzer attached to analytical system. The ammonia absorbed in sulfuric acid was determined by coupling with phenol and hypochlorite to form indophenols blue. Wavelength using ammonia analysis was 630 nm, which was absorbance of indophenols blue.

The flow diagrams and reagents for each parameter are shown in Figures 2.6.2 to 2.6.6.

b). Nitrate + Nitrite Reagents

Imidazole (buffer), 0.06 M (0.4 % w/v)

Dissolved 4 g imidazole, $C_3H_4N_2$, in ca. 1000 ml DIW; added 2 ml concentrated HCl. After mixing, 1 ml Triton®X-100 (50 % solution in ethanol) was added.

Sulfanilamide, 0.06 M (1 % w/v) in 1.2M HCl

Dissolved 10 g sulfanilamide, $4-NH_2C_6H_4SO_3H$, in 900 ml of DIW, added 100 ml concentrated HCl. After mixing, 2 ml Triton®X-100 (50 % solution in ethanol) was added.

N-1-Naphthylethylene-diamine dihydrochloride, 0.004 M (0.1 %f w/v)

Dissolved 1 g NED, $C_{10}H_7NHCH_2CH_2NH_2 \cdot 2HCl$, in 1000 ml of DIW and added 10 ml concentrated HCl. After mixing, 1 ml Triton®X-100 (50 % solution in ethanol) was added. This reagent was stored in a dark bottle.

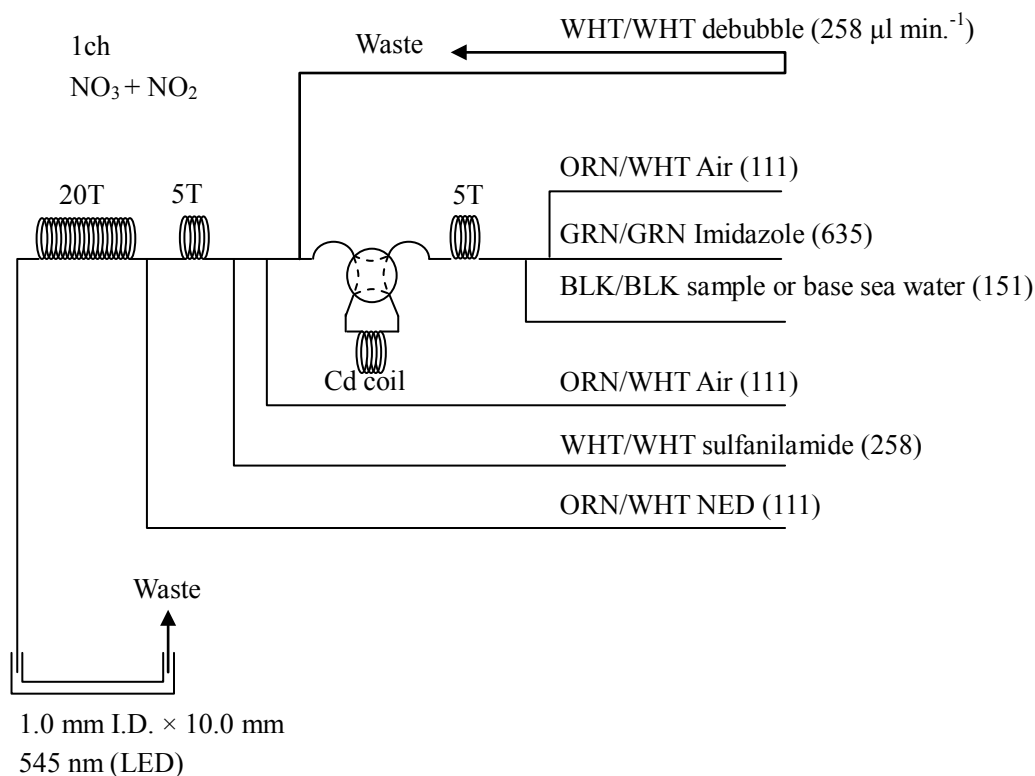


Figure 2.6.2 NO₃ (1ch.) Flow diagram.

c). Nitrite Reagents

Sulfanilamide, 0.06 M (1 % w/v) in 1.2 M HCl

Dissolved 10g sulfanilamide, 4-NH₂C₆H₄SO₃H, in 900 ml of DIW, added 100 ml concentrated HCl. After mixing, 2 ml Triton®X-100 (50 % solution in ethanol) was added.

N-1-Naphthylethylene-diamine dihydrochloride, 0.004 M (0.1 % w/v)

Dissolved 1 g NED, C₁₀H₇NHCH₂CH₂NH₂•2HCl, in 1000 ml of DIW and added 10 ml concentrated HCl. After mixing, 1 ml Triton®X-100 (50 % solution in ethanol) was added. This reagent was stored in a dark bottle.

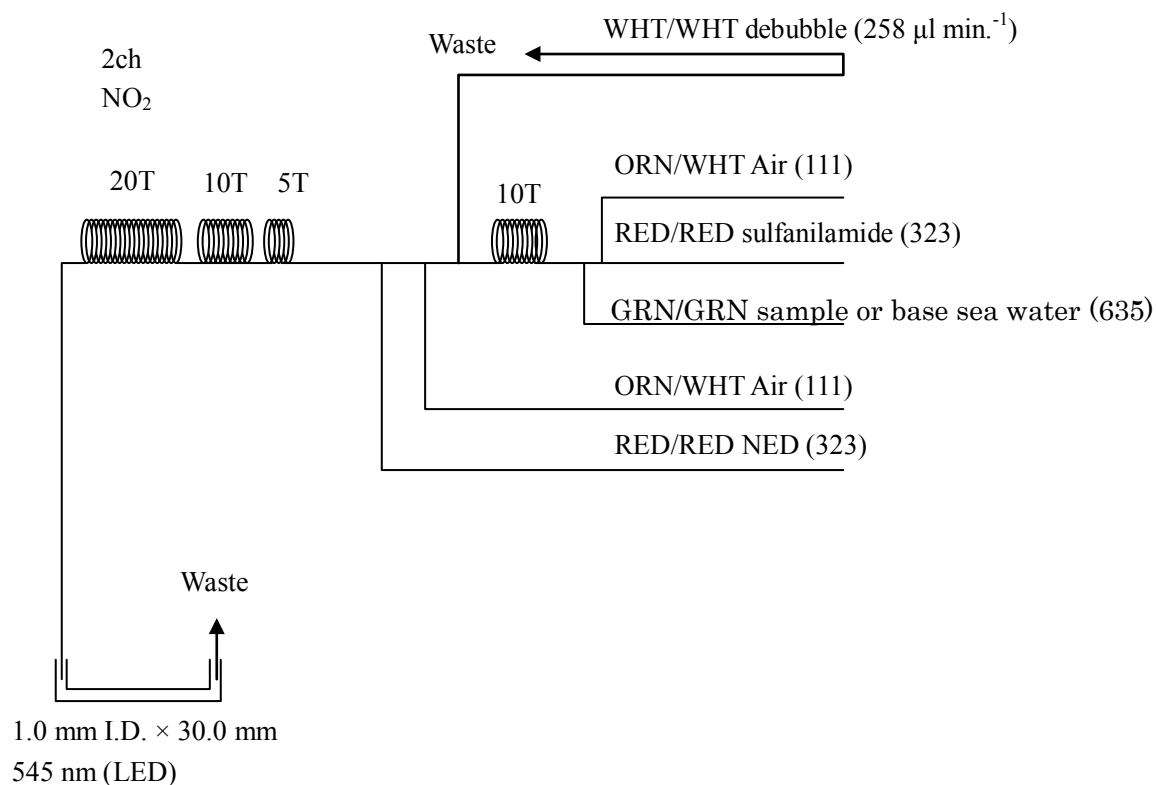


Figure 2.6.3 NO₂ (2ch.) Flow diagram.

d). Silicate Reagents

Molybdic acid, 0.06 M (2 % w/v)

Dissolved 15 g disodium molybdate (VI) dihydrate, $\text{Na}_2\text{MoO}_4 \cdot 2\text{H}_2\text{O}$, in 980 ml DIW, added 8 ml concentrated H_2SO_4 . After mixing, 20 ml sodium dodecyl sulphate (15 % solution in water) was added.

Oxalic acid, 0.6 M (5 % w/v)

Dissolved 50 g oxalic acid anhydrous, HOOC:COOH , in 950 ml of DIW.

Ascorbic acid, 0.01M (3 % w/v)

Dissolved 2.6g L (+)-ascorbic acid, $\text{C}_6\text{H}_8\text{O}_6$, in 100 ml of DIW. This reagent was freshly prepared before every measurement.

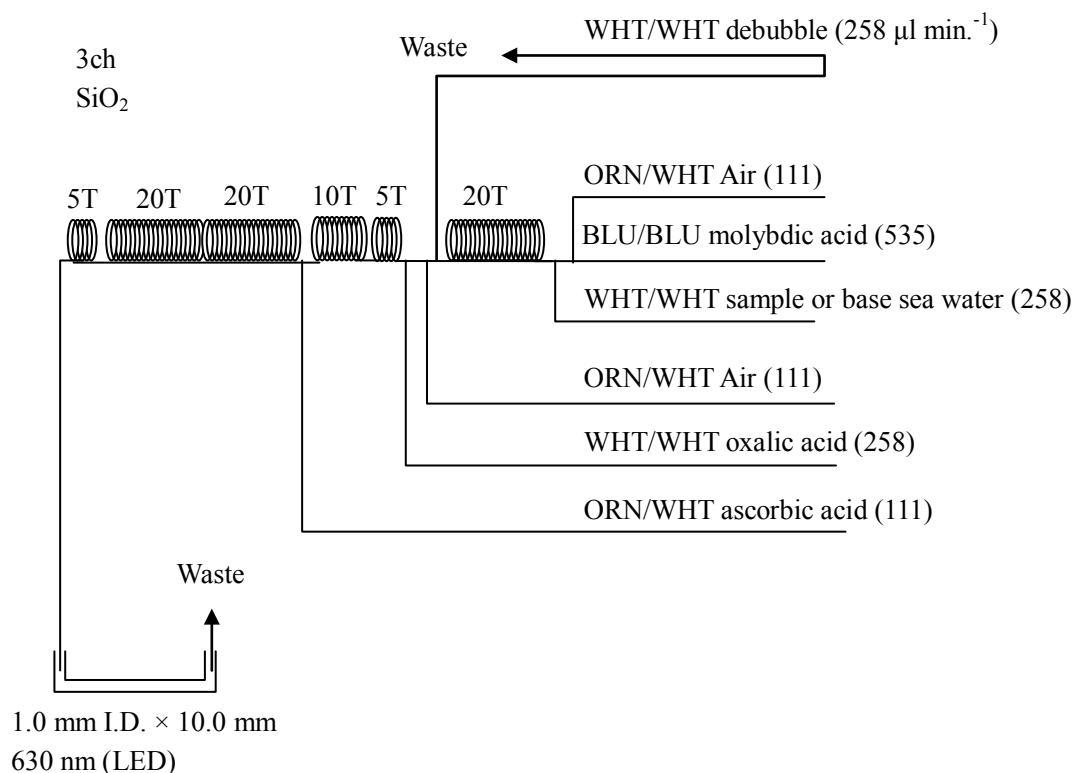


Figure 2.6.4 SiO_2 (3ch.) Flow diagram.

e). Phosphate Reagents

Stock molybdate solution, 0.03M (0.8 % w/v)

Dissolved 8 g disodium molybdate (VI) dihydrate, $\text{Na}_2\text{MoO}_4 \cdot 2\text{H}_2\text{O}$, and 0.17 g antimony potassium tartrate, $\text{C}_8\text{H}_4\text{K}_2\text{O}_{12}\text{Sb}_2 \cdot 3\text{H}_2\text{O}$, in 950 ml of DIW and added 50 ml concentrated H_2SO_4 .

PO_4 Color reagent

Dissolved 1.2 g L (+)-ascorbic acid, $\text{C}_6\text{H}_8\text{O}_6$, in 150 ml of stock molybdate solution. After mixing, 3 ml sodium dodecyl sulphate (15 % solution in water) was added. This reagent was freshly prepared before every measurement.

4ch.

PO_4

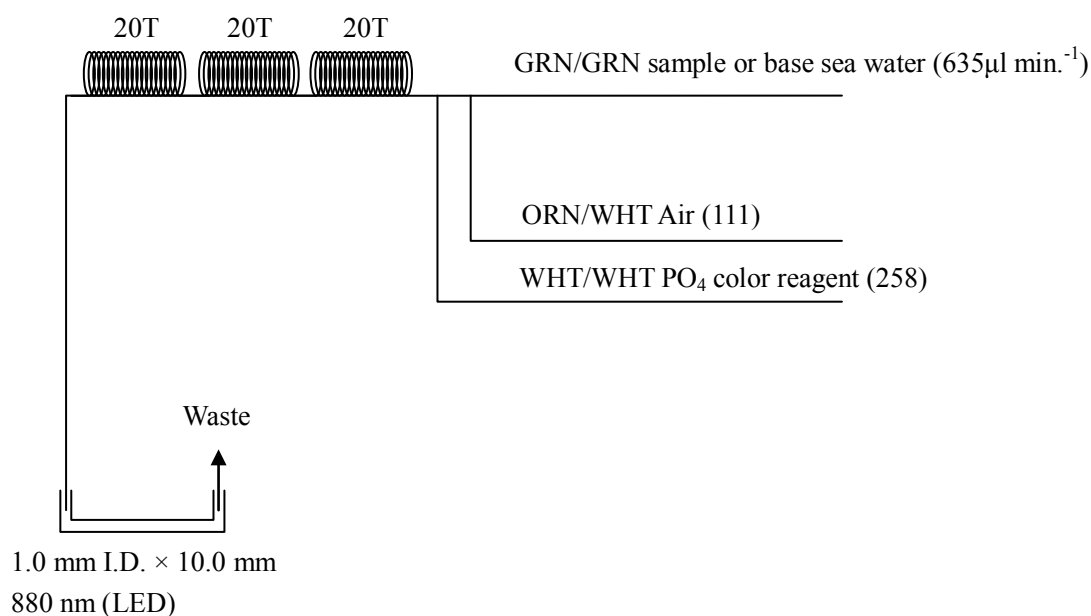


Figure 2.6.5 PO_4 (4ch.) Flow diagram.

We removed a dilution line, an air line, a debubble line and a 5 turns coil, then a flow of phosphate method became simple as shown in Fig. 2.6.5.

f). Ammonia Reagents

EDTA

Dissolved 41 g EDTA (ethylenediaminetetraacetic acid tetrasodium salt), $\text{C}_{10}\text{H}_{12}\text{N}_2\text{O}_8\text{Na}_4 \cdot 4\text{H}_2\text{O}$, and 2 g boric acid, H_3BO_3 , in 200 ml of DIW. After mixing, 1 ml Triton®X-100 (30 % solution in DIW) was added. This reagent was prepared at a week about.

NaOH

Dissolved 5 g sodium hydroxide, NaOH, and 16 g EDTA in 100 ml of DIW. This reagent was prepared at a week about.

Stock Nitroprusside

Dissolved 0.25 g sodium pentacyanonitrosylferrate (II), $\text{Na}_2[\text{Fe}(\text{CN})_5\text{NO}]$, in 100 ml of DIW and added 0.2 ml 1N H_2SO_4 . Stored in a dark bottle and prepared at a month about.

Nitroprusside solution

Mixed 4 ml stock nitroprusside and 5 ml 1N H_2SO_4 in 500 ml of DIW. After mixing, 1 ml Triton®X-100 (30 % solution in DIW) was added. This reagent was stored in a dark bottle and prepared at every 2 or 3 days.

Alkaline phenol

Dissolved 10 g phenol, $\text{C}_6\text{H}_5\text{OH}$, 5 g sodium hydroxide and citric acid, $\text{C}_6\text{H}_8\text{O}_7$, in 200 ml DIW. Stored in a dark bottle and prepared at a week about.

NaClO solution

Mixed 3 ml sodium hypochlorite solution, NaClO, in 47 ml DIW. Stored in a dark bottle and freshly prepared before every measurement. This reagent was prepared 0.3% available chlorine.

ORN/YEL NaOH (79)

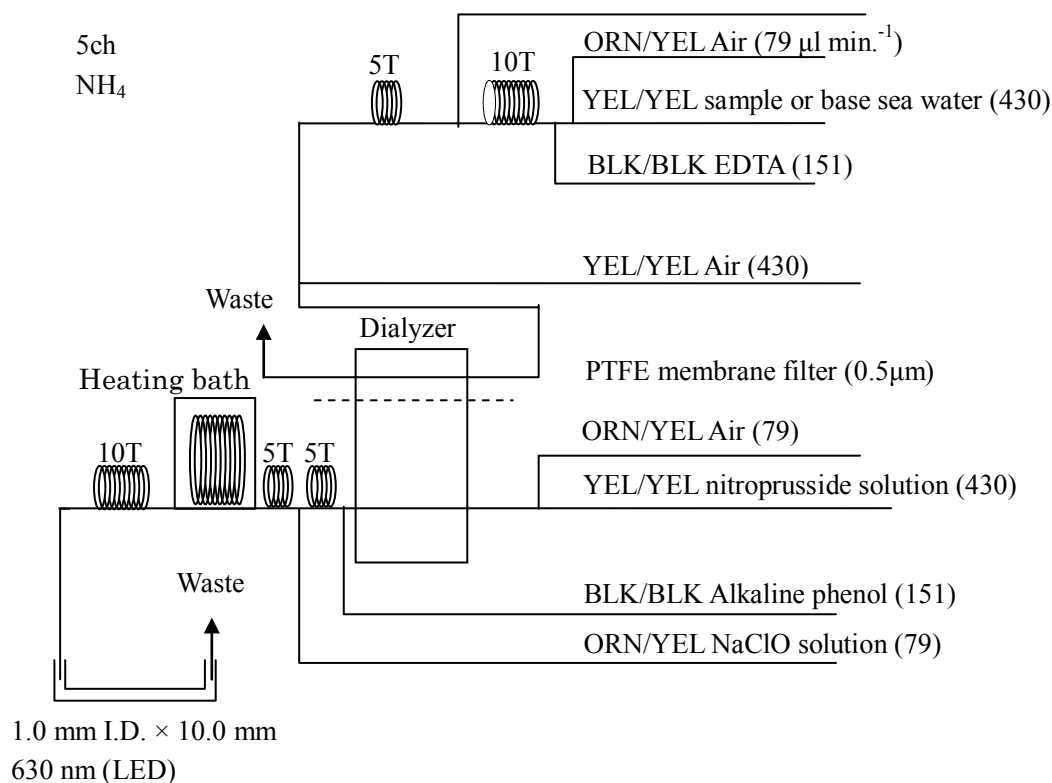


Figure 2.6.6 NH₄ (5ch.) Flow diagram.

We put a 10 turns coil just after a sample inlet line instead of a 5 turns coil and NaOH solution put the main line from the top instead from the bottom.

g). Sampling procedures

Sampling of nutrients followed that oxygen, salinity and trace gases. Samples were drawn into two of virgin 10 ml polyacrylates vials without sample drawing tubes. These were rinsed three times before filling and vials were capped immediately after the drawing. The vials were put into water bath adjusted to ambient temperature, 23 ± 1 deg. C, in about 30 minutes before use to stabilize the temperature of samples in MR13-04.

No transfer was made and the vials were set an auto sampler tray directly. Samples were analyzed after collection basically within 24 hours in MR13-04.

h). Data processing

Raw data from QuAAtro was treated as follows:

- Checked baseline shift.
- Checked the shape of each peak and positions of peak values taken, and then changed the positions of peak values taken if necessary.
- Carry-over correction and baseline drift correction were applied to peak heights of each samples followed by sensitivity correction.
- Baseline correction and sensitivity correction were done basically using liner regression.
- Loaded pressure and bottle salinity from Seafile data to calculate density of seawater.
- Calibration curves to get nutrients concentration were assumed second order equations.

(5) Nutrients standards

a). Volumetric laboratory ware of in-house standards

All volumetric glass ware and polymethylpentene (PMP) ware used were gravimetrically calibrated. Plastic volumetric flasks were gravimetrically calibrated at the temperature of use within 0 to 4 K.

Volumetric flasks

Volumetric flasks of Class quality (Class A) were used because their nominal tolerances are 0.05 % or less over the size ranges likely to be used in this work. Class A flasks were made of borosilicate glass, and the standard solutions were transferred to plastic bottles as quickly as possible after they were made up to volume and well mixed in order to prevent excessive dissolution of silicate from the glass. PMP volumetric flasks were gravimetrically calibrated and used only within 0 to 4 K of the calibration temperature.

The computation of volume contained by glass flasks at various temperatures other than the calibration temperatures were done by using the coefficient of linear expansion of borosilicate crown glass.

Because of their larger temperature coefficients of cubical expansion and lack of tables constructed for these materials, the plastic volumetric flasks were gravimetrically calibrated over the temperature range of intended use and used at the temperature of calibration within 0 to 4 K. The weights obtained in the calibration weightings were corrected for the density of water and air buoyancy.

Pipettes and pipettors

All pipettes had nominal calibration tolerances of 0.1 % or better. These were gravimetrically calibrated in order to verify and improve upon this nominal tolerance.

b). Reagents, general considerations

Specifications

For nitrate standard, “potassium nitrate 99.995 suprapur®” provided by Merck, CAS No.: 7757-91-1, was used.

For nitrite standard, “sodium nitrite” provided by Wako, CAS No.: 7632-00-0, was used. The assay of nitrite salts was determined according JIS K8019 (1992) were 98.73%. We used that value to adjust the weights taken.

For the silicate standard, we use “Silicon standard solution SiO₂ in NaOH 0.5 mol/l CertiPUR®” provided by Merck, CAS No.: 1310-73-2, of which lot number HC097572 was used. The silicate concentration was certified by NIST-SRM3150 with the uncertainty of 0.5 %. Factor of HC097572 was signed 1.000, however we reassigned the factor as 0.976 from the result of comparison among HC074650, HC097572 and RMNS in MR11-E02 cruise.

For phosphate standard, “potassium dihydrogen phosphate anhydrous 99.995 suprapur®” provided by Merck, CAS No.: 7778-77-0, was used.

For ammonia standard, “ammonia sulfate” provided by Wako, CAS No.: 7783-20-2, was used.

Ultra pure water

Ultra pure water (Milli-Q) freshly drawn was used for preparation of reagent, standard solutions and for measurement of reagent and system blanks.

Low-nutrients seawater (LNSW)

Surface water having low nutrient concentration was taken and filtered using 0.45 µm pore size membrane filter. This water was stored in 20 liter cubitainer with paper box. The concentrations of nutrient of this water were measured carefully in Aug 2012.

Treatment of silicate standard due to high alkalinity

Since the silicon standard solution Merck CertiPUR® is in NaOH 0.5 mol/l, we need to dilute and neutralize to avoid make precipitation of Mg (OH)₂ etc. When we make B standard, silicon standard solution is diluted by factor 12 with pure water and neutralized by HCl 1.0 mol/l to be about 7. After that B standard solution is used to prepare C standards.

c). Concentrations of nutrients for A, B and C standards

Concentrations of nutrients for A, B and C standards (working standards) were set as shown in Table 2.6.1. The working standard was prepared according recipes as shown in Table 2.6.2. All volumetric laboratory tools were calibrated prior the cruise as stated in chapter (5). Then the actual concentration of nutrients in each fresh standard was calculated based on the ambient, solution temperature and determined factors of volumetric laboratory wares.

The calibration curves for each run were obtained using 5 levels working standards, C-1, C-2, C-3, C-4 and C-5.

Table 2.6.1 Nominal concentrations of nutrients for A, B and C standards.

	A	B	C-1	C-2	C-3	C-4	C-5
NO ₃ (µM)	22000	900	0.03	9.2	18.3	36.6	55.0
NO ₂ (µM)	4000	20	0.00	0.2	0.4	0.8	1.2
SiO ₂ (µM)	36000	2800	0.80	28	56	111	167
PO ₄ (µM)	3000	60	0.04	0.6	1.2	2.4	3.6
NH ₄ (µM)	4000	200	0.00	0.0	2.0	4.0	6.0

Table 2.6.2 Working standard recipes.

C Std.	B-1 Std.	B-2 Std.	B-3 Std.	DIW
C-1	0 ml	0 ml	0 ml	75 ml
C-2	5 ml	5 ml	0 ml	65 ml
C-3	10 ml	10 ml	5 ml	40 ml
C-4	20 ml	20 ml	10 ml	25 ml
C-5	30 ml	30 ml	15 ml	0 ml

B-1 Std.: Mixture of nitrate, silicate and phosphate.

B-2 Std.: Nitrite.

B-3 Std.: Ammonia.

d). Renewal of in-house standard solutions

In-house standard solutions as stated in paragraph c) were renewed as shown in Table 2.6.3(a) to (c).

Table 2.6.3(a) Timing of renewal of in-house standards.

NO ₃ , NO ₂ , SiO ₂ , PO ₄ , NH ₄	Renewal
--	---------

A-1 Std. (NO ₃)	maximum 1 month
A-2 Std. (NO ₂)	maximum 1 month
A-3 Std. (SiO ₂)	commercial prepared solution
A-4 Std. (PO ₄)	maximum 1 month
A-5 Std. (NH ₄)	maximum 1 month
B-1 Std. (mixture of NO ₃ , SiO ₂ , PO ₄)	8 days
B-2 Std. (NO ₂)	8 days
B-3 Std. (NH ₄)	8 days

Table 2.6.3(b) Timing of renewal of working calibration standards.

Working standards	Renewal
C Std. (mixture of B-1 , B-2 and B-3 Std.)	24 hours

Table 2.6.3(c) Timing of renewal of in-house standards for reduction estimation.

Reduction estimation	Renewal
D-1 Std. (3600 µM NO ₃)	8 days
43 µM NO ₃	when C Std. renewed
47 µM NO ₂	when C Std. renewed

(6) Reference material of nutrients in seawater

To get the more accurate and high quality nutrients data to achieve the objectives stated above, huge numbers of the bottles of the reference material of nutrients in seawater (hereafter RMNS) are prepared (Aoyama et al., 2006, 2007, 2008, 2009). In the previous worldwide expeditions, such as CLIVAR cruises, the higher reproducibility and precision of nutrients measurements were required (Joyce and Corry, 1994). Since no standards were available for the measurement of nutrients in seawater at that time, the requirements were described in term of reproducibility. The required reproducibility was 1 %, 1 to 2 %, 1 to 3 % for nitrate, phosphate and silicate, respectively. Although nutrient data from the WOCE one-time survey was of unprecedented quality and coverage due to much care in sampling and measurements, the differences of nutrients concentration at crossover points are still found among the expeditions (Aoyama and Joyce, 1996, Mordy et al., 2000, Gouretski and Jancke, 2001). For instance, the mean offset of nitrate concentration at deep waters was $0.5 \mu\text{mol kg}^{-1}$ for 345 crossovers at world oceans, though the maximum was $1.7 \mu\text{mol kg}^{-1}$ (Gouretski and Jancke, 2001). At the 31 crossover points in the Pacific WHP one-time lines, the WOCE standard of reproducibility for nitrate of 1 % was fulfilled at about half of the crossover points and the maximum difference was 7 % at deeper layers below 1.6 deg. C in potential temperature (Aoyama and Joyce, 1996).

During the period from 2003 to 2012, RMNS were used to keep comparability of nutrients measurement among the 9 cruises of CLIVAR project (Sato et al., 2010, Aoyama et al., 2012), MR10-05 cruise for Arctic research (Aoyama et al., 2010) and MR10-06 cruise for “Change in material cycles and ecosystem by the climate change and its feedback” (Aoyama et al., 2011).

a). RMNS for this cruise

RMNS lots BA, BS, BU, AY, BT, BD, BV, and BF, which cover full range of nutrients concentrations in the North Pacific Ocean are prepared. These RMNS assignment were completely done based on random number. The RMNS bottles were stored at a room in the ship, REAGENT STORE, where the temperature was maintained 20 - 25 deg. C.

b). Assigned concentration for RMNSs

We assigned nutrients concentrations for RMNS lots BA, BS, BU, AY, BT, BD, BV, and BF as shown in Table 2.6.4.

Table 2.6.4 Assigned concentration of RMNSs.

	unit: $\mu\text{mol kg}^{-1}$				
	Nitrate	Nitrite	Silicate	Phosphate	Ammonia
BA	0.07	0.02	1.60	0.068	0.95
BS	0.07	0.02	1.61	0.063	-
BU	3.96	0.07	20.27	0.378	-
AY	5.60	0.62	29.42	0.516	0.77
BT	18.18	0.47	40.94	1.318	-
BD	29.82	0.05	64.30	2.191	2.83
BV	35.32	0.06	99.55	2.541	1.02
BF	41.39	0.02	149.60	2.809	2.82

(7) Quality control

a). Precision of nutrients analyses during the cruise

Precision of nutrients analyses during the cruise was evaluated based on the 6 to 9 measurements, which are measured every 9 to 12 samples, during a run at the concentration of C-5 std. Summary of precisions are shown as shown in Table 2.6.5. Analytical precisions previously evaluated were 0.08 % for nitrate, 0.10 % for phosphate and 0.07 % for silicate in CLIVAR P21 revisited cruise of MR09-01 cruise in 2009, respectively. During this cruise, analytical precisions were 0.13 % for nitrate, 0.14 % for nitrite, 0.12 % for silicate, 0.10 % for phosphate and 0.18 % for ammonia in terms of median of precision, respectively. Then we can conclude that the analytical precisions for nitrate, phosphate and silicate were maintained throughout this cruise.

Table 2.6.5 Summary of precision based on the replicate analyses.

	Nitrate CV %	Nitrite CV %	Silicate CV %	Phosphate CV %	Ammonia CV%
Median	0.13	0.14	0.12	0.10	0.26
Mean	0.14	0.15	0.12	0.11	0.25
Maximum	0.20	0.23	0.21	0.19	0.33
Minimum	0.06	0.07	0.06	0.05	0.18
N	15	15	15	15	8

b). Carry over

We can also summarize the magnitudes of carry over throughout the cruise. These are small enough within acceptable levels as shown in Table 2.6.6.

Table 2.6.6 Summary of carry over throughout MR13-04.

	Nitrate %	Nitrite %	Silicate %	Phosphate %	Ammonia %
Median	0.20	0.16	0.21	0.21	0.53
Mean	0.19	0.16	0.21	0.21	0.53
Maximum	0.24	0.42	0.29	0.32	0.65
Minimum	0.11	0.00	0.15	0.12	0.37
N	15	15	15	15	8

c). Estimation of uncertainty of nitrate, nitrite, silicate, and phosphate concentrations

Empirical equations, eq. (1), (2) and (3) to estimate uncertainty of measurement of, nitrate, nitrite and silicate are used based on measurements of 140 sets of RMNSs during the cruise MR09-01 in 2009. These empirical equations are as follows, respectively.

Nitrate Concentration Cnat in $\mu\text{mol kg}^{-1}$:

Uncertainty of measurement of nitrate (%) =

$$0.146 + 2.514 * (1/Cnat) + 0.056725 * (1/Cnat) * (1/Cnat)$$

--- (1)

where Cnat is nitrate concentration of sample.

Nitrite Concentration Cnit in $\mu\text{mol kg}^{-1}$:

$$\text{Uncertainty of measurement of nitrite (\%)} = -0.09 + 0.53 * (1/C_{\text{nit}})$$

----- (2)

where Cnit is nitrite concentration of sample.

Silicate Concentration Csil in $\mu\text{mol kg}^{-1}$:

$$\text{Uncertainty of measurement of silicate (\%)} = 0.123 + 9.9377 * (1/C_{\text{sil}}) + 7.6725 * (1/C_{\text{sil}}) * (1/C_{\text{sil}})$$

----- (3)

where Csil is silicate concentration of sample.

Phosphate Concentration Cphs in $\mu\text{mol kg}^{-1}$:

$$\text{Uncertainty of measurement of phosphate (\%)} = 0.23146 + 0.16859 * (1/C_{\text{phs}})$$

----- (4)

where Cphs is phosphate concentration of sample.

Equation (4) is revised based on measurements of 11 sets of RMNSs during the cruise MR13-04 in 2013 because precision of phosphate measurement was improved.

d). Empirical equation for uncertainty of ammonia

Since we do not have RM for ammonia, empirical equation of uncertainty of ammonia is created based on differences of duplicate measurements of samples taken from same niskin bottles during the cruise MR13-04. We use 27 pairs of duplicate measurements and concentration of ammonia ranged from 0.05 to 0.86 $\mu\text{mol kg}^{-1}$ among all 36 pairs.

Based on differences between two measurements, we estimated an empirical equation between uncertainty of measurement of ammonia and ammonia concentration where we adapted $k = 1$ as follows;

Ammonia Concentration Camo in $\mu\text{mol kg}^{-1}$:

$$\text{Uncertainty of measurement of ammonia (\%)} = 0.24836 + 2.7977 * (1/C_{\text{amo}})$$

----- (5)

where Camo is ammonia concentration of sample.

(8) Problems/improvements occurred and solutions.

In the phosphate analysis, peak top became flat by not using dilution water. Analytical precisions previously evaluated were 0.21 % (n=18) in during the cruise MR12-02, while analytical precisions improved up to 0.11 % (n=15) for phosphate during this cruise.

By changed to a 10 turn glass coil from a 5 turn glass coil after the addition of EDTA, samples were mixed well. Analytical precisions previously evaluated were 0.48 % (n=6) in during the cruise MR12-02, while analytical precisions were 0.25 % (n=8) for ammonia during this cruise.

(9) Station list

Table 2.6.7 List of stations

Cruise	Station	Cast	Year	Month	Date	Latitude		Longitude	
MR13-04	F01	01	2013	7	11	36.478	N	141.478	E
MR13-04	S01	01	2013	7	14	29.972	N	144.981	E
MR13-04	S01	02	2013	7	14	29.996	N	145.000	E
MR13-04	S01	04	2013	7	15	29.911	N	144.956	E
MR13-04	S01	05	2013	7	16	30.069	N	144.972	E
MR13-04	KEO	01	2013	7	17	32.314	N	144.529	E
MR13-04	JKO	01	2013	7	18	38.093	N	146.416	E
MR13-04	KNT	01	2013	7	20	44.005	N	155.003	E
MR13-04	K02	01	2013	7	22	47.002	N	160.005	E
MR13-04	K02	02	2013	7	22	47.003	N	160.006	E
MR13-04	K02	03	2013	7	17	47.001	N	159.994	E
MR13-04	E01	01	2013	7	26	41.252	N	146.712	E

(10) Data archive

All data will be submitted to JAMSTEC Data Management Office (DMO) and is currently under its control.

(11) References

- Aminot, A. and Kerouel, R. 1991. Autoclaved seawater as a reference material for the determination of nitrate and phosphate in seawater. *Anal. Chim. Acta*, 248: 277-283.
- Aminot, A. and Kirkwood, D.S. 1995. Report on the results of the fifth ICES intercomparison exercise for nutrients in sea water, ICES coop. Res. Rep. Ser., 213.
- Aminot, A. and Kerouel, R. 1995. Reference material for nutrients in seawater: stability of nitrate, nitrite, ammonia and phosphate in autoclaved samples. *Mar. Chem.*, 49: 221-232.
- Aoyama M., and Joyce T.M. 1996, WHP property comparisons from crossing lines in North Pacific. In Abstracts, 1996 WOCE Pacific Workshop, Newport Beach, California.
- Aoyama, M., 2006: 2003 Intercomparison Exercise for Reference Material for Nutrients in Seawater in a Seawater Matrix, Technical Reports of the Meteorological Research Institute No.50, 91pp, Tsukuba, Japan.
- Aoyama, M., Susan B., Minhan, D., Hideshi, D., Louis, I. G., Kasai, H., Roger, K., Nurit, K., Doug, M., Murata, A., Nagai, N., Ogawa, H., Ota, H., Saito, H., Saito, K., Shimizu, T., Takano, H., Tsuda, A., Yokouchi, K., and Agnes, Y. 2007. Recent Comparability of Oceanographic Nutrients Data: Results of a 2003 Intercomparison Exercise Using Reference Materials. *Analytical Sciences*, 23: 1151-1154.
- Aoyama M., J. Barwell-Clarke, S. Becker, M. Blum, Braga E. S., S. C. Coverly, E. Czobik, I. Dahllhof, M. H. Dai, G. O. Donnell, C. Engelke, G. C. Gong, Gi-Hoon Hong, D. J. Hydes, M. M. Jin, H. Kasai, R. Kerouel, Y. Kiyomono, M. Knockaert, N. Kress, K. A. Kroglund, M. Kumagai, S. Leterme, Yarong Li, S. Masuda, T. Miyao, T. Moutin, A. Murata, N. Nagai, G. Nausch, M. K. Ngirchchol, A. Nybakk, H. Ogawa, J. van Ooijen, H. Ota, J. M. Pan, C. Payne, O. Pierre-Duplessix, M. Pujo-Pay, T. Raabe, K. Saito, K. Sato, C. Schmidt, M. Schuett, T. M. Shammon, J. Sun, T. Tanhua, L. White, E.M.S. Woodward, P. Worsfold, P. Yeats, T. Yoshimura, A. Youenou, J. Z. Zhang, 2008: 2006 Intercomparison Exercise for Reference Material for Nutrients in Seawater in a Seawater Matrix, Technical Reports of the Meteorological Research Institute No. 58, 104pp.
- Aoyama, M., Nishino, S., Nishijima, K., Matsushita, J., Takano, A., Sato, K., 2010a. Nutrients, In: R/V Mirai Cruise Report MR10-05. JAMSTEC, Yokosuka, pp. 103-122.
- Aoyama, M., Matsushita, J., Takano, A., 2010b. Nutrients, In: MR10-06 preliminary cruise report. JAMSTEC, Yokosuka, pp. 69-83
- Gouretski, V.V. and Jancke, K. 2001. Systematic errors as the cause for an apparent deep water property variability: global analysis of the WOCE and historical hydrographic data REVIEW ARTICLE, *Progress In Oceanography*, 48: Issue 4, 337-402.
- Grasshoff, K., Ehrhardt, M., Kremling K. et al. 1983. Methods of seawater analysis. 2nd rev. Weinheim: Verlag Chemie, Germany, West.
- Hydes, D.J., Aoyama, M., Aminot, A., Bakker, K., Becker, S., Coverly, S., Daniel, A., Dickson, A.G., Grosso, O., Kerouel, R., Ooijen, J. van, Sato, K., Tanhua, T., Woodward, E.M.S., Zhang, J.Z., 2010. Determination of Dissolved Nutrients (N, P, Si) in Seawater with High Precision and Inter-Comparability Using Gas-Segmented Continuous Flow Analysers, In: GO-SHIP Repeat Hydrography Manual: A Collection of Expert Reports and Guidelines. IOCCP Report No. 14, ICPO Publication Series No 134.
- Joyce, T. and Corry, C. 1994. Requirements for WOCE hydrographic programmed data reporting. WHPO Publication, 90-1, Revision 2, WOCE Report No. 67/91.

- Kawano, T., Uchida, H. and Doi, T. WHP P01, P14 REVISIT DATA BOOK, (Ryoin Co., Ltd., Yokohama, 2009).
- Kirkwood, D.S. 1992. Stability of solutions of nutrient salts during storage. *Mar. Chem.*, 38: 151-164.
- Kirkwood, D.S. Aminot, A. and Perttila, M. 1991. Report on the results of the ICES fourth intercomparison exercise for nutrients in sea water. *ICES coop. Res. Rep. Ser.*, 174.
- Mordy, C.W., Aoyama, M., Gordon, L.I., Johnson, G.C., Key, R.M., Ross, A.A., Jennings, J.C. and Wilson, J. 2000. Deep water comparison studies of the Pacific WOCE nutrient data set. *Eos Trans-American Geophysical Union*. 80 (supplement), OS43.
- Murphy, J., and Riley, J.P. 1962. *Analytica chim. Acta* 27, 31-36.
- Sato, K., Aoyama, M., Becker, S., 2010. RMNS as Calibration Standard Solution to Keep Comparability for Several Cruises in the World Ocean in 2000s. In: Aoyama, M., Dickson, A.G., Hydes, D.J., Murata, A., Oh, J.R., Roose, P., Woodward, E.M.S., (Eds.), *Comparability of nutrients in the world's ocean*. Tsukuba, JAPAN: MOTHER TANK, pp 43-56.
- Uchida, H. & Fukasawa, M. WHP P6, A10, I3/I4 REVISIT DATA BOOK Blue Earth Global Expedition 2003 1, 2, (Aiwa Printing Co., Ltd., Tokyo, 2005).

2.7 pH

Masahide WAKITA (JAMSTEC MIO): Principal Investigator
Emi DEGUCHI (MWJ)

(1) Objective

Since the global warming is becoming an issue world-widely, studies on the greenhouse gases such as CO₂ are drawing high attention. The ocean plays an important role in buffering the increase of atmospheric CO₂, and studies on the exchange of CO₂ between the atmosphere and the sea becomes highly important. Oceanic biosphere, especially primary production, has an important role concerned to oceanic CO₂ cycle through its photosynthesis and respiration. However, the diverseness and variability of the biological system make difficult to reveal their mechanism and quantitative understanding of CO₂ cycle. Dissolved CO₂ in water alters its appearance into several species, but the concentrations of the individual species of CO₂ system in solution cannot be measured directly. However, two of the four measurable parameters (alkalinity, total dissolved inorganic carbon, pH and pCO₂) can estimate each concentration of CO₂ system (Dickson et al., 2007). Seawater acidification associated with CO₂ uptake into the ocean possibly changes oceanic ecosystem and CO₂ garners in Ocean recently. We here report on board measurements of pH during MR13-04 cruise.

(2) Methods, Apparatus and Performance

(2)-1 Seawater sampling

Seawater samples were collected by 12 liter Niskin bottles mounted on the CTD/Carousel Water Sampling System and a bucket at 7 stations. Among these stations, deep and shallow casts were carried out for 2 stations. Seawater was sampled in a 100 ml glass bottle that was previously soaked in 5 % non-phosphoric acid detergent (pH13) solution at least 3 hours and was cleaned by fresh water for 5 times and Milli-Q ultrapure water for 3 times. A sampling silicone rubber tube with PFA tip was connected to the Niskin bottle when the sampling was carried out. The glass bottles were filled from the bottom smoothly, without rinsing, and were overflowed for 2 times bottle volume (about 10 seconds) with care not to leave any bubbles in the bottle. The water in the bottle was sealed by a glass made cap gravimetrically fitted to the bottle mouth without additional force. After collecting the samples on the deck, the bottles were carried into the lab and put in the water bath kept about 25 deg C before the measurement.

(2)-2 Seawater analyses

pH (-log[H⁺]) of the seawater was measured potentiometrically in the glass bottles. The pH / Ion meter (Radiometer PHM240) is used to measure the electromotive force (e.m.f.) between the glass electrode cell (Radiometer pHG201) and the reference electrode cell (Radiometer REF201) in the sample with its temperature controlled to 25 +/- 0.15 deg C.

To calibrate the electrodes, the TRIS buffer (Lot=130417: pH= 8.0907 pH units at 25 deg C, DelValls and Dickson, 1998) and AMP buffer (Lot=130417: pH=6.7840 pH units at 25 deg C, Dickson and Goyet, 1994) in the synthetic seawater (Total hydrogen ion concentration scale) were applied. pH_T of seawater sample (pH_{spl}) is calculated from the expression:

$$\text{pH}_{\text{spl}} = \text{pH}_{\text{TRIS}} + (E_{\text{TRIS}} - E_{\text{spl}}) / \text{ER},$$

where electrode response ER is calculated as follows:

$$\text{ER} = (E_{\text{AMP}} - E_{\text{TRIS}}) / (\text{pH}_{\text{TRIS}} - \text{pH}_{\text{AMP}}).$$

ER value should be equal to the ideal Nernst value as follows:

$$\text{ER} = RT \ln(10) / F = 59.16 \text{ mV} / \text{pH units at } 25 \text{ deg C},$$

where F is Faraday constant.

(3) Preliminary results

A replicate analysis of seawater sample was made at 4 layers (ex. 0, 125, 2400, and B-10 dbar depth) of deep cast or 2 layers (ex. 40 and 225 dbar depth) of shallow cast. The difference between each pair of analyses was plotted on a range control chart (see Figure 2.7-1). The average of the difference was 0.001 pH units ($n = 30$ pairs) with its standard deviation of 0.001 pH units. These values were lower than the value recommended by Guide (Dickson et al., 2007).

(4) Data Archive

All data will be submitted to JAMSTEC and is currently under its control.

(5) Reference

- DelValls, T. A. and A. G. Dickson (1998). The pH of buffers based on 2-amino-2-hydroxymethyl-1,3-propanediol ('tris') in synthetic sea water, *Deep-Sea Research I* 45, 1541-1554.
- Dickson A. G. and C. Goyet (Eds.) (1994), *Handbook of methods for the analysis of the various parameters of the carbon dioxide system in sea water*, version 2, ORNS/CDIAC-74.
- Dickson, A. G., C. L. Sabine and J. R. Christian (Eds.) (2007), *Guide to best practices for ocean CO₂ measurements*, PICES Special Publication 3, 199pp.

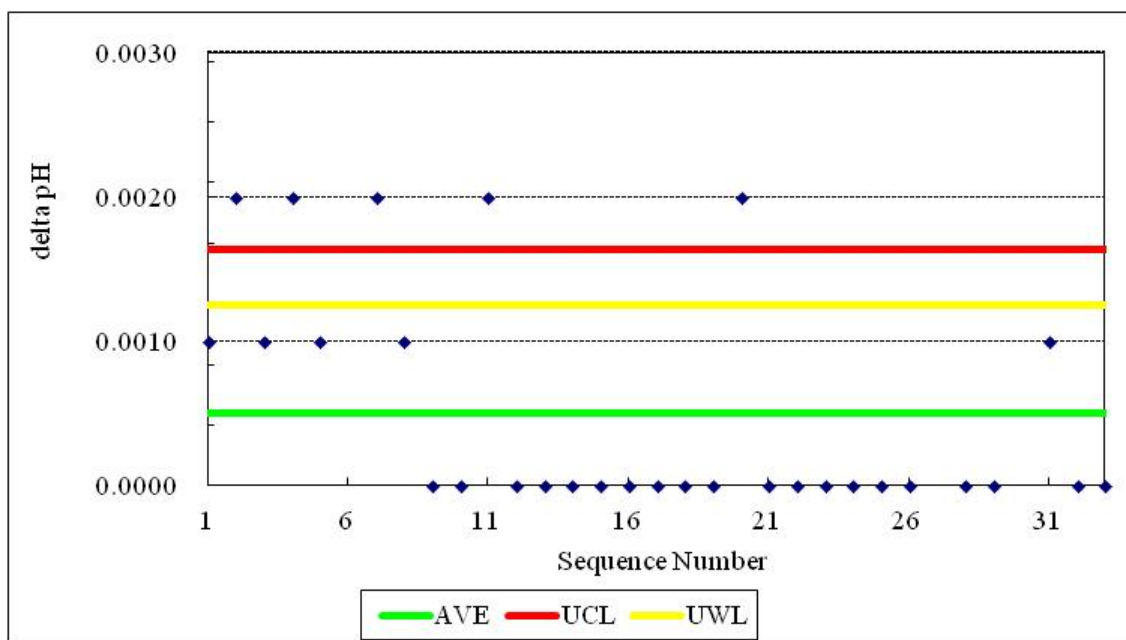


Figure 2.7-1 Range control chart of the absolute differences of replicate measurements of pH carried out during the cruise. AVE represents the average value, UCL upper control limit ($UCL = AVE * 3.267$), and UWL upper warning limit ($UWL = AVE * 2.512$) (Dickson et al., 2007).

2.8 Dissolved inorganic carbon –DIC–

Masahide WAKITA (JAMSTEC MIO): Principal Investigator

Makoto TAKADA (MWJ): Operation Leader

Tomonori WATAI (MWJ)

(1) Objective

Concentration of CO₂ in the atmosphere is now increasing at a rate of 1.5 μmol mol⁻¹ yr⁻¹ owing to human activities such as burning of fossil fuels, deforestation, and cement production. The ocean plays an important role in buffering the increase of atmospheric CO₂, therefore the urgent tasks are to clarify the mechanism of the oceanic CO₂ absorption and to estimate of CO₂ absorption capacity of the oceans. Oceanic biosphere, especially primary production, has an important role concerned to oceanic CO₂ cycle through its photosynthesis and respiration. However, the diverseness and variability of the biological system make difficult to reveal their mechanism and quantitative understanding of the CO₂ cycle. When CO₂ dissolves in water, chemical reaction takes place and CO₂ alters its appearance into several species. Concentrations of the individual species of the CO₂ system in solution cannot be measured directly, but calculated from two of four parameters: total alkalinity, total dissolved inorganic carbon, pH and pCO₂ (Dickson et al., 2007). We here report on-board measurements of DIC performed during the MR13-04 cruise.

(2) Methods, Apparatus and Performance

(2)-1 Seawater sampling

Seawater samples were collected by 12 liter Niskin bottles mounted on the CTD/Carousel Water Sampling System and a bucket at 7 stations. Among these stations, deep and shallow casts were carried out for 2 stations. Seawater was sampled in a 300 ml glass bottle (SHOTT DURAN) that was previously soaked in 5 % non-phosphoric acid detergent (pH = 13) solution at least 3 hours and was cleaned by fresh water for 5 times and Milli-Q deionized water for 3 times. A sampling silicone rubber tube with PFA tip was connected to the Niskin bottle when the sampling was carried out. The glass bottles were filled from the bottom, without rinsing, and were overflowed for 20 seconds. They were sealed using the polyethylene inner lids with its diameter of 29 mm with care not to leave any bubbles in the bottle. After collecting the samples on the deck, the glass bottles were carried to the laboratory to be measured. Within one hour after the sampling, 3 ml of the sample (1 % of the bottle volume) was removed from the bottle and poisoned with 100 μl of over saturated solution of mercury chloride. Then the samples were sealed by the polyethylene inner lids with its diameter of 31.9 mm and stored in a refrigerator at approximately 5 deg C until analyzed. Before the analysis, the samples were put in the water bath kept about 20 deg C for one hour.

(2)-2 Seawater analysis

Measurements of DIC were made with total CO₂ measuring system (Nippon ANS, Inc.). The system comprise of seawater dispensing unit, a CO₂ extraction unit, and a coulometer (SEACAT2000, Nippon ANS, Inc.)

The seawater dispensing unit has an auto-sampler (6 ports), which dispenses the

seawater from a glass bottle to a pipette of nominal 15 ml volume. The pipette was kept at 20 ± 0.05 deg C by a water jacket, in which water circulated through a thermostatic water bath (RTE 10, Thermo).

The CO₂ dissolved in a seawater sample is extracted in a stripping chamber of the CO₂ extraction unit by adding phosphoric acid (10 % v/v). The stripping chamber is made approx. 25 cm long and has a fine frit at the bottom. First, the certain amount of acid is taken to the constant volume tube from an acid bottle and transferred to the stripping chamber from its bottom by nitrogen gas (99.9999 %). Second, a seawater sample kept in a pipette is introduced to the stripping chamber by the same method as that for an acid. The seawater and phosphoric acid are stirred by the nitrogen bubbles through a fine frit at the bottom of the stripping chamber. The stripped CO₂ is carried to the coulometer through two electric dehumidifiers (kept at 0.5 deg C) and a chemical desiccant (Mg(ClO₄)₂) by the nitrogen gas (flow rates of 140 ml min⁻¹).

Measurements of 1.5 % CO₂ standard gas in a nitrogen base, system blank (phosphoric acid blank), and seawater samples (6 samples) were programmed to repeat. The variation of our own made JAMSTEC DIC reference material or 1.5 % CO₂ standard gas signal was used to correct the signal drift results from chemical alternation of coulometer solutions.

(3) Preliminary results

During the cruise, 335 samples were analyzed for DIC. A replicate analysis was performed at the interval decided beforehand and the difference between each pair of analyses was plotted on a range control chart (Figure 2.8-1). The average of the differences was 0.96 μmol kg⁻¹ (n = 23). The standard deviation was 0.83 μmol kg⁻¹, which indicates that the analysis was accurate enough according to the Guide to best practices for ocean CO₂ measurements (Dickson et al., 2007).

(4) Data Archive

These data obtained in this cruise will be submitted to the Data Management Office (DMO) of JAMSTEC, and will open to the public via “R/V Mirai Data Web Page” in JAMSTEC home page.

(5) Reference

Dickson, A. G., C. L. Sabine, and J. R. Christian (2007), *Guide to best practices for ocean CO₂ measurements*, PICES Special Publication 3, 199pp.

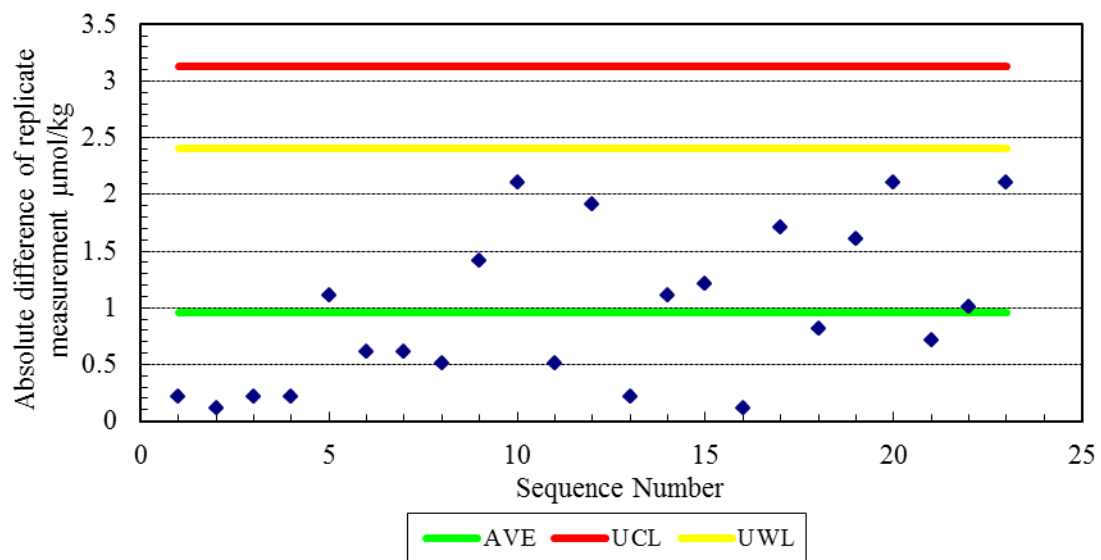


Figure 2.8-1 Range control chart of the absolute differences of replicate measurements of DIC carried out during this cruise. UCL and UWL represents the upper control limit ($\text{UCL} = \text{AVE} \times 3.267$) and upper warning limit ($\text{UWL} = \text{AVE} \times 2.512$), respectively.

2.9 Total alkalinity

Masahide WAKITA (JAMSTEC MIO): Principal Investigator

Tomonori WATAI (MWJ): Operation Leader

Makoto TAKADA (MWJ)

(1) Objective

Global warming is becoming an issue world-widely, therefore studies on green house gases, especially carbon dioxide (CO_2), are indispensable. The ocean currently absorbs one third of the 6 Gt of carbon emitted into the atmosphere each year by human activities, such as burning of fossil fuels, deforestation, and cement production. When CO_2 dissolves in sea water, chemical reaction takes place and CO_2 alters its appearance into several species and make the oceanic CO_2 cycle complicated. Oceanic biological activity, especially oceanic primary production, plays an important role concerned to the CO_2 cycle through its photosynthesis and respiration. The concentrations of the individual CO_2 species cannot be measured directly, however, two of four measurable parameters: total alkalinity, total dissolved inorganic carbon, pH, and pCO_2 , can clarify the whole distribution of the CO_2 species (Dickson et al., 2007). We here report on-board measurements of total alkalinity performed during the MR13-04 cruise.

(2) Methods, Apparatus and Performance

(2)-1 Seawater sampling

Seawater samples were collected by 12 liter Niskin bottles mounted on the CTD/Carousel Water Sampling System and a bucket at 7 stations. Among these stations, deep and shallow casts were carried out for 2 stations. The seawater from the Niskin bottle was filled into the 125 ml borosilicate glass bottles (SHOTT DURAN) using a sampling silicone rubber tube with PFA. The water was filled into the bottle from the bottom smoothly, without rinsing, and overflowed for 2 times bottle volume (10 seconds) with care not to leave any bubbles in the bottle. These bottles were pre-washed in advance by soaking in 5 % non-phosphoric acid detergent (pH = 13) for more than 3 hours, and then rinsed 5 times with tap water and 3 times with Milli-Q deionized water. The samples were stored in a refrigerator at approximately 5 deg C before the analysis, and were put in the water bath with its temperature of about 25 deg C for one hour just before analysis.

(2)-2 Seawater analyses

The TA was measured using a spectrophotometric system (Nippon ANS, Inc.) using a scheme of Yao and Byrne (1998). The constant volume of sample seawater, with its value of approx. 42 ml, was transferred from a sample bottle into the titration cell kept at 25 deg C in a thermostated compartment. Then, the sample seawater was circulated through the tube connecting the titration cell and the pH cell in the spectrophotometer (Carry 50 Scan, Varian) by a peristaltic pump. The length and volume of the pH cell are 8 cm and 13 ml, respectively, and its temperature is also kept at 25 deg C in a thermostated compartment. The TA is calculated by measuring two sets of absorbance at three wavelengths (750, 616 and 444 nm); one is the absorbance of seawater sample before injecting an acid with indicator solution (bromocresol green sodium) and another is the absorbance after the injection. For mixing acid and seawater,

and for degassing CO₂ from the mixed solution sufficiently, they are circulated between the titration and pH cell by a peristaltic pump for 8 and half minutes before the measurement.

The TA is calculated based on the following equation:

$$\begin{aligned} \text{pH}_T = & 4.2699 + 0.002578 * (35 - S) \\ & + \log ((R(25) - 0.00131) / (2.3148 - 0.1299 * R(25))) \\ & - \log (1 - 0.001005 * S), \end{aligned} \quad (1)$$

$$\begin{aligned} A_T = & (N_A * V_A - 10^{\text{pH}_T} * \text{DensSW}(T, S) * (V_S + V_A)) \\ & * (\text{DensSW}(T, S) * V_S)^{-1}, \end{aligned} \quad (2)$$

where R(25) represents the difference of absorbance at 616 and 444 nm between before and after the injection. The absorbance of wavelength at 750 nm is used to subtract the variation of absorbance caused by the system. DensSW (T, S) is the density of seawater at temperature (T) and salinity (S), N_A the concentration of the added acid, V_A and V_S the volume of added acid and seawater, respectively.

To keep the high analysis precision, some treatments were carried out during the cruise. The acid with indicator solution stored in 1 L DURAN bottle is kept in a bath with its temperature of 25 deg C, and about 10 ml of it is discarded at first before the batch of measurement. For mixing the seawater and the acid with indicator solution sufficiently, TYGON tube used on the peristaltic pump was periodically renewed. Absorbance measurements were done 10 times during each analysis, and the stable last five and three values are averaged and used for above listed calculation for before and after the injection, respectively.

(3) Preliminary results

A few replicate samples were taken at most of stations and the difference between each pair of analyses was plotted on a range control chart (see Figure 2.9-1). The average of the difference was 0.7 μmol kg⁻¹ (n = 23) with its standard deviation of 0.7 μmol kg⁻¹, which indicates that the analysis was accurate enough according to the Guide to best practices for ocean CO₂ measurements (Dickson et al., 2007).

(4) Data Archive

These data obtained in this cruise will be submitted to the Data Management Office (DMO) of JAMSTEC, and will be opened to the public via “R/V Mirai Data Web Page” in JAMSTEC home page.

(5) References

- Dickson, A. G., C. L., Sabine, and J. R. Christian (2007), *Guide to best practices for ocean CO₂ measurements*; *PICES Special Publication 3*, 199pp.
- Yao, W., and R. H. Byrne (1998), Simplified seawater alkalinity analysis: Use of linear array spectrometers. *Deep-Sea Research I*, 45, 1383-1392.

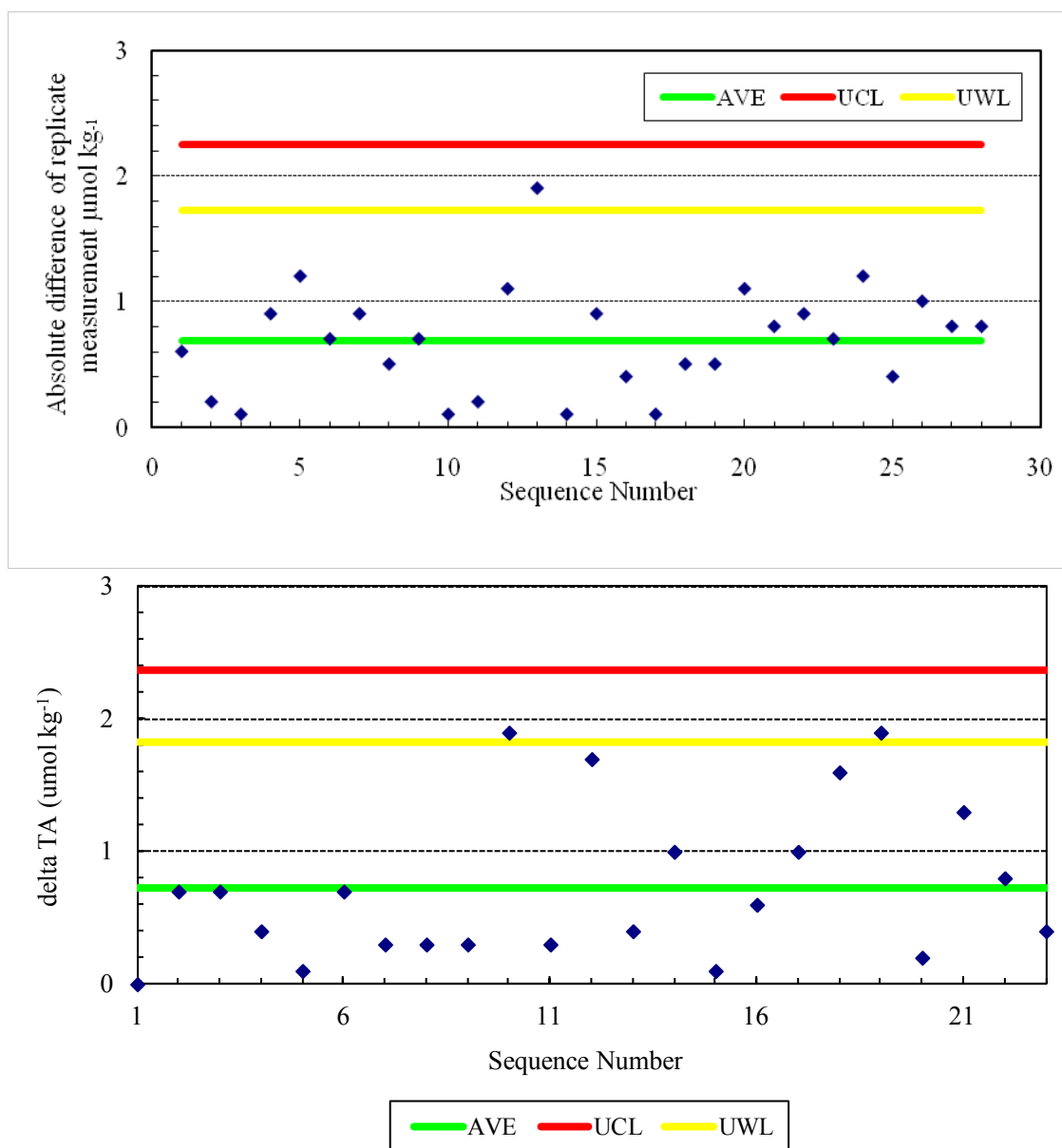


Figure 2.9-1 Range control chart of the absolute differences of replicate measurements carried out in the analysis of TA during the MR13-04 cruise. UCL and UWL represents the upper control limit ($\text{UCL} = \text{AVE} \times 3.267$) and upper warning limit ($\text{UWL} = \text{AVE} \times 2.512$), respectively.

2.10 Underway pCO₂

Masahide WAKITA (JAMSTEC MIO): Principal Investigator

Tomonori WATAI (MWJ): Operation Leader

Makoto TAKADA (MWJ)

Emi DEGUCHI (MWJ)

(1) Objectives

Concentrations of CO₂ in the atmosphere are increasing at a rate of 1.5 ppmv yr⁻¹ owing to human activities such as burning of fossil fuels, deforestation, and cement production. Oceanic CO₂ concentration is also considered to be increased with the atmospheric CO₂ increase, however, its variation is widely different by time and locations. Underway pCO₂ observation is indispensable to know the pCO₂ distribution, and it leads to elucidate the mechanism of oceanic pCO₂ variation. We here report the underway pCO₂ measurements performed during MR13-04 cruise.

(2) Methods, Apparatus and Performance

Oceanic and atmospheric CO₂ concentrations were measured during the cruise using an automated system equipped with a non-dispersive infrared gas analyzer (NDIR; LI-7000, Li-Cor). Measurements were done every about one and a half hour, and 4 standard gasses, atmospheric air, and the CO₂ equilibrated air with sea surface water were analyzed subsequently in this hour. The concentrations of the CO₂ standard gases were 300.081, 349.963, 399.976 and 450.234 ppmv. Atmospheric air taken from the bow of the ship (approx.30 m above the sea level) was introduced into the NDIR by passing through a electrical cooling unit, a mass flow controller which controls the air flow rate of 0.5 L min⁻¹, a membrane dryer (MD-110-72P, perma pure llc.) and chemical desiccant (Mg(ClO₄)₂). The CO₂ equilibrated air was the air with its CO₂ concentration was equivalent to the sea surface water. Seawater was taken from an intake placed at the approximately 4.5 m below the sea surface and introduced into the equilibrator at the flow rate of 4 - 5 L min⁻¹ by a pump. The equilibrated air was circulated in a closed loop by a pump at flow rate of 0.7 - 0.8 L min⁻¹ through two cooling units, a membrane dryer, the chemical desiccant, and the NDIR.

(3) Preliminary results

Cruise track during pCO₂ observation is shown in Figure 2.10-1. Temporal variations of both oceanic and atmospheric CO₂ concentration (xCO₂) are shown in Fig. 2.10-2.

(4) Data Archive

Data obtained in this cruise will be submitted to the Data Management Office (DMO) of JAMSTEC, and will be opened to the public via “R/V Mirai Data Web Page” in JAMSTEC home page.

(5) Reference

Dickson, A. G., Sabine, C. L. & Christian, J. R. (2007), Guide to best practices for ocean CO₂

measurements; PICES Special Publication 3, 199pp.

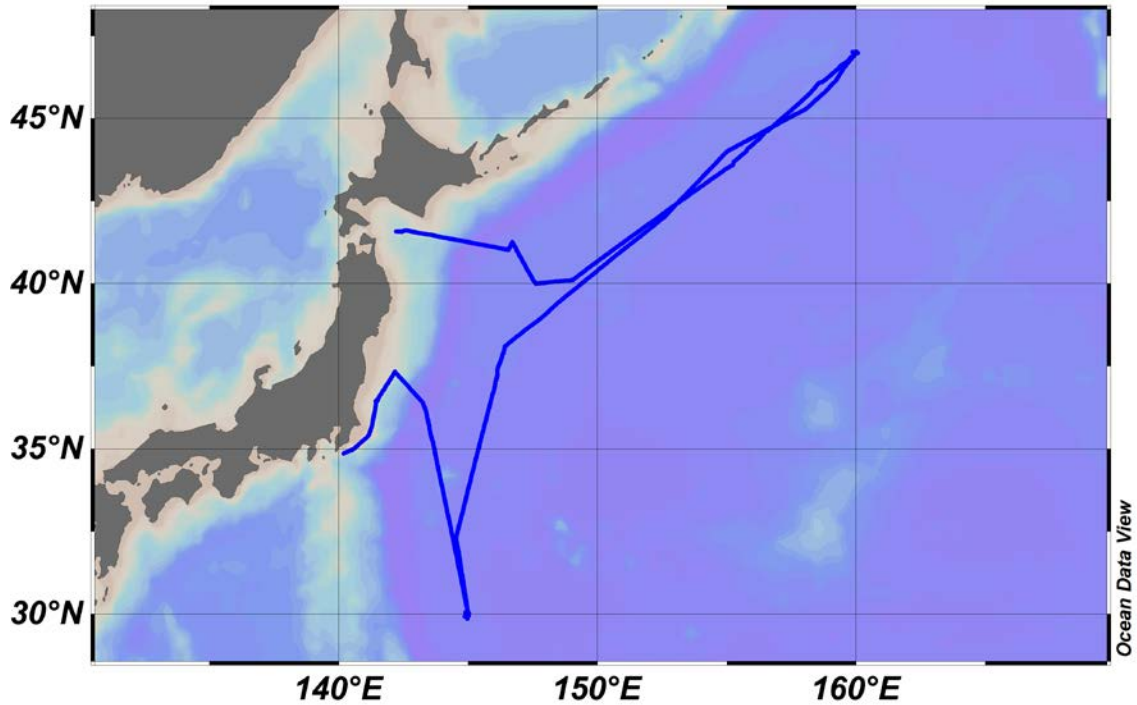


Figure 2.10-1 Observation map

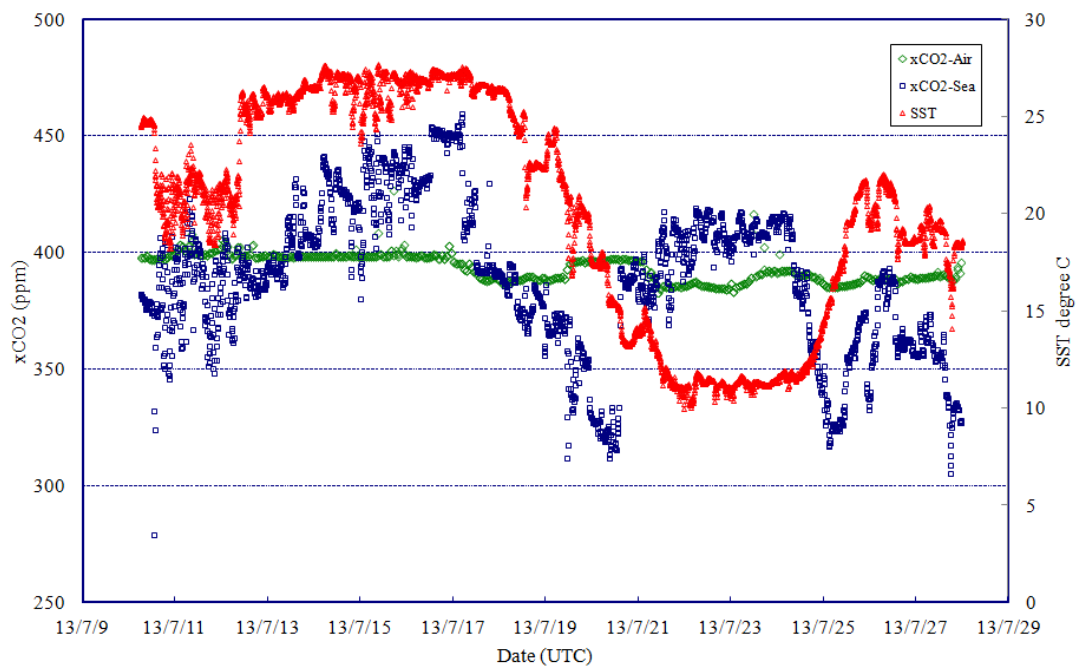


Figure 2.10-2 Temporal variations of oceanic and atmospheric CO₂ concentration (xCO₂). Blue dots represent oceanic xCO₂ variation and green atmospheric xCO₂. SST variation (red) is also shown.

3. Special observation

3.1 BGC mooring

3.1.1 Recovery and deployment

Makio HONDA (JAMSTEC MIO)

Hajime KAWAKAMI (JAMSTEC MIO)

Tomoyuki TAKAMORI (MWJ)

Masaki FURUBATA (MWJ)

The BGC mooring system was designed for biogeochemistry at Station K-2 and S-1 in the Western Subarctic Gyre. We recovered BGC mooring at Station K-2 and S-1 which were deployed at MR12-02 and deployed BGC mooring at Station K-2 and S-1. Before deployment, sea floor topography was surveyed with Sea Beam. In order to place the top of mooring systems 150m depth, precise water depths for mooring positions was measured by an altimeter (Datasonics PSA900D) mounted on CTD / CWS. Mooring works took approximately 4 hours for each mooring system. After sinker was dropped, we positioned the mooring systems by measuring the slant ranges between research vessel and the acoustic releaser. The position of the mooring is finally determined as follow:

Table 3.1.1-1 Mooring positions for respective mooring systems

	Recovery	Deployment	Recovery	Deployment
Station & type	K-2 BGC	K-2 BGC	S-1 BGC	S-1 BGC
Mooring Number	K2BGC120614	K2BGC130724	S1BGC120701	S1BGC130717
Working Date	Jul. 22 st 2013	Jul. 24 st 2013	Jul. 15 th 2013	Jul. 17 th 2013
Latitude	47° 00.40N	47° 00.47N	30° 03.93 N	30° 03.86 N
Longitude	159° 58.22 E	159° 58.40 E	144° 58.21 E	144° 57.80 E
Sea Beam Depth	5,210 m	5,219 m	5,922 m	5,927 m

The BGC mooring consists of a advance buoy with 30m pick up rope, a 64” syntactic top float with 3,000 lbs (1,360 kg) buoyancy, instruments, wire and nylon ropes, glass floats (Benthos 17” glass ball), dual releasers (Edgetech) and 4,660 lbs (2,116 kg), sinker. Two ARGOS compact mooring locators and one submersible recovery strobe are mounted on the top float. This mooring system was planned to keep the following time-series observational instruments are mounted approximately 150 m below sea surface. It is 10 m longer than real depth because recovered depth sensor which was installed on the Sediment trap shows 10 m deeper than our expected by mooring tilt.

The BGC mooring consists of 3 Sediment Traps installed on the 200 m, 500 m and 5,000m. Another K2 BGC mooring is 2 Remote Access Sampler with Ocean Optical Sensor installed on 100 m and 550 m. Also Extra instrument are mounted. Details for each instrument are described below (section 3.1.2). Serial numbers for instruments are as follows:

Table 3.1.1-2 Serial numbers of instruments

	Recover		Deployment	
Station and type Mooring Number	K-2 BGC K2BGC120614	S-1 BGC S1BGC120701	K-2 BGC K2BGC130724	S-1 BGC S1BGC130717
Top Buoy(150m) ARGOS ARGOS ID Strobe JFE Depth sensor Temperature sensor	18842 / 52111 18577 / 05373 NO2-044	18841 / A02-108 18570 / 115728 Benthos 233	A02-058 / 18842 115728 / 18577 B02-016 085I001 101931	A10-058 / A10-057 126529 / 126530 A10-058
RAS (100m) RAS 3-48-500 SBE-37 JFE DO sensor			11241-07 4442 / 1892 0092	
Temperature sensor WIRE(125m) WIRE (150m) WIRE (175m)			101932 101933 101934	
Sediment Trap(200m) Nichiya JFE Depth sensor Rigo Depth sensor SBE-37 JFE DO sensor Back Scattero meter Sediment Trap Mark7-21(4810m)	ST98025 DP1158 905 10558-01	ST98080 DP1142 891 10236-01	ST98025 1893 0080 905 10558-01	ST98080 082U009 891 10236-01
WIRE (300m) SBE-37 JFE DO sensor			2239 0087	
Sediment Trap(500m) Mark7-21 Temperature sensor	10238-02	878	10238-02 101947	62-665
RAS (550m) RAS 3-48-500 SBE-37 JFE DO sensor			11241-09 2289 0088	
Sediment Trap(4810m) Mark7-21	10558-01	10236-01	10558-01	10236-01
Releaser Releaser SBE-37 AREC DO sensor	27824 34040 2731 051	27805 28531 2730 052	27809 28531 2731 051	27815 28386 2730 052

Table 3.1.1-3 Recovery BGC Mooring Record at K-2

Project	Time-Series	Depth	5,206.2	m
Area	North Pacific	Planned Depth	5,216.2	m
Station	K2 BGC	Length	5,068.2	m
Target Position	47°00.350 N 159°58.326 E	Depth of Buoy	150	m
		Period	1	year
ACOUCTIC RELEASERS				
Type	Edgetech	ORE		
Serial Number	27824	34040		
Receive F.	11.0 kHz	11.0 kHz		
Transmit F.	14.0 kHz	14.0 kHz		
RELEASE C.	344674	233770		
Enable C.	361121	221130		
Disable C.	361167	221155		
Battery	2 years	2 years		
Release Test	OK	OK		
RECOVERY				
Recorder	Tomoyuki Takamori	Work Distance	2.3	Nmile
Ship	R/V MIRAI	Send Enable C.	19:46	
Cruise No.	MR13-04	Slant Renge	-	msec
Date	2013/7/22	Send Release C.	19:49	
Weather	O/f	Discovery Buoy	19:51	
Wave Hight	1.1 m	Pos. of Top Buoy	47°00.46	N
Seabeam Depth	5,202 m		159°58.33	E
Ship Heading	<047>	Pos. of Start	47°00.52	N
Ship Ave.Speed	0.8 knot		159°57.82	E
Wind	<030> 3.7 m/s	Pos. of Finish	47°02.08	N
Current	<058> 0.4 knot		160°00.08	E

Table 3.1.1-4 Recovery BGC Mooring Record at S-1

Project	Time-Series		Depth	5,920.0	m
Area	North Pacific		Planned Depth	5,915.0	m
Station	S1 BGC		Length	5,752.3	m
Target Position	30°03.8656	N	Depth of Buoy	150	m
	144°58.0275	E	Period	1	year
ACOUCTIC RELEASERS					
Type	Edgetech		Edgetech		
Serial Number	27805		28531		
Receive F.	11.0	kHz	11.0	kHz	
Transmit F.	14.0	kHz	14.0	kHz	
RELEASE C.	344611		223065		
Enable C.	360631		200405		
Disable C.	360677		200426		
Battery	2 years		2 years		
Release Test	OK		OK		
RECOVERY					
Recorder	Takamori Tomoyuki		Work Distance	2.0	Nmile
Ship	R/V MIRAI		Send Enable C.	3:04	
Cruise No.	MR13-04		Slant Renge	-	msec
Date	2013/7/15		Send Release C.	3:06	
Weather	bc		Discovery Buoy	3:09	
Wave Hight	1.6	m	Pos. of Top Buoy	30°03.80	N
Seabeam Depth	5,911	m		144°57.99	E
Ship Heading	<185>		Pos. of Start	30°03.88	N
Ship Ave.Speed	0.7	knot		144°57.45	E
Wind	<220>	5.0 m/s	Pos. of Finish	30°01.99	N
Current	<257>	0.7 knot		144°56.59	E

Table 3.1.1-5 Deployment BGC Mooring Record at K-2

Project	Time-Series		Depth	5,206.2	m
Area	North Pacific		Planned Depth	5,216.2	m
Station	K2 BGC		Length	5,068.2	m
Target Position	47°00.350	N	Depth of Buoy	150	m
	159°58.326	E	Period	1	year
ACOUCTIC RELEASERS					
Type	Edgetech		Edgetech		
Serial Number	27809		28531		
Receive F.	11.0	kHz	11.0	kHz	
Transmit F.	14.0	kHz	14.0	kHz	
RELEASE C.	344535		223065		
Enable C.	360320		200405		
Disable C.	360366		200426		
Battery	2 years		2 years		
Release Test	OK		OK		
DEPLOYMENT					
Recorder	Tomoyuki Takamori		Start	5.0	Nmile
Ship	R/V MIRAI		Overshoot	-	m
Cruise No.	MR13-04		Let go Top Buoy	21:07	
Date	2013/7/24		Let go Anchor	23:50	
Weather	o		Sink Top Buoy	0:33	
Wave Hight	1.2	m	Pos. of Start	47°01.09	N
Seabeam Depth	5,219	m		159°51.56	E
Ship Heading	<098>		Pos. of Drop. Anc.	47°00.30	N
Ship Ave.Speed	1.8	knot		159°58.76	E
Wind	<065>	6.1 m/s	Pos. of Mooring	47°00.84	N
Current	<036>	0.4 Knot		159°56.94	E

Table 3.1.1-6 Deployment BGC Mooring Record at S-1

Project	Time-Series		Depth	5,920.0	m
Area	North Pacific		Planned Depth	5,915.0	m
Station	S1 BGC		Length	5,752.3	m
Target Position	30°03.8656	N	Depth of Buoy	150	m
	144°58.0275	E	Period	1	year
ACOUCTIC RELEASERS					
Type	Edgetech		ORE		
Serial Number	27815		28386		
Receive F.	11.0	kHz	11.0	kHz	
Transmit F.	14.0	kHz	14.0	kHz	
RELEASE C.	344657		354501		
Enable C.	361035		376513		
Disable C.	361073		376530		
Battery	2 years		2 years		
Release Test	OK		OK		
DEPLOYMENT					
Recorder	Takamori Tomoyuki		Start	3.9	Nmile
Ship	R/V MIRAI		Overshoot	0.3	m
Cruise No.	MR13-04		Let go Top Buoy	0:00	
Date	2013/7/17		Let go Anchor	2:38	
Weather	o		Sink Top Buoy	3:15	
Wave Hight	1.4	m	Pos. of Start	30°03.24	N
Seabeam Depth	5,927	m		144°53.92	E
Ship Heading	<079>		Pos. of Drop. Anc.	30°03.91	N
Ship Ave.Speed	1.4	knot		144°58.38	E
Wind	<025>	5.3 m/s	Pos. of Mooring	30°03.85	N
Current	<272>	0.5 knot		144°57.81	E

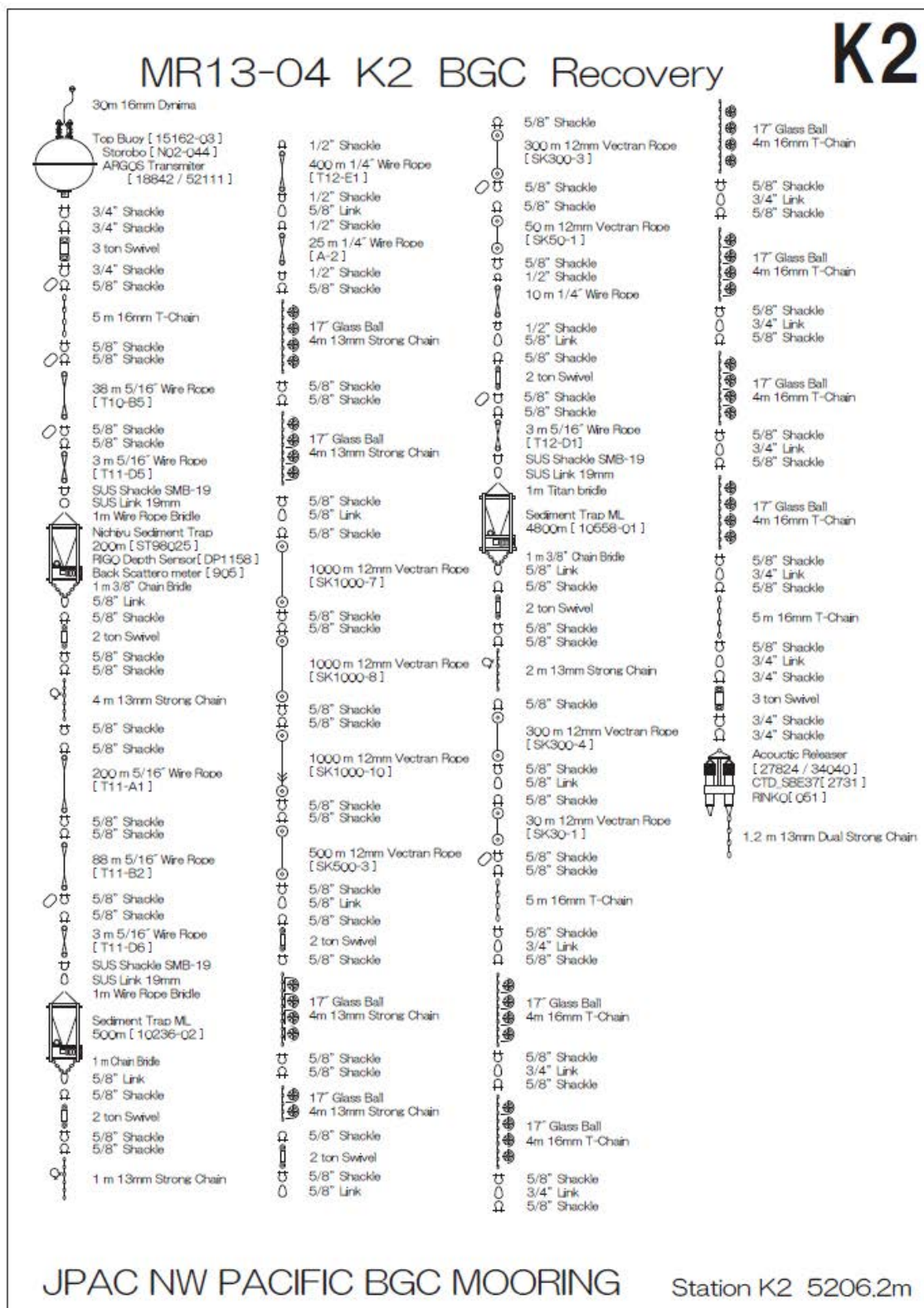
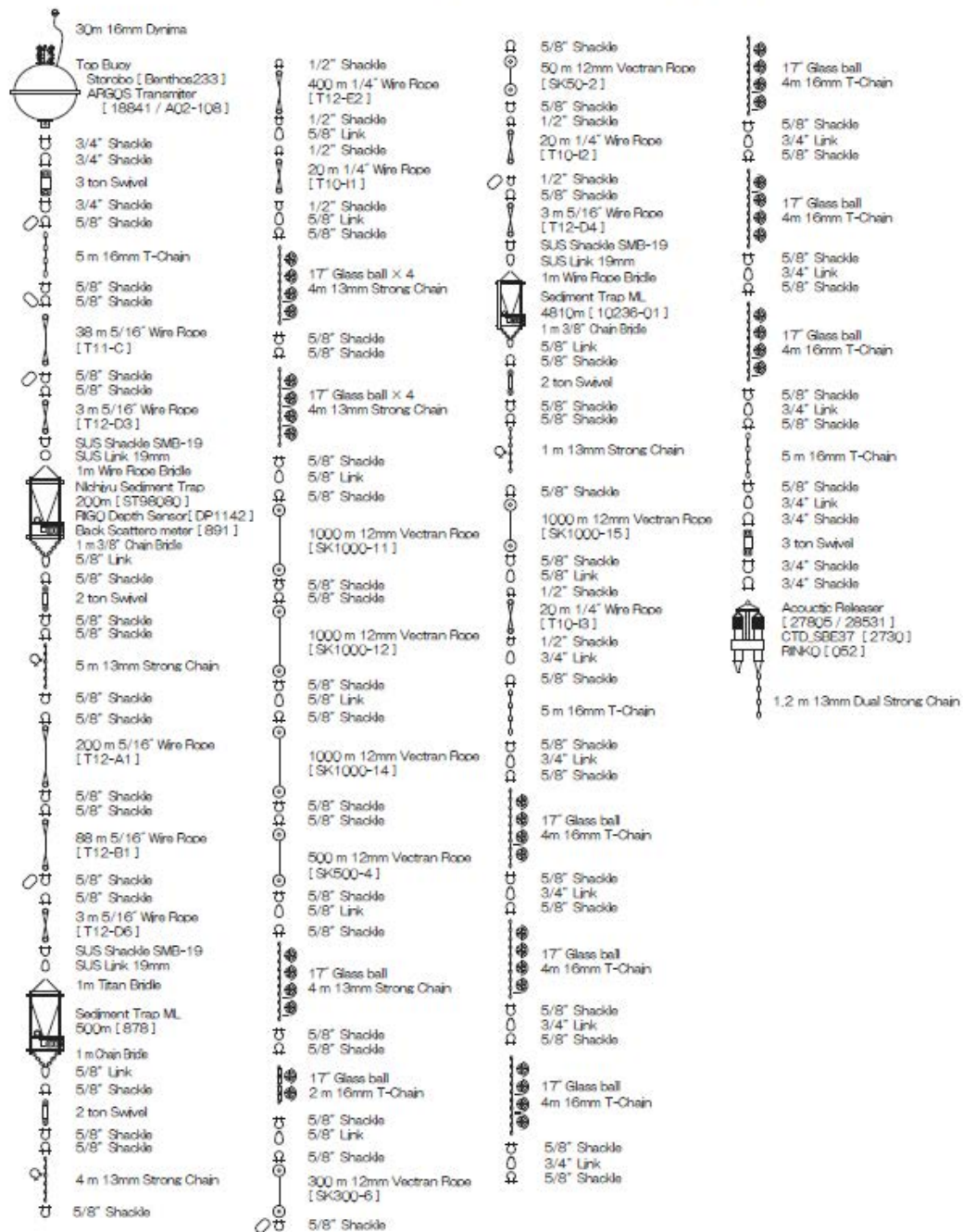


Fig. 3.1.1-1 Recovery BGC Mooring Figure at K-2

MR13-04 S1 BGC Recovery

S1



JPAC NW PACIFIC BGC MOORING

Station S1 5920.0m

Fig. 3.1.1-2 Recovery BGC Mooring Figure at S-1

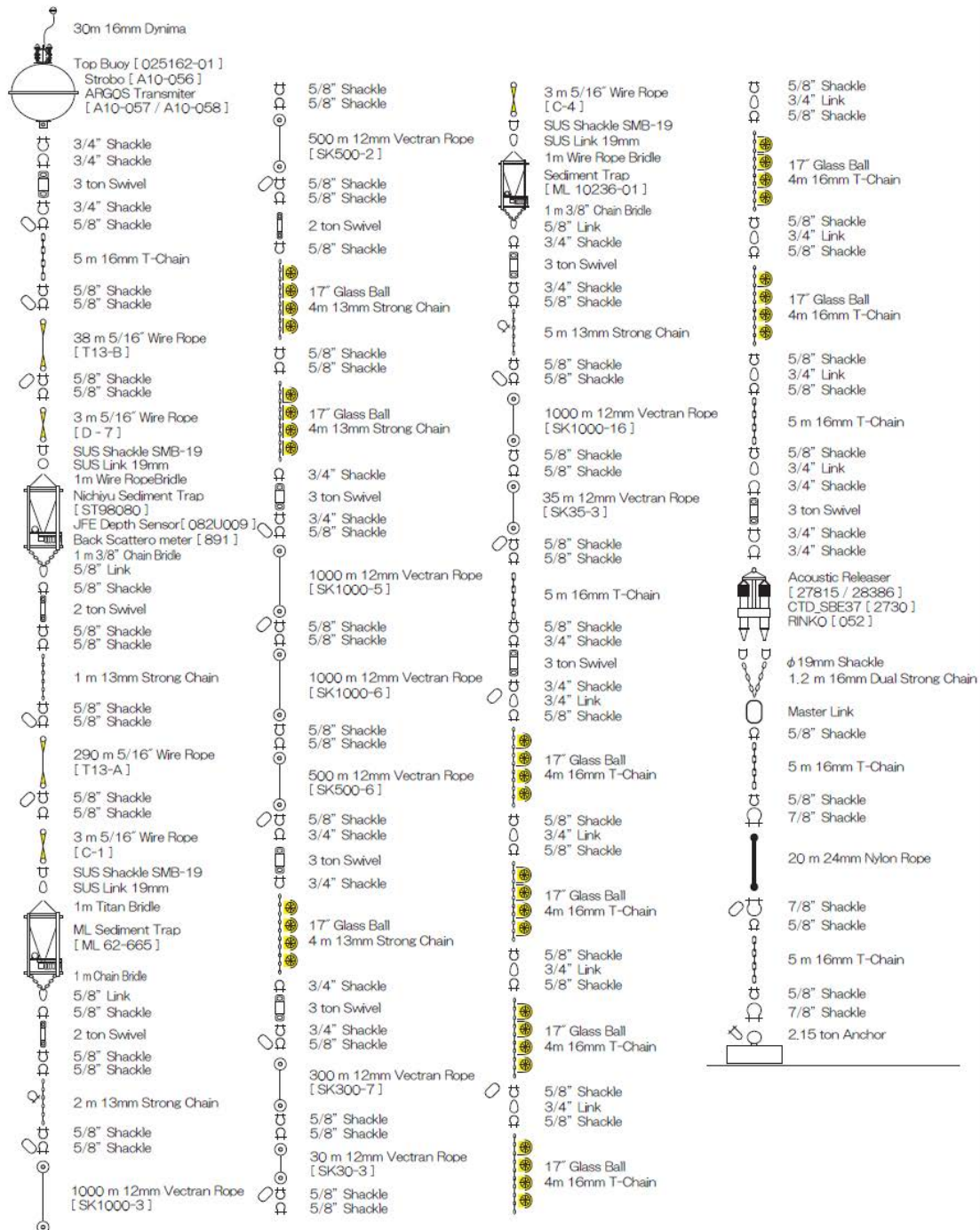
K2



80

MR13-04 S1 BGC Deployment

S1



JPAC NW PACIFIC BGC MOORING

Station S1 5920.2m

Fig. 3.1.1-4 Deployment BGC Mooring Figure at S-1

3.1.2 Instruments

On mooring systems, the following instruments are installed.

(1) ARGOS CML (Compact Mooring Locator)

The Compact Mooring Locator is a subsurface mooring locator based on SEIMAC's Smart Cat ARGOS PTT (Platform Terminal Transmitter) technology. Using CML, we can know when our mooring has come to the surface and its position. The CML employs a pressure sensor at the bottom. When the CML is turned ON, the transmission is started immediately every 90 seconds and then when the pressure sensor works ON by approximately 10 dbar, the transmission is stopped. When the top buoy with the CML comes to the surface, the pressure sensor will work OFF and the transmission will be started. Smart Cat transmissions will be initiated at this time, allowing us to locate our mooring. Depending on how long the CML has been moored, it will transmit for up to 120 days on a 90 second repetition period. Battery life, however, is affected by how long the CML has been moored prior to activation. A longer pre-activation mooring will mean less activation life.

Principle specification is as follows:

(Specification)

Transmitter:	Smart Cat PTT
Operating Temp.:	+35 [deg] to -5 [deg]
Standby Current:	80 microamps
Smart Cat Freq.:	401.650 MHz
Battery Supply:	7-Cell alkaline D-Cells
Ratings:	+10.5VDC nom., 10 Amp Hr
Hull:	6061-T6 Aluminum
Max Depth:	1,000 m
Length:	22 inches
Diameter:	3.4 inches
Upper flange:	5.60 inches
Dome:	Acrylic
Buoyancy:	-2.5 (negative) approx.
Weight	12 pounds approx.

(2) Submersible Recovery Strobe

The NOVATECH Xenon Flasher is intended to aid in the marking or recovery of oceanographic instruments, manned vehicles, remotely operated vehicles, buoys or structures. Due to the occulting (firing closely spaced bursts of light) nature of this design, it is much more visible than conventional marker strobes, particularly in poor sea conditions.

(Specification)

Repetition Rate:	Adjustable from 2 bursts per second to 1 burst every 3 seconds.
Burst Length:	Adjustable from 1 to 5 flashes per burst. 100 ms between flashes nominal.
Battery Type:	C-cell alkaline batteries.
Life:	Dependent on repetition rate and burst length. 150 hours with a one flash burst every 2 seconds.
Construction:	Awl-grip painted, Hard coat anodized 6061 T-6 aluminum housing.
Max. Depth:	7,300m

Daylight-off:	User selected, standard
Pressure Switch:	On at surface, auto off when submerged below 10m.
Weight in Air:	4 pounds
Weight in Water:	2 pounds
Diameter:	1.7 inches nominal
Length:	21-1/2 inches nominal

(3) Small memory Depth Sensor

JFE Depth sensor is digital memory type and designed for mounting on the plankton net and instrument for mooring and so on. It is small and right weight for easy handling. Sampling interval is chosen between 1 and 59 seconds or 1 and 60 minutes and sampled Time and Depth data. MR13-04 Cruise, Data is sampled at 1-hour intervals. The data is converted to personal computer using Infrared rays interface.

(Specification)

Model:	DFFI-D50HG
Operating Depth:	0 ~ 5MPa
Precision:	0.3% (F.S.)
Memory:	859,320 data (8Mbyte)
Battery:	Alkali battery (LRO3XJ) DC1.5V
Sample interval:	1 ~ 59 seconds or 1 ~ 60 minutes
Broken Pressure:	5MPa
Diameter:	26mm
Length:	139.5mm
Main Material:	Titan
Optics Window:	Polycarbonate
Weight:	139g

(4) CTD SBE-37

The SBE 37-SM MicroCAT is a high-accuracy conductivity and temperature (pressure optional) recorder with internal battery and memory. Designed for moorings or other long duration, fixed-site deployments, the MicroCAT includes a standard serial interface and nonvolatile FLASH memory. Constructed of titanium and other non-corroding materials to ensure long life with minimum maintenance, the MicroCAT's depth capability is 7000 meters; it is also available with an optional 250-meter plastic *ShallowCAT* housing. Data is sampled at 1-hour intervals from MR13-04 Cruise.

(Specification)

Measurement Range

Conductivity: 0 - 7 S/m (0 - 70 mS/cm)

Temperature: -5 to 35 °C

Optional Pressure: 7000 (meters of deployment depth capability)

Initial Accuracy

Conductivity: 0.0003 S/m (0.003 mS/cm)

Temperature: 0.002 °C

Optional Pressure: 0.1% of full scale range

Typical Stability (per month)

Conductivity: 0.0003 S/m (0.003 mS/cm)

Temperature: 0.0002 °C
 Optional Pressure: 0.004% of full scale range
 Resolution
 Conductivity: 0.00001 S/m (0.0001 mS/cm)
 Temperature: 0.0001 °C
 Optional Pressure: 0.002% of full scale range
 Time Resolution 1 second
 Clock Accuracy 13 seconds/month
 Quiescent Current * 10 microamps
 Optional External Input Power 0.5 Amps at 9-24 VDC
 Housing, Depth Rating, and Weight (without pressure sensor)
 Standard Titanium, 7000 m (23,000 ft)
 Weight in air: 3.8 kg (8.3 lbs)
 Weight in water: 2.3 kg (5.1 lbs)

(5) JFE Advantech optical dissolved oxygen sensor, Rinko

JFE Advantech optical dissolved oxygen sensor, Rinko, is based on the oxygen luminescence quenching. The Rinko used has a datalogger with an internal battery and memory in a titanium housing designed for mooring observation. Data is sampled at 1-hour intervals.

(Manufacturer's specification)

Model: Riniko I (ARO-USB)
 Sensor Type: Luminescence quenching
 Operating Range: 0 ~ 200%
 Resolution: 0.01 ~ 0.04%
 Precision: ±2%FS (linearity)
 Memory: 1GB mini SD card
 Sampling interval: 0.1 ~ 600 seconds
 Burst time: 1 ~ 1,440 minutes
 Sample number: 1 ~ 18,000
 Battery: CR-V3 lithium battery, 3.3Ah (maximum 2 batteries)
 Housing material: Titanium
 Size: φ54 mm × 232 mm
 Weight: 0.9 kg in air, 0.6 kg in water
 Depth rating: 7000 m

(6) JFE Advantech miniature temperature sensor

JFE Advantech miniature temperature sensor (MDS MkV/T) is 8 cm long, 18mm wide, a weight of 50 g; it has a sampling frequency of 1 Hz and autonomously record data through a lithium ion battery. These instruments are ideal for long-term deployments for up to 2 years, and they can be used for tagging and tracking marine mammals. Through a convenient computer interface (via RS-232C) you can easily download the recorded data, or program the MkV for a variety of sampling strategies. Data is sampled at 1-hour intervals from MR13-04 Cruise.

(Specification)

SENSOR TYPE: Temperature

PARAMETERS: Ultra-Miniature Temperature Recorder

ACCURACY: $\pm 0.05^{\circ}\text{C}$

DEPTH RATING: 2000m

OUTPUT: RS-232C

SAMPLE RATE: 1 sec, 1 min, 2 min, 10 min

RESOLUTION: 0.015°C

DIMENSIONS: 18 mm (diameter) x 80 mm (length)

POWER SUPPLY: 1 ea Lithium battery (2CR1/3N)

3.1.3 Sampling schedule

After retrieving sample / data, replacement of new battery and initialization of schedule (Table 3.1.3), sediment trap mooring system at S1 (K2) was deployed on 17 July 2013 (24 July 2013). These mooring systems will be recovered during cruises held in 2014 (candidate cruises by R/V Hakuohmaru and R/V Kaiyo).

K2			
	21cup		26cup
	500 m, 4810 m		200m
Int	14		14
1	2013/7/25	1	2013/7/25
2	2013/8/8	2	2013/8/1
3	2013/8/22	3	2013/8/8
4	2013/9/5	4	2013/8/15
5	2013/9/19	5	2013/8/22
6	2013/10/3	6	2013/9/5
7	2013/10/17	7	2013/9/19
8	2013/10/31	8	2013/10/3
9	2013/11/14	9	2013/10/17
10	2013/11/28	10	2013/10/31
11	2013/12/12	11	2013/11/14
12	2013/12/26	12	2013/11/28
13	2014/1/9	13	2013/12/12
14	2014/1/23	14	2013/12/26
15	2014/2/6	15	2014/1/9
16	2014/2/20	16	2014/1/23
17	2014/3/6	17	2014/2/6
18	2014/3/20	18	2014/2/20
19	2014/4/3	19	2014/3/6
20	2014/4/17	20	2014/3/20
21	2014/5/1	21	2014/4/3
	2014/5/15	22	2014/4/10
		23	2014/4/17
		24	2014/4/24
		25	2014/5/1
		26	2014/5/8
			2014/5/15
Int. 7 days			
K2			
Deployment date		2013/7/24	
Hakuho start date		ca. 2014.5.20	
Recovery date		ca. 2014.5.22	

S1			
	21cup		26cup
	500 m, 4810 m		200m
Int	18		18
1	2013/7/18	1	2013/7/18
2	2013/8/5	2	2013/8/5
3	2013/8/23	3	2013/8/23
4	2013/9/10	4	2013/9/10
5	2013/9/28	5	2013/9/28
6	2013/10/16	6	2013/10/16
7	2013/11/3	7	2013/11/3
8	2013/11/21	8	2013/11/21
9	2013/12/9	9	2013/12/9
10	2013/12/27	10	2013/12/27
11	2014/1/14	11	2014/1/14
12	2014/2/1	12	2014/1/23
13	2014/2/19	13	2014/2/1
14	2014/3/9	14	2014/2/10
15	2014/3/27	15	2014/2/19
16	2014/4/14	16	2014/2/28
17	2014/5/2	17	2014/3/9
18	2014/5/20	18	2014/3/18
19	2014/6/7	19	2014/3/27
20	2014/6/25	20	2014/4/5
21	2014/7/13	21	2014/4/23
	2014/7/31	22	2014/5/11
		23	2014/5/29
		24	2014/6/16
		25	2014/7/4
		26	2014/7/22
			2014/7/31
Int. 9 days			
S1			
Deployment date		2013/7/17	
Next cruise		?	
Recovery date		?	

3.1.4 Preliminary results

Onboard, heights of sinking particle collect in collecting cups were measured with scale in order to know general view of seasonal variability. Using diameter of collecting cups, we estimated total mass flux in volume for each collecting period (18 days).

(1) S1 Sediment Trap

At 200 m, total mass flux (TMF) increased between August and September 2012 and between March and May 2013 (Fig. 3.1.4.1 upper panel). Water depth of 200 m sediment trap is also shown in Fig. 3.1.4.1 (upper panel). After deployment in July 2013, water depth of 200 m sediment trap slightly decreased. It is likely attributed to the extension of wire / Vectran rope used for mooring system. After November 2013, minimum water depth was about 220 m on average. Water depths thereafter sometimes increased. Maximum water depth of 260 m was observed in December 2012. However change of water depth was smaller compared to that for 2011-2012 deployment (see MR12-02 preliminary cruise report).

Although TMF were smaller than that at 200 m, seasonal variability in TMF at 500 m (middle panel) and 4810 m (bottom panel) synchronized well with that at 200 m: increases in TMF were observed between August and September 2012 and between March and April 2013.

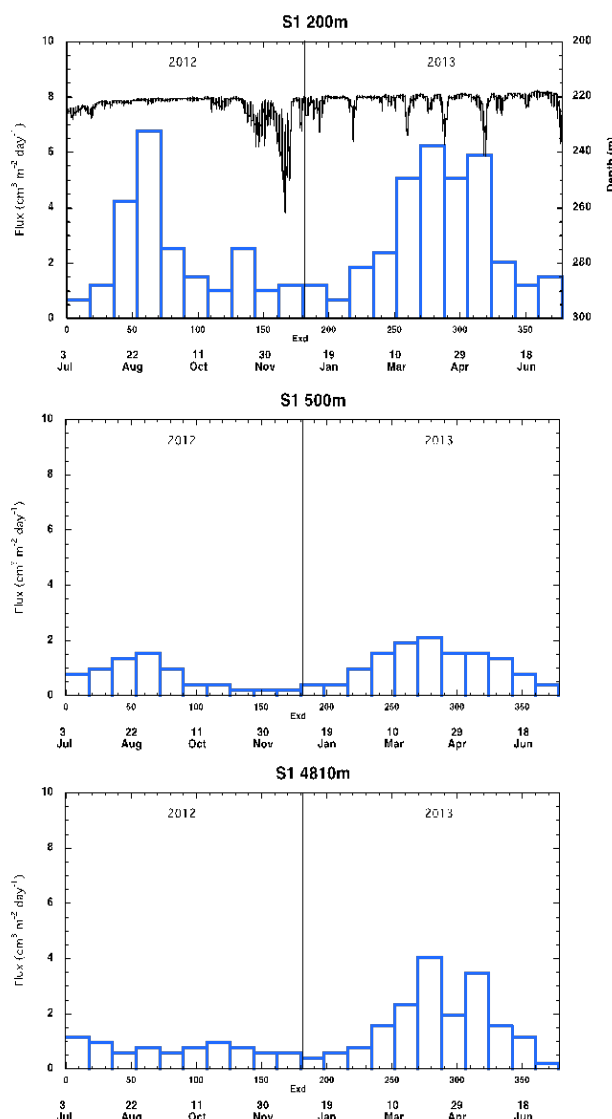


Fig. 3.1.4.1 Total mass flux (bar graphs) at 200 m (upper), 500 m (middle) and 4810 m (bottom) of S1. Line graph in upper panel is water depth of 200 m sediment trap.

(2) K2 Sediment Trap

At 200m, TMF was high in June 2012 when collection of sinking particle started (Fig. 3.1.4.2 upper panel). However TMF suddenly decreased in July 2012 and, thereafter, sinking particles were quite little or were not collected. Sediment trap was recovered on 22 July 2013 when the last bottle was still under open hole. In this bottle, there was large sinking particle collected. This seasonal variability was strange and should be artifact. We suspected that large sinking particle during June and July 2012 clogged the mouth of collecting cups and sinking particle was accumulated at the mouth and, these particles dropped into the last collecting cup when sediment trap was recovered in July 2013.

At 500 m, TMF was large in June 2012 (Fig. 3.1.4.2 middle panel). This flux corresponded to the large flux observed at 200m described above. TMF decreased gradually toward late September 2012. In October and December 2012, relatively high TMF were observed. Between January and May 2013, TMF was small. The highest TMF was observed in June 2013.

At 4810 m, TMF in July 2012 was relatively high and decreased gradually by June 2013 (Fig. 3.1.4.2 lower panel). In late June 2013, the highest flux was observed and corresponded to the highest TMF observed at 500m in early June 2013. Based on the time lag between 500m and 4810 m, sinking velocity of sinking particle was estimated to be about 240 m day^{-1} .

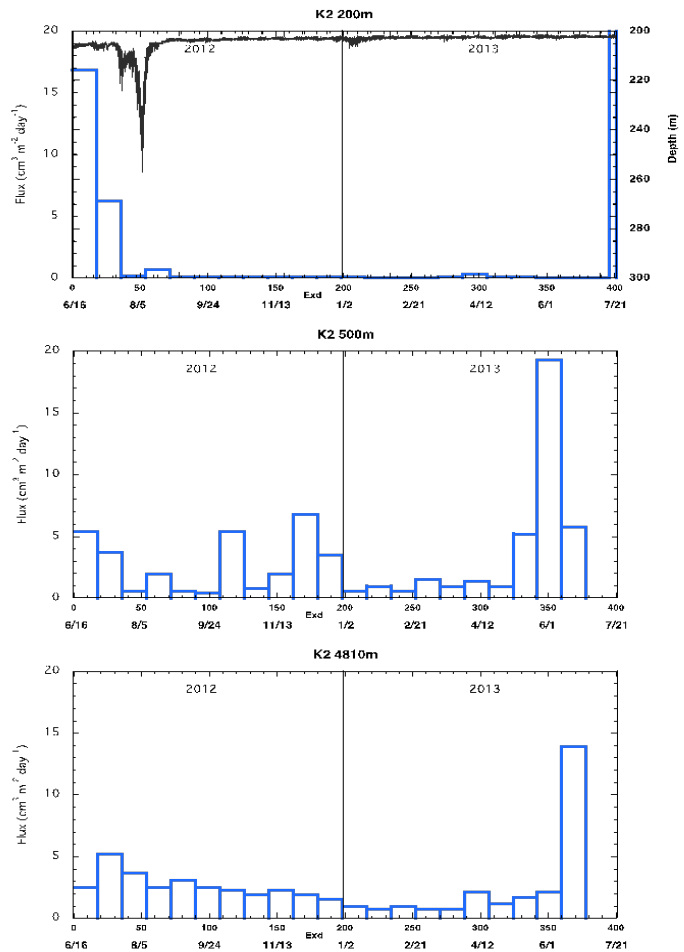


Fig.3.1.4.2 Total mass flux (bar graphs) at 200 m (upper), 500 m (middle) and 4810 m (bottom) of K2. Depth of 200 m sediment trap is shown in upper panel.

3.2 Underwater profiling buoy system (Primary productivity profiler)

3.2.1 POPPS

Tetsuichi FUJIKI (JAMSTEC)

Tomoyuki TAKAMORI (MWJ)

Tetsuya NAKAMURA (Nichiyu Giken Kogyo)

(1) Objective

An understanding of the variability in phytoplankton productivity provides a basic knowledge of how aquatic ecosystems are structured and functioning. The primary productivity of the world oceans has been measured mostly by the radiocarbon tracer method or the oxygen evolution method. As these traditional methods use the uptake of radiocarbon into particulate matter or changes in oxygen concentration in the bulk fluid, measurements require bottle incubations for periods ranging from hours to a day. This methodological limitation has hindered our understanding of the variability of oceanic primary productivity. To overcome these problems, algorithms for estimating primary productivity by using satellite ocean color imagery have been developed and improved. However, one of the major obstacles to the development and improvement of these algorithms is a lack of *in situ* primary productivity data to verify the satellite estimates.

During the past decade, the utilization of active fluorescence techniques in biological oceanography has brought marked progress in our understanding of phytoplankton photosynthesis in the oceans. Above all, fast repetition rate (FRR) fluorometry reduces the primary electron acceptor (Q_a) in photosystem (PS) II by a series of subsaturating flashlets and can measure a single turnover fluorescence induction curve in PSII. The PSII parameters derived from the fluorescence induction curve provide information on the physiological state related to photosynthesis and can be used to estimate gross primary productivity. FRR fluorometry has several advantages over the above-mentioned traditional methods. Most importantly, because measurements made by FRR fluorometry can be carried out without the need for time-consuming bottle incubations, this method enables real-time high-frequency measurements of primary productivity. In addition, the FRR fluorometer can be used in platform systems such as moorings, drifters, and floats.

The current study aimed to assess the vertical and temporal variations in PSII parameters and primary productivity in the western Pacific, by using an underwater profiling buoy system that uses the FRR fluorometer (system name: Primary productivity profiler)

(2) Methods

a) Primary productivity profiler

The primary productivity profiler (original design by Nichiyu Giken Kogyo) consisted mainly of an observation buoy equipped with a submersible FRR fluorometer (Diving Flash, Kimoto Electric), a scalar irradiance sensor (QSP-2200, Biospherical Instruments), a CTD sensor (MCTD, Falmouth Scientific) and a dissolved oxygen sensor (Compact Optode, Alec Electronics), an underwater winch, an acoustic Doppler current profiler (Workhorse Long Ranger, Teledyne RD Instruments) and an acoustic releaser (Fig. 1). The observation buoy

moved between the winch depth and the surface at a rate of 0.2 m s^{-1} and measured the vertical profiles of phytoplankton fluorescence, irradiance, temperature, salinity and dissolved oxygen. The profiling rate of the observation buoy was set to 0.2 m s^{-1} to detect small-scale variations (approx. 1 m) in the vertical profile. To minimize biofouling of instruments, the underwater winch was placed below the euphotic layer so that the observation buoy was exposed to light only during the measurement period. In addition, the vertical migration of observation buoy reduced biofouling of instruments.

b) Measurement principle of FRR fluorometer

The FRR fluorometer consists of closed dark and open light chambers that measure the fluorescence induction curves of phytoplankton samples in darkness and under actinic illumination. To allow relaxation of photochemical quenching of fluorescence, the FRR fluorometer allows samples in the dark chamber to dark adapt for about 1 s before measurements. To achieve cumulative saturation of PSII within $150 \mu\text{s}$ — i.e., a single photochemical turnover — the instrument generates a series of subsaturating blue flashes at a light intensity of $25 \text{ mmol quanta m}^{-2} \text{ s}^{-1}$ and a repetition rate of about 250 kHz. The PSII parameters are derived from the single-turnover-type fluorescence induction curve by using the numerical fitting procedure described by Kolber et al. (1998). Analysis of fluorescence induction curves measured in the dark and light chambers provides PSII parameters such as fluorescence yields, photochemical efficiency and effective absorption cross section of PSII, which are indicators of the physiological state related to photosynthesis. Using the PSII parameters, the rate of photosynthetic electron transport and the gross primary productivity can be estimated.

c) Site description and observations

The primary productivity profiler deployed at station S1 in MR12-02 was recovered on 14 July 2013 (UTC). In addition, the primary productivity profiler was newly-deployed on 16 July 2013 (UTC) (Fig. 2, target position: $29^{\circ} 56.268 \text{ N}$, $144^{\circ} 58.513 \text{ E}$, 5915 m; actual position: $29^{\circ} 56.152 \text{ N}$, $144^{\circ} 58.449 \text{ E}$, 5912 m). The measurements began on 18 July 2013 and will continue until 1 July 2014.

Measurement schedule at station S1 (Japan time)

1. 13/07/18 02:00	2. 13/07/18 11:00	3. 13/07/22 02:00	4. 13/07/22 11:00
5. 13/07/26 02:00	6. 13/07/26 11:00	7. 13/07/30 02:00	8. 13/07/30 11:00
9. 13/08/03 02:00	10. 13/08/03 11:00	11. 13/08/07 02:00	12. 13/08/07 11:00
13. 13/08/11 02:00	14. 13/08/11 11:00	15. 13/08/15 02:00	16. 13/08/15 11:00
17. 13/08/19 02:00	18. 13/08/19 11:00	19. 13/08/23 02:00	20. 13/08/23 11:00
21. 13/08/27 02:00	22. 13/08/27 11:00	23. 13/08/31 02:00	24. 13/08/31 11:00
25. 13/09/04 02:00	26. 13/09/04 11:00	27. 13/09/08 02:00	28. 13/09/08 11:00
29. 13/09/12 02:00	30. 13/09/12 11:00	31. 13/09/16 02:00	32. 13/09/16 11:00
33. 13/09/20 02:00	34. 13/09/20 11:00	35. 13/09/24 02:00	36. 13/09/24 11:00
37. 13/09/28 02:00	38. 13/09/28 11:00	39. 13/10/02 02:00	40. 13/10/02 11:00
41. 13/10/06 02:00	42. 13/10/06 11:00	43. 13/10/10 02:00	44. 13/10/10 11:00
45. 13/10/14 02:00	46. 13/10/14 11:00	47. 13/10/18 02:00	48. 13/10/18 11:00

49. 13/10/22 02:00	50. 13/10/22 11:00	51. 13/10/26 02:00	52. 13/10/26 11:00
53. 13/10/30 02:00	54. 13/10/30 11:00	55. 13/11/03 02:00	56. 13/11/03 11:00
57. 13/11/07 02:00	58. 13/11/07 11:00	59. 13/11/11 02:00	60. 13/11/11 11:00
61. 13/11/15 02:00	62. 13/11/15 11:00	63. 13/11/19 02:00	64. 13/11/19 11:00
65. 13/11/23 02:00	66. 13/11/23 11:00	67. 13/11/27 02:00	68. 13/11/27 11:00
69. 13/12/01 02:00	70. 13/12/01 11:00	71. 13/12/05 02:00	72. 13/12/05 11:00
73. 13/12/09 02:00	74. 13/12/09 11:00	75. 13/12/13 02:00	76. 13/12/13 11:00
77. 13/12/17 02:00	78. 13/12/17 11:00	79. 13/12/21 02:00	80. 13/12/21 11:00
81. 13/12/25 02:00	82. 13/12/25 11:00	83. 13/12/29 02:00	84. 13/12/29 11:00
85. 14/01/02 02:00	86. 14/01/02 11:00	87. 14/01/06 02:00	88. 14/01/06 11:00
89. 14/01/10 02:00	90. 14/01/10 11:00	91. 14/01/14 02:00	92. 14/01/14 11:00
93. 14/01/18 02:00	94. 14/01/18 11:00	95. 14/01/22 02:00	96. 14/01/22 11:00
97. 14/01/26 02:00	98. 14/01/26 11:00	99. 14/01/30 02:00	100. 14/01/30 11:00
101. 14/02/03 02:00	102. 14/02/03 11:00	103. 14/02/07 02:00	104. 14/02/07 11:00
105. 14/02/11 02:00	106. 14/02/11 11:00	107. 14/02/15 02:00	108. 14/02/15 11:00
109. 14/02/19 02:00	110. 14/02/19 11:00	111. 14/02/23 02:00	112. 14/02/23 11:00
113. 14/02/27 02:00	114. 14/02/27 11:00	115. 14/03/03 02:00	116. 14/03/03 11:00
117. 14/03/07 02:00	118. 14/03/07 11:00	119. 14/03/11 02:00	120. 14/03/11 11:00
121. 14/03/15 02:00	122. 14/03/15 11:00	123. 14/03/19 02:00	124. 14/03/19 11:00
125. 14/03/23 02:00	126. 14/03/23 11:00	127. 14/03/27 02:00	128. 14/03/27 11:00
129. 14/03/31 02:00	130. 14/03/31 11:00	131. 14/04/04 02:00	132. 14/04/04 11:00
133. 14/04/08 02:00	134. 14/04/08 11:00	135. 14/04/12 02:00	136. 14/04/12 11:00
137. 14/04/16 02:00	138. 14/04/16 11:00	139. 14/04/20 02:00	140. 14/04/20 11:00
141. 14/04/24 02:00	142. 14/04/24 11:00	143. 14/04/28 02:00	144. 14/04/28 11:00
145. 14/05/02 02:00	146. 14/05/02 11:00	147. 14/05/06 02:00	148. 14/05/06 11:00
149. 14/05/10 02:00	150. 14/05/10 11:00	151. 14/05/14 02:00	152. 14/05/14 11:00
153. 14/05/18 02:00	154. 14/05/18 11:00	155. 14/05/22 02:00	156. 14/05/22 11:00
157. 14/05/26 02:00	158. 14/05/26 11:00	159. 14/05/30 02:00	160. 14/05/30 11:00
161. 14/06/03 02:00	162. 14/06/03 11:00	163. 14/06/07 02:00	164. 14/06/07 11:00
165. 14/06/11 02:00	166. 14/06/11 11:00	167. 14/06/15 02:00	168. 14/06/15 11:00
169. 14/06/19 02:00	170. 14/06/19 11:00	171. 14/06/23 02:00	172. 14/06/23 11:00
173. 14/06/27 02:00	174. 14/06/27 11:00	175. 14/07/01 02:00	176. 14/07/01 11:00

(3) References

Kolber, Z. S., O. Prášil and P. G. Falkowski. 1998. Measurements of variable chlorophyll fluorescence using fast repetition rate techniques: defining methodology and experimental protocols. *Biochim. Biophys. Acta*. 1367: 88-106.

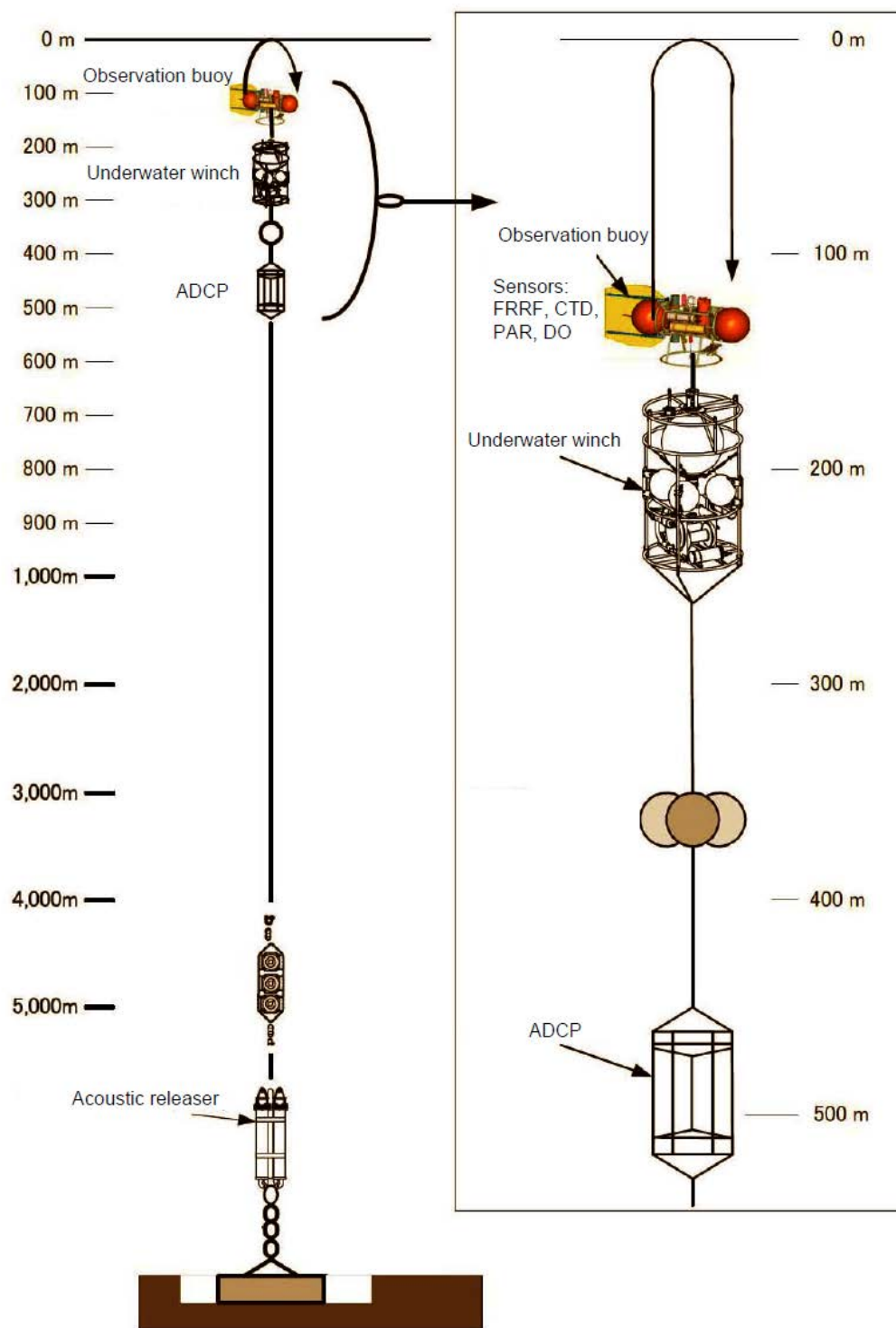


Figure 1. Schematic diagram of the primary productivity profiler.

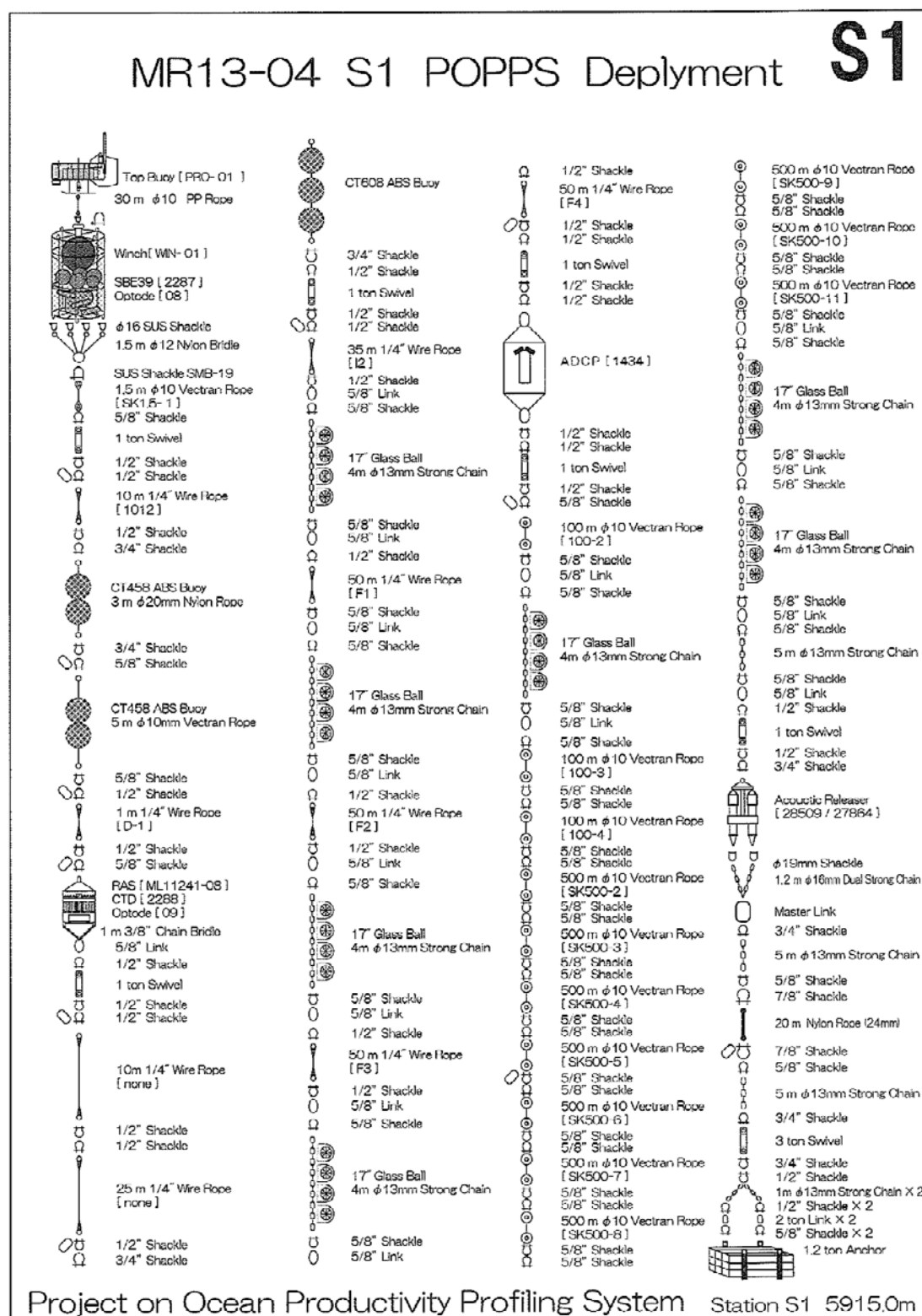


Figure 2. Detailed design of the primary productivity profiler deployed at station S1 in MR13-04.

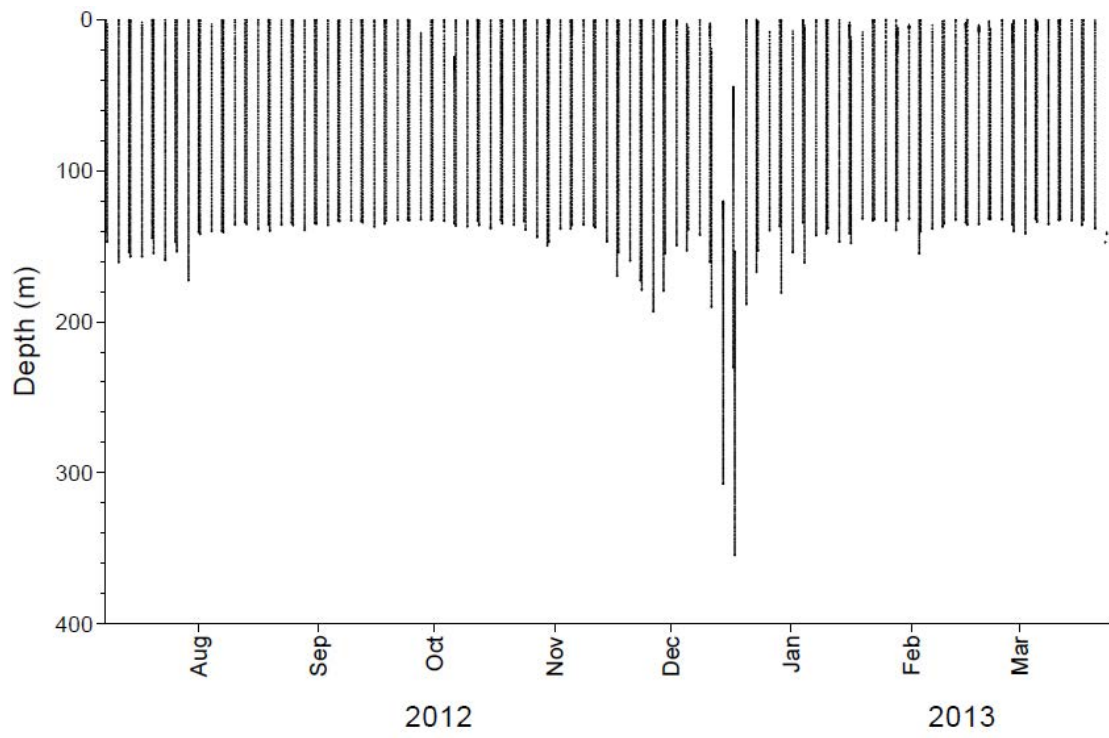


Figure 3. The operating condition of observation buoy in the primary productivity profiler recovered from station S1.

3.2.2 RAS

Masahide WAKITA (JAMSTEC, MIO)

3.1.4.1. Preliminary results

(1) Pressure, temperature and salinity at remote automatic water sampler (RAS)

Pressure, temperature and salinity by SBE-37 SM (Sea-birds) were observed every a half hour attached on RAS and POPPS WINCH frames. RAS and POPPS WINCH were located at ~200 db and ~180 db, respectively (Fig. 1a). Temperature and salinity at RAS and WINCH were generally constant all year around (Fig. 1b and 1c). However, both RAS and WINCH were sometimes deepened by approximately 20 db. It was noteworthy that both RAS and WINCH were deepened in winter 2011. It is suspected that strong current took place and mooring system might be largely forced to be tilted.

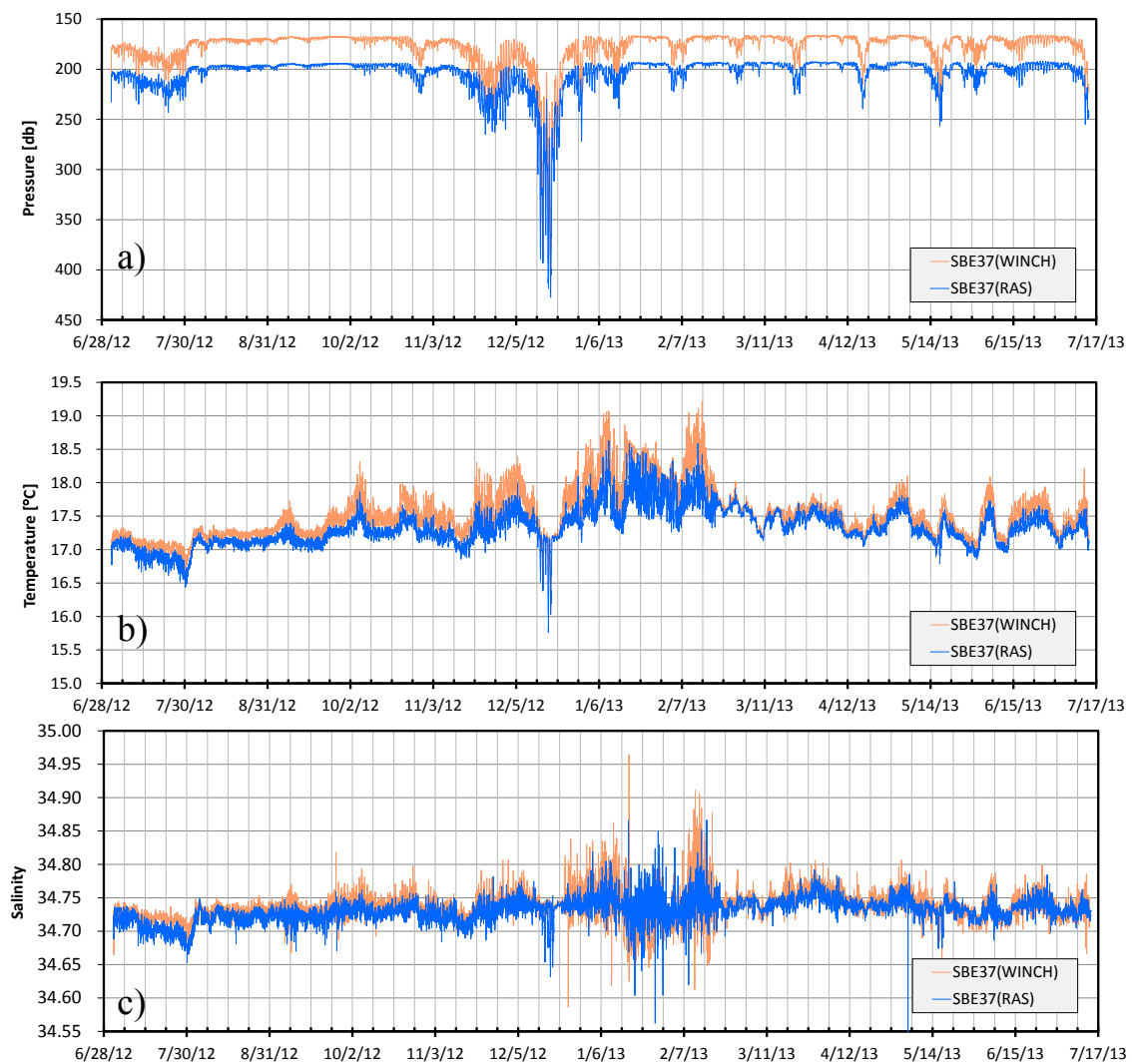


Figure 1 Pressure (a), temperature (b) and Salinity (c) at RAS and POPPS during deployment.

(2) Chemical analysis of RAS sample

RAS worked following schedule and obtained samples of dissolved inorganic carbon (DIC), total alkalinity (TA), nutrients (Phosphate, Nitrate + Nitrite, Silicate), density, $^{15}\text{NO}_3^-$ and salinity (Table 1). $^{15}\text{NO}_3^-$ will be measured by Nagoya Univ/RIGC. However, the volume of last sample bag after collecting (#48) was quite small. This samples leaked with holes and couldn't measure DIC, TA, nutrients, density, $^{15}\text{NO}_3^-$ and salinity

Salinity of RAS seawater samples will be measured by salinometer (Model 8400B "AUTOSAL" Guildline Instruments). Salinity of RAS samples should be lower than ambient seawater, because RAS samples were diluted with HgCl_2 solution and Milli-Q water. Salinity measured by salinometer will be slightly lower than that observed by SBE-37 sensor (CTD). RAS samples (~500ml) were diluted with 0.5 ml of HgCl_2 for preservative and 1.0 ml of Milli-Q water for pressure-resistance of sample tube. For chemical properties, the dilutions of RAS samples by HgCl_2 must be corrected by a ratio of salinity by SBE-37 to that by salinometer. Preliminary results of uncorrected chemical analysis of RAS sample are shown in Figs. 2a to 2b.

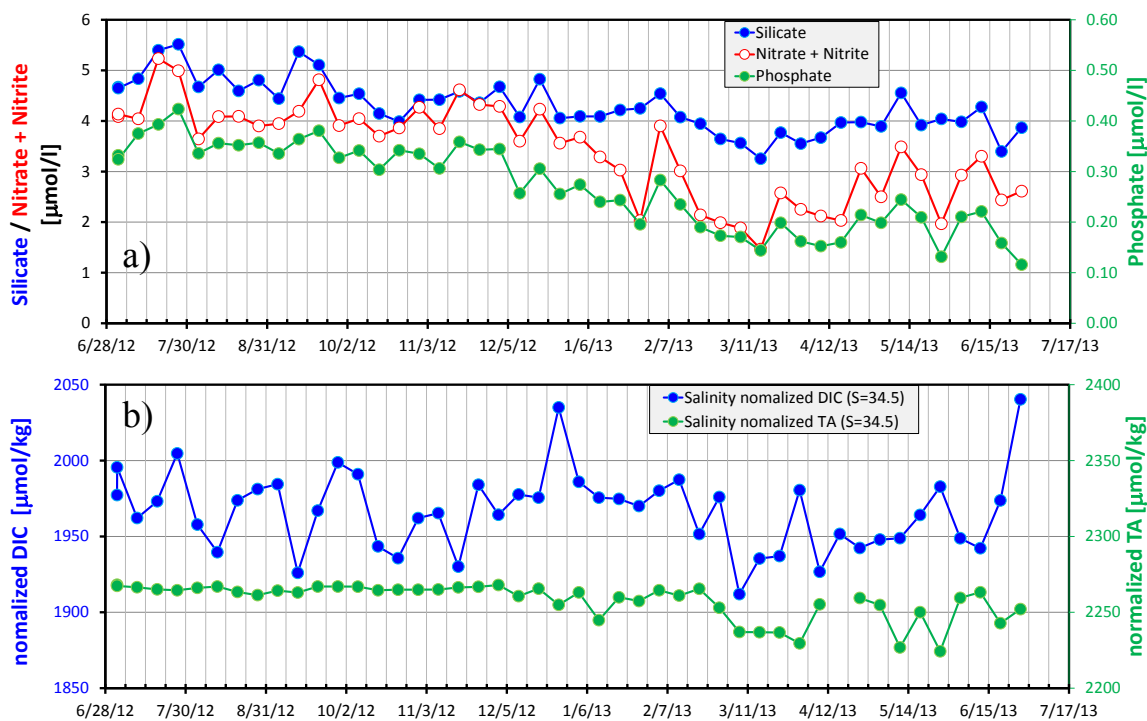


Figure 2 Measurements of nutrients (phosphate, nitrate, and silicate) (a) and, TA and DIC (b) collected by RAS during deployment.

Table 1 RAS sample list at S1.

RAS No.	Date		Memo	RIGC					RIGC/NU	RIGC	Memo
	Interval 8 days			Volume	DIC	TA	Nutrients	Density	¹⁵ NO ₃ ⁻	Salinity	
	#	mm/dd/yyyy									
1	07/02/2012	19:00:00	Saturated HgCl ₂ 0.5ml	L	1	1	2	1	1	1	
2	07/02/2012	19:40:00	Saturated HgCl ₂ 0.5ml	L	1	1	2	1	1	1	
3	07/10/2012	19:00:00	Saturated HgCl ₂ 0.5ml	L	1	1	2	1	1	1	
4	07/18/2012	19:00:00	Saturated HgCl ₂ 0.5ml	L	1	1	2	1	1	1	
5	07/26/2012	19:00:00	Saturated HgCl ₂ 0.5ml	L	1	1	2	1	1	1	
6	08/03/2012	19:00:00	Saturated HgCl ₂ 0.5ml	L	1	1	2	1	1	1	
7	08/11/2012	19:00:00	Saturated HgCl ₂ 0.5ml	L	1	1	2	1	1	1	
8	08/19/2012	19:00:00	Saturated HgCl ₂ 0.5ml	L	1	1	2	1	1	1	
9	08/27/2012	19:00:00	Saturated HgCl ₂ 0.5ml	L	1	1	2	1	1	1	
10	09/04/2012	19:00:00	Saturated HgCl ₂ 0.5ml	L	1	1	2	1	1	1	
11	09/12/2012	19:00:00	Saturated HgCl ₂ 0.5ml	L	1	1	2	1	1	1	
12	09/20/2012	19:00:00	Saturated HgCl ₂ 0.5ml	L	1	1	2	1	1	1	
13	09/28/2012	19:00:00	Saturated HgCl ₂ 0.5ml	L	1	1	2	1	1	1	
14	10/06/2012	19:00:00	Saturated HgCl ₂ 0.5ml	L	1	1	2	1	1	1	
15	10/14/2012	19:00:00	Saturated HgCl ₂ 0.5ml	L	1	1	2	1	1	1	
16	10/22/2012	19:00:00	Saturated HgCl ₂ 0.5ml	L	1	1	2	1	1	1	
17	10/30/2012	19:00:00	Saturated HgCl ₂ 0.5ml	L	1	1	2	1	1	1	
18	11/07/2012	19:00:00	Saturated HgCl ₂ 0.5ml	L	1	1	2	1	1	1	
19	11/15/2012	19:00:00	Saturated HgCl ₂ 0.5ml	L	1	1	2	1	1	1	
20	11/23/2012	19:00:00	Saturated HgCl ₂ 0.5ml	L	1	1	2	1	1	1	
21	12/01/2012	19:00:00	Saturated HgCl ₂ 0.5ml	L	1	1	2	1	1	1	
22	12/09/2012	19:00:00	Saturated HgCl ₂ 0.5ml	L	1	1	2	1	1	1	
23	12/17/2012	19:00:00	Saturated HgCl ₂ 0.5ml	L	1	1	2	1	1	1	
24	12/25/2012	19:00:00	Saturated HgCl ₂ 0.5ml	L	1	1	2	1	1	1	
25	01/02/2013	19:00:00	Saturated HgCl ₂ 0.5ml	L	1	1	2	1	1	1	
26	01/10/2013	19:00:00	Saturated HgCl ₂ 0.5ml	L	1	1	2	1	1	1	
27	01/18/2013	19:00:00	Saturated HgCl ₂ 0.5ml	L	1	1	2	1	1	1	
28	01/26/2013	19:00:00	Saturated HgCl ₂ 0.5ml	L	1	1	2	1	1	1	
29	02/03/2013	19:00:00	Saturated HgCl ₂ 0.5ml	L	1	1	2	1	1	1	
30	02/11/2013	19:00:00	Saturated HgCl ₂ 0.5ml	L	1	1	2	1	1	1	
31	02/19/2013	19:00:00	Saturated HgCl ₂ 0.5ml	L	1	1	2	1	1	1	
32	02/27/2013	19:00:00	Saturated HgCl ₂ 0.5ml	L	1	1	2	1	1	1	
33	03/07/2013	19:00:00	Saturated HgCl ₂ 0.5ml	L	1	1	2	1	1	1	
34	03/15/2013	19:00:00	Saturated HgCl ₂ 0.5ml	L	1	1	2	1	1	1	
35	03/23/2013	19:00:00	Saturated HgCl ₂ 0.5ml	L	1	1	2	1	1	1	
36	03/31/2013	19:00:00	Saturated HgCl ₂ 0.5ml	L	1	1	2	1	1	1	
37	04/08/2013	19:00:00	Saturated HgCl ₂ 0.5ml	L	1	1	2	1	1	1	
38	04/16/2013	19:00:00	Saturated HgCl ₂ 0.5ml	L	1	1	2	1	1	1	
39	04/24/2013	19:00:00	Saturated HgCl ₂ 0.5ml	L	1	1	2	1	1	1	
40	05/02/2013	19:00:00	Saturated HgCl ₂ 0.5ml	L	1	1	2	1	1	1	
41	05/10/2013	19:00:00	Saturated HgCl ₂ 0.5ml	L	1	1	2	1	1	1	
42	05/18/2013	19:00:00	Saturated HgCl ₂ 0.5ml	L	1	1	2	1	1	1	
43	05/26/2013	19:00:00	Saturated HgCl ₂ 0.5ml	L	1	1	2	1	1	1	
44	06/03/2013	19:00:00	Saturated HgCl ₂ 0.5ml	L	1	1	2	1	1	1	
45	06/11/2013	19:00:00	Saturated HgCl ₂ 0.5ml	L	1	1	2	1	1	1	
46	06/19/2013	19:00:00	Saturated HgCl ₂ 0.5ml	L	1	1	2	1	1	1	
47	06/27/2013	19:00:00	Saturated HgCl ₂ 0.5ml	L	1	1	2	1	1	1	
48	07/05/2013	19:00:00	Saturated HgCl ₂ 0.5ml	S	0	0	0	0	0	0	Hole in bag

3.1.4.2. RAS sampling schedule

Sampling schedule of time-series remote automatic water sampler (RAS) of POPPS mooring at station S1 is as follows;

S1 RAS 250m POPPS

RAS No.	Date		Memo
	Interval 8 days		
#	mm/dd/yyyy	Time(JST)	
1	07/17/2013	7:00:00	20% Saturated HgCl ₂ 2.5ml
2	07/17/2013	7:40:00	20% Saturated HgCl ₂ 2.5ml
3	07/25/2013	7:00:00	20% Saturated HgCl ₂ 2.5ml
4	08/02/2013	7:00:00	20% Saturated HgCl ₂ 2.5ml
5	08/10/2013	7:00:00	20% Saturated HgCl ₂ 2.5ml
6	08/18/2013	7:00:00	20% Saturated HgCl ₂ 2.5ml
7	08/26/2013	7:00:00	20% Saturated HgCl ₂ 2.5ml
8	09/03/2013	7:00:00	20% Saturated HgCl ₂ 2.5ml
9	09/11/2013	7:00:00	20% Saturated HgCl ₂ 2.5ml
10	09/19/2013	7:00:00	20% Saturated HgCl ₂ 2.5ml
11	09/27/2013	7:00:00	20% Saturated HgCl ₂ 2.5ml
12	10/05/2013	7:00:00	20% Saturated HgCl ₂ 2.5ml
13	10/13/2013	7:00:00	20% Saturated HgCl ₂ 2.5ml
14	10/21/2013	7:00:00	20% Saturated HgCl ₂ 2.5ml
15	10/29/2013	7:00:00	20% Saturated HgCl ₂ 2.5ml
16	11/06/2013	7:00:00	20% Saturated HgCl ₂ 2.5ml
17	11/14/2013	7:00:00	20% Saturated HgCl ₂ 2.5ml
18	11/22/2013	7:00:00	20% Saturated HgCl ₂ 2.5ml
19	11/30/2013	7:00:00	20% Saturated HgCl ₂ 2.5ml
20	12/08/2013	7:00:00	20% Saturated HgCl ₂ 2.5ml
21	12/16/2013	7:00:00	20% Saturated HgCl ₂ 2.5ml
22	12/24/2013	7:00:00	20% Saturated HgCl ₂ 2.5ml
23	01/01/2014	7:00:00	20% Saturated HgCl ₂ 2.5ml
24	01/09/2014	7:00:00	20% Saturated HgCl ₂ 2.5ml
25	01/17/2014	7:00:00	20% Saturated HgCl ₂ 2.5ml
26	01/25/2014	7:00:00	20% Saturated HgCl ₂ 2.5ml
27	02/02/2014	7:00:00	20% Saturated HgCl ₂ 2.5ml
28	02/10/2014	7:00:00	20% Saturated HgCl ₂ 2.5ml
29	02/18/2014	7:00:00	20% Saturated HgCl ₂ 2.5ml
30	02/26/2014	7:00:00	20% Saturated HgCl ₂ 2.5ml
31	03/06/2014	7:00:00	20% Saturated HgCl ₂ 2.5ml
32	03/14/2014	7:00:00	20% Saturated HgCl ₂ 2.5ml
33	03/22/2014	7:00:00	20% Saturated HgCl ₂ 2.5ml
34	03/30/2014	7:00:00	20% Saturated HgCl ₂ 2.5ml
35	04/07/2014	7:00:00	20% Saturated HgCl ₂ 2.5ml
36	04/15/2014	7:00:00	20% Saturated HgCl ₂ 2.5ml
37	04/23/2014	7:00:00	20% Saturated HgCl ₂ 2.5ml
38	05/01/2014	7:00:00	20% Saturated HgCl ₂ 2.5ml
39	05/09/2014	7:00:00	20% Saturated HgCl ₂ 2.5ml
40	05/17/2014	7:00:00	20% Saturated HgCl ₂ 2.5ml
41	05/25/2014	7:00:00	20% Saturated HgCl ₂ 2.5ml
42	06/02/2014	7:00:00	20% Saturated HgCl ₂ 2.5ml
43	06/10/2014	7:00:00	20% Saturated HgCl ₂ 2.5ml
44	06/18/2014	7:00:00	20% Saturated HgCl ₂ 2.5ml
45	06/26/2014	7:00:00	20% Saturated HgCl ₂ 2.5ml
46	07/04/2014	7:00:00	20% Saturated HgCl ₂ 2.5ml
47	07/12/2014	7:00:00	20% Saturated HgCl ₂ 2.5ml
48	07/12/2014	7:40:00	20% Saturated HgCl ₂ 2.5ml

Interval 40 minutes

for duplicate sampling

Interval 40 minutes

for duplicate sampling

Sampling schedule of time-series remote automatic water sampler (RAS) of BGC mooring in 100m at station K2 is as follows;

K2 RAS 100m BGC

RAS No.	Date		Memo	
	Interval 8 days			
#	mm/dd/yyyy	Time(JST)		
1	07/25/2013	16:00:00	20% Saturated HgCl ₂ 2.5ml	Interval 40 minutes for duplicate sampling
2	07/25/2013	16:40:00	20% Saturated HgCl ₂ 2.5ml	
3	08/02/2013	16:00:00	20% Saturated HgCl ₂ 2.5ml	
4	08/10/2013	16:00:00	20% Saturated HgCl ₂ 2.5ml	
5	08/18/2013	16:00:00	20% Saturated HgCl ₂ 2.5ml	
6	08/26/2013	16:00:00	20% Saturated HgCl ₂ 2.5ml	
7	09/03/2013	16:00:00	20% Saturated HgCl ₂ 2.5ml	
8	09/11/2013	16:00:00	20% Saturated HgCl ₂ 2.5ml	
9	09/19/2013	16:00:00	20% Saturated HgCl ₂ 2.5ml	
10	09/27/2013	16:00:00	20% Saturated HgCl ₂ 2.5ml	
11	10/05/2013	16:00:00	20% Saturated HgCl ₂ 2.5ml	
12	10/13/2013	16:00:00	20% Saturated HgCl ₂ 2.5ml	
13	10/21/2013	16:00:00	20% Saturated HgCl ₂ 2.5ml	
14	10/29/2013	16:00:00	20% Saturated HgCl ₂ 2.5ml	
15	11/06/2013	16:00:00	20% Saturated HgCl ₂ 2.5ml	
16	11/14/2013	16:00:00	20% Saturated HgCl ₂ 2.5ml	
17	11/22/2013	16:00:00	20% Saturated HgCl ₂ 2.5ml	
18	11/30/2013	16:00:00	20% Saturated HgCl ₂ 2.5ml	
19	12/08/2013	16:00:00	20% Saturated HgCl ₂ 2.5ml	
20	12/16/2013	16:00:00	20% Saturated HgCl ₂ 2.5ml	
21	12/24/2013	16:00:00	20% Saturated HgCl ₂ 2.5ml	
22	01/01/2014	16:00:00	20% Saturated HgCl ₂ 2.5ml	
23	01/09/2014	16:00:00	20% Saturated HgCl ₂ 2.5ml	
24	01/17/2014	16:00:00	20% Saturated HgCl ₂ 2.5ml	
25	01/25/2014	16:00:00	20% Saturated HgCl ₂ 2.5ml	
26	02/02/2014	16:00:00	20% Saturated HgCl ₂ 2.5ml	Interval 4 day for winter sampling
27	02/06/2014	16:00:00	20% Saturated HgCl ₂ 2.5ml	
28	02/10/2014	16:00:00	20% Saturated HgCl ₂ 2.5ml	
29	02/14/2014	16:00:00	20% Saturated HgCl ₂ 2.5ml	
30	02/18/2014	16:00:00	20% Saturated HgCl ₂ 2.5ml	
31	02/22/2014	16:00:00	20% Saturated HgCl ₂ 2.5ml	
32	02/26/2014	16:00:00	20% Saturated HgCl ₂ 2.5ml	
33	03/02/2014	16:00:00	20% Saturated HgCl ₂ 2.5ml	
34	03/06/2014	16:00:00	20% Saturated HgCl ₂ 2.5ml	
35	03/10/2014	16:00:00	20% Saturated HgCl ₂ 2.5ml	
36	03/14/2014	16:00:00	20% Saturated HgCl ₂ 2.5ml	
37	03/18/2014	16:00:00	20% Saturated HgCl ₂ 2.5ml	
38	03/22/2014	16:00:00	20% Saturated HgCl ₂ 2.5ml	
39	03/26/2014	16:00:00	20% Saturated HgCl ₂ 2.5ml	
40	03/30/2014	16:00:00	20% Saturated HgCl ₂ 2.5ml	
41	04/03/2014	16:00:00	20% Saturated HgCl ₂ 2.5ml	
42	04/07/2014	16:00:00	20% Saturated HgCl ₂ 2.5ml	
43	04/11/2014	16:00:00	20% Saturated HgCl ₂ 2.5ml	
44	04/15/2014	16:00:00	20% Saturated HgCl ₂ 2.5ml	
45	04/19/2014	16:00:00	20% Saturated HgCl ₂ 2.5ml	
46	04/27/2014	16:00:00	20% Saturated HgCl ₂ 2.5ml	
47	05/05/2014	16:00:00	20% Saturated HgCl ₂ 2.5ml	Interval 40 minutes for duplicate sampling
48	05/05/2014	16:40:00	20% Saturated HgCl ₂ 2.5ml	

3.3 Phytoplankton

3.3.1 Chlorophyll *a* measurements by fluorometric determination

Kazuhiko MATSUMOTO (JAMSTEC)

Hideki YAMAMOTO (MWJ)

Hironori SATO (MWJ)

1. Objective

Phytoplankton biomass can estimate as the concentration of chlorophyll *a* (chl-*a*), because all oxygenic photosynthetic plankton contain chl-*a*. Phytoplankton exist various species in the ocean, but the species are roughly characterized by their cell size. The objective of this study is to investigate the vertical distribution of phytoplankton and their size fractionations as chl-*a* by using the fluorometric determination.

2. Sampling

Samplings of total chl-*a* were conducted from 7-16 depths between the surface and 200 m at all observational stations. At the cast for primary production, water samples were collected at 16 depths between the surface and 200 m at the station of S1 and K2.

3. Instruments and Methods

Water samples (0.25L) for total chl-*a* were filtered (<0.02 MPa) through 25mm-diameter Whatman GF/F filter. Size-fractionated chl-*a* were obtained by sequential filtration (<0.02 MPa) of 1-L water sample through 10- μ m, 3- μ m and 1- μ m polycarbonate filters (47-mm diameter) and Whatman GF/F filter (25-mm diameter). Phytoplankton pigments retained on the filters were immediately extracted in a polypropylene tube with 7 ml of N,N-dimethylformamide (Suzuki and Ishimaru, 1990). Those tubes were stored at -20°C under the dark condition to extract chl-*a* for 24 hours or more.

Fluorescences of each sample were measured by Turner Design fluorometer (10-AU-005), which was calibrated against a pure chl-*a* (Sigma-Aldrich Co.). We applied two kind of fluorometric determination for the samples of total chl-*a*: “Non-acidification method” (Welschmeyer, 1994) and “Acidification method” (Holm-Hansen *et al.*, 1965). Size-fractionated samples were applied only “Non-acidification method”. Analytical conditions of each method were listed in table 1.

4. Preliminary Results

The results of total chl-*a* at station S1 and K2 were shown in Figure 1 and 2. The results of total chl-*a* at station F1, KEO, JKEO, KNOT and E01 were shown in Figure 3. The results of size fractionated chl-*a* were shown in Figure4.

5. Data archives

The processed data file of pigments will be submitted to the JAMSTEC Data Integration and Analysis Group (DIAG) within a restricted period. Please ask PI for the latest information.

6. Reference

- Suzuki, R., and T. Ishimaru (1990), An improved method for the determination of phytoplankton chlorophyll using N, N-dimethylformamide, *J. Oceanogr. Soc. Japan*, 46, 190-194.
- Holm-Hansen, O., Lorenzen, C. J., Holmes, R.W. and J. D. H. Strickland (1965), Fluorometric determination of chlorophyll. *J. Cons. Cons. Int. Explor. Mer.* 30, 3-15.
- Welschmeyer, N. A. (1994), Fluorometric analysis of chlorophyll *a* in the presence of chlorophyll *b* and pheopigments. *Limnol. Oceanogr.* 39, 1985-1992.

Table 1. Analytical conditions of “Non-acidification method” and “Acidification method” for chlorophyll *a* with Turner Designs fluorometer (10-AU-005).

	Non-acidification method	Acidification method
Excitation filter (nm)	436	340-500
Emission filter (nm)	680	>665
Lamp	Blue Mercury Vapor	Daylight White

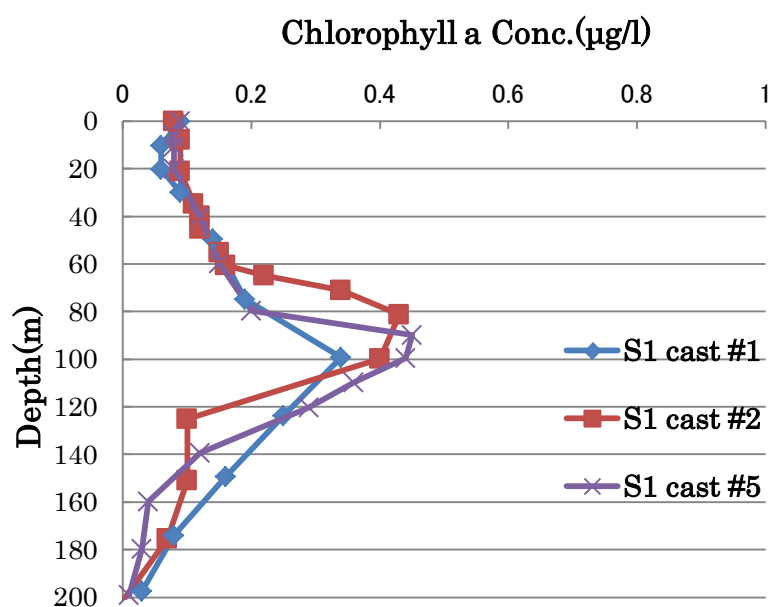


Figure1. Vertical distribution of chlorophyll *a* at Stn.S1 cast1,2 and 5

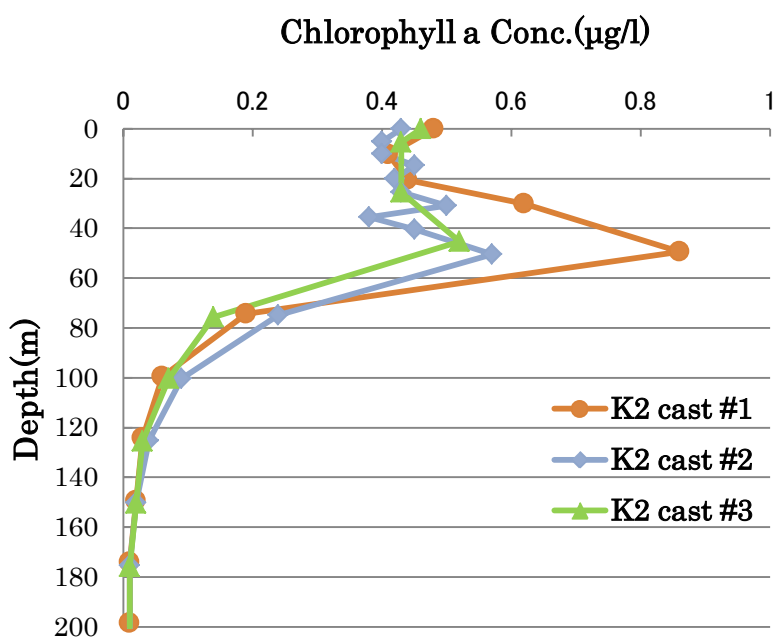


Figure2. Vertical distribution of chlorophyll *a* at Stn.K2 cast1,2, and 3

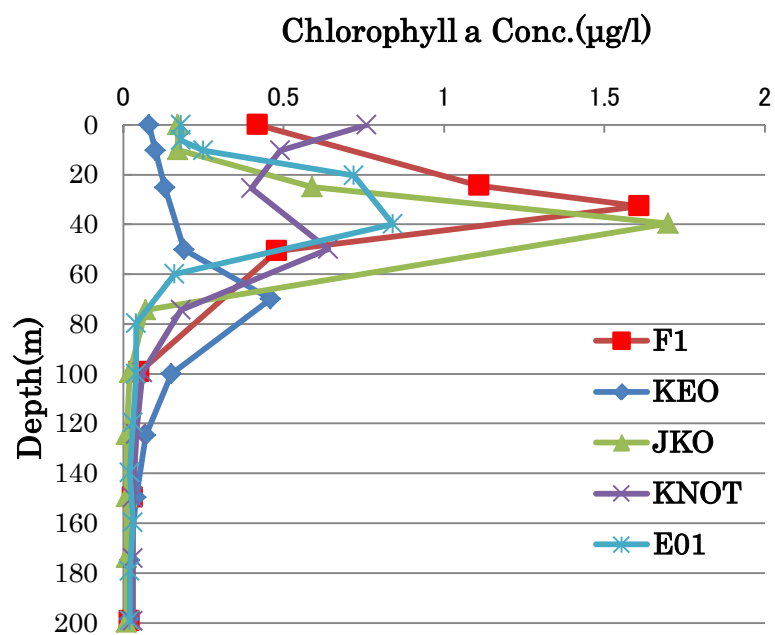


Figure3. Vertical distribution of chlorophyll *a* at Stn.F1, KEO, JKEO and KNOT.

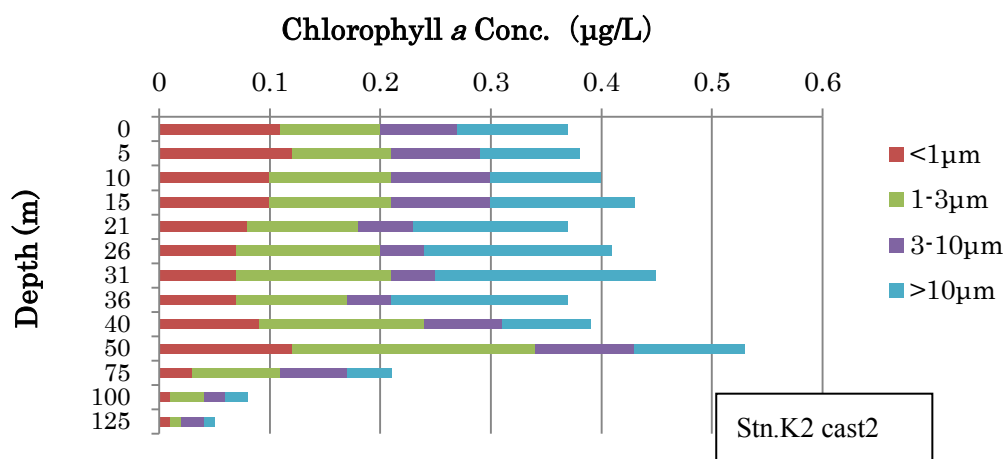
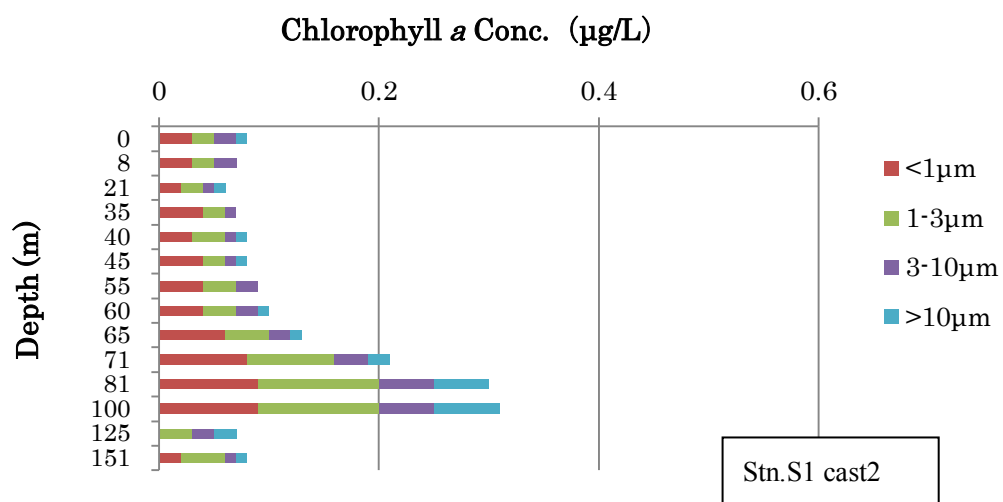


Figure4. Vertical distribution of size-fractionated chlorophyll *a*

3.3.2 HPLC measurements of marine phytoplankton pigments

Kazuhiko MATSUMOTO (JAMSTEC RIGC): Principal Investigator

Hironori SATO (Marine Works Japan Ltd.): Operation Leader

Hideki YAMAMOTO (Marine Works Japan Ltd.)

(1) Objective

The chemotaxonomic assessment of phytoplankton populations present in natural seawater requires taxon-specific algal pigments as good biochemical markers. A high-performance liquid chromatography (HPLC) measurement is an optimum method for separating and quantifying phytoplankton pigments in natural seawater. In this cruise, we measured the marine phytoplankton pigments by HPLC to investigate the marine phytoplankton community structure in the western North Pacific.

(2) Methods, Apparatus and Performance

Seawater samples were collected from 13 or 14 depths between the surface and 200 m at the cast for the primary production. Seawater samples were collected using Niskin bottles, except for the surface water, which was taken by a bucket. Seawater samples (2 to 3L) were filtered (<0.02 MPa) through the 47-mm diameter Whatman GF/F filter. To remove retaining seawater in the sample filters, GF/F filters were vacuum-dried in a freezer (0 °C) within 6 hours. Subsequently, phytoplankton pigments retained on a filter were extracted in a glass tube with 4 ml of N,N-dimethylformamide (HPLC-grade) for at least 24 hours in a freezer (-20 °C), and analyzed by HPLC within a few days.

Residua cells and filter debris were removed through polypropylene syringe filter (pore size: 0.2 µm) before the analysis. The samples injection of 500 µl was conducted by auto-sampler with the mixture of extracted pigments (350 µl), pure water (150 µl) and internal standard (10 µl). Phytoplankton pigments were quantified based on C₈ column method containing pyridine in the mobile phase (Zapata *et al.*, 2000).

(i) HPLC System

HPLC System was composed by Agilent 1200 modular system, G1311A Quaternary pump (low-pressure mixing system), G1329A auto-sampler and G1315D photodiode array detector.

(ii) Stationary phase

Analytical separation was performed using a YMC C₈ column (150×4.6 mm). The column was thermostatted at 35 °C in the column heater box.

(iii) Mobile phases

The eluant A was a mixture of methanol: acetonitrile: aqueous pyridine solution (0.25M pyridine), (50:25:25, v:v:v). The eluant B was a mixture of methanol: acetonitrile: acetone (20:60:20, v:v:v). Organic solvents for mobile phases were used reagents of HPLC-grade.

(iv) Calibrations

HPLC was calibrated using the standard pigments (Table 1).

(v) Internal standard

Ethyl-apo-8'-carotenoate was added into the samples prior to the injection as the internal standard. The mean chromatogram area and coefficient of variation (CV) of internal standard were estimated as the following two samples:

Standard samples (Figure 1): 202.5 ± 1.1 (n = 38), CV=0.5%

Seawater samples: 207.0 ± 2.7 (n = 51), CV=1.3%

(vi) Pigment detection and identification

Chlorophylls and carotenoids were detected by photodiode array spectroscopy (350~800 nm). Pigment concentrations were calculated from the chromatogram area at different five channels (Table 1). First channel was allocated at 409 nm of wavelength for the absorption maximum of Pheophorbide *a* and Pheophytin *a*. Second channel was allocated at 431 nm for the absorption maximum of chlorophyll *a*. Third channel was allocated at 440 nm for the absorption maximum of [3,8-divinyl]-protochlorophyllide. Fourth channel was allocated at 450 nm for other pigments. Fifth channel was allocated at 462 nm for chlorophyll *b*.

(3) Preliminary results

Vertical profiles of major pigments (Chlorophyll *a*, Chlorophyll *b*, Divinyl Chlorophyll *a*, Fucoxanthin, 19'-hexanoyloxyfucoxanthin, 19'-butanoyloxyfucoxanthin and zeaxanthin) at the station K2 and S1 were shown in Figure 2 and 3.

(4) Data archives

The processed data file of pigments will be submitted to the JAMSTEC Data Integration and Analyses Group (DIAG) within a restricted period. Please ask PI for the latest information.

(5) Reference

Zapata M, Rodriguez F, Garrido JL (2000), Separation of chlorophylls and carotenoids from marine phytoplankton: a new HPLC method using a reversed phase C₈ column and pyridine-containing mobile phases, *Mar. Ecol. Prog. Ser.*, 195, 29-45.

Table 1. Retention time and wavelength of identification for pigment standards.

No.	Pigment	Productions	Retention Time (minute)	Wavelength of identification (nm)
1	Chlorophyll <i>c3</i>	DHI Co.	8.057	462
2	Chlorophyllide <i>a</i>	DHI Co.	9.997	431
3	[3,8-Divinyl]-Protochlorophyllide	DHI Co.	10.583	440
4	Chlorophyll <i>c2</i>	DHI Co.	11.309	450
5	Peridinin	DHI Co.	14.415	450
6	Pheophorbide <i>a</i>	DHI Co.	16.481	409
7	19'-butanoyloxyfucoxanthin	DHI Co.	17.731	450
8	Fucoxanthin	DHI Co.	19.031	450
9	Neoxanthin	DHI Co.	19.269	440
10	Prasincoxanthin	DHI Co.	20.706	450
11	19'-hexanoyloxyfucoxanthin	DHI Co.	21.422	450
12	Violaxanthin	DHI Co.	21.514	440
13	Diadinoxanthin	DHI Co.	24.122	450
14	Dinoxanthin	DHI Co.	25.541	440
15	Antheraxanthin	DHI Co.	25.536	450
16	Alloxanthin	DHI Co.	26.869	450
17	Diatoxanthin	DHI Co.	27.858	450
18	Zeaxanthin	DHI Co.	28.612	450
19	Lutein	DHI Co.	28.807	450
20	Ethyl-apo-8'-carotenoate	Sigma-Aldrich Co.	30.565	462
21	Crococanthin	DHI Co.	32.654	450
22	Chlorophyll <i>b</i>	Sigma-Aldrich Co.	33.028	462
23	Divinyl Chlorophyll <i>a</i>	DHI Co.	34.146	440
24	Chlorophyll <i>a</i>	Sigma-Aldrich Co.	34.380	431
25	Pheophytin <i>a</i>	DHI Co.	36.514	409
26	Alpha-carotene	DHI Co.	37.145	450
27	Beta-carotene	DHI Co.	37.359	450

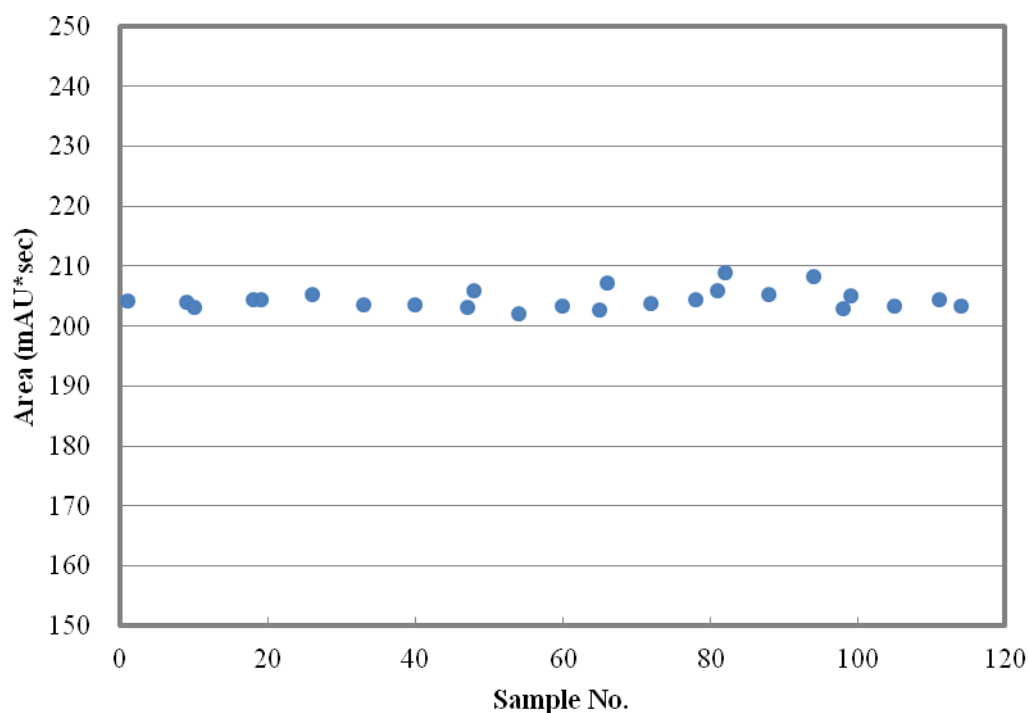


Figure 1. Variability of chromatogram areas for the internal standard.

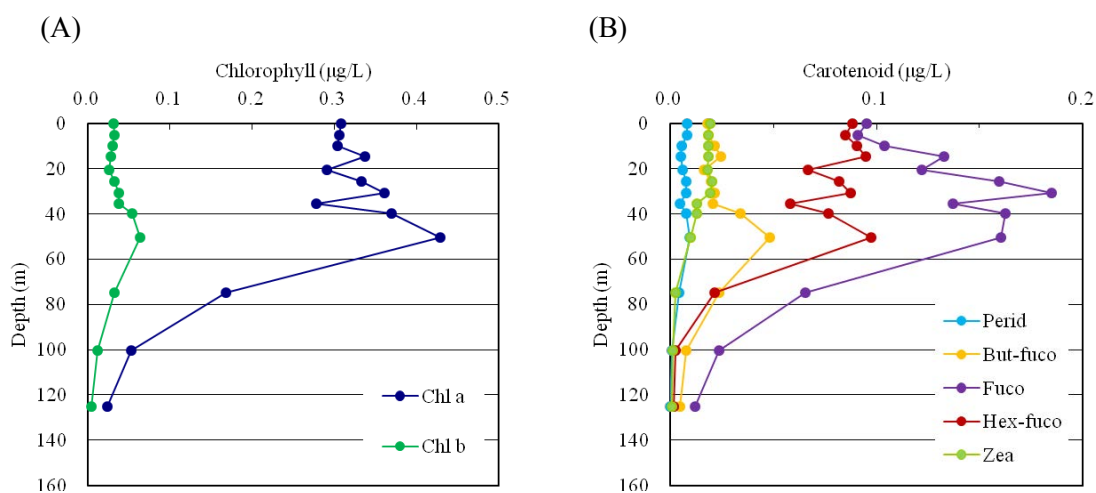


Figure 2-(A). Vertical distributions of major phytoplankton pigments (Chlorophyll *a*, Chlorophyll *b*) at Stn.K2 cast2.

Figure 2-(B). Vertical distributions of major phytoplankton pigments (Fucoxanthin, 19'-hexanoyloxyfucoxanthin, 19'-butanoyloxyfucoxanthin, Peridinin and Zeaxanthin) at Stn.K2 cast2.

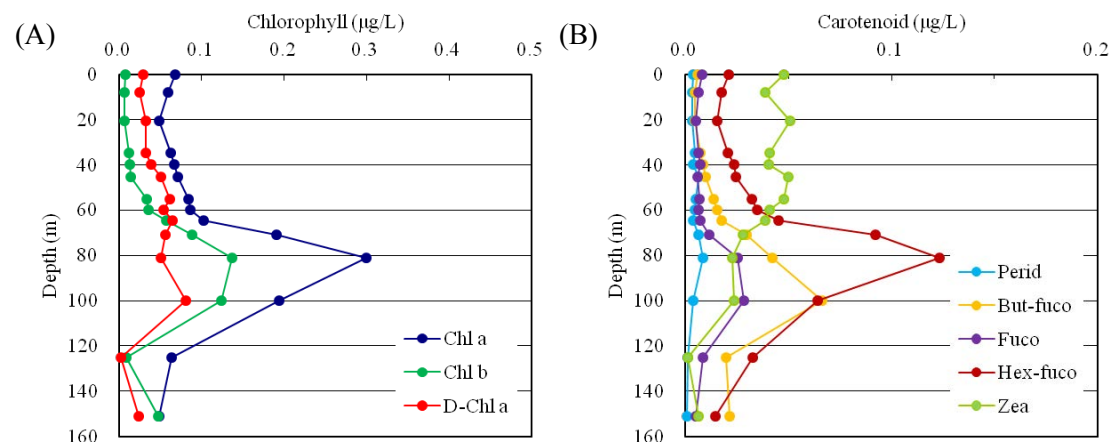


Figure 3-(A). Vertical distributions of major phytoplankton pigments (Chlorophyll *a*, Chlorophyll *b*, Divinyl Chlorophyll *a*) at Stn.S1 cast2.

Figure 3-(B). Vertical distributions of major phytoplankton pigments (Fucoxanthin, 19'-hexanoyloxyfucoxanthin, 19'-butanoyloxyfucoxanthin, Peridinin and Zeaxanthin) at Stn.S1 cast2.

3.3.3 Phytoplankton abundance

Kazuhiko MATSUMOTO (JAMSTEC RIGC)

(1) Objectives

The main objective of this study is to estimate phytoplankton abundances and their taxonomy in the subarctic gyre and the subtropical gyre in the western North Pacific. Phytoplankton abundances were measured with two kinds of methods: microscopy for large size phytoplankton and flowcytometry for small size phytoplankton.

(2) Sampling

Samplings were conducted using Niskin bottles, except for the surface water, which was taken by a bucket. Samplings were carried out at the two observational stations of K2 and S1.

(3) Methods

1) Microscopy

Water samples were placed in 500 ml plastic bottle at station K2 and in 1000 ml plastic bottle at station S1. Samples were fixed with neutral-buffered formalin solution (1% final concentration). The microscopic measurements are scheduled after the cruise.

2) Flowcytometry

2)-1 Equipment

The flowcytometry system used in this research was BRYTE HS system (Bio-Rad Laboratories Inc). System specifications are follows:

Light source: 75W Xenon arc lamp

Excitation wavelength: 350-650 nm

Detector: high-performance PMT

Analyzed volume: 75 μ l

Flow rate: 10 μ l min⁻¹

Sheath fluid: Milli-Q water

Filter block: B2 as excitation filter block, OR1 as fluorescence separator block

B2 and OR1 have ability as follows:

B2: Excitation filter 390-490 nm

 Beam-splitter 510 nm

 Emission filter 515-720 nm

OR1: Emission filter 1 565-605 nm

 Beam-splitter 600 nm

 Emission filter 2 >615 nm

2)-2 Measurements

The water samples were fixed immediately with glutaraldehyde (1% final concentration) and stored in the dark at 4°C. The analysis by the flow cytometer was acquired on board within 24 hours after the sample fixation. Calibration was achieved with standard beads

of 0.356 – 9.146 µm (Polysciences, Inc.). Standard beads of 2.764 µm were added into each sample prior to the injection of flow cytometer as internal standard. Phytoplankton cell populations were estimated from the forward light scatter signal. Acquired data were stored in list mode file and analyzed with WinBryte software. Phytoplankton are classified with prokaryotic cyanobacteria (*Prochlorococcus* and *Synechococcus*) and other eukaryotes on the basis of scatter and fluorescence signals. *Synechococcus* is discriminated by phycoerythrin as the orange fluorescence, while other phytoplankton are recognized by chlorophylls as the red fluorescence without the orange fluorescence. *Prochlorococcus* and picoeukaryotes were distinguished with their cell size, but it was difficult to identify the abundance of *Prochlorococcus* accurately in the surface mixed layer due to its decreased chlorophyll fluorescence. The cell size was estimated using the empirically-determined relationship between cell diameter (d_{cell}) and bead diameter (d_{bead}) with the forward light scatter signal (FS) by Blanchot *et al.*, (2001) as follows.

$$d_{\text{cell}} = d_{\text{bead}} (\text{FS})^{1/5}$$

(4) Data Archive

All data will be submitted to Data Integration and Analysis Group (DIAG), JAMSTEC.

(5) Reference

Blanchot J, André J-M, Navarette C, Neveux J, Radenac M-H (2001), Picophytoplankton in the equatorial Pacific: vertical distributions in the warm pool and in the high nutrient low chlorophyll conditions, *Deep-Sea Research I* 48, 297-314.

3.3.4 Primary production and new production

Kazuhiko MATSUMOTO (JAMSTEC RIGC)

Kanako YOSHIDA (MWJ)

Keitaro MATSUMOTO (MWJ)

Yuta IIBUCHI (MWJ)

(1) Objective

Quantitative assessment of temporal and spatial variation in carbon and nitrate uptake in the surface euphotic layer should be an essential part of biogeochemical studies in the western North Pacific. Primary production (PP) was measured as incorporation of inorganic C^{13} , and new production (NP), measurement of nitrate uptake rate was conducted with ^{15}N stable isotope tracer at K2, and S1 stations.

(2) Methods

1) *Sampling, incubation bottle and filter*

Sampling was conducted at predawn immediately before the incubation experiment. Seawater samples were collected using Teflon-coated and acid-cleaned Niskin bottles, except for the surface water, which was taken by a bucket. Samplings were conducted at eight depths in the euphotic layer in response to the light levels of the incubation containers adjusted with the blue acrylic plate. Two kinds of baths were prepared for PP and NP (bath-1), and for oxygen evolution (bath-2). The light levels of the incubation containers in each bath were shown in Table 3.3.4-1. The light depths relative to the surface had been estimated by the underwater optical sensor on the previous day of the sampling. Seawater samples were placed into acid-cleaned clear polycarbonate bottles in duplicate for PP and NP, and in a single for the dark and the time-zero samples. The time-zero sample was filtered immediately after the addition of ^{13}C and ^{15}N solution. Filtration of seawater sample was conducted with pre-combusted glass fiber filters (Whatman GF/F 25 mm) with temperature of 450 degree C for at least 4 hours.

2) *Incubation*

Each bottle was spiked with sufficient $NaH^{13}CO_3$ just before incubation so that ^{13}C enrichment was about 10% of ambient dissolved inorganic carbon as final concentration of 0.2 mmol dm^{-3} (Table 3.3.4-2). The ^{15}N -enriched NO_3 , $K^{15}NO_3$ solution, was injected with two levels (about 10% of ambient nitrate and the sufficient) to the incubation bottles except PP bottles (Table 3.3.4-3). Incubation was begun at predawn and continued for 24 h. The simulated *in situ* method was conducted in the on-deck bath cooled by running surface seawater or by immersion cooler.

3) *Measurement*

After 24 hours incubation, samples were filtered through GF/F filter, and the filters were kept in a freezer (-20 degree C) on board until analysis. Before analysis, the filters were dried in the oven (45 degree C) for at least 20 hours, and inorganic carbon was removed by acid treatment in HCl vapor bath for 30 minutes. All samples were measured by a mass spectrometer ANCA-SL system at MIRAI during this cruise.

Instruments: preprocessing equipment ANCA-SL (Europa Scientific Ltd.; now SerCon Ltd.)
stable isotope ratio mass spectrometer 20-20 (Europa Scientific Ltd.; now SerCon Ltd.)

Methods: Dumas method, Mass spectrometry

Precision: All specifications are for n=5 samples.

It is a natural amount and five time standard deviation of the analysis as for amount 100 µg of the sample. We measured repeatability 5 times in this cruise. ^{13}C (0.05 - 0.08 ‰), ^{15}N (0.03 - 0.14 ‰)

Reference Material: The third-order reference materials L-Alanine (SI Science Co.,Ltd.)

4) Calculation

(a) Primary Production

Based on the balance of ^{13}C , assimilated organic carbon (ΔPOC) is expressed as follows (Hama *et al.*, 1983):

$$^{13}\text{C}_{(\text{POC})} * \text{POC} = ^{13}\text{C}_{(\text{sw})} * \Delta\text{POC} + (\text{POC} - \Delta\text{POC}) * ^{13}\text{C}_{(0)}$$

This equation is converted to the following equation;

$$\Delta\text{POC} = \text{POC} * (^{13}\text{C}_{(\text{POC})} - ^{13}\text{C}_{(0)}) / (^{13}\text{C}_{(\text{sw})} - ^{13}\text{C}_{(0)})$$

where $^{13}\text{C}_{(\text{POC})}$ is concentration of ^{13}C of particulate organic carbon after incubation, *i.e.*, measured value(‰). $^{13}\text{C}_{(0)}$ is that of particulate organic carbon before incubation, *i.e.*, that for samples as a blank.

$^{13}\text{C}_{(\text{sw})}$ is concentration of ^{13}C of ambient seawater with a tracer. This value for this study was determined based on the following calculation;

$$^{13}\text{C}_{(\text{sw})} (\text{‰}) = [(\text{TDIC} * 0.011) + 0.0002] / (\text{TDIC} + 0.0002) * 100$$

where TDIC is concentration of total dissolved inorganic carbon at respective bottle depth(mol dm^{-3}) and 0.011 is concentration of ^{13}C of natural seawater (1.1%). 0.0002 is added ^{13}C (mol) as a tracer. Taking into account for the discrimination factor between ^{13}C and ^{12}C (1.025), primary production (PP) was, finally, estimated by

$$\text{PP} = 1.025 * \Delta\text{POC}$$

(b) New production

NO_3 uptake rate or new production (NP) was estimated with following equation:

$$\text{NP} (\mu\text{g dm}^{-3} \text{ day}^{-1}) = (^{15}\text{N}_{\text{excess}} * \text{PON}) / (^{15}\text{N}_{\text{enrich}}) / \text{day}$$

where $^{15}\text{N}_{\text{excess}}$, PON and $^{15}\text{N}_{\text{enrich}}$ are excess ^{15}N (measured ^{15}N minus ^{15}N natural abundance, 0.366 atom‰) in the post-incubation particulate sample (‰), particulate nitrogen content of the

sample after incubation (mg dm^{-3}) and ^{15}N enrichment in the dissolved fraction (%), respectively.

(3) Preliminary results

Fig. 3.3.4.1 and 3.3.4.2 show the vertical profile of primary production (PP) and the diurnal change of photosynthetically available radiation (PAR) observed by PUV-510B (Biospherical Instruments Inc.).

(4) Data archives

All data will be submitted to JAMSTEC Data Integration and Analyses Group (DIAG).

Table 3.3.4-1 Light levels of the incubation containers

Number	Bath 1	Bath 2
#1	100%	100%
#2	65%	66%
#3	37.5%	40%
#4	18.1%	13.4%
#5	13.3%	9.3%
#6	6.3%	4.6%
#7	3.8%	3.1%
#8	0.7%	1.7%

Table 3.3.4-2 Sampling cast table and spike ^{13}C concentration

Incubation type	CTD cast	$\text{NaH}^{13}\text{CO}_3$ ($\mu\text{mol dm}^{-3}$)
SIS	S01M02	200
SIS	K02M02	200

Table 3.3.4-3 Sampling cast table and spike ^{15}N concentration

Incubation type	CTD cast	Light Intensity	K^{15}NO_3 ($\mu\text{mol dm}^{-3}$)
SIS	S01M02	100% - 13.3%	0.05
		6.3% - 0.7%	0.01
		100% - 0.7%	10
SIS	K02M02	100% - 0.7%	1.7
		100% - 0.7%	10

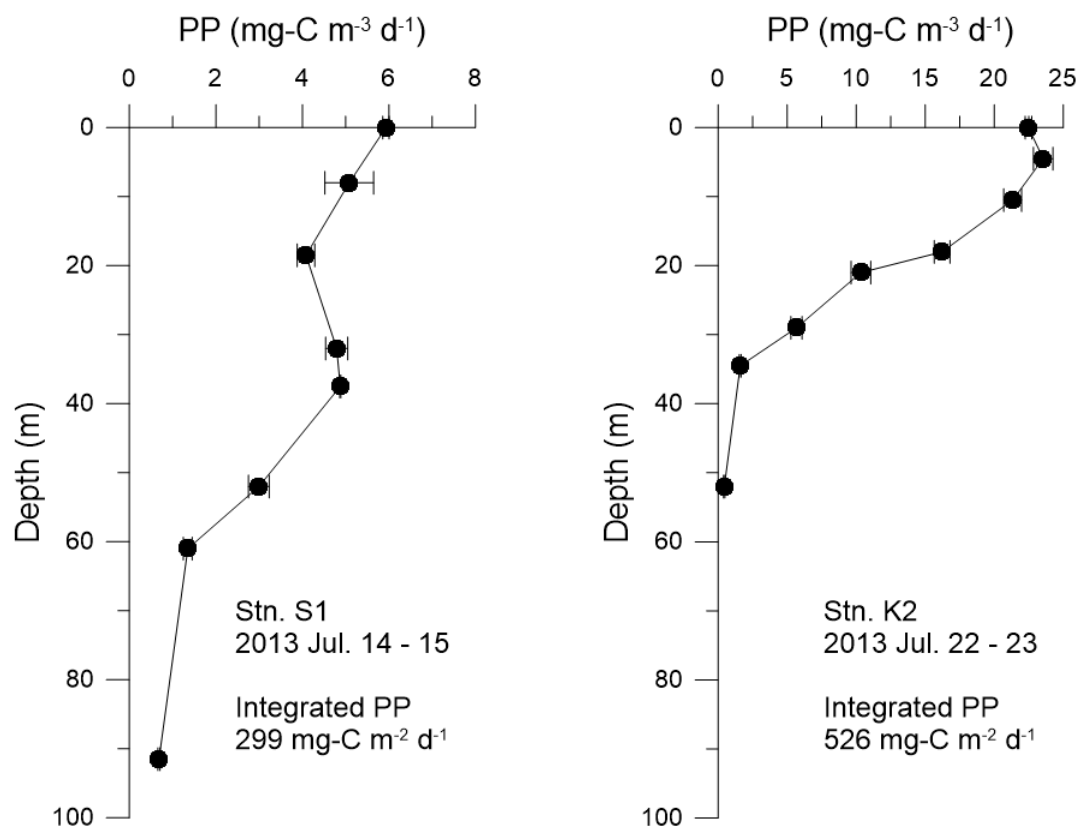


Figure 3.3.4.1 Vertical profile of primary production

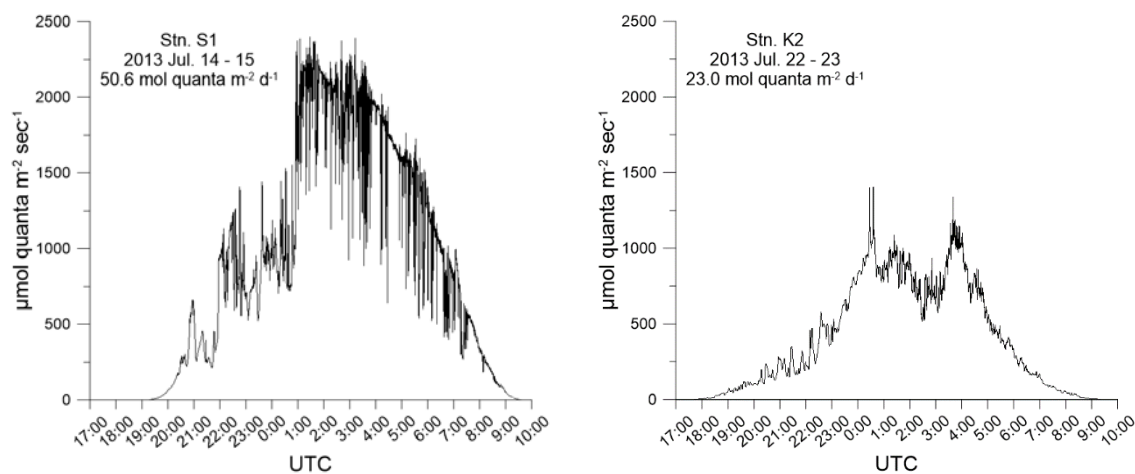


Figure 3.3.4.2 Photosynthetically available radiation (PAR) during the incubation experiment

3.3.5 P vs. E curve

Kazuhiko MATSUMOTO (JAMSTEC RIGC)

Kanako YOSHIDA (MWJ)

Keitaro MATSUMOTO (MWJ)

Yuta IIBUCHI (MWJ)

(1) Objectives

The objective of this study is to estimate the relationship between phytoplankton photosynthetic rate (P) and scalar irradiance (E) in the western North Pacific.

(2) Methods

1) Sampling

Samplings were carried out at two observational stations of K2 and S1. Sample water was collected at two depths of different irradiance level, using Teflon-coated and acid-cleaned Niskin bottles.

2) Incubation

Three incubators filled in water were used, illuminated at one end by a 500W halogen lamp. Water temperature was controlled by circulating water cooler (Fig. 3.3.5-1). Water samples were poured into acid-cleaned clear nine flasks (approx. 1 liter) and were arranged in the incubator linearly against the lamp after adding the isotope solutions. The isotope solutions of 0.2 mmol dm⁻³ (final concentration) of NaH¹³CO₃ solution were spiked. All flasks were controlled light intensity by shielding with a neutral density filter on lamp side. The light intensities inside the flasks were shown in Table 3.3.5. The incubations were begun before local noon and continued for 3 h. Filtration of seawater sample was conducted with glass fiber filters (Whatman GF/F 25 mm) which precombusted with temperature of 450 degree C for at least 4 hours.

3) Measurement

After the incubation, samples were treated as same as the primary production experiment. All incubator samples were measured by a mass spectrometer ANCA-SL system at MIRAI during the cruise. The analytical function and parameter values used to describe the relationship between the photosynthetic rate (P) and scalar irradiance (E) are best determined using a least-squares procedure from the following equation.

$$P = P_{\max}(1 - e^{-\alpha E/P_{\max}})e^{-b\alpha E/P_{\max}} : (\text{Platt et al., 1980})$$

where, P_{\max} is the light-saturated photosynthetic rate, α is the initial slope of the P vs. E curve, b is a dimensionless photoinhibition parameter.

(3) Preliminary results

The P vs. E curve obtained at the station of K2 and S1 is shown in Fig. 3.3.5-2.

(4) Data archives

All data will be submitted to JAMSTEC Data Integration and Analyses Group (DIAG) .

(5) Reference

Platt, T., Gallegos, C.L. and Harrison, W.G., 1980. Photoinhibition of photosynthesis in natural assemblages of marine phytoplankton. *Journal of Marine Research*, 38, 687-701.

Table 3.3.5 Light Intensity of each flask

	Bath A	Bath B	Bath C
Bottle No.	Light intensity ($\mu\text{E m}^{-2} \text{sec}^{-1}$)		
1	2050	2000	2000
2	1000	1000	950
3	410	450	450
4	180	200	190
5	88	94	86
6	40	42	37
7	17	18.5	16
8	7.4	7.2	6.6
9	0	0	0

Halogen lamp : 500W

Fig. 3.3.5-1 Look down view of the incubator

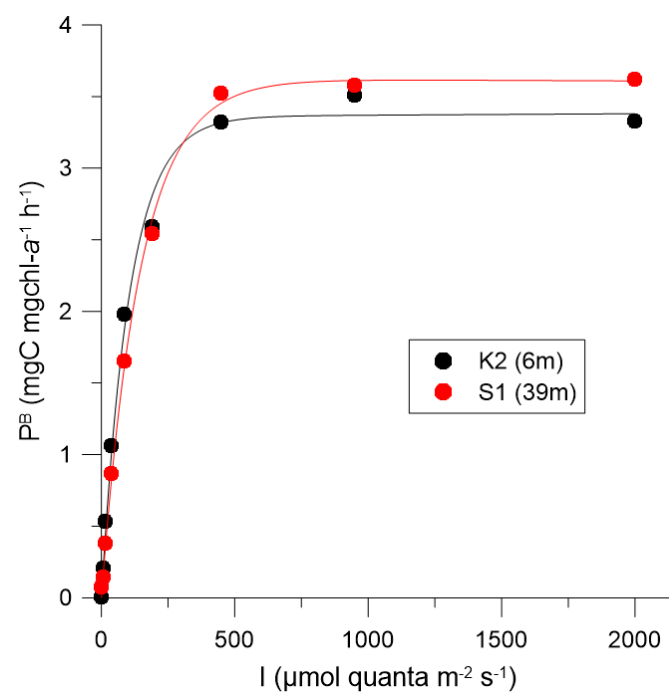


Fig. 3.3.5-2 P vs. E curve

3.3.6 Oxygen evolution (gross primary production)

Osamu ABE (Nagoya University)

Tetsuichi FUJIKI (JAMSTEC RIGC)

(1) Objective

An understanding of the variability in phytoplankton productivity provides a basic knowledge of how aquatic ecosystems are structured and functioning. Primary productivity in the world ocean has been measured mostly with the methods of carbon tracer or oxygen evolution. In incubations of 24 hours, the former method provides the values closest to net primary productivity (NPP), while the latter comes closest to gross primary productivity (GPP). The GPP is defined as total amount of oxygen released by phytoplankton photosynthesis. The NPP/GPP ratio provides fundamental information on the metabolic balance and carbon cycle in the ocean. In the MR13-04, the GPP were measured using following three approaches, as light and dark bottle incubation for dissolved O₂ concentration, light bottle incubation for dissolved O₂ spiked with H₂¹⁸O and fast repetition rate (FRR) fluorometry.

(2) Description of instruments deployed

Light and Dark bottle incubation of dissolved O₂

Seawater samples were collected at Station S1 and K2, from eight depths corresponding to light levels approximately 100, 60, 35, 13, 7, 5, 3, 1 % of surface light intensity. At each depth, duplicate samples were collected respectively for light and dark incubations, along with duplicate time zero samples. All samples were collected using 12-L Niskin-X sampler attached to CTD rosette system, except for surface water by a bucket sampling. For dark incubation, bottles were wrapped with aluminum foil, packed into plastic container and incubated in temperature-controlled water bath. For light incubation, bottled water were incubated under eight light conditions corresponding to those of original sample depths, in temperature-controlled water bath. After 24-hour incubation, their oxygen concentrations were determined with Winkler titration described in Section 2.5.

GPP is calculated from the difference of oxygen concentration between light and dark incubation.

Light bottle incubation of dissolved O₂ spiked with H₂¹⁸O

Seawater samples were collected at S1 and K2 from the same depths as light and dark bottle incubation experiment. Samples for light incubation were then spiked with 1 mL of ¹⁸O-labeled water (approximately 10 % H₂¹⁸O water) in order to obtain 0.1 % ¹⁸O concentration, and then sealed. Time zero samples were also collected accordingly. Spiked samples were incubated in the same way of light and dark incubation. After 24-hour incubation, ~80 mL of subsample were collected into pre-evacuated vacuum flasks for the determination of δ¹⁸O of dissolved oxygen. Two milliliter of water were collected from the residual samples for the determination of δ¹⁸O of water. These subsamples are brought back to laboratory and δ¹⁸O ratios of oxygen and water are determined using isotope-ratio mass spectrometer.

GPP is calculated from δ¹⁸O of oxygen for time zero and final (incubated), δ¹⁸O of water, oxygen concentration for time zero and final according to the following equation (Bender et al. 2000).

$$GPP = [(\delta^{18}O_f - \delta^{18}O_{avg})O_{2f} - (\delta^{18}O_i - \delta^{18}O_{avg})O_{2i}] / [\delta^{18}O_{water} - (\delta^{18}O_{avg} + \epsilon_R)]$$

where the subscripts i, f, avg are time zero, final and average of them, respectively, $\delta^{18}O_{water}$ denotes isotope ratio of incubating water, and ϵ_R denotes isotope fractionation factor during oxygen consumption.

FRR fluorometry

Principle of FRR fluorometer can be found in the section 3.2.1 (POPPS mooring). The FRR fluorometer together with a scalar irradiance sensor (QSP-2200, Biospherical Instruments) and a pressure gauge (ABH500PSC1B, Honeywell International) were deployed several times a day using a ship winch. These instrument packages lowered gently through the water column to 100m (150m for S1) depth and up again at a rate of 0.2 m s^{-1} and measured vertical profiles of GPP.

(3) Preliminary results

At stations K2 and S1, the vertical profiles of GPP measured with the light-dark bottle method were shown in figure 3.3.6.1. Since the surface GPP at S1 indicated a negative value, the result was excluded from the figure.

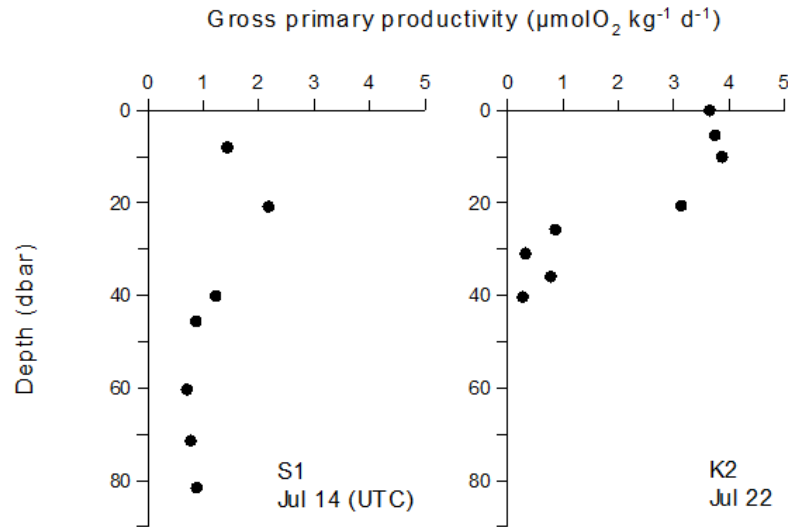


Figure 3.3.6.1. Vertical profiles of GPP at stations K2 and S1, measured with the light-dark bottle method.

(4) Data archives

The data will be submitted to JAMSTEC Data Management Office.

(5) References

Bender, M. L., M. L. Dickson and J. Orchard. 2000. Net and gross production in the Ross Sea as determined by incubation experiments and dissolved O_2 studies. *Deep-Sea Res. II* 47: 3141–3158.

3.3.7 Absorption coefficients of phytoplankton and colored dissolved organic matter (CDOM)

Kosei SASAOKA (JAMSTEC RIGC)

(1) Objectives

Absorption coefficients of particulate matter (phytoplankton and non-phytoplankton particles, defined as ‘detritus’) and colored dissolved organic matter (CDOM) play an important role in determining the optical properties of seawater. In particular, light absorption by phytoplankton is a fundamental process of photosynthesis, and their chlorophyll *a* (Chl-*a*) specific coefficient, a^*_{ph} , can be essential factors for bio-optical models to estimate primary productivities. Absorption coefficients of CDOM are also important parameters to validate and develop the bio-optical algorithms for ocean color sensors, because the absorbance spectrum of CDOM overlaps that of Chl-*a*. The global colored detrital and dissolved materials (CDM) distribution appears regulated by a coupling of biological, photochemical, and physical oceanographic processes all acting on a local scale, and greater than 50% of blue light absorption is controlled by CDM (Siegel et al., 2002). The objectives of this study are to characterize the absorption spectra of phytoplankton and CDOM in the western North Pacific.

(2) Methods

Seawater samples for absorption coefficient of total particulate matter ($a_p(\lambda)$) were performed using Niskin bottles and a bucket. Samples were collected in 3000ml dark bottles and filtered (800 – 3000 ml) through 25-mm What-man GF/F glass-fiber filters under a gentle vacuum (< 0.013 MPa) on board. After filtration, the optical density of total particulate matter on filter ($OD_{fp}(\lambda)$) between 350 and 750 nm at a rate of 0.5 nm was immediately measured by a dual beam multi-purpose spectrophotometer (MPS-2400, Shimadzu Co.), and absorption coefficient was determined from the OD according to the quantitative filter technique (QFT) (Mitchell, 1990). A blank filter with filtered seawater was used as reference. All spectra were normalized to 0.0 at 750nm to minimize difference between sample and reference filter. To determine the optical density of non-pigment detrital particles ($OD_{fd}(\lambda)$), the filters were then soaked in methanol for a few hours and rinsed with filtered seawater to extract and remove the pigments (Kishino et al., 1985), and its absorption coefficient was measured again by MPS-2400. These measured optical densities on filters ($OD_{fp}(\lambda)$ and $OD_{fd}(\lambda)$) were converted to optical densities in suspensions ($OD_{sp}(\lambda)$ and $OD_{sd}(\lambda)$) using the pathlength amplification factor of Cleveland and Weidemann (1993) as follows:

$$\begin{aligned} OD_{sp}(\lambda) &= 0.378 OD_{fp}(\lambda) + 0.523 OD_{fp}(\lambda)^2 \text{ and} \\ OD_{sd}(\lambda) &= 0.378 OD_{fd}(\lambda) + 0.523 OD_{fd}(\lambda)^2. \end{aligned}$$

The absorption coefficient of total particles ($a_p(\lambda)$ (m^{-1})) and non-pigment detrital particles ($a_d(\lambda)$ (m^{-1})) are computed from the corrected optical densities ($OD_s(\lambda)$):

$$a_p(\lambda) = 2.303 \times OD_{sp}(\lambda) / L \quad (L = V / S), \text{ and}$$

$$a_d(\lambda) = 2.303 \times OD_{sd}(\lambda) / L \quad (L = V / S),$$

Where S is the clearance area of the filter (m²) and V is the volume filtered (m³). Absorption coefficient of phytoplankton ($a_{ph}(\lambda)$) was obtained by subtracting $a_d(\lambda)$ from $a_p(\lambda)$ as follows:

$$a_{ph}(\lambda) = a_p(\lambda) - a_d(\lambda).$$

Finally, we will calculate chl-*a* normalized specific absorption spectra (a_{ph}^*) to divide a_{ph} by chl-*a* concentrations obtained from HPLC.

Seawater samples for absorption coefficient of CDOM ($a_y(\lambda)$) were collected in 250ml bottles using a bucket. After letting the CDOM samples rest for a few hours to equilibrate to room temperature, samples were filtered through a 47-mm Nuclepore membrane filter (pore size = 0.2 µm). Optical densities of the CDOM ($OD_y(\lambda)$) in this filtered seawater were measured in the range from 300 to 800 nm using 10-cm pathlength glass cells with MPS-2400. Milli-Q water was used as a reference. A blank (Milli-Q water versus Milli-Q water) was subtracted from each wavelength of the spectrum. The absorption coefficient of CDOM ($a_y(\lambda)$ (m⁻¹)) was calculated from measured optical densities ($OD_y(\lambda)$) as follows:

$$a_y(\lambda) = 2.303 \times OD_y(\lambda) / L \quad (L \text{ is the cuvette pathlength (m)}).$$

(3) Preliminary results

Some examples of absorption spectra of phytoplankton ($a_{ph}(\lambda)$) and CDOM ($a_y(\lambda)$) were shown in Fig.3.3.7-1 and Fig.3.3.7-2, respectively.

(4) Data archive

The data from this study will be submitted to Data Integration and Analysis Group (DIAG) of JAMSTEC.

(5) References

- Mitchell, B.G., 1990, Algorithms for determining the absorption coefficient of aquatic particulates using the quantitative filter technique (QFT), *Ocean Optics X*, SPIE 1302, 137-148.
- Kishino, M., Takahashi, M., Okami, N. and Ichimura, S., 1985, Estimation of the spectral absorption coefficients of phytoplankton in the sea, *Bulletin of Marine Science*, 37, 634-642.
- Cleveland, J.S. and Weidemann, A.D., 1993, Quantifying absorption by aquatic particles: a multiple scattering correction for glass fiber filters, *Limnology and Oceanography*, 38, 1321-1327.
- Siegel, D.A., Maritorena, S., Nelson, N.B., Hansell, D.A., Lorenzi-Kayser, M., 2002, Global distribution and dynamics of colored dissolved and detrital organic materials. *J. Geophys. Res.*, 107, C12, 3228, doi:10.1029/2001JC000965.

Table 3.3.7-1 List of sampling for absorption coefficients of phytoplankton and CDOM during MR13-04.

Station	Date (UT)	Time (UT)	Latitude	Longitude	Sampling type	Cast No.	Particle absorbance	CDOM absorbance	Remarks
F1	2013/07/11	07:40-07:55	36-28.67N	141-28.67E	Bucket	1	○(0m)	○(0m)	Routine
S1	2013/07/14	17:04-17:52	29-59.73N	145-00.02E	CTD+Bucket	2	○	○(0m)	Shallow (P.P)
S1	2013/07/15	20:34-21:59	29-54.68N	144-57.33E	CTD	4	○	-	Shallow (PE)
KEO	2013/07/17	15:46-16:02	32-18.82N	144-31.74E	Bucket	1	○(0m)	○(0m)	Routine
JKEO	2013/07/18	21:32-21:49	38-05.56N	146-24.98E	Bucket	1	○(0m)	○(0m)	Routine
KNOT	2013/07/20	18:28-18:44	44-00.29N	155-00.17E	Bucket	1	○(0m)	○(0m)	Routine
K2	2013/07/22	15:08-15:58	47-00.15N	160-00.37E	CTD+Bucket	2	○	○(0m)	Shallow (P.P.)
K2	2013/07/23	02:03-03:35	47-00.23N	159-59.74E	CTD	4	○	-	Shallow (PE)
E03	2013/07/26	04:46-04:56	40-07.02N	149-02.17E	Bucket	1	-	○(0m)	ARGO
E01	2013/07/27	19:01-19:13	41-15.13N	146-42.73E	Bucket	1	○(0m)	○(0m)	ARGO

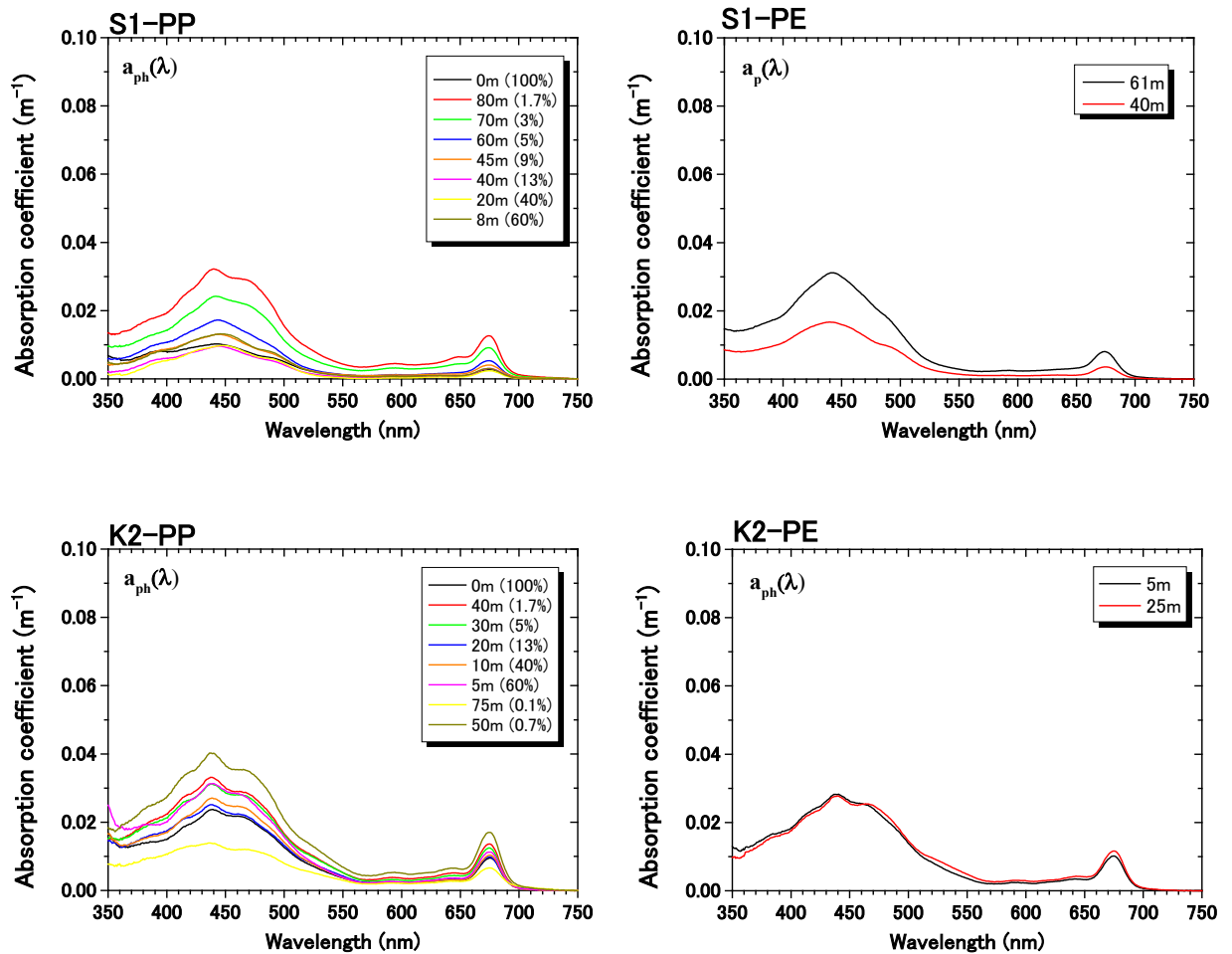


Fig.3.3.7-1 Absorption spectra of phytoplankton ($a_{ph}(\lambda)$) at Stn.S1 and K2. All spectra were normalized to 0.0 at 750nm.

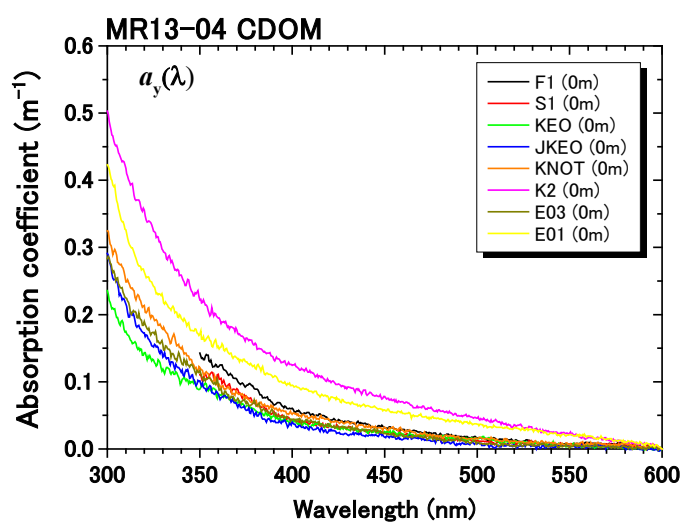


Fig.3.3.7-2 Absorption spectra of CDOM ($a_y(\lambda)$) collected by a bucket (0m depth) at each stations. All spectra were normalized to 0.0 at 600nm.

3.3.8 Taxonomy and genome analysis of eukaryotic picophytoplankton originated from cryopreserved marine environmental specimens

Haruyo YAMAGUCHI (NIES)

Masanobu KAWACHI (NIES)

(1) Objective and strategies

Our knowledge regarding eukaryotic phytoplankton diversity in open sea has been still fragmented. Especially, basic information about eukaryotic picophytoplankton is limited because of its small cell size and few morphological features. In this cruise, we will investigate morphological, phylogenetic and genomic features for marine eukaryotic picophytoplankton to unveil the diversity in open sea.

Flow cytometry (FCM) is a powerful tool to analyze the diversity of picophytoplankton. However equipping such precision machine on ship laboratory is hard and troublesome work. Our strategy is that we firstly cryopreserve environmental specimen on shipboard during cruise and after the cruise we analyze the specimen by FCM equipped with a cell sorter. This approach will allow long-term preservation of natural biodiversity and also repeated analyses on the morphological, phylogenetic and genomic feature in the laboratory.

We will use a light microscope, inverted light microscope and scanning electron microscope (SEM) for their morphological observations. In addition, we have continuously established unialgal culture strains for more detailed works during/after the cruise. On the FCM sorted cells, we will perform metagenomic analyses using next generation sequencing techniques. The same methods will be applied regarding raw, not cryopreserved, seawater samples obtained during the cruise.

Here, we summarize the preliminary species list and photographs taken during the cruise. In the list, we added electron micrographs taken by SEM in the laboratory. In this preliminary cruise report, we focus on both pico and nano-sized phytoplankton to understand whole species composition in this cruise area.

(2) Sample treatments and preliminary observations of phytoplankton

Seawater samples were collected from sea surface and chlorophyll maximum layer using the continuous sea surface water monitoring system and Niskin water sampler system, respectively. Detailed sampling sites were listed in Table 3.3.8.1. For efficient sample treatment of picophytoplankton, the seawater sample was initially pre-filtered using a plankton net with a mesh size of 5 μm , and then concentrated about 100 fold by tangential flow filtration. For concentration of large-sized phytoplankton, we used a plankton net with a mesh size of 5 or 20 μm . The resultant samples were used for the several treatments; sub-culturing, cryopreservation, DNA analyses, light and scanning electron microscopy. As for the cryopreservation, samples were cooled with cryoprotectant (5% DMSO) with a rate of $-1^{\circ}\text{C}/\text{min}$ to -35°C by using a programmable freezer and then frozen rapidly to -196°C into liquid nitrogen.

During the cruise, the concentrated samples were cultivated in ESM or MNK culture media (Kasai et al. 2009) at $4\text{--}20^{\circ}\text{C}$. We observed both raw concentrated samples and the sub-cultured samples using inverted light microscope equipped with a tablet photograph device on shipboard. The phytoplankton diversity, including pico and nano-sized phytoplankton was

partly recorded by taking photos. Colorless protists, less species number, were also documented. The species name was listed in Table 3.3.8.2 to 10. Although this is a preliminary observation with low magnification images using the inverted light microscope, dominant phytoplankton species in each site was partly indicated. Additional information from the SEM observations was also used for correction of species identification. Furthermore, we performed single cell isolations to establish culture strains which will be useful materials to investigate precise diversity and detailed taxonomy.

(3) Preliminary results

During this cruise, we obtained 19 samples as listed in Table 3.3.8.1.

Table 3.3.8.1 Sampling information

#	Date (JST)	Station name	Sample name	Depth (m)	Remarks
1	2013/7/11	F1	F1-surface	0	CSMS ^{*2}
2	2013/7/11	F1	F1-chlorophyll_max	33	Niskin bottle
3	2013/7/12	Kuroshio ^{*1}	Kuroshio-surface	0	CSMS ^{*2}
4	2013/7/14	S1	S1- chlorophyll_max	100	Niskin bottle
5	2013/7/15	S1	S1- surface	0	CSMS ^{*2}
6	2013/7/16	S1	S1- chlorophyll_max	61	Niskin bottle
7	2013/7/17	S1	S1- chlorophyll_max	100	Niskin bottle
8	2013/7/18	KEO	KEO- chlorophyll_max	70	Niskin bottle
9	2013/7/19	JKEO	JKEO- surface	0	CSMS ^{*2}
10	2013/7/19	JKEO	JKEO- chlorophyll_max	40	Niskin bottle
11	2013/7/21	KNOT	KNOT- chlorophyll_max	50	Niskin bottle
12	2013/7/21	KNOT	KNOT- surface	0	CSMS ^{*2}
13	2013/7/22	K2	K2- surface	0	CSMS ^{*2}
14	2013/7/23	K2	K2- chlorophyll_max_upper	15	Niskin bottle
15	2013/7/23	K2	K2- chlorophyll_max_lower	35	Niskin bottle
16	2013/7/23	K2	K2- chlorophyll_max	40	Niskin bottle
17	2013/7/24	K2	K2- surface	0	Niskin bottle
18	2013/7/26	E03	E03- chlorophyll_max	45	Niskin bottle
19	2013/7/26	E01	E01- chlorophyll_max	30	Niskin bottle

^{*1} “Kuroshio” is not a station name. Considering the salinity and vessel speed of the surface seawater, we performed sampling of seawater originated from the Kuroshio Current from the continuous sea surface water monitoring system (CSMS).

^{*2} “CSMS” stands for the continuous sea surface water monitoring system.

These samples were size-fractionated using two sets of plankton net. We used mainly inverted light microscope to identify species name. To do further reliable identification, we also used light microscope and scanning electron microscope. Table 3.3.8.2–3.3.8.10 show preliminary species list observed in this cruise.

Table 3.3.8.2 Preliminary species list observed in F1

#	Sample name	Fraction size	Taxon	Species	Remarks
---	-------------	---------------	-------	---------	---------

1	F1-surface	< 5 µm	Bacillariophyceae	<i>Fragillaria</i> sp.	D
2			Cryptophyceae	<i>Teleaulax</i> sp.	
3			Dinophyceae	<i>Gymnodinium</i> sp. 1	
4			Dinophyceae	<i>Katodinium</i> sp.	
5			Mamiellophyceae	<i>Mamiella</i> sp.	
6			unknown	pico-cocoids	D
7			unknown	yellow-nano cocoids	D
8	F1-chlorophyll_max	< 5 µm	Bacillariophyceae	<i>Nitzschia</i> sp.	D
9			Dinophyceae	<i>Amphidinium acutissimum</i>	
10			Dinophyceae	<i>Gymnodinium</i> sp. 2	
11			Dinophyceae	<i>Gymnodinium</i> sp. 3	
12			Dinophyceae	<i>Torodinium</i> sp.?	
13			Mamiellophyceae	<i>Mamiella</i> sp.	
14			Katablepharida	<i>Leucocryptos</i> sp.	
15			Prasinophyceae	<i>Pyramimonas</i> sp.	
16			Prymnesiophyceae	<i>Chrysoculter</i> sp.?	
17			Prymnesiophyceae	<i>Haptolina hirta</i>	
18			Prymnesiophyceae	<i>Gephyrocapsa</i> sp.	
19			Prymnesiophyceae	<i>Syracosphaera corrugis</i>	
20			Prymnesiophyceae	<i>Umbilicosphaera sibogae</i>	
21			unknown	nano-cocoids	D
22			unknown	pico-cocoids	D
23		> 5 µm	Dinophyceae	<i>Ceratium tripos</i>	
			Prymnesiophyceae	coccolithophorid	

Abbreviations in the Remarks column, C: growth was confirmed in sub-cultured samples, D: dominant species, S: species observed by scanning electron microscopy.

Table 3.3.8.3 Preliminary species list observed in Kuroshio

#	Sample name	Fraction size	Taxon	Species	Remarks
1	Kuroshio-surface	< 5 µm	Bacillariophyceae	<i>Nitzschia</i> sp.	D
2			Dinophyceae	<i>Gymnodinium</i> sp. 1	
3			Dinophyceae	<i>Gymnodinium</i> sp. 2	
4			Dinophyceae	<i>Torodinium</i> sp.	
5			Euglenophyceae	Euglenophyceae sp.	
6			Prasinophyceae	<i>Pyramimonas</i> sp.	
7			Prymnesiophyceae	coccolithophorid	
8			unknown	yellow cocoids	
9		> 20 µm	Bacillariophyceae	<i>Bacteriastrum</i> sp.	D
10			Bacillariophyceae	<i>Chaetoceros</i> sp.	
11			Bacillariophyceae	<i>Guinardia cylindrus</i>	
12			Bacillariophyceae	<i>Hemiaulus</i> sp.	
13			Bacillariophyceae	<i>Leptocylindrus mediterraneus</i>	
14			Bacillariophyceae	<i>Rhizosolenia</i> sp.	
15			Bacillariophyceae	<i>Thalassionema</i> sp.	

16			Bacillariophyceae	<i>Thalassiosira</i> sp.	
17			Cyanobacteria	<i>Richelia</i> sp.	
18			Cyanobacteria	symbiotic cyanobacteria	
19			Cyanobacteria	in <i>Amphisolenia</i>	
20			Cyanobacteria	<i>Trichodesmium</i> sp.	
21			Dinophyceae	<i>Amphisolenia bidentata</i>	
22			Dinophyceae	<i>Ceratium fusus</i>	
23			Dinophyceae	<i>Ceratium horridum</i>	
24			Dinophyceae	<i>Gymnodinium</i> sp. 3	
25			Dinophyceae	<i>Phalacroma rapa</i>	
26			Dinophyceae	<i>Prorocentrum triestinum</i>	
27			Dinophyceae	<i>Protoperdinium</i> sp.	
28			Dinophyceae	<i>Pyrophacus steinii</i>	
29			Dinophyceae	<i>Scropsiella</i> sp.?	
30			Nanomonadea	<i>Solenicola setigera</i>	
			Prymnesiophyceae	<i>Discosphaera tubifer</i>	

Table 3.3.8.4 Preliminary species list observed in S1

#	Sample name	Fraction size	Taxon	Species	Remarks
1	S1-surface	< 5 µm	Bacillariophyceae	<i>Nitzschia</i> sp.	
2			Cryptophyceae	<i>Chroomonas</i> sp.	
3			Cryptophyceae	<i>Rhodomonas</i> sp.	
4			Cyanobacteria	<i>Richelia</i> sp.	
5			Cyanobacteria	<i>Trichodesmium</i> sp.	
6			Dictyochophyceae	<i>Dictyocha fibula</i>	S
7			Dinophyceae	<i>Gymnodinium</i> sp. 1	
8			Dinophyceae	<i>Karenia</i> sp.	
9			Dinophyceae	<i>Prorocentrum</i> sp. 1	S
10			Dinophyceae	<i>Warnowia</i> sp. 1	
11			Pelagophyceae	<i>Pelagomonas</i> sp.	
12			Prasinophyceae	Prasinophyceae sp.	C
13			Prasinophyceae	<i>Pyramimonas</i> sp.	
14			Prymnesiophyceae	<i>Chrysochromulina</i> sp. 1	D
15			Prymnesiophyceae	<i>Discosphaera tubifer</i>	S
16			Prymnesiophyceae	<i>Rhabdosphaera clavigera</i> var. <i>stylifera</i>	S
17			Prymnesiophyceae	<i>Syracocphaera histrica</i>	S

7					
1					
8			Prymnesiophyceae	<i>Syracocphaera pulchra</i>	S
1					
9			Prymnesiophyceae	<i>Umbellosphaera irregularis</i>	S
2					
0			Prymnesiophyceae	<i>Umbellosphaera tenuis</i>	S
2					
1			Telonemia	<i>Telonema</i> sp.	
2					
2			unknown	green flagellate	C
2					
3		> 20 µm	Bacillariophyceae	<i>Guinardia cylindrus</i>	
2					
4			Bacillariophyceae	<i>Hemiaulus</i> sp.	
2					
5			Bacillariophyceae	<i>Nitzschia</i> sp.	
2					
6			Bacillariophyceae	<i>Rhizosolenia</i> sp.	
2					
7			Bacillariophyceae	<i>Skeletonema</i> sp.	
2					
8			Ciliophora	<i>Favella</i> sp.	
2					
9			Cyanobacteria	<i>Richelia</i> sp.	
3					
0			Dinophyceae	<i>Amphisolenia bidentata</i>	
3					
1			Dinophyceae	<i>Ceratium contortum</i>	
3					
2			Dinophyceae	<i>Goniodoma polyedricum</i>	
3					
3			Dinophyceae	<i>Gymnodinium</i> sp. 2	
3					
4			Dinophyceae	<i>Gyrodinium</i> sp.	
3					
5			Dinophyceae	<i>Oxytoxum</i> sp.	
3					
6			Dinophyceae	<i>Phalacroma rapa</i>	
3					
7			Dinophyceae	<i>Podolampus</i> sp.	
3					
8			Dinophyceae	<i>Prorocentrum</i> sp. 2	
3			Euglenophyceae	<i>Pelanema</i> sp.	

9					
4					
0			Prymnesiophyceae	<i>Discosphaera tubifer</i>	
4			Prymnesiophyceae	<i>Helicosphaera</i> sp.	
1			Prymnesiophyceae	Prymnesiophyceae sp.	
4			Prymnesiophyceae	<i>Syracocphaera prolongata</i>	
2			Syndiniophyceae	<i>Euduboscquella</i> sp.	
4					
4	S1-chlorophyll_ma				
5	x	< 5 µm	Bacillariophyceae	<i>Asteromphalus</i> sp.	
4			Cryptophyceae	<i>Rhodomonas</i> sp.	
6			Dinophyceae	<i>Amphidinium acutissimum</i>	
4			Dinophyceae	green dinoflagellate	
7			Dinophyceae	<i>Gymnodinium</i> sp. 3	D
4			Dinophyceae	<i>Gyrodinium</i> sp.	
8			Dinophyceae	<i>Torodinium</i> sp.	
4			Dinophyceae	<i>Warnowia</i> sp.	
9			Katablepharida	<i>Leucocryptos</i> sp.	
5			Nephroselmidophyceae	<i>Nephroselmis pyriformis</i>	C
4			Prymnesiophyceae	<i>Chrysochromulina</i> sp. 2	D
5			Prymnesiophyceae	<i>Gephyrocapsa</i> sp.	D
5			Prymnesiophyceae	<i>Imantonia</i> sp.	
6			Trebouxiophyceae	<i>Picochlorum</i> sp.?	C
5			unknown	brown coccoids	
7			unknown	yellow coccoids	D
5					
8		> 20 µm	Bacillariophyceae	<i>Bacteriastrium</i> sp.	
6					

1					
6					
2			Bacillariophyceae	<i>Cerataulina</i> sp?	
6					
3			Bacillariophyceae	<i>Chaetoceros atlanticus</i>	
6					
4			Bacillariophyceae	<i>Chaetoceros</i> sp.	
6					
5			Bacillariophyceae	<i>Cylindrotheca</i> sp.	
6					
6			Bacillariophyceae	<i>Fragillariopsis</i> sp.	
6					
7			Bacillariophyceae	<i>Hemiaulus</i> sp.	
6					
8			Bacillariophyceae	<i>Leptocylindrus mediterraneus</i>	
6					
9			Bacillariophyceae	<i>Nitzschia</i> sp.	
7					
0			Bacillariophyceae	<i>Planktoniella sol</i>	
7					
1			Bacillariophyceae	<i>Pseudo-nitzschia</i> sp. 1	
7					
2			Bacillariophyceae	<i>Pseudo-nitzschia</i> sp. 2	
7					
3			Bacillariophyceae	<i>Thalassionema</i> sp.	
7					
4			Bacillariophyceae	<i>Thalassiosira</i> sp.	
7					
5			Dictyochophyceae	<i>Dictyocha fibula</i>	
7					
6			Dictyochophyceae	<i>Dictyocha speculum</i>	
7					
7			Dinophyceae	<i>Ceratium horridum</i>	
7					
8			Dinophyceae	<i>Cochlodinium convolutum</i>	
7					
9			Dinophyceae	green dinoflagellate	
8					
0			Dinophyceae	<i>Protoperidinium</i> sp.	
8					
1			Dinophyceae	<i>Torodinium</i> sp.	
8					
2			Dinophyceae	<i>Toropidoneis</i> sp.	
8			Dinophyceae	<i>Warnowia</i> sp. 2	

3					
8					
4			Prasinophyceae	<i>Halosphaera</i> sp.	
8					
5			Prymnesiophyceae	<i>Acanthoica quattropina</i>	S
8					
6			Prymnesiophyceae	<i>Corisphaera gracilis</i>	S
8					
7			Prymnesiophyceae	<i>Gephyrocapsa ericsonii</i>	S
8					
8			Prymnesiophyceae	<i>Michaelsarsia elegans</i>	
8					
9			Prymnesiophyceae	<i>Phaeocystis</i> sp.	S
9					
0			Prymnesiophyceae	<i>Rhabdosphaera claviger</i>	
9					
1			Prymnesiophyceae	<i>Scyphosphaera apsteinii</i>	
9					
2			Prymnesiophyceae	<i>Syracosphaera borealis</i>	S
9					
3			Prymnesiophyceae	<i>Syracosphaera orbiculus</i>	S

Table 3.3.8.5 Preliminary species list observed in KEO

#	Sample name	Fraction size	Taxon	Species	Remarks
1	KEO-surface	> 5 µm	unknown	yellow coccoids	
2		5-100 µm	Bacillariophyceae	<i>Bacteriastrum</i> sp.	
3			Bacillariophyceae	<i>Chaetoceros affinis</i>	
4			Bacillariophyceae	<i>Chaetoceros danicus</i>	
5			Bacillariophyceae	<i>Chaetoceros</i> sp.	
6			Bacillariophyceae	<i>Corethron</i> sp.	
7			Bacillariophyceae	<i>Cylindrotheca</i> sp.	
8			Bacillariophyceae	<i>Dactyliosolen phuketensis</i>	
9			Bacillariophyceae	<i>Eucampia</i> sp.	
10			Bacillariophyceae	<i>Guinardia cylindrus</i>	
11			Bacillariophyceae	<i>Hemiaulus</i> sp.	
12			Bacillariophyceae	<i>Leptocylindrus mediterraneus</i>	
13			Bacillariophyceae	<i>Rhizosolenia</i> sp.	
14			Bacillariophyceae	<i>Thalassionema</i> sp.	
15			Bacillariophyceae	<i>Thalassiosira</i> sp.	
16			Bacillariophyceae	<i>Tropidoneis</i> sp.	
17			Cyanobacteria	<i>Richelia</i> sp.	
18			Cyanobacteria	<i>Trichodesmium</i> sp.	
19			Dinophyceae	<i>Gymnodinium</i> sp.	
20			Dinophyceae	<i>Gonyaulax polygramma?</i>	

21			Dinophyceae	<i>Lepidodinium</i> sp.	
22			Dinophyceae	<i>Phalacroma rapa</i>	
23			Dinophyceae	<i>Prorocentrum</i> sp.	C
24			Nephroselmndophyceae	<i>Nephroselmis</i> sp.	C
25			Prymnesiophyceae	<i>Chrysochromulina</i> sp.	
26			Prymnesiophyceae	<i>Discosphaera tubifer</i>	
27			Prymnesiophyceae	<i>Gephyrocapsa</i> sp.	
28			Prymnesiophyceae	<i>Michaelsarsia elegans</i>	
29			Prymnesiophyceae	<i>Umbilicosphaera sibogae</i>	
30	KEO-chlorophyll_max	> 5 µm	Cryptophyceae	Cryptophyceae sp.	C

Table 3.3.8.6 Preliminary species list observed in JKEO

#	Sample name	Fraction size	Taxon	Species	Remarks
1	JKEO-surface	< 5 µm	Bacillariophyceae	<i>Nitzschia</i> sp.	
2			Ciliophora	<i>Myrionecta rubra</i>	
3			Dinophyceae	<i>Amphidinium acutissimum</i>	
4			Dinophyceae	<i>Gymnodinium</i> sp. 1	D
5			Dinophyceae	<i>Torodinium</i> sp.	
6			Prymnesiophyceae	<i>Emiliana huxleyi</i>	S
7		> 20 µm	Bacillariophyceae	<i>Asterionellopsis glacialis</i>	
8			Bacillariophyceae	<i>Chaetoceros lorenzianus</i>	
9			Bacillariophyceae	<i>Chaetoceros</i> sp.	
10			Bacillariophyceae	<i>Ditylum brightwellii</i>	
11			Bacillariophyceae	<i>Fragillariopsis</i> sp.	
12			Bacillariophyceae	<i>Leptocylindrus mediterraneus</i>	
13			Bacillariophyceae	<i>Thalassiosira</i> sp.	
14			Dictyochophyceae	<i>Dictyocha speculum</i>	
15			Dinophyceae	<i>Actiniscus pentasterias</i>	
16			Dinophyceae	<i>Ceratium tripos</i>	
17			Dinophyceae	<i>Gymnodinium</i> sp. 2	D
18			Dinophyceae	<i>Gymnodinium</i> sp. 3	
19			Dinophyceae	<i>Lepidodinium</i> sp.	
20			Dinophyceae	<i>Phalacroma</i> sp.	
21			Prymnesiophyceae	<i>Gephyrocapsa</i> sp.	
22			unknown	brown coccoids	
23	JKEO-chlorophyll_max	< 5 µm	Bacillariophyceae	<i>Asterionellopsis glacialis</i>	
24			Bacillariophyceae	<i>Thalassiosira</i> sp.	
			Ciliophora	<i>Myrionecta rubra</i>	
25			Dinophyceae	<i>Warnowia</i> sp.	
26			Katablepharida	<i>Leucocryptos</i> sp.	
27			Prasinophyceae	<i>Pycnococcus</i> sp.?	D
28			Prasinophyceae	<i>Pyramimonas</i> sp.	
29			Prymnesiophyceae	<i>Chrysocromulina</i> sp.	
30			Prymnesiophyceae	<i>Coccolithus</i> sp.?	

Table 3.3.8.7 Preliminary species list observed in KNOT

#	Sample name	Fraction size	Taxon	Species	Remarks
1	KNOT-surface	< 5 µm	Bacillariophyceae	<i>Pseudo-nitzschia</i> sp.	
2			Bolidophyceae	<i>Tetraparma pelagica</i>	S
3			Bolidophyceae	<i>Triparma columacea</i>	S
4			Bolidophyceae	<i>Triparma laevis</i>	S
5			Bolidophyceae	<i>Triparma strigata</i>	S
6			Cryptophyceae	Cryptophyceae sp. 1	
7			Dinophyceae	<i>Gymnodinium</i> sp. 1	
8			Katablepharida	<i>Leucocryptos</i> sp.	
9			Prasinophyceae	<i>Pyramimonas</i> sp.	
10		> 20 µm	Bacillariophyceae	<i>Azpeitia</i> sp.?	
11			Bacillariophyceae	<i>Chaetoceros peruvianus</i>	
12			Bacillariophyceae	<i>Corethron</i> sp.	
13			Prymnesiophyceae	<i>Coccolithus pelagicus</i>	S
14	KNOT-chlorophyll_max	< 5 µm	Bacillariophyceae	<i>Chaetoceros</i> sp.	
15			Bacillariophyceae	<i>Cylindrotheca</i> sp.	
16			Cryptophyceae	Cryptophyceae sp. 2	
17			Dinophyceae	<i>Gymnodinium</i> sp. 2	

Table 3.3.8.8 Preliminary species list observed in K2

#	Sample name	Fraction size	Taxon	Species	Remarks
1	K2-surface	< 5 µm	Bacillariophyceae	<i>Nitzschia</i> sp.	
2			Bacillariophyceae	<i>Pseudo-nitzschia</i> sp.	
3			Bacillariophyceae	<i>Thalassiothrix</i> sp.	
4			Bolidophyceae	<i>Triparma columacea</i>	S
5			Bolidophyceae	<i>Tetraparma pelagica</i>	S
6			Cryptophyceae	<i>Teleaulax</i> sp.	
7			Dinophyceae	<i>Gymnodinium</i> sp. 1	
8			Dinophyceae	<i>Gymnodinium</i> sp. 2	
9			Dinophyceae	<i>Gyrodinium</i> sp.	
10			Katablepharida	<i>Leucocryptos</i> sp.	
11			Prasinophyceae	<i>Pyramimonas</i> sp. 1	
12			Prasinophyceae	<i>Pyramimonas</i> sp. 2	
13			Prymnesiophyceae	<i>Chrysochromulina</i> sp.	
14			Prymnesiophyceae	<i>Phaeocystis</i> sp.	D
15			unknown	brown nano coccoids	
16			unknown	pico elongate	D
17			unknown	yellow pico coccoids	
18			unknown	yellow nano coccoids 1	
19		> 20 µm	Bacillariophyceae	<i>Asteromphalus</i> sp.	
20			Bacillariophyceae	<i>Azpeitia</i> sp?	D
21			Bacillariophyceae	<i>Chaetoceros atlanticus</i>	D
22			Bacillariophyceae	<i>Corethron</i> sp.	

23			Bacillariophyceae	<i>Licmophora</i> sp.	
24			Bacillariophyceae	melosirid	
25			Bacillariophyceae	<i>Pseudo-nitzschia</i> sp.	
26			Bacillariophyceae	<i>Rhizosolenia</i> sp.	
27			Bacillariophyceae	<i>Thalassionema</i> sp.	D
			Bacillariophyceae	<i>Thalassiothrix</i> sp.	
28			Bacillariophyceae	<i>Undatella</i> sp.	
29			Dinophyceae	<i>Ceratium fusus</i>	
30			Dinophyceae	<i>Ceratium pentagonum</i>	
31			Dinophyceae	<i>Dinophysis acuminata</i>	
32			Dinophyceae	<i>Protoperidinium</i> sp.	
33			Prasinophyceae	<i>Pyramimonas</i> sp.	
34			unknown	yellow nano coccoids 2	
35	K2-chlorophyll_max	< 5 µm	Bacillariophyceae	<i>Nitzschia</i> sp.	
			Bolidophyceae	<i>Triparma columacea</i>	S
36			Cryptophyceae	<i>Rhodomonas</i> sp.	C
37			Dinophyceae	<i>Gymnodinium</i> sp. 3	D
38			Dinophyceae	<i>Torodinium</i> sp.	
39			Pavlovophyceae	<i>Pavlova</i> sp.	D
		> 20 µm	Prymnesiophyceae	<i>Chrysochromulina</i> sp.	
40			Bacillariophyceae	<i>Chaetoceros atlanticus</i>	D
			Bacillariophyceae	<i>Chaetoceros</i> sp.	C
			Bacillariophyceae	<i>Corethron</i> sp.	
41			Bacillariophyceae	<i>Eucampia</i> sp.	C
42			Bacillariophyceae	<i>Leptocylindrus danicus</i>	C
			Bacillariophyceae	melosirid	
43			Bacillariophyceae	<i>Proboscia alata</i>	
			Bacillariophyceae	<i>Pseudo-nitzschia</i> sp.	
			Bacillariophyceae	<i>Rhizosolenia</i> sp.	C
44			Bacillariophyceae	<i>Thalassionema</i> sp.	D
45			Bacillariophyceae	<i>Thalassiosira</i> sp.	C
			Bacillariophyceae	<i>Thalassiothrix</i> sp.	
46			Dictyochophyceae	<i>Dictyocha speculum</i>	
47			unknown	yellow nano coccoids 3	

Table 3.3.8.9 Preliminary species list observed in E03

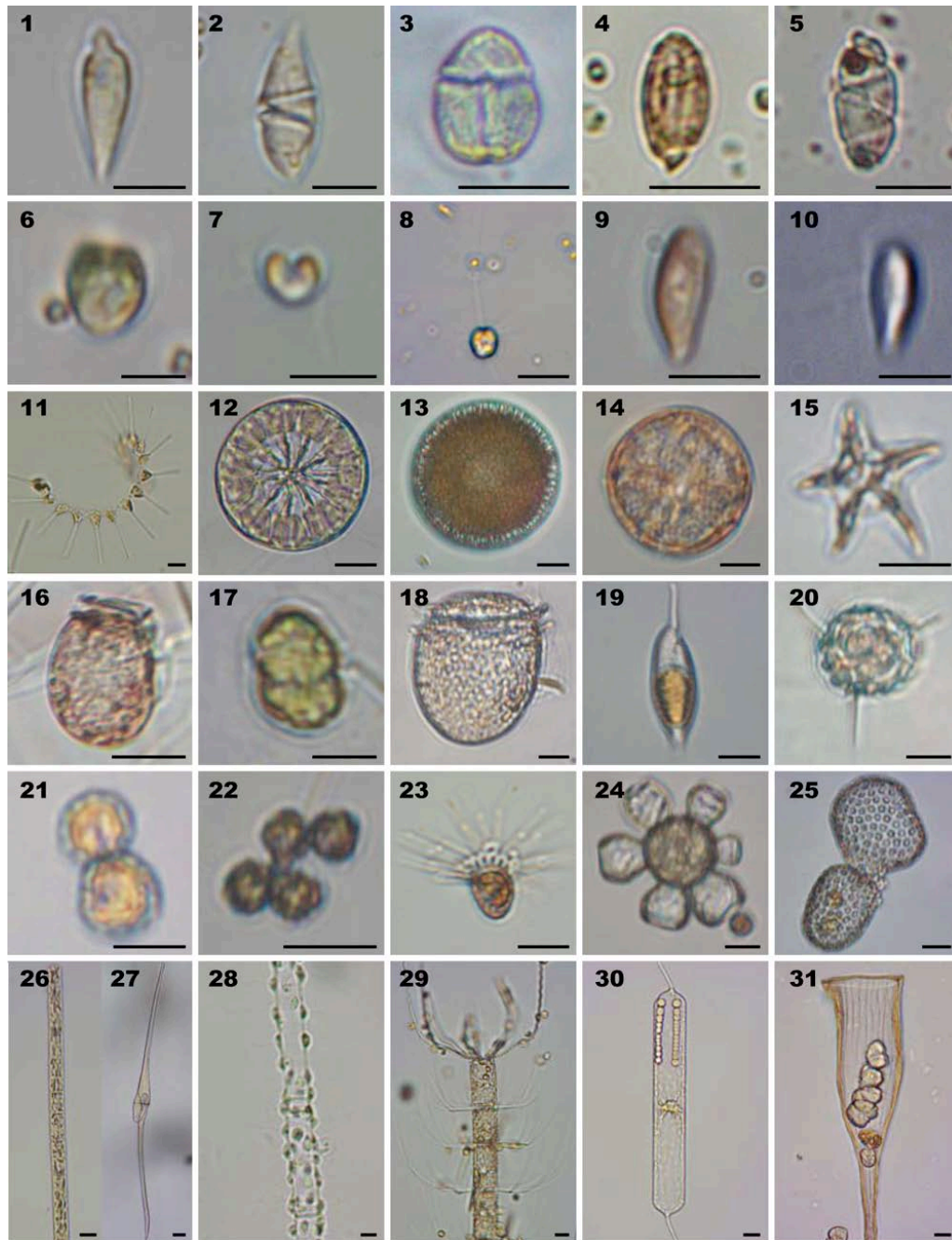
#	Sample name	Fraction size	Taxon	Species	Remarks
1	E03-chlorophyll_max	< 5 µm	Bacillariophyceae	<i>Nitzschia</i> sp.	
2			Cryptophyceae	<i>Hemiselmis</i> sp.	
3			Dinophyceae	<i>Amphidinium acutissimum</i>	
4			Dinophyceae	<i>Gymnodinium</i> sp.1	
5			Dinophyceae	<i>Gymnodinium</i> sp. 2	
6			Prymnesiophyceae	<i>Chrysochromulina</i> sp.?	
7			Prymnesiophyceae	coccolithophorid	

8		> 20 µm	Bacillariophyceae	<i>Actinoptycus senarius</i>	
9			Bacillariophyceae	<i>Coscinodiscus</i> sp.	
10			Bacillariophyceae	<i>Cylindrotheca</i> sp.	C
11			Bacillariophyceae	" <i>Navicula</i> " sp.	
12			Bacillariophyceae	<i>Nitzschia</i> sp.	C
13			Bacillariophyceae	<i>Pseudo-nitzschia</i> sp.	C
14			Bacillariophyceae	<i>Thalassiosira</i> sp.	
15			Dictyochophyceae	<i>Dictyocha speculum</i>	
16			Dinophyceae	<i>Cochlodinium</i> sp.?	
17			Dinophyceae	<i>Gymnodinium</i> sp. 3	
18			Dinophyceae	<i>Gymnodinium</i> sp. 4	
19			Dinophyceae	<i>Gonyaulax polygramma</i> ?	
20			Dinophyceae	<i>Prorocentrum triestinum</i>	
21			Dinophyceae	<i>Protoperidinium</i> sp.	
22			Noctilucofhyceae	<i>Pronoctiluca pelagica</i>	
23			Prymnesiophyceae	<i>Calyptrosphaera</i> sp.?	

Table 3.3.8.10 Preliminary species list observed in E01

#	Sample name	Fraction size	Taxon	Species	Remarks
1	E01-chlorophyll_max	< 5 µm	Bacillariophyceae	<i>Cylindrotheca</i> sp.	
2			Bacillariophyceae	<i>Nitzschia</i> sp. 1	
3			Bolidophyceae	<i>Triparma columacea</i>	S
4			Bolidophyceae	<i>Triparma laevis</i>	S
5			Bolidophyceae	<i>Triparma retinervis</i>	S
6			Bolidophyceae	<i>Triparma strigata</i>	S
7			Dinophyceae	<i>Heterocapsa rotundata</i>	
8			Prymnesiophyceae	coccolithophorid 1	
9			unknown	yellow nano coccoids 1	D
10			unknown	yellow nano coccoids 2	
11		> 20 µm	Bacillariophyceae	<i>Nitzschia</i> sp. 2	
12			Chlorodendrophyceae	<i>Tetraselmis</i> sp.	
13			Dinophyceae	<i>Gonyaulax polygramma</i> ?	
			Dinophyceae	<i>Heterocapsa rotundata</i>	
14			Dinophyceae	<i>Phalacroma</i> sp.	
15			Prymnesiophyceae	<i>Acanthoica quattropsina</i>	
16			Prymnesiophyceae	coccolithophorid 2	D

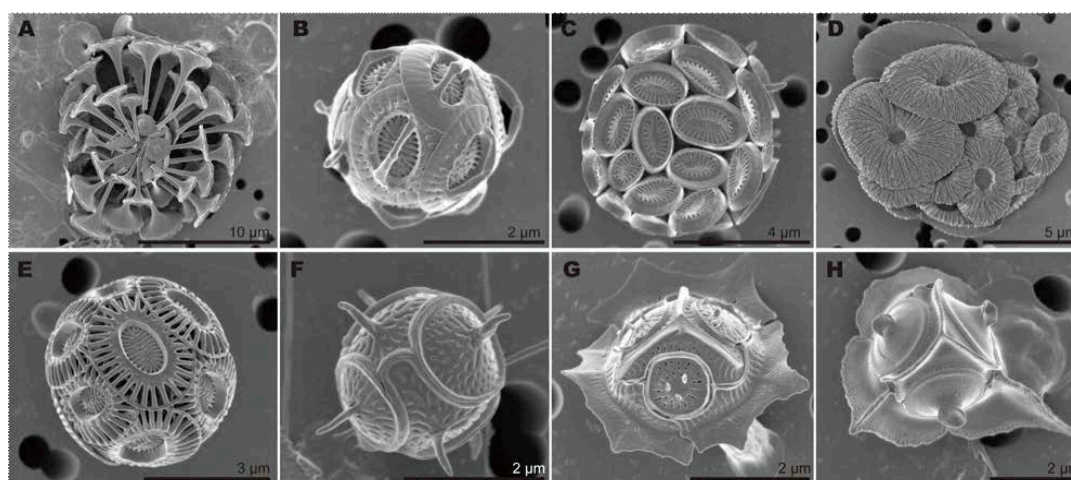
Figure 3.3.8.1 Selected photos taken by inversed light microscope during this cruise



1–10: species observed in fractions of $< 5 \mu\text{m}$, 1: *Amphidinium acutissimum* (Dinophyceae, E03-chlorophyll_max), 2: *Gyrodinium* sp. (Dinophyceae, K2-surface), 3: *Karenia* sp. (Dinophyceae, S1-surface), 4: *Torodinium* sp. (Dinophyceae, S1-chlorophyll_max), 5: *Warnowia* sp. (Dinophyceae, JKEO-chlorophyll_max), 6: *Pyramimonas* sp. (Prasinophyceae, K2-surface), 7: *Chrysochromulina* sp. (Prymnesiophyceae, K2-surface), 8: *Haptolina hirta* (Prymnesiophyceae, F1-chlorophyll_max), 9: *Rhodomonas* sp. (Cryptophyceae, K2-chlorophyll_max), 10: *Leucocryptos* sp. (Katablepharida, S1-chlorophyll_max).
 11–31: species observed in large fractions, 11: *Asterionellopsis glacialis* (Bacillariophyceae, JKEO-surface), 12: *Asteromphalus* sp. (Bacillariophyceae, K2-surface), 13: *Azpeitia* sp.? (Bacillariophyceae, K2-surface), 14: *Thalassiosira* sp. (Bacillariophyceae, E03-chlorophyll_max), 15: *Actiniscus pentasterias* (Dinophyceae, JKEO-surface), 16: *Dinophysis acuminata* (Dinophyceae, JKEO-surface), 17: *Lepidodinium* sp. (Dinophyceae, JKEO-surface),

18: *Phalacroma* sp. (Dinophyceae, E01-chlorophyll_max), 19: *Pronoctiluca pelagica* (Noctilucopephyceae, E03-chlorophyll_max), 20: *Acanthoica quattropsina*, (Prymnesiophyceae, E01-chlorophyll_max), 21: *Calyptrorpha* sp.? (Prymnesiophyceae, E03-chlorophyll_max), 22: *Gephyrocapsa* sp. (Prymnesiophyceae, JKEO-surface), 23: *Michaelsarsia elegans* (Prymnesiophyceae, KEO-surface), 24: *Scyphosphaera apsteinii* (Prymnesiophyceae, S1-chlorophyll_max), 25: *Umbellosphaera sibogae* (Prymnesiophyceae, KEO-surface), 26: *Trichodesmium* sp. (Cyanobacteria, KEO-surface), 27: *Ceratium fusus* (Dinophyceae, K2-surface), 28: *Leptocylindrus mediterraneus* (Bacillariophyceae, S1-chlorophyll_max)+ *Solenicola setigera* (Nanomonadea), 29: *Bacteriastrum* sp. (Bacillariophyceae, S1-chlorophyll_max) + *Phaeocystis* sp. (Prymnesiophyceae), 30: *Guinardia cylindrus* (Bacillariophyceae, Kuroshio-surface) + *Richelia* sp. (Cyanobacteria), 31: *Euduboscquella* sp. (Syndiniophyceae, S1-surface) in *Favella* sp. (Ciliophora), bars= 10 μ m.

Figure 3.3.8.2 Selected electron micrographs observed in this cruise



A: *Discosphaera tubifer* (Prymnesiophyceae, S1-surface), B: *Gephyrocapsa oceanica* (Prymnesiophyceae, S1-chlorophyll_max), C: *Syracosphaera orbiculus* (Prymnesiophyceae, S1-chlorophyll_max), D: *Umbellosphaera tenuis* (Prymnesiophyceae, S1-surface), E: *Emiliania huxleyi* (Prymnesiophyceae, JKEO-surface), F: *Tetraparma pelagica* (Bolidophyceae, KNOT-surface), G: *Triparma columacea* (Bolidophyceae, E01- chlorophyll_max), H: *Triparma laevis* (Bolidophyceae, E01- chlorophyll_max)

(4) Future plans

We will establish culture strains using the cryopreserved samples. We will also analyze the picophytoplankton diversity of the cryopreserved samples using flow cytometry and then sequence the DNA. These data could help us to understand genuine diversity of the picophytoplankton in open sea.

(5) References

Kasai F, Kawachi M, Erata M, Mori F, Yumoto K, Sato M, Ishimoto M (2009) NIES-collection list of strains, 8th edition. The Japanese Journal of Phycology (Sôru) 57 (Suppl.): 1–350.

3.4 Optical measurement

Makio HONDA (JAMSTEC RIGC)

Kazuhiko MATSUMOTO (JAMSTEC RIGC)

(1) Objective

The objective of this measurement is to investigate the air and underwater light conditions at respective stations and to determine depths for *in situ* or simulated *in situ* measurement of primary production by using carbon stable isotope (C-13) during late autumn. In addition, optical data can be used for the validation of satellite data.

(2) Description of instruments deployed

The instrument consisted of the SeaWiFS Profiling Multichannel Radiometer (SPMR) and SeaWiFS Multichannel Surface Reference (SMSR). The SPMR was deployed in a free fall mode through the water column (see right picture). The SPMR profiler called “Free Fall” has a 13 channel irradiance sensors (Ed), a 13 channel radiance sensors (Lu), tilt sensor, and fluorometer. The SMSR has a 13 channel irradiance sensors (Es) and tilt meter (Table 1). These instruments observed the vertical profiles of visible and ultra violet light and chlorophyll concentration.



Table 1. Center wavelength (nm) of the SPMR/SMSR

Es	379.5	399.6	412.2	442.8	456.1	490.9	519.0	554.3	564.5	619.5	665.6	683.0	705.9
Ed	380.0	399.7	412.4	442.9	455.2	489.4	519.8	554.9	565.1	619.3	665.5	682.8	705.2
Lu	380.3	399.8	412.4	442.8	455.8	489.6	519.3	554.5	564.6	619.2	665.6	682.6	704.5

Optical measurements by Free Fall were conducted at our time-series station K2 and S1. Measurements should be ideally conducted at median time. However observations were conducted irregularly because of limited ship-time and other observation's convenience (Table 2). The profiler was dropped twice a each deployment to a depth of 200 m. The SMSR was mounted on the anti-rolling system's deck and was never shadowed by any ship structure. The profiler descended at an average rate of 1.0 m/s with tilts of less than 3 degrees except near surface.

Observed data was analyzed by using software “Satlantic PPROSOFT 6” and extinction rate and photosynthetically available radiation (PAR) were computed.

Table 2 Locations of optical observation and principle characteristics
(Date and Time in LST: UTC+9hr at station S1)

Date and Time	Station	Lat./Long.	Surface PAR (quanta cm ⁻² sec ⁻¹)	Euphotic layer* (m)	Memo
2013.07.15 11:20	S1	30N/145E	1.3×10^{17}	~ 93	during PP incubation #1

* Euphotic layer: 0.5% of surface PAR

(3) Preliminary result

Because of malfunction (later investigation clarified that disconnection was the cause), we deployed “Free Fall sensor” only at station S1 (Table 2). Surface PAR was about 1.3×10^{17} quanta cm⁻² sec⁻¹. The euphotic layers, that is defined as water depth with 0.5 % of surface PAR, were approximately 93 m.

(4) Data archive

Optical data were filed on two types of file.

(BIN file) digital data of upwelling radiance and downwelling irradiance each 1 m from near surface to approximately 150 m for respective wave-lengths with surface PAR data during “Free Fall” deployment

(PAR file) in situ PAR each 1 m from near surface to approximately 100 m with extinction coefficient with surface PAR data during “Free Fall” deployment

These data files will be submitted to JAMSTEC Data Integration and Analyses Group (DIAG).

3.5 Biological study for phytoplankton and zooplankton

Katsunori KIMOTO (RIGC, JAMSTEC)

Haruka TAKAGI (Waseda University/ RIGC, JAMSTEC)

3.5.1 Planktic Foraminifer and radiolarian study in the western Pacific

(1) Objective

Planktic foraminifers and radiolarians produce calcium carbonate (CaCO_3) and siliceous ($\text{SiO}_2 + \text{nH}_2\text{O}$) tests respectively and that contribute to the material cycles of the ocean. Such shell-bearers show wide distribution in the water column. Recent molecular biological studies revealed the high genetic variations within many planktic foraminifera species. These intra-specific genetic variations considered to be the indications of the cryptic speciation and their ecologies could be different among these cryptic species. Moreover, morphological variations which correspond to the genetic populations is confirmed on several species. The water mass structure is considered as one of the factors which affect the distribution of the genetic populations. However, the relationships between genetic variability of the planktic foraminifers and property of water are not fully understood. In this cruise, we have following objectives for shell-bearers zooplankton: 1) Clarify the populations of planktic foraminifers and radiolarians in each water depths 2) Understanding of genetic variability in the planktic foraminifers and radiolarians between the North Pacific Subpolar gyre and the Subtropical gyre.

In addition, we tested a new analytical method to measure photosynthetic activities of symbiotic algae living in planktic foraminifer and radiolarian cells by using FRRF (Fast Repetition Rate Fluorometry) in this cruise. That is reported in Chapter 3.5.3.

(2) Methods

Living planktic foraminifera samples were collected by filtration of surface seawater and vertical towing of a NORPAC net (Fig. 3-5-1). Surface seawater taken from onboard seawater tap was filtered using filtration apparatus (100 μm opening mesh). The NORPAC net towing was conducted at station K2 and S1. A closing NORPAC net (63 μm opening) was used in order to obtain depth-stratified samples. The sampling depths of the NORPAC net tows are summarized in Table 3-5-1. Obtained NORPAC net samples were divided using sample separation apparatus and the half volume of the sample were used for DNA analysis. The other half were used for faunal assemblages.

All samples were stored at 4 °C immediately after collection. Living planktic foraminifer and radiolarian individuals were picked under a stereomicroscope in the laboratory. Picked specimens were cleaned in filtered seawater with fine brushes. Specimens were air dried on the faunal slides and stored at -80 °C. Remnant materials were

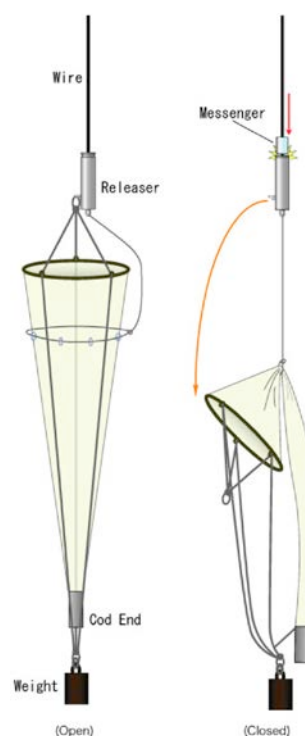


Fig.3-5-1 Schematic illustration of closing NORPAC net. Plankton net is open during towing (left), and closed at the top of the sampling depth range by deploying a messenger (right).

fixed by 99.5 % Ethanol and stored in the refrigerator.

(3) Preliminary result on shipboard analysis

Species identifications under stereomicroscope show that planktic foraminifer species at K2 consist of subpolar species while species at S1 is consist of subtropical species. Samples collected station K2 contained *Globigerina bulloides*, *Neogloboquadrina pachyderma*, *Turborotalita quinqueloba*, and *Globigerinita uvula* and *Globigerinita glutinata*. Planktic foraminifera species observed in the samples collected in the Subtropical Gyre region include *Globigerinoides ruber*, *Globigerinoides sacculifer*, *Globigerinoides tenellus*, *Globigerinoides conglobatus*, *Orbulina universa*, *Hastigerina pelagica*, *Globorotalia truncatulinoides*, *Globigerinella aequilateralis*, and *Streptochilus globulosus*. The number of individuals collected at S1 was very few compared with the samples collected at Stn. K2.

(4) Data archive

Planktic foraminifers and radiolarians sample is stored at JAMSTEC. Molecular phylogenetic analyses and morphological observations will be conducted.

Table 3-5-1. Summary of plankton tow sampling.

Station	Latitude			Longitude			Depth (m)	Equipments	Date			Time
Stn. S1	29	57	N	144	58	E	0-20	NORPAC Net	2013	7	14	8:28 UTC
Stn. S1	29	57	N	144	58	E	20-50	NORPAC Net	2013	7	14	8:34 UTC
Stn. S1	29	57	N	144	58	E	50-100	NORPAC Net	2013	7	14	8:47 UTC
Stn. S1	29	57	N	144	58	E	100-150	NORPAC Net	2013	7	14	8:59 UTC
Stn. S1	29	57	N	144	58	E	150-200	NORPAC Net	2013	7	14	9:13 UTC
Stn. S1	29	57	N	144	58	E	200-300	NORPAC Net	2013	7	14	9:29 UTC
Stn. S1	29	57	N	144	58	E	0-100	NORPAC Net	2013	7	14	9:55 UTC
Stn. S1	30	0	N	145	0	E	0-25	NORPAC Net	2013	7	15	9:00 UTC
Stn. S1	30	0	N	145	0	E	25-75	NORPAC Net	2013	7	15	9:06 UTC
Stn. S1	30	0	N	145	0	E	25-75	NORPAC Net	2013	7	15	9:17 UTC
Stn. S1	30	0	N	145	0	E	75-125	NORPAC Net	2013	7	15	9:27 UTC
Stn. S1	30	0	N	145	0	E	75-125	NORPAC Net	2013	7	15	9:39 UTC
Stn. S1	30	0	N	145	0	E	125-200	NORPAC Net	2013	7	15	9:52 UTC
Stn. S1	30	0	N	145	0	E	25-75	NORPAC Net	2013	7	15	10:08 UTC
Stn. K2	47	0	N	160	0	E	0-20	NORPAC Net	2013	7	22	6:30 UTC
Stn. K2	47	0	N	160	0	E	20-50	NORPAC Net	2013	7	22	6:39 UTC
Stn. K2	47	0	N	160	0	E	50-100	NORPAC Net	2013	7	22	6:48 UTC
Stn. K2	47	0	N	160	0	E	100-150	NORPAC Net	2013	7	22	6:59 UTC
Stn. K2	47	0	N	160	0	E	150-200	NORPAC Net	2013	7	22	7:12 UTC
Stn. K2	47	0	N	160	0	E	200-300	NORPAC Net	2013	7	22	7:27 UTC
Stn. K2	47	0	N	160	0	E	0-50	NORPAC Net	2013	7	22	7:46 UTC
Stn. K2	47	0	N	160	0	E	0-20	NORPAC Net	2013	7	23	5:49 UTC
Stn. K2	47	0	N	160	0	E	20-50	NORPAC Net	2013	7	23	5:56 UTC
Stn. K2	47	0	N	160	0	E	50-100	NORPAC Net	2013	7	23	6:05 UTC
Stn. K2	47	0	N	160	0	E	100-150	NORPAC Net	2013	7	23	6:17 UTC
Stn. K2	47	0	N	160	0	E	150-200	NORPAC Net	2013	7	23	6:32 UTC
Stn. K2	47	0	N	160	0	E	200-300	NORPAC Net	2013	7	23	6:47 UTC

3.5.2 Shell-bearing phytoplankton studies in the western North Pacific

(1) Objectives

Shell-beared phytoplankton (Diatoms, Silicoflagellates, and Coccolithophorids) are main primary producer of the ocean, therefore it is important to know their seasonal distribution, interactions, and transgressions of assemblages. Furthermore, hard skeletons of phytoplankton remains in the deep sea sediments and it provide useful information for paleoceanographic changes of sea surface water conditions. In this study, we collected water samples from Stn. K2 and S1 to investigate vertical distributions and ecological features of each phytoplankton.

(2) Methods

Seawater samples were obtained from upper 200 m water depths at all hydrocast stations by CTD/Niskin systems of 12 L bottle capacity. The locations that were collected seawater were listed in Table 3.5.2.

For coccolithophorid separations, maximally 10 litter seawaters were filtered using 0.45 μm membrane filter (ADVANTEC MFS, Inc., JAPAN) immediately after collection. For diatoms and silicoflagellates separations, 10 litter seawaters were also filtered using 0.45 μm membrane filter. After seawater filtration, membrane filters were rinsed by nano-pure water (Milli-Q water: $>18.2\text{M}\Omega$) and dried under room temperature.

(3) Future works

Collected samples were analyzed assemblages, diversities and spatial distributions for each taxon at onshore laboratory. These data will be compared with the sediment trap datasets that are moored at St. S1 and K2, same locations with water sampling points in this time. That should be provided the important information of seasonal and spatial variability of phytoplankton related with oceanographic changes in the western north Pacific.

Table3-5-2. Summary of seawater filtration sampling.

Station	Latitude			Longitude			Equipments	Depth (m)	Date			Time		water volume (ℓ)
Stn. S1	30	0	N	145	0	E	Niskin bottol	200	2013	7	14	23:30	UTC	20
Stn. S1	30	0	N	145	0	E	Niskin bottol	175	2013	7	14	23:30	UTC	20
Stn. S1	30	0	N	145	0	E	Niskin bottol	150	2013	7	14	23:30	UTC	20
Stn. S1	30	0	N	145	0	E	Niskin bottol	125	2013	7	14	23:30	UTC	20
Stn. S1	30	0	N	145	0	E	Niskin bottol	100	2013	7	14	23:30	UTC	20
Stn. S1	30	0	N	145	0	E	Niskin bottol	75	2013	7	14	23:30	UTC	20
Stn. S1	30	0	N	145	0	E	Niskin bottol	50	2013	7	14	23:30	UTC	20
Stn. S1	30	0	N	145	0	E	Niskin bottol	30	2013	7	14	23:30	UTC	20
Stn. S1	30	0	N	145	0	E	Niskin bottol	10	2013	7	14	23:30	UTC	20
Stn. S1	30	0	N	145	0	E	Bucket	0	2013	7	14	23:30	UTC	20
Stn. K2	47	0	N	160	0	E	Niskin bottol	200	2013	7	23	7:30	UTC	20
Stn. K2	47	0	N	160	0	E	Niskin bottol	175	2013	7	23	7:30	UTC	20
Stn. K2	47	0	N	160	0	E	Niskin bottol	150	2013	7	23	7:30	UTC	20
Stn. K2	47	0	N	160	0	E	Niskin bottol	125	2013	7	23	7:30	UTC	20
Stn. K2	47	0	N	160	0	E	Niskin bottol	100	2013	7	23	7:30	UTC	20
Stn. K2	47	0	N	160	0	E	Niskin bottol	75	2013	7	23	7:30	UTC	20
Stn. K2	47	0	N	160	0	E	Niskin bottol	50	2013	7	23	7:30	UTC	20
Stn. K2	47	0	N	160	0	E	Niskin bottol	30	2013	7	23	7:30	UTC	20
Stn. K2	47	0	N	160	0	E	Niskin bottol	10	2013	7	23	7:30	UTC	20
Stn. K2	47	0	N	160	0	E	Bucket	0	2013	7	23	7:30	UTC	20

3.5.3 Symbiotic algae studies in the western North Pacific

(1) Objectives

In modern oceans, about 45 species of living planktic foraminifers are known, and about 1/4 of them are “photosymbiotic” species which have photosynthetic algae in their cells. Photosynthetic algae (e.g., dinoflagellates, chrysophytes) are incorporated from ambient environment and harbored as symbionts within the host foraminiferal cytoplasm. Since the number of symbionts maintained in the host’s cell is quite large (around 10^3 - 10^4 cells per foraminifer, Spero and Parker, 1985), their photosynthetic activity cannot be ignored when considering primary production of the ocean. Photosymbiotic species are distributed mainly in warm, rather less nutritious regions. On the other hand, they become rare or cannot be found in high latitudinal nutritious regions. Therefore, their photosynthesis might contribute on primary production especially in warm regions where ocean productivity is low. In order to measure photosynthetic performance of symbiotic algae, we conducted FRRF measurement (Fast Repetition Rate Fluorometry) of individual planktic foraminifer-algal consortium. In addition, some radiolarian species are also known as symbiotic, thereby photosynthetic performance of radiolarians was also investigated in the same way.



Figure 3-5-2. Photomicrograph of a photosymbiotic planktic foraminifer. Figured specimen is *Globigerinoides sacculifer* obtained and cultured during MR13-04 cruise.

(2) Methods

Planktic foraminifers were collected by vertical towing of a closing NORPAC net or filtration of surface seawater (see 3.5.1 for detail). Living foraminifers were sorted and isolated using Pasteur pipette. Selected foraminiferal specimens were used for on board culturing and FRRF measurements.

Specimens were cultured in the Nunclon Multidish-12 wells (one individual per well) filled with filtered seawater (0.45 μ m filtration), and they were maintained in an incubator. White LED light was set at the top and the bottom of the incubator, in which irradiance was controlled to 150 μ mol·m⁻²·sec⁻¹, automatically turned on during the daytime (4:30–18:30), and turned off during the nighttime (18:30–4:30). Temperature was maintained at 20°C. During the culturing period, the specimens were fed *Artemia salina* (nauplii) about every 2 days. Only for herbivorous species, diatoms (*Thalassiosira* sp.) were supplied. FRRF measurement, which is non-destructive analysis, was done repeatedly on each cultured specimen during the culturing

period.

A FRR fluorometer was used to assess the photosynthetic competence of symbiotic algae within foraminifers and radiolarians (Diving Flash; Kimoto Electric; for details, see Fujiki et al. 2008). Samples were put into a quartz glass cuvette and placed on the detection window of the FRR fluorometer. To obtain the fluorescence induction curve in photosystem II (PSII), this instrument generates a series of blue flashes (a wavelength of 470 nm with a 25-nm bandwidth) at a repetition rate of about 250 kHz and an excitation light intensity of 25 mmol quanta m⁻² s⁻¹. We derived the PSII parameters from the fluorescence induction curve by using the numerical fitting procedure described by Kolber et al. (1998): these parameters included the minimum fluorescence (F_0), maximum fluorescence (F_m), variable fluorescence [F_v ($=F_m - F_0$)], potential photochemical efficiency (F_v/F_m), effective absorption cross-section of PSII (σ_{PSII}) and minimum turnover time (τ).

After the measurement of FRRF, some specimens were prepared for on shore DNA analysis of symbiotic algae. Living specimens for DNA analysis were picked up by brushes and put in milli-Q water within micro-tubes, then stored at -80°C. Some radiolarian specimens were treated in the same way for study of symbiotic algal DNA.

(3) Preliminary results

18 foraminiferal species were investigated; *Globigerinoides sacculifer*, *Gs. ruber*, *Gs. conglobatus*, *Orbulina universa*, *Globigerinella siphonifera*, *Globigerina bulloides*, *Neogloboquadrina dutertrei*, *N. incompta*, *N. pachyderma*, *Globorotalia menardii*, *Gr. inflata*, *Gr. truncatulinoidea*, *Pulleniatina obliquiloculata*, *Hastigerina pelagica*, *Globigerinita glutinata*, *Gt. uvula*, *Turborotalita quinqueloba*, and *Globoturborotalita tenella*. The results of on board FRRF measurement are summarized in Table 3-5-3. The FRRF result showed clear photosynthetic profiles for all *Globigerinoides* species, *Orbulina universa*, *Globigerinella siphonifera*, *Neogloboquadrina dutertrei*, and *Globorotalia menardii*. A few specimens of *Globigerinita glutinata*, *Gt. uvula*, and *Globoturborotalita tenella* showed significant fluorescence induction curve, though most of the specimens did not. For these species, further investigations are needed to identify photosymbiotic relationships.

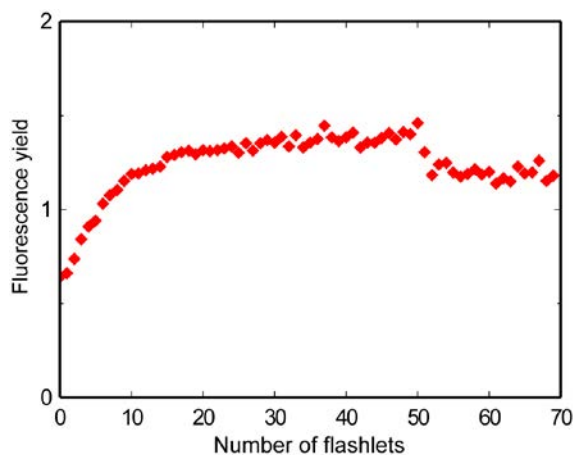


Figure 3-5-3. An example of fluorescence induction curve obtained by FRRF measurement of a photosymbiotic planktic foraminifer *Globigerinoides sacculifer*.

Table 3-5-3. Summary of on board FRRF measurement of planktic foraminifers.

Species	Number of specimens	Presence/absence of symbionts based on FRRF
<i>Globigerinoides sacculifer</i>	14	P
<i>Globigerinoides ruber</i>	14	P
<i>Globigerinoides conglobatus</i>	3	P
<i>Orbulina universa</i>	15	P
<i>Globigerinella siphonifera</i>	14	P
<i>Globigerina bulloides</i>	6	A
<i>Neogloboquadrina dutertrei</i>	13	P
<i>Neogloboquadrina incompta</i>	3	A
<i>Neogloboquadrina pachyderma</i>	3	A
<i>Globorotalia menardii</i>	3	P
<i>Globorotalia inflata</i>	1	A
<i>Globorotalia truncatulinoides</i>	3	A
<i>Pulleniatina obliquiloculata</i>	2	A
<i>Hastigerina pelagica</i>	2	A
<i>Globigerinita glutinata</i>	11	depends
<i>Globigerinita uvula</i>	9	depends
<i>Globoturborotalita tenella</i>	2	depends
<i>Turborotalita quinqueloba</i>	1	A

4) Data archive

The planktic foraminifer samples are stored at JAMSTEC. Morphological observations and isotopic analysis of foraminiferal chambers will be conducted on some selected specimens.

References

- Spero, H. J., and S. L., Parker, 1985, Photosynthesis in the symbiotic planktonic foraminifer *Orbulina universa*, and its potential contribution to oceanic primary productivity. *Journal of Foraminiferal Research*, 15: 273-281.
- Fujiki, T., T. Hosaka, H. Kimoto, T. Ishimaru, and T. Saino. 2008. In situ observation of phytoplankton productivity by an underwater profiling buoy system: use of fast repetition rate fluorometry. *Mar. Ecol. Prog. Ser.* 353: 81–88.
- Kolber, Z. S., O. Prášil and P. G. Falkowski. 1998. Measurements of variable chlorophyll fluorescence using fast repetition rate techniques: defining methodology and experimental protocols. *Biochim. Biophys. Acta.* 1367: 88-106.

3.6 Community structures and metabolic activities of microbes

(Studies on the microbial-geochemical processes that regulate the operation of the biological pump in the subarctic and subtropical regions of the western North Pacific)

Mario UCHIMIYA

(Atmosphere and Ocean Research Institute, The University of Tokyo: AORI)

Hideki FUKUDA (AORI)

Naomi SATO (AORI)

Hiroshi OGAWA (AORI)

Toshi NAGATA (AORI)

Koji HAMASAKI (AORI)

(1) Objective

A significant fraction of dissolved and particulate organic matter produced in the euphotic layer of oceanic environments is delivered to meso- and bathypelagic layers, where substantial transformation and decomposition of organic matter proceeds due to the actions of diverse microbes thriving in these layers. Spatio-temporal variations in organic matter transformation and decomposition in the ocean's interior largely affect patterns in carbon cycling in the global ocean. Thus elucidating activities and distribution patterns of microbes in deep oceanic waters is fundamentally important in order to better understand major controls of oceanic material cycling in the ocean.

The objective of this study is to determine seasonal variability of microbial activities during the time-series observation of vertical fluxes at the two distinctive oceanic stations located in the subarctic and subtropical western North Pacific. We investigated i) full-depth profiles of prokaryotic abundance and related biogeochemical parameters including dissolved organic carbon and nitrogen concentrations (potential resources of prokaryotes), and the abundances of viruses (potential predators of prokaryotes), ii) metabolic activities of Bacteria and Archaea, iii) temporal variation of prokaryote and labile organic matter and iv) sinking velocity and physico-chemical properties of suspended particles in the mixing layer.

(2) Method

Seawater samples were collected from predetermined depths of routine CTD cast and one or two additional casts, conducted at Stations K2 and S1 (see the meta-data sheet for details). Time series seawater sampling was conducted by using remote access sampler (RAS).

i) Full-depth profiles of prokaryotic activity and abundance and related biogeochemical parameters

- a) Prokaryotic abundance: Flowcytometry
- b) Prokaryotic production: ^3H -leucine incorporation
- c) Virus abundance: Flowcytometry
- d) DOC/DON: Concentrations of dissolved organic carbon and total dissolved nitrogen will be determined by the high temperature catalytic oxidation (HTCO) method. The concentration of dissolved organic nitrogen will be calculated by subtracting the

- concentration of dissolved inorganic nitrogen (determined by Auto-analyzer) from that of total dissolved nitrogen.
- e) Radio isotope composition of organic and inorganic carbon (see the meta-data sheet for details): $^{14}\text{C}/^{13}\text{C}$ ratio will be determined by using AMS (accelerator mass spectrometry).
- ii) Sinking velocity and physic-chemical properties of suspended particles
- a) Concentrations of particulate organic carbon and nitrogen: elemental analyzer for samples collected on GF/F filters.
- b) in situ observation of size distribution of suspended particles: Determined using in situ particle sizing instruments, LISST-100X and holographic camera, LISST-HOLO.
- iii) Time series seawater sampling for prokaryote and related biogeochemical parameters
- a) Prokaryote abundance: Flowcytometry
- b) DOC/DON: HTCO method (see above).
- (3) All results will be submitted to Data Management Office, JAMSTEC after analysis and validation and be opened to public via the web site.

3.7 Particle in the water column

3.7.1 LISST

Hideki FUKUDA

(Atmosphere and Ocean Research Institute, The University of Tokyo)

(1) Objective

The fate of particulate organic matter (POM) produced by primary producer in the surface layer have been one of the most major concern in biogeochemical oceanography during past three decades. Both physical behavior of POM in fluid and its biological availability are critically affected by its physical size. Thus development of *in situ* particle size distribution is supposed to be dominant process to control the fate of POM. On the other hand, increasing recognition that sinking flux of POC is related closely with that of biominerals such as opal and calcite, which act as ballast of settling particles, indicates importance of chemical composition and physical structure of POM. Therefore size dependency of effective density (excess density) of suspended particles in the surface layer of oceanic environments, its spatial variability and its controlling mechanism are key issue to understanding POM dynamics in global material cycling.

In this cruise I examined spatial patterns of i) the high resolution vertical profile of size spectrum of suspended particles (5-252 μm in diameter), which are potentially constituent of settling large aggregates, by using a low-angle light scattering instrument (LISST-100X, Sequoia Scientific Inc., USA), ii) the type of suspended particles (25-2500 μm in diameter) by using a submersible particle imaging system (LISST-HOLO, Sequoia Scientific Inc., USA), which can obtain 3D hologram of suspended particles and planktonic organisms and iii) settling velocity of suspended particles (5-252 μm in diameter).

(2) Method

The observation using LISST-100X and LISST-HOLO was conducted at station S1 and K2 from surface to 200 m in depth. Hodograph was intensively taken at 8 depth levels corresponding to the sampling layer of large volume pump (LVP) sampling (10, 20, 30, 50, 75, 100, 150 and 200 m). Water samples for measurement of effective density were collected from 10 m in depth by CTD-RMS. Settling velocity will be determined with small chamber attached on lesser pass of LISST-100X in land facility. Then a fractal dimension of suspended particles and excess density of solid in suspended particles will be estimated from a relationship between particle size and settling velocity assuming that suspended particles had spherical shape.

(3) All results will be submitted to Data Management Office, JAMSTEC after analysis and validation and be opened to public via the web site.

3.7.2 Suspended particles

Hajime KAWAKAMI (JAMSTEC MIO)

Makio C. HONDA (JAMSTEC RIGC)

Yoshihisa MINO (Nagoya University/JAMSTEC RIGC)

(1) Purpose of the study

To understand the vertical distributions of various size of organic particles and its behavior (formation, decomposition, transportation, etc.) in the western North Pacific Ocean

(2) Sampling

In situ filtering (suspended particulate) samples were taken at 10, 20, 30, 50, 75, 100, 150, and 200 m depths at stations K2, S1, and F1 using large volume pump sampler (Large Volume Water Transfer System WTS-6-1-142LV04, McLane Inc.). Approximately 800 L seawater was filtered through nylon mesh filter with a nominal pore size 250 and 53 μm , and glass-fiber filter with a nominal pore size of 0.7 μm at each station. The particles on 250 and 53 μm nylon filters were re-filtered through glass-fiber filter with a nominal pore size of 0.7 μm .

(3) Chemical analyses

The filter samples are exposed to HCl fumes overnight to remove carbonates and then dried. The particulate organic carbon (POC) and nitrogen (PON) are measured using an elemental analyzer (NC-2000, CE Instruments) in land-based laboratory. Nitrogen stable isotope is measured using a mass spectrometer (DELTA plus, Thermo Fisher Scientific).

(4) Preliminary result

The distributions of POC and PON of 0.7–53, 53–250, and >250 μm particle sizes will be determined as soon as possible after this cruise. This work will help further understanding of particle dynamics at the euphotic layers.

3.8. Dissolved Organic Carbon

Masahide WAKITA (Mutsu Institute for Oceanography, JAMSTEC)

(1) Purpose of the study

Fluctuations in the concentration of dissolved organic carbon (DOC) in seawater have a potentially great impact on the carbon cycle in the marine system, because DOC is a major global carbon reservoir. A change by < 10% in the size of the oceanic DOC pool, estimated to be ~ 700 GtC, would be comparable to the annual primary productivity in the whole ocean. In fact, it was generally concluded that the bulk DOC in oceanic water, especially in the deep ocean, is quite inert based upon ^{14}C -age measurements. Nevertheless, it is widely observed that in the ocean DOC accumulates in surface waters at levels above the more constant concentration in deep water, suggesting the presence of DOC associated with biological production in the surface ocean. This study presents the distribution of DOC during spring in the northwestern North Pacific Ocean.

(2) Sampling

Seawater samples were collected at stations E01, K2 (Cast 1 and 3), S1 (Cast 1 and 5) and F1, and brought the total to ~270. Seawater from each Niskin bottle was transferred into 60 ml High Density Polyethylene bottle (HDPE) rinsed with same water three times. Water taken from the surface to 250 m is filtered using precombusted (450°C) GF/F inline filters as they are being collected from the Niskin bottle. At depths > 250 m, the samples are collected without filtration. After collection, samples are frozen upright and preserved at ~ -20 °C cold until analysis in our land laboratory. Before use, all glassware was muffled at 550 °C for 5 hrs.

(3) Analysis

Prior to analysis, samples are returned to room temperature and acidified to pH < 2 with concentrated hydrochloric acid. DOC analysis was basically made with a high-temperature catalytic oxidation (HTCO) system improved a commercial unit, the Shimadzu TOC-V (Shimadzu Co.). In this system, the non-dispersive infrared was used for carbon dioxide produced from DOC during the HTCO process (temperature: 680 °C, catalyst: 0.5% Pt-Al₂O₃).

(4) Preliminary result

The distributions of DOC will be determined as soon as possible after this cruise.

(5) Data Archive

All data will be submitted to JAMSTEC Data Management Office (DMO) within 2 years.

3.9 Chlorofluorocarbons and sulfur hexafluoride

Masahide WAKITA (JAMSTEC MIO)

Ken-ichi SASAKI (JAMSTEC MIO)

(1) Objective

Chlorofluorocarbons (CFCs) and sulfur hexafluoride (SF_6) are man-made stable gases. These atmospheric gases can slightly dissolve in sea surface water by air-sea gas exchange and then are spread into the ocean interior. So dissolved these gases could be used as chemical tracers for the ocean circulation. We measured concentrations of three chemical species of CFCs, CFC-11 (CCl_3F), CFC-12 (CCl_2F_2), and CFC-113 ($\text{C}_2\text{Cl}_3\text{F}_3$), and SF_6 in seawater.

(2) Apparatus

We use three measurement systems. One is SF_6 /CFCs simultaneous analyzing system. Other two are CFCs analyzing system. Both systems are basically purging and trapping gas chromatography.

Table 3-5-1 Instruments

SF_6 /CFCs simultaneous analyzing system

Gas Chromatograph: GC-14B (Shimadzu Ltd.)

Detector 1: ECD-14 (Shimadzu Ltd)

Detector 2 ECD-14 (Shimadzu Ltd)

Analytical Column:

Pre-column: Silica Plot capillary column [OD: 0.32 mm, length: 10 m, film thickness: 4 μm]

Main column 1: Connected two columns (MS 5A packed column [1/16" OD, 10 cm length stainless steel tubing packed the section of 7 cm with 80/100 mesh Molecular Sieve 5A] followed by Gas Pro [OD: 0.32 mm, length: 35 m])

Main column2: Silica Plot capillary column [OD: 0.32mm, length: 30 m, film thickness: 4 μm]

Purging & trapping: Developed in JAMSTEC. Cold trap columns are 30 cm length stainless steel tubing packed the section of 5cm with 100/120 mesh Porapak T and followed by the section of 5cm of 100/120 mesh Carboxen 1000. OD of the main and focus trap columns are 1/8" and 1/16", respectively.

CFCs analyzing system

Gas Chromatograph: GC-14B (Shimadzu Ltd.)

Detector: ECD-14 (Shimadzu Ltd)

Analytical Column:

Pre-column: Silica Plot capillary column [OD: 0.53mm, length: 8 m, film thickness: 6 μm]

Main column:	Connected two capillary columns (Pola Bond-Q [OD: 0.53mm, length: 9 m, film thickness: 10 m] followed by Silica Plot [OD: 0.53mm, length: 14 m, film thickness: 6μm])
Purging & trapping:	Developed in JAMSTEC. Cold trap columns are 1/16" OD stainless steel tubing packed the section of 5cm with Porapak T.

(3) Procedures

3-1 Sampling

Seawater sub-samples were collected from 12 liter Niskin bottles to 300 ml and 400 ml of glass bottles for CFC and SF₆ measurements, respectively, at stations K2 and S1. The bottles were filled by nitrogen gas before sampling. Two times of the bottle volumes of seawater sample were overflowed. The bottles filled by seawater sample were kept in water bathes controlled at 5°C until analysis in our land-based laboratory. The CFCs and SF₆ concentrations were determined as soon as possible after this cruise.

In order to confirm CFC/SF₆ concentrations of standard gases and their stabilities and also to check saturation levels in sea surface water, mixing ratios in background air were analyzed. Air samples were collected into a 200ml glass cylinder at outside of our laboratory.

3-2 Analysis

SF₆/CFCs simultaneous analyzing system

Constant volume of sample water (200 ml) is taken into a sample loop. The sample is sent into stripping chamber and dissolved SF₆ and CFCs are de-gassed by N₂ gas purging for 9 minutes. The gas sample is dried by magnesium perchlorate desiccant and concentrated on a main trap column cooled down to -80 °C. Stripping efficiencies are frequently confirmed by re-stripping of surface layer samples and more than 99 % of dissolved SF₆ and CFCs are extracted on the first purge. Following purging & trapping, the main trap column is isolated and moved into slit of heater block electrically heated to 170 °C. After 1 minute, the desorbed gases are sent onto focus trap cooled down to -80 °C for 30 seconds. Gaseous sample on the focus trap are desorbed by same manner of the main trap, and lead into the pre-column. Sample gases are roughly separated in the pre-column. SF₆ and CFC-12 are sent on to main column 1 (MC 1) and CFC-11 and CFC-113 still remain on the pre-column. Main column connected on pre-column is switched to the main column 2 (MC 2). Another carrier gas line is connected to MC 1 and SF₆ and CFC-12 are further separated and detected by an electron capture detector, ECD 1. CFC-11 and CFC-113 lead to MC 2 are detected by ECD 2. When CFC-113 eluted from pre-column onto MC 2, the pre-column is switched onto another line and flushed by counter flow of pure nitrogen gas.

CFCs analyzing system

Constant volume of sample water (50 ml) is taken into a sample loop. The sample is sent into stripping chamber and dissolved CFCs are de-gassed by N₂ gas purging for 8 minutes.

The gas sample is dried by magnesium perchlorate desiccant and concentrated on a main trap column cooled down to -50 °C. Stripping efficiencies are frequently confirmed by re-stripping of surface layer samples and more than 99.5 % of dissolved CFCs are extracted on the first purge. Following purging & trapping, the trap column is isolated and electrically heated to 140 °C. The desorbed gases are lead into the pre-column. Sample gases are roughly separated in the pre-column. When CFC-113 eluted from pre-column onto main column, the pre-column is switched onto another line and flushed by counter flow of pure nitrogen gas.

Nitrogen gases used in these systems was filtered by gas purifier tube packed with Molecular Sieve 13X (MS-13X).

Table 3-5-2 Analytical conditions

SF₆/CFCs simultaneous analyses

Temperature

Analytical Column:	95 °C
Detector (ECD):	300 °C
Trap column:	-80 °C (at adsorbing) & 170 °C (at desorbing)

Mass flow rate of nitrogen gas (99.99995%)

Carrier gas 1:	5 ml/min
Carrier gas 2:	5 ml/min
Detector make-up gas 1:	35 ml/min
Detector make-up gas 2:	35 ml/min
Back flush gas:	7 ml/min
Sample purge gas:	200 ml/min

CFCs analyses

Temperature

Analytical Column:	95 °C
Detector (ECD):	240 °C
Trap column:	-50 °C (at adsorbing) & 140 °C (at desorbing)

Mass flow rate of nitrogen gas (99.99995%)

Carrier gas :	13 ml/min
Detector make-up gas :	24 ml/min
Back flush gas:	20 ml/min
Sample purge gas:	130 ml/min

(4) Preliminary result

The distributions of CFCs and SF₆ will be determined as soon as possible after this cruise. The standard gases used in this analysis will be calibrated with respect to SIO scale standard gases and then the data will be corrected.

(5) Data archive

All data will be submitted to JAMSTEC Data Management office (DMO) and under its control.

3.10 Vertical distribution of isotopic composition of dissolved oxygen

Osamu ABE (Nagoya University)

(1) Objective

$\Delta^{17}\text{O}$ of dissolved O_2 , which is defined approximately as $\delta^{17}\text{O} - 0.5\delta^{18}\text{O}$, is a unique tracer for primary productivity and gas transfer between atmosphere and water. This can be treated as a conservative component in subsurface (hypolimnion) waters, thus we could reconstruct past changes of productivity from subsurface $\Delta^{17}\text{O}$ values when the water was in the surface. Objective of this study is to clarify inter-annual variation of primary productivity at the subduction area of north Pacific intermediate water (NPIW) using vertical distribution $\Delta^{17}\text{O}$.

(2) Sampling

In this cruise, vertical water sampling was conducted at Station F1, K2 and S1. At coastal Station F1, 13 samples were obtained from 25 to bottom. One hundred and fifty milliliter of water was collected to vacuum flasks of 300mL except for anoxic layer, which expands below 600 m. In this layer, 1L water was collected to vacuum flasks of 2L for gaining sufficient signals in IRMS. At Station S1, 35 sample were obtained from 10 m to bottom. Between 1000 and 1800m, large vacuum flaks were used for sampling, and small flasks were used for other all depths. At Station K2, 34 samples were obtained from 10m to bottom including 4 duplicate samples. Large vacuum flasks were used between 300 and 1200 m, others collected with small flasks.

After the bottling, less soluble gases such as oxygen, argon and nitrogen are released to vacuum headspaces within 24 hours at room temperature. These gases will be collected using a vacuum line in the laboratory. Then O_2 gas will be purified using molecular sieve packed column and measured by isotope ratio mass spectrometer (IRMS) for $\Delta^{17}\text{O}$.

(3) Expected results

Previous investigations for $\Delta^{17}\text{O}$ has been limited to surface mixed layer and used for “present” primary productivity at the surface water. This study will first investigate whether this parameter would be really conserved the surface condition. On that basis, $\Delta^{17}\text{O}$ values for NPIW water masses from each location can be regarded as those surface values when water masses were at the surface. Compare to surface $\Delta^{17}\text{O}$, subsurface $\Delta^{17}\text{O}$ values would be controlled not only by primary productivity and gas transfer between atmosphere and water, but also by the amount of isopycnal and diapycnal mixing. With regard to gas exchanges between air-water, and stratified water masses could be quantified by measuring degrees of super-saturation for nitrogen and/or noble gases.

3.11 Argo float

Toshio SUGA (JAMSTEC RIGC, not on board): Principal Investigator

Shigeki HOSODA (JAMSTEC RIGC) Operation Leader

Taiyo KOBAYASHI (JAMSTEC RIGC not on board)

Kanako SATO (JAMSTEC RIGC: not on board)

Mizue HIRANO (JAMSTEC RIGC: not on board)

Ryuichiro INOUE (JAMSTEC RIGC: not on board)

Shinya KOUKETSU (JAMSTEC RIGC: not on board)

Shingo OSHITANI (MWJ)

(1) Objective

The recent studies have shown that the oceanic physical phenomena of a small scale from tens to hundreds kilometers such as meso-scale eddies have the potential to affect significantly the transport of material such as nutrients and the biological activity of phytoplankton. To clarify relationship between meso-scale eddy and biological activity, we investigate the observation project from FY2010, named INBOX (Western North Pacific Integrated Physical-Biogeochemical Ocean Observation Experiment). In MR11-05 cruise in FY2011, we observed physical and biogeochemical process around the mooring point S1 (30N, 145E) where is at the south of Kuroshio Extension, deploying 22 floats with dissolved oxygen sensors (DO-float) in the 150-km square area. In MR12-02 cruise in FY2012, we focused on meso-scale eddy activity and its growth and decay process, and decide a warm core eddy as the target in the mixed water region off Japan (41N, 147E). To capture the activity and decay process, we carried out launching 9 DO-floats at the center of the eddy, measuring temperature and salinity structures using data of XCTD, shipboard CTD with water sampling, and surface drifting buoys. In MR13-04, the purpose of the observation is to get long term data of physical-biogeochemical parameters such as temperature, salinity, and dissolved oxygen, launching one DO-float in the same eddy. As ship-board CTD measurements with water sampling are conducted, we can also validate the accuracy of the float's sensors. These observations totally make it possible to evaluate the relationship between meso-scale eddies and the biological activity together with the data of mooring buoys and research vessels.

In addition to the observation of physical-biogeochemical process in the meso-scale eddy, we launched two Argo floats to contribute maintaining the global Argo float array. Another aim of launching the floats is to clarify the structure and temporal/spatial variability of water masses in the North Pacific such as the North Pacific central mode water. The Argo floats can automatically measure vertical profiles of temperature and salinity with fine vertical resolution every ten days. The obtained data enable us to understand the variability and the formation mechanism of the water masses.

Further, we deployed one Deep Ninja at the S1 mooring point. The Deep Ninja can measure temperature and salinity at a depth of up to 4000m, which is far deeper than normal Argo float. Therefore, it is expected to capture long-term variations of the oceanic structure in wider area using Deep Ninjas. The development of Deep Ninja was started in 2009, and the long term observation in the Southern Ocean was succeeded in 2012-2013. In MR13-04, we will check technical data to improve the ability of Deep Ninja.

(2) Method

We launched one APEX float manufactured by Teledyne Webb Research (DO-APEX; point E01), two ARVOR floats manufactured by nke Inc. (point S1 and 42N), and one Deep Ninja manufactured by Tsurumi Seiki Co. LTD (point S1). All floats equip a CTD sensor of SBE41CP manufactured by Sea-Bird Electronics Inc (SBE) to measure temperature, salinity, and pressure and the DO-APEX has optode4330 DO sensor manufactured by Aanderaa Data Instruments (AADI) to measure dissolved oxygen additionally. The CTD sensors and the optode4330 on the DO-APEX had been calibrated in laboratory before shipping. The specifications for each float are shown in Tables 3.11-1 for DO-APEX, 3.11-2 for ARVORs and 3.11-3 for Deep Ninja. Shipboard CTD observation and water sampling were conducted at all points where the floats had been launched (point S1, 42N, and E01).

The DO-APEX usually drifts at 500 dbar and profiles from a depth of 2000 dbar once per two days (later changed the parameters to 600 dbar drifting /1000 dbar profiling every day). The DO-APEX has the Iridium transmitting system so that it can change their operation by commands from a base station. The Deep Ninja is set to drift at 1000 dbar and dives to 4000 dbar to measure CTD profiles every 5 days (later changed to 3000 and then 4000 dbar drifting and 4000 dbar profiling every 10 days). The Deep Ninja also can control its mission through the iridium telecommunication system. The ARVORs have ARGOS telecommunication system which can only send data via satellites from floats, which is the same as normal Argo floats. The ARVORs usually drifts at 1000 dbar and profiles from 2000 dbar every 10 days.

Table 3.11-1: Specification of launched float (APEX with Iridium transmission system)

Float Type	APEX float (manufactured by Teledyne Webb Research.)
CTD sensor	SBE41CP (manufactured by Sea-Bird Electronics Inc.)
Dissolved oxygen	Optode 4330 (manufactured by Aanderaa Data Instruments)
Cycle	2 days
Iridium transmit timeout	90 minutes (The timeout period at the sea surface)
Target Parking Pressure	1000 dbar
Sampling levels	Pressure, temperature, and salinity: each 2dbar from 2000dbar to surface (High resolution mode) Dissolved oxygen:75 levels (2000,1900,1800,1700,1600,1500,1450,1400,1350,1300,1250,1200,1150,1100,1050,1000,950,900,850,800,750,700,650,625,600,575,550,525,500,475,450,425,400,375,350,340,330,320,310,300,290,280,270,260,250,240,230,220,210,200,190,180,170,160,150,140,130,120,110,100,90,80,70,60,50,45,40,35,30,25,20,15, 10,6,and surface,dbar)

Table 3.11-2: Specification of launched float (Arvor with ARGOS transmission system)

Float Type	Arvor float (manufactured by nke Instrumentation.)
CTD sensor	SBE41CP (manufactured by Sea-Bird Electronics Inc.)
Dissolved oxygen	N/A
Cycle	10 days

ARGOS transmit timeout	11 hours(S1), 9 hours(42N)
Target Parking Pressure	2020 dbar
Sampling layers	Pressure, temperature, salinity:115 layers
	(2000,1950,1900,1850,1800,1750,1700,1650,1600,1550,1500,1450,1400,1350,1300,1250,1200,1150,1100,1050,1000,980,960,940,920,900,880,860,840,820,800,780,760,740,720,700,680,660,640,620,600,580,560,540,520,500,490,480,470,460,450,440,430,420,410,400,390,380,370,360,350,340,330,320,310,300,290,280,270,260,250,240,230,220,210,200,195,190,185,180,175,170,165,160,155,150,145,140,135,130,125,120,115,110,105,100,95,90,85,80,75,70,65,60,55,50,45,40,35,30,25,20,15,10,5and surface dbar)

Table 3.11-3: Specification of launched float (Deep Ninja with Iridium transmission system)

Float Type	Deep Ninja float manufactured by The Tsurumi-seiki Co., Ltd.
CTD sensor	SBE41CP for deep float manufactured by Sea-Bird Electronics Inc.
Dissolved oxygen	N/A
Cycle	5 days
Iridium transmit timeout	90 minutes (The timeout period at the sea surface)
Target Parking Pressure	1000 dbar
Sampling levels	Pressure, temperature, and salinity520 layers
	The deepest, every 20 dbar from 4000 to 2000 dbar, every 10 dbar from 2000 to 1000 dbar, every 5 dbar from 1000 to 400 dbar, and every 2 dbar from 400 dbar to surface (High resolution mode)

(3) Preliminary result

The Float S/N, ARGOS ID or IMEI Number, launched date/ time, launched position, and observation cycle of the float are summarized in Table. 3.11-4.

Table 3.11-4: Launched position and date/time

Float S/N	ARGOS/IMEI ID	Date and Time of Reset (UTC)	Date and Time of launch (UTC)	Launch position (point name)	Observation cycle	Remarks
0007	30023401 1985560	2013/7/17 02 : 28	2013/7/17 03 : 48	30 -03.91[N] 144-58.09[E] (S1)	5 days	Deep Ninja
OIN 13JAP- ARL-04	123564	2013/7/17 02 : 34	2013/7/17 03 : 50	30 -03.97[N] 144-58.06[E] (S1)	10 days	Arvor
OIN 13JAP- ARL-05	123565	2013/7/20 00 : 19	2013/7/20 01 : 53	42 -00.44[N] 152-33.89[E] (42N)	10 days	Arvor
6207	30002501 0719390	2013/7/26 19 : 36	2013/7/26 20 : 59	41 -15.48[N] 146-44.21[E] (E01)	2 days	APEX (Optode4330)

Launched position of the DO-APEX (S/N: 8349) and sea surface height anomaly is displayed in Fig. 3.11-1. The warm core eddy positioned around 42N, 147E still alive from previous Mirai's INBOX observation in MR12-02, although some detach and deformation were occurred during one year. The DO-APEX was launched around the center of the eddy with ship-board CTD and water sampling observations. Temporal changes of temperature, salinity, $\sigma\theta$, and dissolved oxygen by middle August are shown in Fig. 3.11-2.

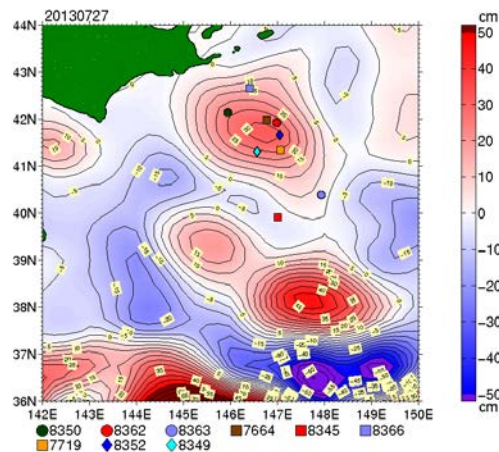


Figure 3.11-1. Float position (DO-APEX; S/N 8349) on July 27, 2013. Background color and contour is sea surface height anomaly map obtained from AVISO. Nine floats were deployed in the warm core eddy, drifting anti-cyclonically with current of meso-scale eddy.

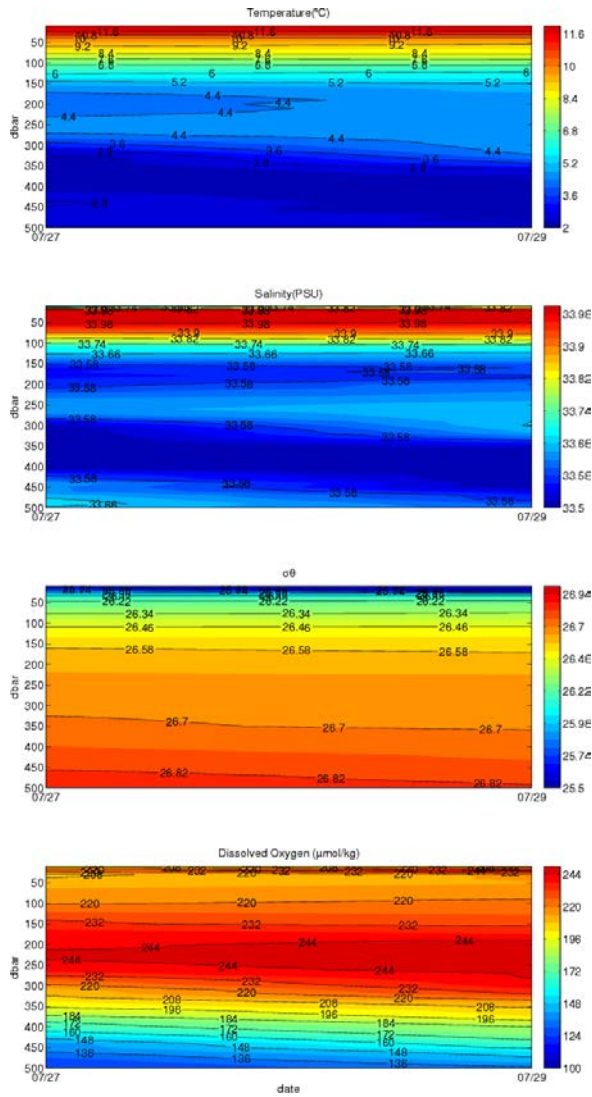


Figure 3.11-2. Time series of temperature, salinity, σ_t , and dissolved oxygen in 0-500 dbar. Those are obtained from the DO-APEX (S/N: 8349).

Deep Ninja has moved anti-cyclonically and measured four CTD profiles from 4000 dbar to the surface since the deployment. for almost a month. It has operated very well (as of the middle of August 2013). Figure 3.11-3 shows the summary of its performance.

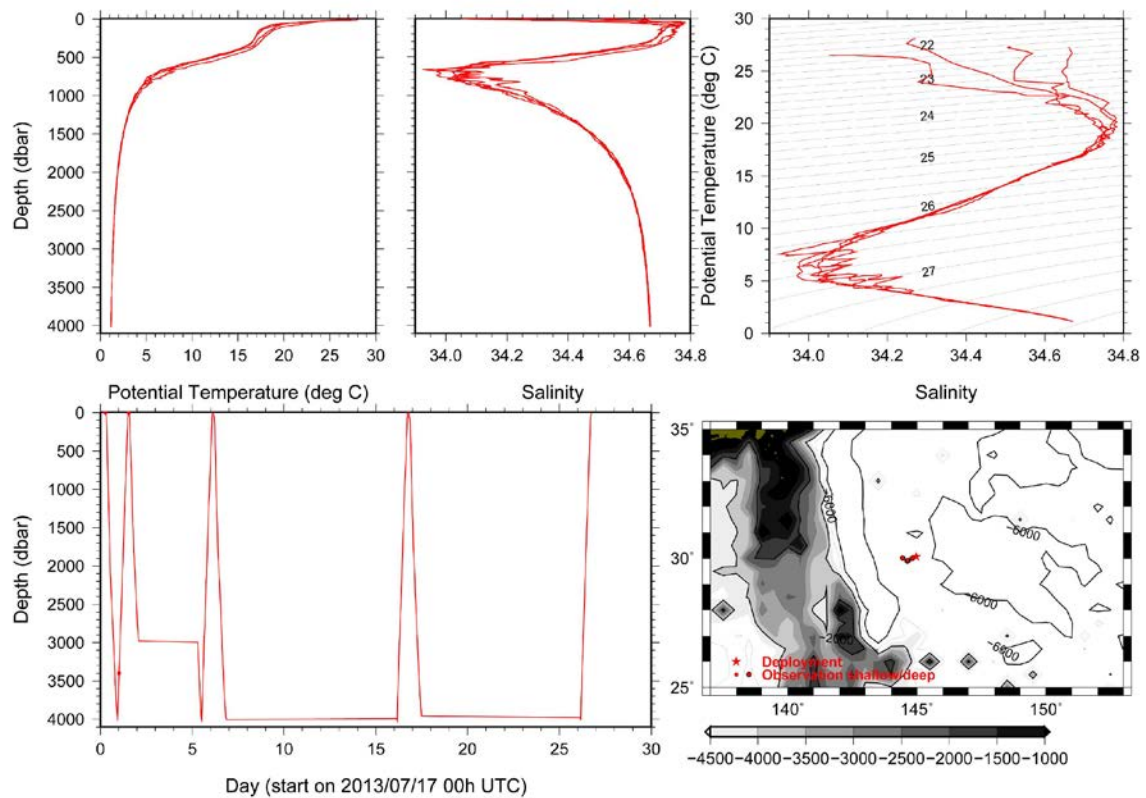


Figure 3.11-3. Summary of the operation of Deep Ninja (S/N: 0007) since the deployment at S1 (as of the middle of August). The lower left panel shows the vertical movement of Deep Ninja.

(4) Data archive

The data of ARVORs are produced from Global Data Assembly Center (GDAC: <http://www.usgodae.org/argo/argo.html>, or <http://www.coriolis.eu.org/>) and Global Telecommunication System (GTS) in real-time, with real-time quality control. The data of DO-APEX and Deep Ninja will be released via the GDAC within two years.

3.12 Temporal changes in water properties of abyssal water in the western North Pacific

Hiroshi UCHIDA (JAMSTEC RIGC) (Principal Investigator)

Masahide WAKITA (JAMSTEC MIO)

Akihiko MURATA (JAMSTEC RIGC) (not on board)

(1) Objective

The objective of this study is to clarify temporal changes in water properties of abyssal water in the western North Pacific by means of moored CTD/O₂ observations. The time series data will be used to evaluate sampling error caused by short-term temperature fluctuation for the estimation of bottom water warming in recent decades derived from land-to-land repeat hydrographic data, and to monitor long-term fluctuation of water properties of the abyssal water.

(2) Materials and methods

CTDs used in the mooring observations were SBE-37 SM (Sea-Bird Electronics, Inc., Bellevue, Washington, USA). The SBE-37s had no pump, but included an optional pressure sensor with a range of 7000 m (Paine Electronics, LLC, East Wenatchee, Washington, USA). Oxygen sensors used in the mooring observations were Oxygen Optode model 3830 (Aanderaa Data Instruments AS, Bergen, Norway) from October 2008 to June 2012, and Rinko I (JFE Advantech Co., Ltd., Kobe, Japan) from June 2012. The Oxygen Optode sensor was attached to a datalogger with an internal battery and memory in a titanium housing designed for mooring observation (Compact OPTODE; Alec Electronics Co., Ltd., Kobe, Japan) (Uchida et al., 2008).

The CTD and oxygen sensors were attached to the acoustic releaser of the BGC mooring system (Table 3.12.1). Depth of the acoustic releasers was 34 m above the sea floor. The data were obtained at a sampling interval of 1 hour.

For in situ calibration before mooring deployment or after mooring recovery, these sensors were attached to the CTD/water-sampling frame and the data sampled at 10 or 12 second intervals will be compared with the simultaneously obtained shipboard CTD/O₂ data. For the oxygen sensors, laboratory calibration was also performed at JAMSTEC.

(3) Quality control of the CTD/O₂ data

The data processing sequence for quality control of the CTD/O₂ data was as follows:

- 1) The exponential time drift of the pressure sensor was corrected. The time drift was estimated by fitting an exponential-linear curve, $P = c_0 \exp[c_1 t] + c_2 t + c_3$, where t is time. Then the exponential time drift ($c_0 \exp[c_1 t]$) was subtracted from the pressure data.
- 2) Offset of the pressure sensor and linear time drift of the temperature sensor were estimated from the results of the in situ comparison with shipboard CTD data obtained during the cruises MR10-01 and MR12-02. Data obtained during the bottle firing stops for depths deeper than 5000 dbar were averaged and used to estimate offset and linear time drift relative to January 1, 2008.

Pressure offset: 11.2 dbar for S/N 2730, 12.6 dbar for S/N 2731

Temperature offset: 0.0015 °C for S/N 2730, -0.0018 °C for S/N 2731

Temperature time drift: 4.58255×10^{-7} °C/day for S/N 2730, 5.40917×10^{-7} °C/day for S/N

- 3) Salinity measured by the moored CTD is very noisy. Therefore, salinity was estimated from the temperature–salinity relation obtained from the shipboard CTD data. Linear relations for the data deeper than 4500 dbar of the CTD profiles obtained during the cruises MR10-01, MR11-02, MR11-03, MR11-05, MR12-02, and MR13-04 were calculated for each of the K2 and S1 stations. Salinity were measured referred to the IAPSO Standard Seawater P152 for MR10-01, MR11-02, MR11-03 and MR11-05, and P154 for MR12-02 and MR13-04. The IAPSO Standard Seawater batch offset correction (+0.0005) was applied for the salinity data from MR12-02 and MR13-04. Firstly, salinity was preliminarily estimated by using temperature of the moored CTD and the in situ temperature–salinity relation. Secondly, potential temperature was calculated pressure and temperature of the moored CTD and the estimated salinity. Finally, salinity was estimated by using the potential temperature and the potential temperature–salinity relation. The temperature–salinity relations are as follows.

$$\text{Salinity} = 34.6324 + 0.0377726 \times (\text{in situ temperature}) \text{ for station K2}$$

$$\text{Salinity} = 34.8123 - 0.113345 \times (\text{potential temperature}) \text{ for station K2}$$

$$\text{Salinity} = 34.6314 + 0.0389634 \times (\text{in situ temperature}) \text{ for station S1}$$

$$\text{Salinity} = 34.8008 - 0.102767 \times (\text{potential temperature}) \text{ for station S1}$$

- 4) Oxygen Optode sensors were calibrated by using the results from post-recovery laboratory calibrations performed at JAMSTEC. The calibration coefficients for the equation of Uchida et al. (2010) are as follows.

For S/N 3, 2012/08/07

$$c0 = 2.420219\text{e-}3$$

$$c1 = 1.039146\text{e-}4$$

$$c2 = 1.691735\text{e-}6$$

$$d0 = -1.522458\text{e-}3$$

$$d1 = -8.646764\text{e-}2$$

$$d2 = 1.764567\text{e-}2$$

$$cp = 0.032$$

For S/N 5, 2012/08/30

$$c0 = 2.385680\text{e-}3$$

$$c1 = 1.048169\text{e-}4$$

$$c2 = 1.751023\text{e-}6$$

$$d0 = -1.457683\text{e-}3$$

$$d1 = -9.247459\text{e-}2$$

$$d2 = 1.776070\text{e-}2$$

$$cp = 0.032$$

For the first mooring period of station K2, the moored CTD data was not available. Pressure was estimated to be constant and same as average for the second mooring period (5279.4 dbar). Temperature measured by the Oxygen Optode was used with offset correction (+0.01°C).

- 5) Rinko sensors were calibrated by using the results from pre-deployment laboratory calibrations performed at JAMSTEC. The calibration equation was slightly modified as follows.

$$[\text{O}_2] \text{ (in } \mu\text{mol/L)} = \left[\left\{ (1 + d0) / (d1 + d2) \right\}^{e0} - 1 \right] / (c0 + c1T + c2T^2)$$

The calibration coefficients are as follows.

For S/N 51, 2013/05/28

$c0 = 5.487803e-3$
 $c1 = 2.200586e-4$
 $c2 = 4.116919e-6$
 $d0 = -1.060837e-3$
 $d1 = 3.926398e-2$
 $d2 = 0.1756096$
 $e0 = 1.5$
 $cp = 0.032$

For S/N 52, 2013/05/28

$c0 = 5.936116e-3$
 $c1 = 2.511621e-4$
 $c2 = 5.147401e-6$
 $d0 = -1.167789e-4$
 $d1 = 2.416130e-2$
 $d2 = 0.1789840$
 $e0 = 1.5$
 $cp = 0.032$

(4) Preliminary result

Time series of CTD/O₂ data obtained by the mooring observations were shown in Figs. 3.12.1 and 3.12.2. The oxygen data were drifted in time during the mooring period, probably due to a slow time-dependent, pressure-induced effect. Similar drifts were observed in the Wake Island passage Flux Experiment (Uchida et al., 2009). The pressure-induced effect is larger for the Rinko than for the Oxygen Optode. The effect is not corrected for the oxygen data.

(5) Data archive

The quality-controlled moored CTD/O₂ data were submitted to JAMSTEC Data Integration and Analyses Group (DIAG).

(6) References

- Uchida, H., T. Kawano, I. Kaneko and M. Fukasawa (2008): In situ calibration of optode-based oxygen sensors. *J. Atmos. Oceanic Technol.*, 25, 2271-2281.
- Uchida, H., H. Yamamoto, K. Ichikawa, M. Kawabe and M. Fukasawa (2009): Wake Island Passage Flux Experiment Data Book, JAMSTEC, Yokosuka, Japan, 93 pp.
- Uchida, H., G. C. Johnson and K. E. McTaggart (2010): CTD oxygen sensor calibration procedures, The GO-SHIP Repeat Hydrography Manual: A Collection of Expert Reports and Guidelines, IOCCP Report No. 14, ICPO Publication Series No. 134, Version 1.

Table 3.12.1. Summary of mooring observations of abyssal water.

Cruise	Mooring	K2	S1
MR08-05	Deployment	2008/10/28 01:13 (K-2 BGC) 47-00.36 N, 159-58.16 E, 5206 m SBE37 S/N 2757 (5172 m) OPTODE S/N 5 (5172 m)	None
MR10-01	Recovery	2010/01/24 11:20 The SBE 37 was leaked and no data is available for the SBE 37.	None
	In situ calibration	Station S01 cast 2 (SBE37 and OPTODE)	Station S01 cast 2 (SBE37 and OPTODE)
	Deployment	2010/02/15 05:05 (K2 BGC) 47-00.34 N, 159-58.24 E, 5206 m SBE37 S/N 2731 (5172 m) OPTODE S/N 5 (5172 m)	2010/02/03 03:06 (S1 BGC) 30-03.88 N, 144-57.96 E, 5926 m SBE37 S/N 2730 (5892 m) OPTODE S/N 3 (5892 m)
MR10-06	Recovery	2010/10/25 01:41	2010/11/06 01:44
	Deployment	2010/10/31 05:35 (K2 BGC) 47-00.37 N, 159-58.24 E, 5218 m SBE37 S/N 2731 (5184 m) OPTODE S/N 5 (5184 m)	2010/11/10 01:52 (S1 BGC) 30-03.92 N, 144-57.98 E, 5927 m SBE37 S/N 2730 (5893 m) OPTODE S/N 3 (5893 m)
MR11-05	Recovery	2011/06/30 02:04	2011/07/24 21:19
	Deployment	2011/07/04 00:24 (K2 BGC) 47-00.34 N, 159-58.42 E, 5218 m SBE37 S/N 2731 (5184 m) OPTODE S/N 5 (5184 m)	2011/07/28 23:04 (S1 BGC) 30-03.93 N, 144-58.03 E, 5924 m SBE37 S/N 2730 (5890 m) OPTODE S/N 3 (5890 m)
MR12-02	Recovery	2012/06/09 19:38	2012/06/25 21:50
	In situ calibration	Station K02 cast 6 (SBE37, OPTODE and Rinko)	Station K02 cast 6 (Rinko) Station S01 cast 5 (SBE37)
	Deployment	2012/06/14 23:57 (K2 BGC) 47-00.40 N, 159-58.22 E, 5222 m SBE37 S/N 2731 (5188 m) Rinko I S/N 51 (5188 m)	2012/07/02 02:30 (S1 BGC) 30-03.93 N, 144-58.21 E, 5930 m SBE37 S/N 2730 (5896 m) Rinko I S/N 52 (5896 m)
MR13-04	Recovery	2013/07/21 23:49	2013/07/15 07:07
	Deployment	2013/07/23 23:50 (K2 BGC) 47-00.47 N, 159-58.40 E, 5219 m SBE37 S/N 2731 (5185 m) Rinko I S/N 51 (5185 m)	2013/07/17 02:38 (S1 BGC) 30-03.86 N, 144-57.81 E, 5927 m SBE37 S/N 2730 (5893 m) Rinko I S/N 52 (5893 m)

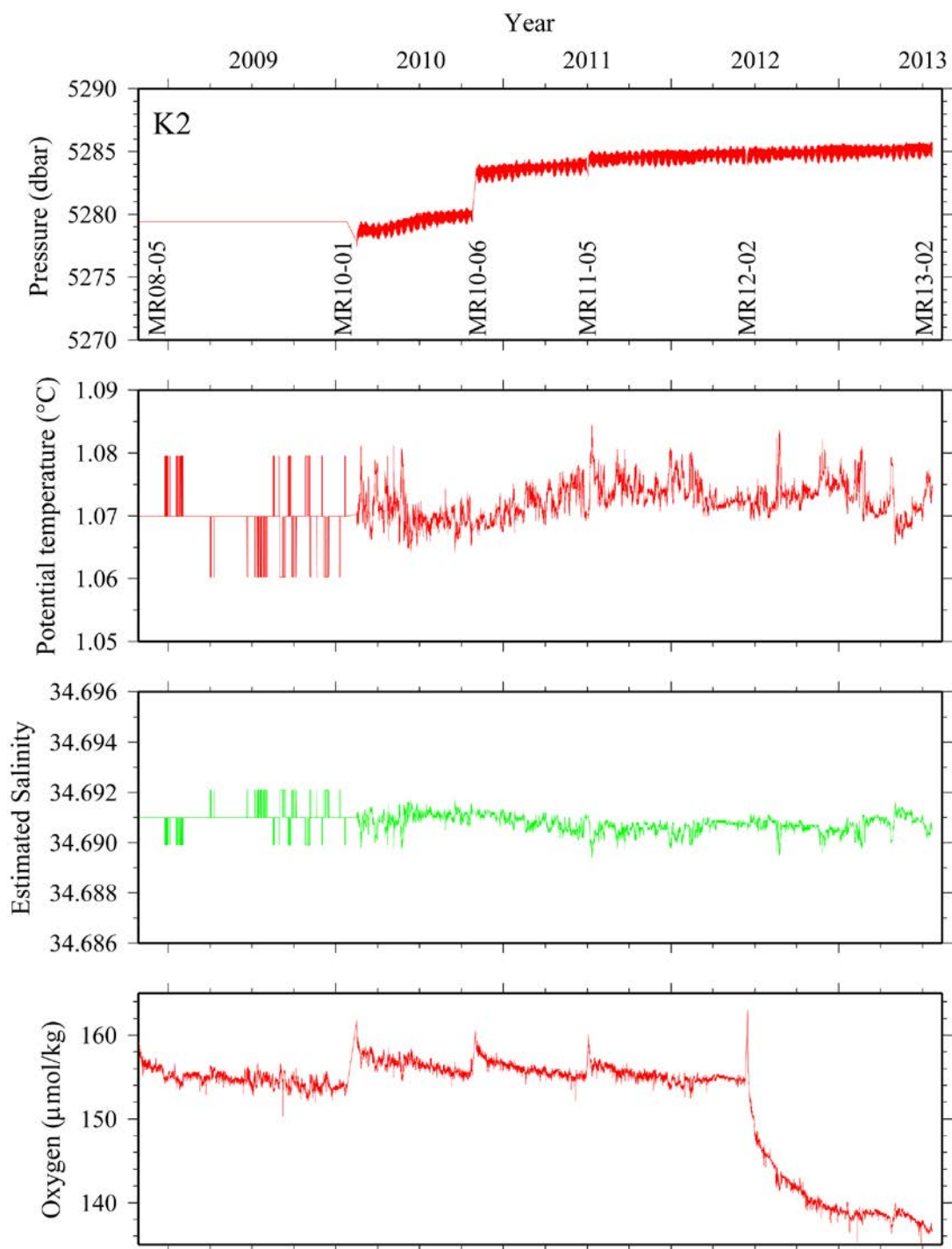


Fig. 3.12.1. Time series of pressure, potential temperature, estimated salinity and oxygen at 34 m above the sea floor for K2 station.

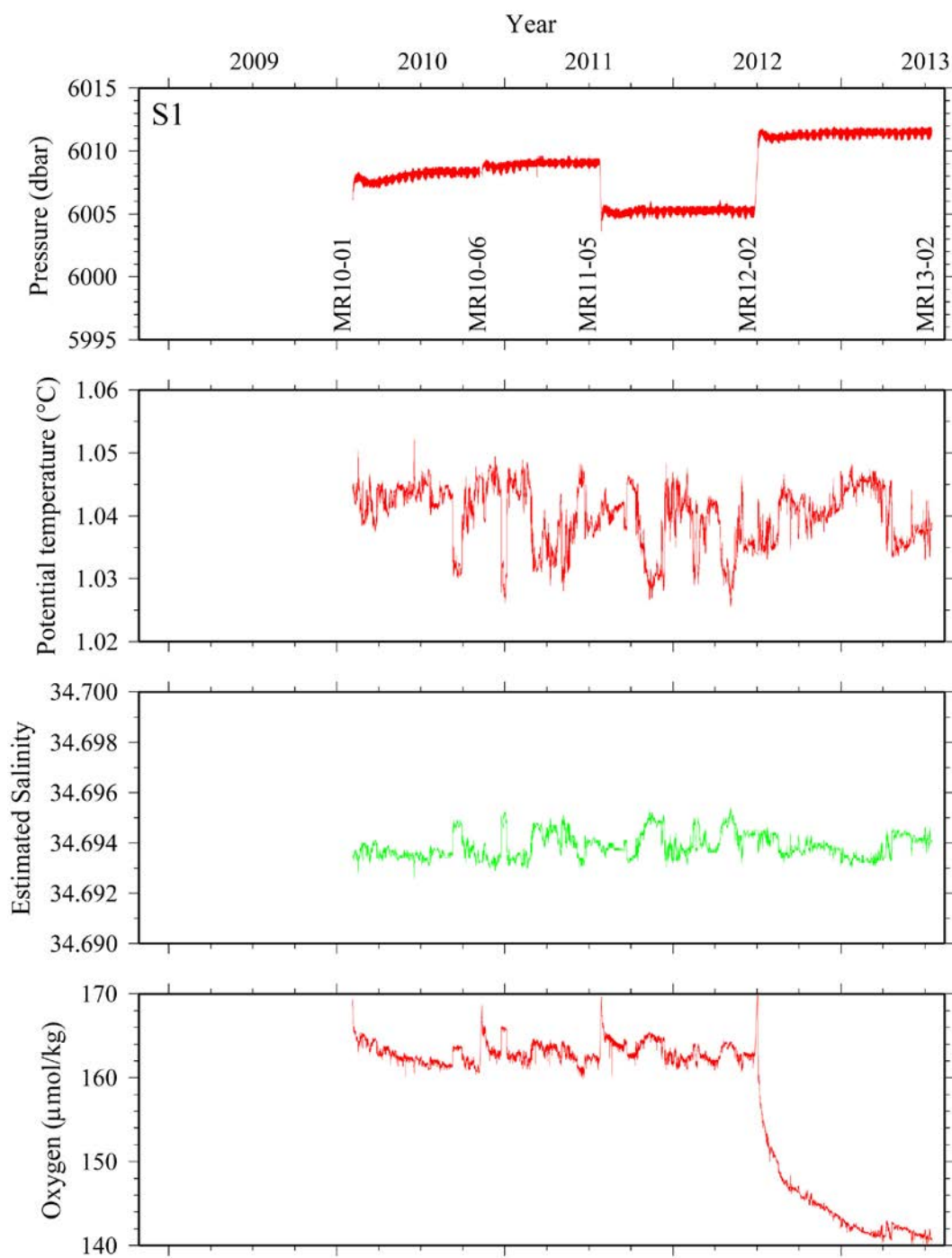


Fig. 3.12.2. Same as Fig. 3.12.1, but for S1 station.

3.13 Fukushima related observation

3.13.1 The concentrations of radionuclides in the western North Pacific

Miho FUKUDA (National Institute of Radiological Science: NIRS)

Tatsuo AONO (NIRS)

Hajime KAWAKAMI (JAMSTEC)

Makio HONDA (JAMSTEC)

(1) Objective

Artificial radionuclides such as radioactive caesium in the ocean were mainly delivered by global fallout before the TEPCO's Fukushima Daiichi Nuclear Power Station (FDNPS) accident. The accident caused emission of radionuclides to atmosphere and ocean, and the large volume of radioactively contaminated water containing high concentrations of radionuclides were discharged to ocean from the FDNPS. In order to clarify the distributions and behavior of radioactive caesium in the western North Pacific, as the activities of caesium in seawater have not decreased by pre-accident level of 1.5 ~ 2 mBq/L, seawater samples were collected during this cruise.

(2) Seawater sampling

Surface seawater samples were collected along the cruise track with an underway surface pump and deep seawater samples were collected by 12 liter Niskin bottles on the CTD/Carousel Water sampling system and a bucket at the time series stations (F1, S1, KEO, JKEO, KNOT and K2) (Table 1).

(3) Future work

The radioactive caesium in seawater will be determined with the AMP method and a gamma spectrometry using extended range coaxial Ge detector. A comparison between obtained results and those of previous cruise (MR11-05 and MR 12-02) will be done in order to clarify the diffusive situation in the western North Pacific.

Table 1 The list and information of seawater samples collected in the cruise of MR 13-04.

Sample number	Date	Time (UTC)	Location		Note
			Latitude	Longitude	
MR13-04-1	2013/7/10	07:07-07:20	35° 00.0' N	140° 35.0' E	Off Boso peninsula (→F1) (0m) in Lab
MR13-04-2	2013/7/10	07:07-07:20	35° 00.0' N	140° 35.0' E	Off Boso peninsula (→F1) (0m) in Lab
MR13-04-3	2013/7/10	07:07-07:20	35° 00.0' N	140° 35.0' E	Off Boso peninsula (→F1) (0m) in Lab
MR13-04-4	2013/7/11	07:15-07:50	36° 29.1' N	141° 29.6' E	F1(0m) in Lab.
MR13-04-5	2013/7/11	07:15-07:50	36° 29.1' N	141° 29.6' E	F1(0m) in Lab.
MR13-04-6	2013/7/11	07:15-07:50	36° 29.1' N	141° 29.6' E	F1(0m) in Lab.
MR13-04-7	2013/7/11	07:15-07:50	36° 29.1' N	141° 29.6' E	F1(0m) in Lab.
MR13-04-8	2013/7/11	07:15-07:50	36° 29.1' N	141° 29.6' E	F1(0m) in Lab.
MR13-04-9	2013/7/11	07:32-08:50	36° 28.7' N	141° 28.7' E	F1(800m) in a Niskin sampler
MR13-04-10	2013/7/11	07:32-08:50	36° 28.7' N	141° 28.7' E	F1(600m) in a Niskin sampler
MR13-04-11	2013/7/11	07:32-08:50	36° 28.7' N	141° 28.7' E	F1(400m) in a Niskin sampler
MR13-04-12	2013/7/11	07:32-08:50	36° 28.7' N	141° 28.7' E	F1(200m) in a Niskin sampler
MR13-04-13	2013/7/11	07:32-08:50	36° 28.7' N	141° 28.7' E	F1(150m) in a Niskin sampler
MR13-04-14	2013/7/11	07:32-08:50	36° 28.7' N	141° 28.7' E	F1(100m) in a Niskin sampler
MR13-04-15	2013/7/11	07:32-08:50	36° 28.7' N	141° 28.7' E	F1(50m) in a Niskin sampler
MR13-04-16	2013/7/11	07:32-08:50	36° 28.7' N	141° 28.7' E	F1(25m) in a Niskin sampler
MR13-04-17	2013/7/12	06:50-07:15	37° 15.2' N	142° 14.9' E	F1→FS1 (0m) in Lab.
MR13-04-18	2013/7/12	07:18-07:30	37° 11.1' N	142° 15.0' E	F1→FS1 (0m) in Lab.
MR13-04-19	2013/7/12	07:37-07:50	37° 07.8' N	142° 24.2' E	F1→FS1 (0m) in Lab.
MR13-04-20	2013/7/12	07:52-08:03	37° 05.7' N	142° 26.6' E	F1→FS1 (0m) in Lab.
MR13-04-21	2013/7/12	08:05-08:19	37° 03.0' N	142° 29.7' E	F1→FS1 (0m) in Lab.
MR13-04-22	2013/7/13	01:20-01:32	33° 41.4' N	144° 01.9' E	FS1→F1 (0m) in Lab.
MR13-04-23	2013/7/13	01:35-01:42	33° 39.8' N	144° 02.3' E	FS1→F1 (0m) in Lab.
MR13-04-24	2013/7/13	01:45-01:51	33° 38.2' N	144° 02.8' E	FS1→F1 (0m) in Lab.
MR13-04-25	2013/7/13	01:52-01:58	33° 37.1' N	144° 03.1' E	FS1→F1 (0m) in Lab.
MR13-04-26	2013/7/13	01:58-02:04	33° 35.6' N	144° 03.5' E	FS1→F1 (0m) in Lab.
MR13-04-27	2013/7/14	04:07-04:12	29° 58.5' N	144° 59.3' E	S1(0m) in Lab.
MR13-04-28	2013/7/14	04:12-04:18	29° 58.5' N	144° 59.3' E	S1(0m) in Lab.
MR13-04-29	2013/7/14	04:18-04:23	29° 58.5' N	144° 59.2' E	S1(0m) in Lab.
MR13-04-30	2013/7/14	04:24-04:30	29° 58.4' N	144° 59.2' E	S1(0m) in Lab.
MR13-04-31	2013/7/14	04:31-04:37	29° 58.4' N	144° 59.2' E	S1(0m) in Lab.
MR13-04-32	2013/7/14	23:27-00:12	30° 00.0' N	145° 00.0' E	S1(200m) in a Niskin sampler
MR13-04-33	2013/7/14	23:27-00:12	30° 00.0' N	145° 00.0' E	S1(175m) in a Niskin sampler
MR13-04-34	2013/7/14	23:27-00:12	30° 00.0' N	145° 00.0' E	S1(150m) in a Niskin sampler
MR13-04-35	2013/7/14	23:27-00:12	30° 00.0' N	145° 00.0' E	S1(125m) in a Niskin sampler
MR13-04-36	2013/7/14	23:27-00:12	30° 00.0' N	145° 00.0' E	S1(100m) in a Niskin sampler
MR13-04-37	2013/7/14	23:27-00:12	30° 00.0' N	145° 00.0' E	S1(75m) in a Niskin sampler
MR13-04-38	2013/7/14	23:27-00:12	30° 00.0' N	145° 00.0' E	S1(50m) in a Niskin sampler
MR13-04-39	2013/7/14	23:27-00:12	30° 00.0' N	145° 00.0' E	S1(25m) in a Niskin sampler
MR13-04-40	2013/7/14	23:27-00:12	30° 00.0' N	145° 00.0' E	S1(10m) in a Niskin sampler
MR13-04-41	2013/7/15	04:22-04:29	30° 03.7' N	144° 57.4' E	S1(0m) in Lab.
MR13-04-42	2013/7/15	04:32-04:41	30° 03.4' N	144° 57.4' E	S1(0m) in Lab.
MR13-04-43	2013/7/15	04:42-04:50	30° 03.2' N	144° 57.5' E	S1(0m) in Lab.
MR13-04-44	2013/7/15	04:52-05:00	30° 03.1' N	144° 57.4' E	S1(0m) in Lab.
MR13-04-45	2013/7/15	05:01-05:09	30° 02.9' N	144° 57.3' E	S1(0m) in Lab.
MR13-04-46	2013/7/15	20:31-21:02	30° 00.0' N	145° 00.0' E	S1(0m) in Bucket
MR13-04-47	2013/7/15	20:31-21:02	30° 00.0' N	145° 00.0' E	S1(0m) in Bucket
MR13-04-48	2013/7/15	20:31-21:02	30° 00.0' N	145° 00.0' E	S1(0m) in Bucket
MR13-04-49	2013/7/15	20:31-21:02	30° 00.0' N	145° 00.0' E	S1(0m) in Bucket
MR13-04-50	2013/7/15	20:31-21:02	30° 00.0' N	145° 00.0' E	S1(0m) in Bucket
MR13-04-51	2013/7/16	20:31-21:59	30° 00.0' N	145° 00.0' E	S1(800m) in a Niskin sampler
MR13-04-52	2013/7/16	20:31-21:59	30° 00.0' N	145° 00.0' E	S1(600m) in a Niskin sampler
MR13-04-53	2013/7/16	20:31-21:59	30° 00.0' N	145° 00.0' E	S1(400m) in a Niskin sampler
MR13-04-54	2013/7/16	20:31-21:59	30° 00.0' N	145° 00.0' E	S1(200m) in a Niskin sampler
MR13-04-55	2013/7/16	20:31-21:59	30° 00.0' N	145° 00.0' E	S1(150m) in a Niskin sampler
MR13-04-56	2013/7/16	20:31-21:59	30° 00.0' N	145° 00.0' E	S1(100m) in a Niskin sampler
MR13-04-57	2013/7/16	20:31-21:59	30° 00.0' N	145° 00.0' E	S1(50m) in a Niskin sampler
MR13-04-58	2013/7/16	20:31-21:59	30° 00.0' N	145° 00.0' E	S1(25m) in a Niskin sampler
MR13-04-59	2013/7/17	10:09-10:17	31° 36.3' N	144° 41.0' E	S1→KEO(0m) in Lab.
MR13-04-60	2013/7/17	10:19-10:27	31° 38.9' N	144° 40.4' E	S1→KEO(0m) in Lab.
MR13-04-61	2013/7/17	10:29-10:38	31° 41.4' N	144° 40.0' E	S1→KEO(0m) in Lab.
MR13-04-62	2013/7/17	10:40-10:45	31° 44.1' N	144° 39.4' E	S1→KEO(0m) in Lab.
MR13-04-63	2013/7/17	10:47-10:55	31° 45.8' N	144° 39.0' E	S1→KEO(0m) in Lab.
MR13-04-64	2013/7/17	13:09-16:53	32° 18.8' N	144° 31.7' E	KEO(100m) in a Niskin sampler
MR13-04-65	2013/7/17	13:58-14:06	32° 18.9' N	144° 31.8' E	KEO (0m) in Lab.
MR13-04-66	2013/7/17	14:07-14:16	32° 18.8' N	144° 31.8' E	KEO (0m) in Lab.
MR13-04-67	2013/7/17	14:18-14:26	32° 18.8' N	144° 31.8' E	KEO (0m) in Lab.
MR13-04-68	2013/7/17	14:28-14:36	32° 18.8' N	144° 31.8' E	KEO (0m) in Lab.
MR13-04-69	2013/7/17	14:41-14:49	32° 18.8' N	144° 31.7' E	KEO (0m) in Lab.
MR13-04-70	2013/7/18	11:43-11:50	36° 46.5' N	145° 31.7' E	KEO→JKEO(0m) in Lab.
MR13-04-71	2013/7/18	11:53-12:00	36° 48.3' N	146° 00.1' E	KEO→JKEO(0m) in Lab.
MR13-04-72	2013/7/18	12:01-12:10	36° 50.3' N	146° 00.7' E	KEO→JKEO(0m) in Lab.
MR13-04-73	2013/7/18	12:11-12:10	36° 52.3' N	146° 01.3' E	KEO→JKEO(0m) in Lab.
MR13-04-74	2013/7/18	12:22-12:28	36° 54.6' N	146° 01.9' E	KEO→JKEO(0m) in Lab.
MR13-04-75	2013/7/18	19:03-22:39	38° 05.6' N	146° 25.0' E	JKEO(100m) in a Niskin sampler
MR13-04-76	2013/7/18	20:01-20:09	38° 05.4' N	146° 24.9' E	JKEO(0m) in Lab.

Table 1 The list and information of seawater samples collected in the cruise of MR 13-04.

Sample number	Date	Time (UTC)	Location		Note
			Latitude	Longitude	
MR13-04-77	2013/7/18	20:11-20:19	38° 05.5' N	146° 25.0' E	JKEO(0m) in Lab.
MR13-04-78	2013/7/18	20:20-20:30	38° 05.5' N	146° 25.0' E	JKEO(0m) in Lab.
MR13-04-79	2013/7/18	20:34-20:41	38° 05.6' N	146° 25.0' E	JKEO(0m) in Lab.
MR13-04-80	2013/7/18	20:42-20:50	38° 05.6' N	146° 25.0' E	JKEO(0m) in Lab.
MR13-04-81	2013/7/19	12:12-12:19	40° 13.5' N	149° 43.4' E	JKEO→ARGO42° N (0m) in Lab.
MR13-04-82	2013/7/19	12:20-12:26	40° 14.7' N	149° 43.4' E	JKEO→ARGO42° N (0m) in Lab.
MR13-04-83	2013/7/19	12:27-12:34	40° 15.7' N	149° 47.1' E	JKEO→ARGO42° N (0m) in Lab.
MR13-04-84	2013/7/19	12:35-12:42	40° 16.8' N	149° 49.0' E	JKEO→ARGO42° N (0m) in Lab.
MR13-04-85	2013/7/19	12:44-12:48	40° 18.1' N	149° 51.1' E	JKEO→ARGO42° N (0m) in Lab.
MR13-04-86	2013/7/19	23:58-01:49	42° 00.2' N	152° 33.3' E	ARGO42° N (800 m) in a Niskin sampler
MR13-04-87	2013/7/19	23:58-01:49	42° 00.2' N	152° 33.3' E	ARGO42° N (600 m) in a Niskin sampler
MR13-04-88	2013/7/19	23:58-01:49	42° 00.2' N	152° 33.3' E	ARGO42° N (400 m) in a Niskin sampler
MR13-04-89	2013/7/19	23:58-01:49	42° 00.2' N	152° 33.3' E	ARGO42° N (200 m) in a Niskin sampler
MR13-04-90	2013/7/19	23:58-01:49	42° 00.2' N	152° 33.3' E	ARGO42° N (100 m) in a Niskin sampler
MR13-04-91	2013/7/19	23:58-01:49	42° 00.2' N	152° 33.3' E	ARGO42° N (60 m) in a Niskin sampler
MR13-04-92	2013/7/19	23:58-01:49	42° 00.2' N	152° 33.3' E	ARGO42° N (40 m) in a Niskin sampler
MR13-04-93	2013/7/19	23:58-01:49	42° 00.2' N	152° 33.3' E	ARGO42° N (20 m) in a Niskin sampler
MR13-04-94	2013/7/19	23:58-01:49	42° 00.2' N	152° 33.3' E	ARGO42° N (10 m) in a Niskin sampler
MR13-04-95	2013/7/20	00:55-1:04	42° 00.3' N	152° 33.4' E	ARGO42° N(0m) in Lab.
MR13-04-96	2013/7/20	01:05-1:12	42° 00.3' N	152° 33.4' E	ARGO42° N (0m) in Lab.
MR13-04-97	2013/7/20	01:13-1:19	42° 00.3' N	152° 33.5' E	ARGO42° N (0m) in Lab.
MR13-04-98	2013/7/20	01:19-1:25	42° 00.3' N	152° 33.5' E	ARGO42° N (0m) in Lab.
MR13-04-99	2013/7/20	01:26-1:34	42° 00.4' N	152° 33.5' E	ARGO42° N (0m) in Lab.
MR13-04-100	2013/7/20	10:58-11:07	43° 28.2' N	152° 20.7' E	ARGO42° N→KNOT (0m) in Lab.
MR13-04-101	2013/7/20	11:08-11:08	43° 25.5' N	152° 33.4' E	ARGO42° N→KNOT (0m) in Lab.
MR13-04-102	2013/7/20	11:16-11:24	43° 30.7' N	154° 24.0' E	ARGO42° N→KNOT (0m) in Lab.
MR13-04-103	2013/7/20	11:25-11:31	43° 31.9' N	154° 25.6' E	ARGO42° N→KNOT (0m) in Lab.
MR13-04-104	2013/7/20	11:32-11:37	43° 32.8' N	154° 26.8' E	ARGO42° N→KNOT (0m) in Lab.
MR13-04-105	2013/7/20	18:27-18:39	44° 00.5' N	155° 00.5' E	KNOT (0m) in Lab.
MR13-04-106	2013/7/20	18:40-18:46	44° 00.6' N	155° 00.3' E	KNOT (0m) in Lab.
MR13-04-107	2013/7/20	18:40-18:56	44° 00.6' N	155° 00.3' E	KNOT (0m) in Lab.
MR13-04-108	2013/7/20	18:57-19:05	44° 00.6' N	155° 00.3' E	KNOT (0m) in Lab.
MR13-04-109	2013/7/20	19:06-19:16	44° 00.7' N	155° 00.3' E	KNOT (0m) in Lab.
MR13-04-110	2013/7/20	19:40-20:48	44° 00.2' N	155° 00.2' E	KNOT (100m) in a Niskin sampler
MR13-04-111	2013/7/21	04:25-04:33	44° 48.9' N	156° 54.9' E	KNOT→K2 (0m) in Lab.
MR13-04-112	2013/7/21	04:34-04:40	44° 49.8' N	156° 57.0' E	KNOT→K2 (0m) in Lab.
MR13-04-113	2013/7/21	04:41-04:47	44° 50.7' N	156° 58.7' E	KNOT→K2 (0m) in Lab.
MR13-04-114	2013/7/21	04:49-04:56	44° 51.7' N	157° 01.2' E	KNOT→K2 (0m) in Lab.
MR13-04-115	2013/7/21	04:57-05:03	44° 52.6' N	157° 03.2' E	KNOT→K2 (0m) in Lab.
MR13-04-116	2013/7/23	02:09-02:22	47° 00.0' N	160° 00.0' E	K2(0m) in Bucket
MR13-04-117	2013/7/23	02:09-02:22	47° 00.0' N	160° 00.0' E	K2(0m) in Bucket
MR13-04-118	2013/7/23	02:09-02:22	47° 00.0' N	160° 00.0' E	K2(0m) in Bucket
MR13-04-119	2013/7/23	02:09-02:22	47° 00.0' N	160° 00.0' E	K2(0m) in Bucket
MR13-04-120	2013/7/23	02:09-02:22	47° 00.0' N	160° 00.0' E	K2(0m) in Bucket
MR13-04-121	2013/7/23	03:41-04:14	47° 00.0' N	160° 00.0' E	K2(800m) in a Niskin sampler
MR13-04-122	2013/7/23	03:41-04:14	47° 00.0' N	160° 00.0' E	K2(600m) in a Niskin sampler
MR13-04-123	2013/7/23	03:41-04:14	47° 00.0' N	160° 00.0' E	K2(400m) in a Niskin sampler
MR13-04-124	2013/7/23	03:41-04:14	47° 00.0' N	160° 00.0' E	K2(200m) in a Niskin sampler
MR13-04-125	2013/7/23	03:41-04:14	47° 00.0' N	160° 00.0' E	K2(150m) in a Niskin sampler
MR13-04-126	2013/7/23	03:41-04:14	47° 00.0' N	160° 00.0' E	K2(100m) in a Niskin sampler
MR13-04-127	2013/7/23	03:41-04:14	47° 00.0' N	160° 00.0' E	K2(50m) in a Niskin sampler
MR13-04-128	2013/7/23	03:41-04:14	47° 00.0' N	160° 00.0' E	K2(25m) in a Niskin sampler
MR13-04-129	2013/7/23	05:34-06:11	47° 00.0' N	160° 00.0' E	K2(10m) in a Niskin sampler
MR13-04-130	2013/7/23	05:34-06:11	47° 00.0' N	160° 00.0' E	K2(200m) in a Niskin sampler
MR13-04-131	2013/7/23	05:34-06:11	47° 00.0' N	160° 00.0' E	K2(175m) in a Niskin sampler
MR13-04-132	2013/7/23	05:34-06:11	47° 00.0' N	160° 00.0' E	K2(150m) in a Niskin sampler
MR13-04-133	2013/7/23	05:34-06:11	47° 00.0' N	160° 00.0' E	K2(125m) in a Niskin sampler
MR13-04-134	2013/7/23	05:34-06:11	47° 00.0' N	160° 00.0' E	K2(100m) in a Niskin sampler
MR13-04-135	2013/7/23	05:34-06:11	47° 00.0' N	160° 00.0' E	K2(75m) in a Niskin sampler
MR13-04-136	2013/7/23	05:34-06:11	47° 00.0' N	160° 00.0' E	K2(50m) in a Niskin sampler
MR13-04-137	2013/7/23	05:34-06:11	47° 00.0' N	160° 00.0' E	K2(10m) in a Niskin sampler
MR13-04-138	2013/7/23	05:38-05:44	47° 00.0' N	160° 00.0' E	K2(0m) in Bucket
MR13-04-139	2013/7/26	05:00-05:08	40° 07.1' N	149° 02.1' E	High pressure eddy E03 (0m) in Lab.
MR13-04-140	2013/7/26	05:13-05:19	40° 07.0' N	149° 02.2' E	High pressure eddy E03 (0m) in Lab.
MR13-04-141	2013/7/26	05:20-05:27	40° 07.1' N	149° 02.2' E	High pressure eddy E03 (0m) in Lab.
MR13-04-142	2013/7/26	05:28-05:34	40° 07.0' N	149° 02.2' E	High pressure eddy E03 (0m) in Lab.
MR13-04-143	2013/7/26	05:35-05:42	40° 07.0' N	149° 02.2' E	High pressure eddy E03 (0m) in Lab.
MR13-04-144	2013/7/26	05:43-05:52	40° 06.9' N	149° 02.2' E	High pressure eddy E03 (0m) in Lab.
MR13-04-145	2013/7/26	22:34-22:42	41° 05.1' N	146° 35.3' E	High pressure eddy E01→E02 (0m) in Lab.
MR13-04-146	2013/7/26	22:45-22:52	41° 04.2' N	146° 34.7' E	High pressure eddy E01→E02 (0m) in Lab.
MR13-04-147	2013/7/26	22:53-23:00	41° 03.5' N	146° 34.2' E	High pressure eddy E01→E02 (0m) in Lab.
MR13-04-148	2013/7/26	23:01-23:08	41° 02.8' N	146° 33.7' E	High pressure eddy E01→E02 (0m) in Lab.

3.13.2 Zooplankton

Minoru KITAMURA (JAMSTEC, BioGeos)

Hajime KAWAKAMI (JAMSTEC, MIO)

Makio HONDA (JAMSTEC, RIGC)

(1) Objective

The magnitude of the 9.0 Tohoku earthquake and the ensuing tsunami on March 11, 2011, inflicted heavy damage on the Fukushima Dai-ichi nuclear power plant (FNPP1). The loss of power supply and subsequent overheating, meltdowns, and hydrogen explosions at the FNPP1 resulted in airborne release and subsequent fallout over the land and the ocean. In addition to atmospheric fallout, water contaminated with radionuclides leaked into the ocean. These Fukushima-derived radionuclides were contaminated in not only coastal but also oceanic marine biota (e.g. Buesseler et al., 2012; Honda et al., 2012; Kitamura et al., 2013). Although the three papers reported snapshot contamination of radionuclides in zooplankton, researches on temporal changes of the contaminations are also needed. Thus, we have observed radiocesium (^{134}Cs and ^{137}Cs) concentrations in zooplankton since April 2011 (at stations K2 and S1) or June 2011 (at station F1). In this cruise, we aimed to understand radiocesium concentrations in zooplankton in the three stations, F1, S1 and K2 two years after the accident.

(2) Methods

For collection of stratified sample sets, multiple opening/closing plankton net system, IONESS, was used. This is a rectangular frame trawl with nine nets. Net mouth area is 1.5 m^2 when the net frame is towed at 45° in angle, and mesh size is 0.33-mm. The net system was towed obliquely. Ship speed during net tow was about 2 knot, speeds of wire out and reeling were 0.1-0.5 m/s and 0.1-0.3 m/s, respectively. Volume of filtering water of each net was estimated using net mouth area, towing distance and filtering efficiency. The former two parameters were obtained from frame angle during tows and revolutions of flow-meter, respectively. And the filtering efficiency is 96% which was directly measured previously. Total three tows of IONESS were done. Date, time, sampling layers and filtering volumes of water are summarized in the Table 3.13.2-1. All samplings were conducted during night. Aliquots (one sixteenth) of the fresh samples were preserved with formalin to analyze community structure of zooplankton. Remaining samples for the measurement of radiocesium were frozen at -20°C after separation from fish.

After the cruise, the frozen samples were weighed (wet weight), dried and reweighed (dry weight). Water contents (%) of the samples were calculated from the equation; Water content = (Wet weight - dry weight) / wet weight \times 100.

Table 3.13.2-1. Summary of zooplankton collections using IONESS. Local ship times (LST) were as follows; UTC +11 hours at the station K2, +9 hours at the stations F1 and S1 (same as JST).

Stn.	Tow ID	Date & Time				Position	Sampling layer (upper, m) and filtering volume (bottom, m ³)										
		LST	in	UTC	in		out	out	Net No.	0	1	2	3	4	5	6	7
F1	I130711A	2013.7.11	20:03	2013.7.11	11:03	36°28.41'N, 141°28.72'E	0-220-200	200-15	15-0	0-220-200	200-15	15-0	0-200	200-15	15-0		
			21:59		12:59	36°26.54'N, 141°25.80'E		2219.9	260.0	1392.1	1457.5	786.1	869.9	1384.1	859.3		
S1	I130714A	2013.7.14	20:08	2013.7.14	11:08	29°57.10'N, 144°59.42'E	0-220-200	200-30	30-0	0-220-200	200-25	25-0	0-205-200	200-25	25-0		
			22:59		13:59	30°01.44'N, 145°00.97'E		3518.8	982.8	1324.7	2519.5	1045.2	1013.3	3433.4	1354.1		
K2	I130722A	2013.7.22	21:05	2013.7.22	10:05	46°58.56'N, 159°58.13'E	0-216-200	200-20	20-0	0-210-200	200-20	20-0	0-216-200	200-20	20-0		
			22:59		11:59	46°58.65'N, 160°03.07'E		2172.9	264.8	823.5	1914.2	695.4	575.8	1652.7	663.9		

(3) Preliminary results

Biomasses (based on the dry weight) and water contents of zooplankton communities in the station S1 are summarized in the Table 3.13.2-2. Those in the stations K2 and F1 will be measured because samples are still drying. Dominant taxa in each sample were preliminary and qualitatively observed and listed up in the table. The radiocesium concentrations in zooplankton will be analyzed using Ge detector at Mutsu Institute for Oceanography, JAMSTEC.

Table 3.13.2-2. Biomasses, water contents and dominant taxa of zooplankton communities collected during the MR13-04 cruise. Abbreviations are as follows; Cop (Copepoda), Eup (Euphausiacea), Dia (Diatom). Measurement of biomass and water content for the samples collected in F1 and K2 are still working.

Station	Net ID	Depth (m)	Biomass (mg-dw m ⁻³)	Water content (%)	Dominant taxa
F1	I130711A-1	200~15	-	-	No formalin sample
	I130711A-2	15~0	-	-	No formalin sample
	I130711A-4	200~15	-	-	Cop., Eup.
	I130711A-5	15~0	-	-	Cop.
	I130711A-7	200~15	-	-	Cop., Eup.
	I130711A-8	15~0	-	-	Cop.
S1	I130714A-1	200~30	3.98	87.9	Cop., Eup.
	I130714A-2	30~0	7.50	84.9	Cop., Eup.
	I130714A-4	200~25	3.98	87.0	Cop., Eup.
	I130714A-5	25~0	10.22	85.4	Cop., Eup.
	I130714A-7	200~25	4.03	87.1	Cop., Eup.
	I130714A-8	25~0	7.18	86.9	Cop., Eup.
K2	I130722A-1	200~20	-	-	Cop., Eup., Dia.
	I130722A-2	20~0	-	-	Cop.
	I130722A-4	200~20	-	-	Cop., Eup., Dia.
	I130722A-5	20~0	-	-	Cop., Eup.
	I130722A-7	200~20	-	-	Cop., Eup.
	I130722A-8	20~0	-	-	Cop., Eup.

(4) Data archives

The data will be submitted to the Data management Group of JAMSTEC after the analysis, which will be <2 years after the end of the cruise.

3. 13. 3 Sediment trap experiment at station F1

Makio HONDA (JAMSTEC)

Hajime KAWAKAMI (JAMSTEC)

Cris GERMAN (Woods Hole Oceanographic Institution, WHOI)

Steven J. MANGANINI (WHOI)

Ken BUESSELER (WHOI)

In order to collect time-series sinking particle and certify how and when artificial radioactive nuclides are transported vertically near the Fukushima Daiichi nuclear power plant, time-series sediment traps were deployed at approximately 500 m and 1000 m at station F1 in July 2012. Sampling interval were 18 days at 1000 m and 36 days at 500 m (18 days in March and April 2012). Before deployment, collecting cups were filled up with seawater based 10% buffered formalin. This observation is cooperative research between JAMSTEC and Woods Hole Oceanographic Institution (PI: Cris German). This mooring system was recovered and redeployed during this cruise.

1. Preliminary result

500 m sediment trap collected sinking particle on schedule. However 1000 m sediment trap had lost three bottles when mooring system was recovered. In addition, based on archival record, rotation of turntable was not sometimes conducted on schedule and several cups collected sinking particles for two interval (36 days). Some external force must damage this sediment trap.

(1) Total Mass Flux

Onboard, we measured heights of sinking particle collect in collecting cups with scale in order to know general view of seasonal variability. Using diameter of collecting cups, we estimated total mass flux in volume.

In July 2012 when sediment trap started collection of sinking particle, total mass flux (TMF) at 500 m were relatively high (Fig. 3.13.3.1). Thereafter TMF decreased gradually and low during winter. TMF re-increased in late February and early March 2013 and peaked in late April. Although sample collection at 1000 m was not perfect, seasonal variability in TMF synchronized well with that at 500m: relatively higher TMF was observed in late July-middle August 2012 and late April-middle May 2013.

2. Future analysis

On land laboratory, sediment trap sample will be pretreated (splitting, filtration, dry-up, pulverization) and major chemical components such as organic carbon, inorganic carbon, biogenic opal, CaCO_3 and Al and radionuclides such as radiocesium will be analyzed.

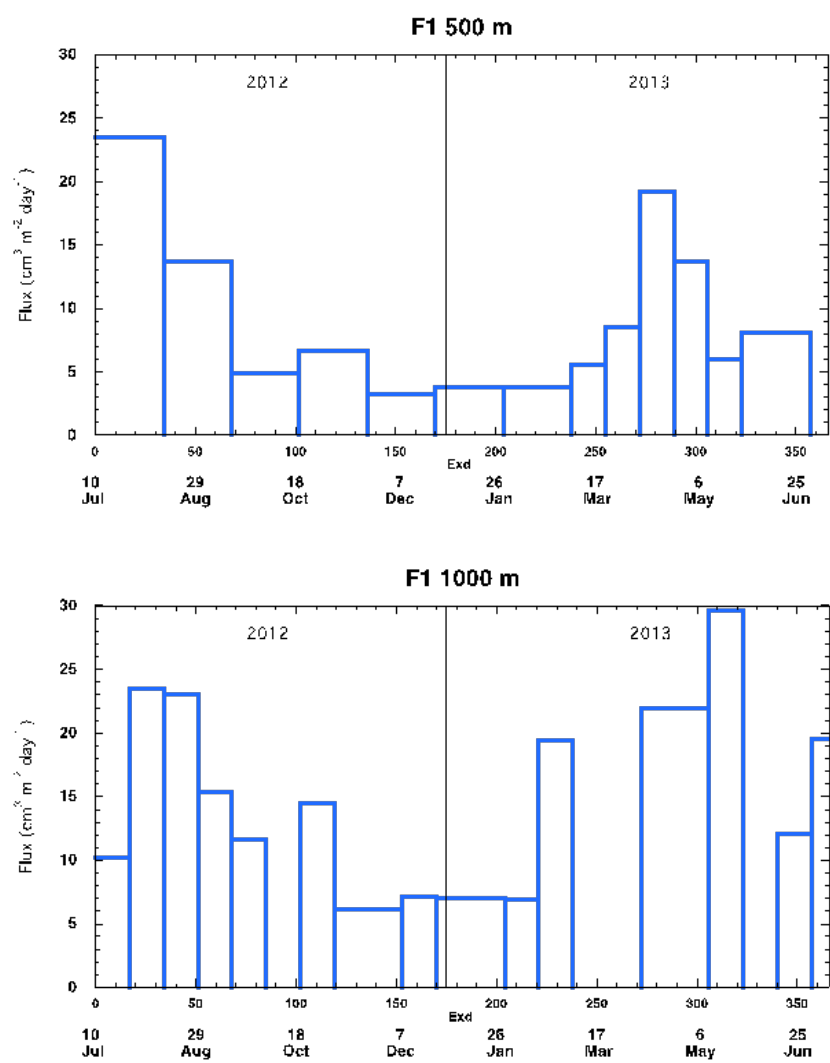


Fig. 3.13.3.1 Seasonal variability in total mass flux (volume).

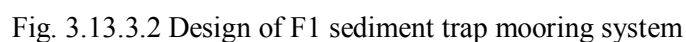
3. Redeployment

After retrieving sample / data, replacement of new battery and initialization of schedule (Table 3.13.3.1), sediment trap mooring system was deployed on 12 July 2013. Designs of mooring system are shown in Fig. 3.13.3.2. Anchor position and ambient topography is shown in Fig. 3.13.3.3. Various information about deployment (Releaser, anchor position, and working log) are shown in Table 3.13.3.2. It is planned that this mooring system will be recovered in autumn 2014.

Table 3.13.3.1 Schedule (opening day of each cup)

F1

	1000m		500m	
	cup #21		cup #13	
	18		36	
1	2013/7/13	1	2013/7/13	
2	2013/7/31	2	2013/8/18	
3	2013/8/18	3	2013/9/23	
4	2013/9/5	4	2013/10/29	
5	2013/9/23	5	2013/12/4	
6	2013/10/11	6	2014/1/9	
7	2013/10/29	7	2014/2/14	
8	2013/11/16	8	2014/3/22	
9	2013/12/4	9	2014/4/9	interval
10	2013/12/22	10	2014/4/27	18
11	2014/1/9	11	2014/5/15	
12	2014/1/27	12	2014/6/2	
13	2014/2/14	13	2014/6/20	
14	2014/3/4		2014/7/26	
15	2014/3/22			
16	2014/4/9			
17	2014/4/27			
18	2014/5/15			
19	2014/6/2			
20	2014/6/20			
21	2014/7/8			
	2014/7/26			



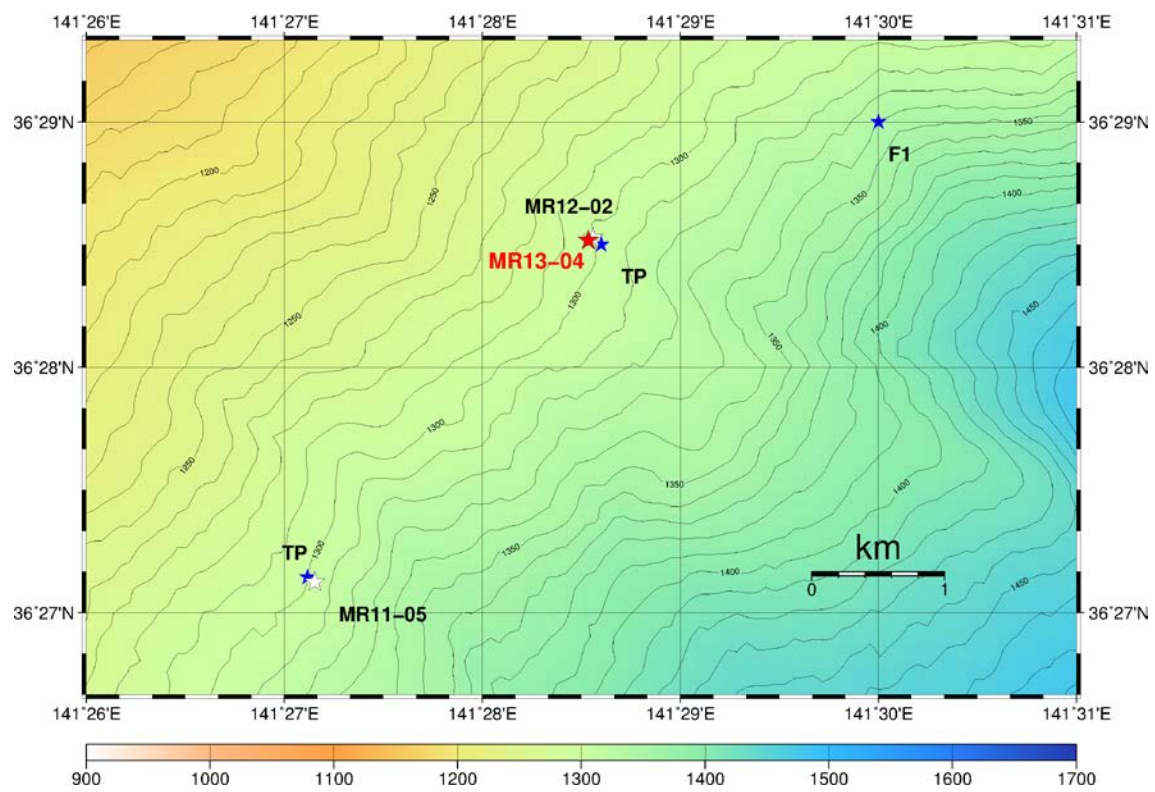


Fig. 3.13.3.3 Anchor position of F1 sediment trap (MR13-04).
Former anchor positions (MR11-05, MR12-02) are also shown for comparison.

Table 3.13.3.3 Deployment log sheet

Mooring Number		F1WHOI130712	
Project	Time-Series	Depth	1,300.0 m
Area	North Pacific	Planned Depth	1,300.0 m
Station	F1	Length	842.0 m
Target Position	36°28.50 N	Depth of Buoy	457 m
	141°28.60 E	Period	1 year
ACOUCTIC RELEASERS			
Type	BENTHOS	BENTHOS	
Serial Number	614	673	
Receive F.	11.0 kHz	13.0 kHz	
Transmit F.	14.0 kHz	14.0 kHz	
RELEASE C.	C	D	
Enable C.	B	B	
Disable C.	-	-	
Battery	1 years	1 years	
Release Test	-	-	
DEPLOYMENT			
Recorder	Takamori Tomoyuki	Start	0.7 Nmile
Ship	R/V MIRAI	Overshoot	- m
Cruise No.	MR13-04	Let go Top Buoy	23:13
Date	2013/7/12	Let go Anchor	0:17
Weather	f	Sink Top Buoy	-
Wave Hight	1.1 m	Pos. of Start	36°28.55 N
Seabeam Depth	1,299 m		141°29.29 E
Ship Heading	<260>	Pos. of Drop. Anc.	36°28.51 N
Ship Ave.Speed	- knot		141°28.38 E
Wind	<003> 5.0 m/s	Pos. of Mooring	- N
Current	<073> 0.6 knot		- E

3.13.4 Biogeochemical cycle and accumulation of anthropogenic radionuclides derived from the accident of Fukushima-Daiichi Nuclear Power Plant

Shigeyoshi OTOSAKA (Japan Atomic Energy Agency)

Takashi SUZUKI (Japan Atomic Energy Agency)

Hisashi NARITA (Tokai University)

3.13.4.1 Sediment trap experiment in the region off Fukushima (station FS1)

(1) Background and objective

The accident of TEPCO's Fukushima Dai-ichi Nuclear Power Plant (1FNPP), occurred on March 2011, released a large amount of anthropogenic radionuclides into the environment, and is still affecting people who are living in the surrounding regions. Although concentration of radionuclides in seawater decreased by less than 1/100 of that at the post-accidental stage, significant amount of radionuclides are still be remained in the coastal sediments. Therefore, it is crucial to understand factors controlling transport of radionuclides between coastal and offshore regions. The objective of this study is to investigate the transport process of particulate radiocesium by a sediment trap experiment.

(2) Methods

On July 11 2013, mooring array equipped with a sediment trap (Fig. 3.13.4.1) was recovered at Stas. FS1 (37°19.88' N, 142°10.05' E). This mooring system was deployed on July 14 2012 by R/V *Soyo-maru* (National Institute of Fisheries Science, Fisheries Research Agency, Japan). A sediment trap with double sampling cone (Nichiyu SMD-13W) was installed at 873 m depth and it collected sinking particles for 13 periods with 26 days interval. Sampling cups were filled with 5% formalin or 0.3% mercury chloride to avoid biodegradation of samples.

(3) Preliminary result

As an index of total mass flux, heights of sinking particles collect in the receiving cups were measured with a scale. Obtained "volume flux" ranged between 2 and 18 mL/m²/day. The flux showed three maxima; autumn (August-September), winter (January-February) and spring (April-May)(Fig. 3.13.4.2). These characteristics agreed well with those observed in the previous observation between 2011 and 2012. Volume fluxes obtained by the two cones independently were comparable except for the period 13 May-June, 2012)(Fig. 3.13.4.3).

It can be considered that the higher mass flux observed in autumn and spring is caused by high biological production in the surface and vertical sinking of the biogenic particles. Maximum of mass flux in winter, on the other hand, is probably due to secondary transport of sediment surface in the surrounding region. Considering that temperature at sampling depth varied temporally when high mass fluxes were observed (Fig. 3.13.4.2), switching of the abyssal current might affected vertical transport of particulate materials in this region.

(4) Future study

Detailed parameters, such as dry mass-based flux and composition of the particles, will be analyzed on land and factors controlling transport of particulate materials in the regions will be

investigated. By comparing data obtained in the 2011-2012 periods as well as those of previous studies (e.g., Otsuka and Noriki, 2005), inter-annual variations of mass flux and properties of sinking particles will be investigated. In addition, fluxes of anthropogenic radionuclides originating from the Fukushima-Daiichi NPP are also estimated by a radiochemical analysis of sinking particles. Since sediment trap is installed at a depth 100m above the bottom, we expect to understand transport processes of particulate radiocesium from the surface waters as well as those transported laterally from the continental shelf (e.g., Otsuka and Kobayashi, 2013). Detailed transport processes of particulate radionuclides will also be inferred from isotopic/elemental proxies such as ^{14}C and lead isotopes (e.g., Otsuka et al., 2008).

(5) References

- Otsuka, S., S. Noriki (2005): Relationship between composition of settling particles and organic carbon flux in the western North Pacific and the Japan Sea. *J. Oceanogr.* **61**, 25-40.
- Otsuka, S., T. Kobayashi (2013): Sedimentation and remobilization of radiocesium in the coast of Ibaraki, 70 km south of the Fukushima Dai-ichi Nuclear Power Plant. *Environ. Monit. Assess.* **185**, 5419-5433.
- Otsuka, S., T. Tanaka, O. Togawa, H. Amano, E.V. Karasev, M. Minakawa, S. Noriki (2008): Deep sea circulation of particulate organic carbon in the Japan Sea. *J. Oceanogr.* **64**, 911-923.

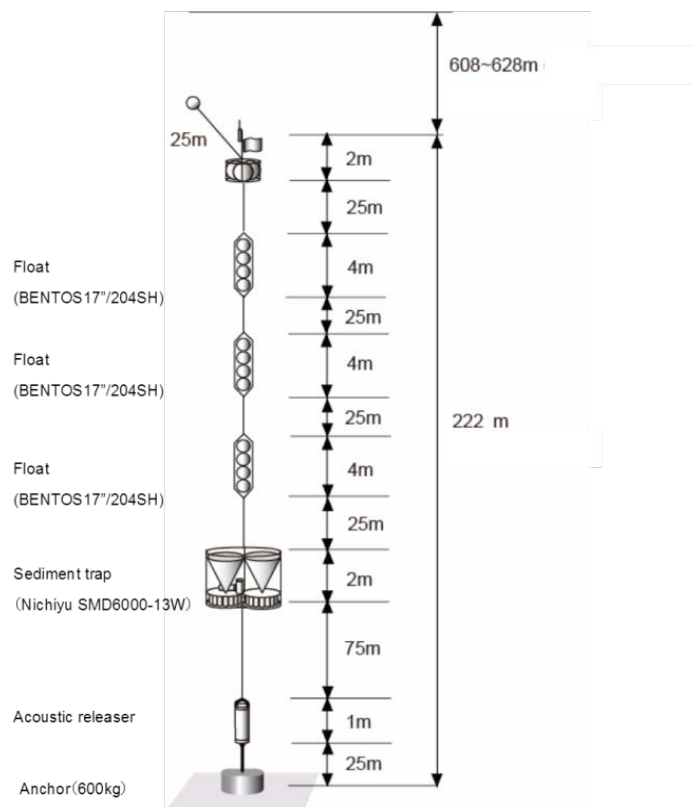


Fig. 3.13.4.1 Schematic of mooring system recovered at station FS1.

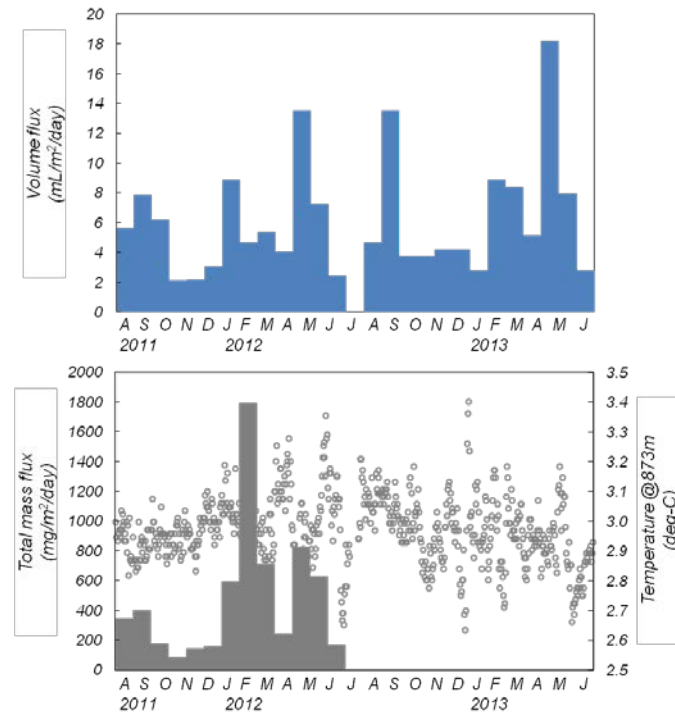


Fig. 3.13.4.2 Upper panel: Seasonal variation of “volume- based” sinking flux obtained at station FS1 (873 m depth). Lower panel: Seasonal variation of total mass flux (bars/left axis) and temperature at 873 m depth (dots/right axis).

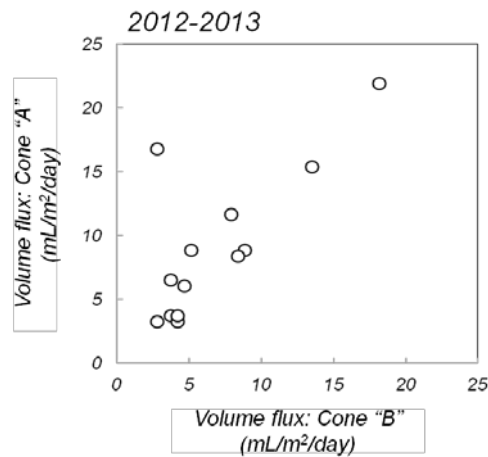


Fig. 3.13.4.3 Relationship of volume-based sinking flux between the two cones.

3.13.4.2 Collection of seawater samples for measurement of ^{129}I

(1) Background and objective

Radioiodine is mainly produced by atomic fission of uranium and trans-uranium isotopes. Among 23 radioisotopes of iodine, ^{131}I (half life = 8.1d) is known as significant contributors to the health effect from the accident of 1FNPP. Because of their short half-lives, however, it is difficult to assess their behavior and fate in the marine environment. Iodine-129 (^{129}I) with long half-life (15.7 Myr) is regarded as one of the most important radionuclides that should be assessed for its biogeochemical cycling on a global scale. In fact, it is reported that significant amount of ^{129}I supplied to the North Pacific (e.g., Suzuki et al., 2013a). In this study, we investigate distribution and fate of the accident-derived ^{129}I over the western North Pacific. In addition, by comparing previous data obtained from the neighboring region (Suzuki et al., 2013b), the impact of the accident will be assessed.

(2) Methods

In this cruise, seawater samples for ^{129}I measurement were collected at 6 stations; stations FS1, S1, KEO, JKEO, KNOT and K2 (Table 3.13.4.1). Seawater samples were collected by a 12L Niskin-X bottle with CTD system except surface seawater, which was collected by a bucket. The seawater sample for ^{129}I was collected into a 1-L plastic bottle.

Measurements of iodine and radioiodine in seawater samples will be conducted at on-shore laboratory after Suzuki et al. (2008). Briefly, iodine in the seawater samples is extracted by the solvent extraction technique. Extracted iodine is then precipitated as silver iodide by the addition of the silver nitrate. Iodine isotopic ratios ($^{129}\text{I}/^{127}\text{I}$) of the silver iodide are measured by the Accelerator Mass Spectrometry (AMS) at the Aomori Research and Development Center in the Japan Atomic Energy Agency (JAEA). To evaluate the ^{129}I concentration in the seawater samples, iodine concentration (^{127}I) will also be measured by voltammetry.

(3) References

- Suzuki, T., S. Kabuto, H. Amano, O. Togawa (2008): Measurement of iodine-129 in seawater samples collected from the Japan Sea area using accelerator mass spectrometry: Contribution of nuclear fuel reprocessing plants *Quat. Geochronol.* **3**, 268-275.
- Suzuki, T., S. Otsuka, J. Kuwabara, H. Kawamura, T. Kobayashi (2013a): Iodine-129 concentration in seawater near Fukushima before and after the accident at the Fukushima Daiichi Nuclear Power Plant. *Biogeoscience* **10**, 3839-3747.
- Suzuki, T., S. Otsuka, O. Togawa (2013b): Concentration of iodine-129 in surface seawater at subarctic and subtropical circulations in the Japan Sea. *Nucl. Inst. Methods Phys. Res. B* **294**, 563-567.

Table 3.13.4.1 Sampling stations and number of samples for ^{129}I measurement.

Station	Lat. (N)	Long. (E)	Sampling Date (UTC)	Number of samples	Max. Pressure (dbar)
F1	36-28.7	141.28.7	2013/07/11	17	1295
S1	30-04.2	144-58.3	2013/07/16	29	2003
KEO	32-18.8	144-31.7	2013/07/17	23	2000
JKEO	38-05.6	146-25.0	2013/07/18	23	2000
KNOT	44-00.2	155-00.2	2013/07/20	23	2001
K2	47-00.1	159-59.6	2013/7/22	5	2028
Total	-	-	-	120	-

3.14 A study of the cycles of global warming related materials using their isotopomers in the western North Pacific

Chisato YOSHIKAWA (JAMSTEC)

Haruka TAMADA (Rakuno Gakuen University)

Florian BREIDER (Tokyo Institute of Technology)

Osamu YOSHIDA (Rakuno Gakuen University)

Sakae TOYODA (Tokyo Institute of Technology)

Naohiro YOSHIDA (Tokyo Institute of Technology)

3.14.1 Aims of this study

This study aims to reduce the uncertainties of sinks and sources of global warming related materials by using “isotopomers”, a useful tracer of material cycles. In this study, to understand the cycles of global warming related materials in the western North Pacific, we conducted air and water sampling for isotopomer analysis of methane (CH_4), nitrous oxide (N_2O) and related substances (NO_3^- , NH_4^+ and Chlorophyll-a). Moreover, to quantitatively understand the cycles and estimate the budgets, we develop a marine isotopomer model for global warming related materials and evaluate the model by using the results of isotopomer analysis.

3.14.2 Sampling elements

All sampling elements of Tokyo Institute of Technology and Rakuno Gakuen University group at hydrographic sampling stations are listed below.

Table 1. Parameters and hydrographic station names for samples collection.

Parameters	Hydrographic stations
1. Concentrations of dissolved CH_4	F1, S1, KNOT, JKEO, KEO, K2, Eddy
2. Concentrations of dissolved N_2O	F1, S1, KNOT, JKEO, KEO, K2, Eddy
3. $\delta^{15}\text{N}$ and $\delta^{18}\text{O}$ values of NO_3^-	F1, S1, KNOT, JKEO, KEO, K2, Eddy
4. $\delta^{15}\text{N}$, SP and $\delta^{18}\text{O}$ values of dissolved N_2O	K2, S1, Eddy
5. $\delta^{13}\text{C}$ values of dissolved CH_4	KNOT, JKEO, KEO
6. δD values of dissolved CH_4	KNOT, JKEO, KEO
7. $\delta^{15}\text{N}$ of Chlorophyll <i>a</i>	F1, S1, KNOT, JKEO, KEO, K2, Eddy
8. Nitrification rate	K2, S1, Eddy

3.14.3 Methane

(1) Introduction

Atmospheric methane (CH_4) is a trace gas playing an important role in the global carbon cycle as a greenhouse gas. Its concentration has increased by about 1050 ppbv from 700 ppbv since the pre-industrial era (IPCC, 2007). In order to understand the current global methane cycle, it is necessary to quantify its sources and sinks. At present, there remain large uncertainties in the estimated methane fluxes from sources to sinks. The ocean's source strength for atmospheric methane should be examined in more detail, even though it might be a relatively minor source, previously reported to be 0.005 to 3% of the total input to the

atmosphere (Cicerone and Oremland, 1988; Bange et al., 1994; Lelieveld et al., 1998).

To estimate an accurate amount of the methane exchange from the ocean to the atmosphere, it is necessary to explore widely and vertically. Distribution of dissolved methane in surface waters from diverse locations in the world ocean is often reported as a characteristic subsurface maximum representing a supersaturation of several folds (Yoshida et al., 2004). Although the origin of the subsurface methane maximum is not clear, some suggestions include advection and/or diffusion from local anoxic environment nearby sources in shelf sediments, and in situ production by methanogenic bacteria, presumably in association with suspended particulate materials (Karl and Tilbrook, 1994; Katz et al., 1999). These bacteria are thought to probable live in the anaerobic microenvironments supplied by organic particles or guts of zooplankton (Alldredge and Cohen, 1987).

So, this study investigates in detail profile of methane concentration and stable isotopic distribution in the water column in the western North Pacific to clarify methane dynamics and estimate the flux of methane to the atmosphere.

(2) Materials and methods

Seawater samples are taken by CTD-CAROUSEL system attached Niskin samplers of 12 L at 5-22 layers and surface layer taken by plastic bucket at hydrographic stations as shown in Table 1. Each sample was carefully subsampled into 30, 125, 600 ml glass vials to avoid air contamination for analysis of methane concentration, carbon isotope ratio, and hydrogen isotope ratio respectively. The seawater samples were poisoned by 20 μ l (30 and 125 ml vials) or 100 μ l (600 ml vial) of mercuric chloride solution (Tilbrook and Karl, 1995; Watanabe et al., 1995), and were closed with rubber and aluminum caps. These were stored in a dark and cool place until we got to land, where we conducted gas chromatographic analysis of methane concentration and mass spectrometric analysis of carbon and hydrogen isotopic composition at the laboratory.

The analytical method briefly described here: The system consists of a purge and trap unit, a desiccant unit, rotary valves, a gas chromatograph equipped with a flame ionization detector for concentration of methane, GC/C/IRMS for carbon isotope ratio of methane, GC/TC/IRMS for hydrogen isotope ratio of methane, and data acquisition units. The entire volume of seawater in each glass vial was processed all at once to avoid contamination and loss of methane. Precisions obtained from replicate determinations of methane concentration, and carbon and hydrogen isotope ratios were estimated to be better than 5%, and 0.3‰ and 3‰, respectively, for the usual concentration of methane in seawater.

(3) Expected results

Subsurface maximum concentrations of methane (>3 nmol kg⁻¹) were expected to be observed in the western North Pacific. A commonly-encountered distribution in the upper ocean with a methane peak within the pycnocline (e.g., Ward et al., 1987; Owens et al., 1991; Watanabe et al., 1995). Karl and Tilbrook (1994) suggested the suboxic conditions would further aid the development of microenvironments within particles in which methane could be produced. The organic particles are accumulated in the pycnocline, and methane is produced in the micro reducing environment by methanogenic bacteria. Moreover, in situ microbial methane production in the guts of zooplankton can be expected (e.g., Owens et al., 1991; de Angelis and

Lee, 1994; Oudot et al., 2002; Sasakawa et al., 2008). Watanabe et al. (1995) pointed out that the diffusive flux of methane from subsurface maxima to air-sea interface is sufficient to account for its emission flux to the atmosphere. In the mixed layer above its boundary, the methane is formed and discharged to the atmosphere in part, in the below its boundary, methane diffused to the bottom vertically. By using concentration and isotopic composition of methane and hydrographic parameters for vertical water samples, it is possible to clarify its dynamics such as production and/or consumption in the water column.

(4) References

- Aldredge, A. A., Y. Cohen: Can microscale chemical patches persist in the sea? Microelectrode study of marine snow, fecal pellets, *Science*, 235, 689–691, 1987.
- Bange, H. W., U. H. Bartell, S. Rapsomanikis, and M. O. Andreae: Methane in the Baltic and the North seas and a reassessment of the marine emissions of methane, *Global Biogeochem. Cycles*, 8, 465–480, 1994.
- Cicerone, R. J., and R. S. Oremland: Biogeochemical aspects of atmospheric methane, *Global Biogeochem. Cycles*, 2, 299–327, 1988.
- de Angelis, M. A., and C. Lee: Methane production during zooplankton grazing on marine phytoplankton, *Limnol. Oceanogr.*, 39, 1298–1308, 1994.
- Karl, D. M., and B. D. Tilbrook: Production and transport of methane in oceanic particulate organic matter, *Nature*, 368, 732–734, 1994.
- Katz, M. E., D. K. Pak, G. R. Dickens, and K. G. Miller (1999), The source and fate of massive carbon input during the latest Paleocene thermal maximum, *Science*, 286, 1531–1533.
- Lelieveld, J., P. J. Crutzen, and F. J. Dentener (1998), Changing concentration, lifetime and climate forcing of atmospheric methane, *Tellus Ser. B*, 50, 128–150.
- Oudot, C., P. Jean-Baptiste, E. Fourre, C. Mormiche, M. Guevel, J-F. Ternon, and P. L. Corre: Transatlantic equatorial distribution of nitrous oxide and methane, *Deep-Sea Res., Part I*, 49, 1175–1193, 2002.
- Owens, N. J. P., C. S. Law, R. F. C. Mantoura, P. H. Burkill, and C. A. Llewellyn: Methane flux to the atmosphere from the Arabian Sea, *Nature*, 354, 293–296, 1991.
- Sasakawa, M., U. Tsunogai, S. Kameyama, F. Nakagawa, Y. Nojiri, and A. Tsuda (2008), Carbon isotopic characterization for the origin of excess methane in subsurface seawater, *J. Geophys. Res.*, 113, C03012, doi: 10.1029/2007JC004217.
- Tilbrook, B. D., and D. M. Karl: Methane sources, distributions and sinks from California coastal waters to the oligotrophic North Pacific gyre, *Mar. Chem.*, 49, 51–64, 1995.
- Ward, B. B., K. A. Kilpatrick, P. C. Novelli, and M. I. Scranton: Methane oxidation and methane fluxes in the ocean surface layer and deep anoxic waters, *Nature*, 327, 226–229, 1987.
- Watanabe, S., N. Higashitani, N. Tsurushima, and S. Tsunogai: Methane in the western North Pacific, *J. Oceanogr.*, 51, 39–60, 1995.
- Yoshida, O., H. Y. Inoue, S. Watanabe, S. Noriki, M. Wakatsuchi: Methane in the western part of the Sea of Okhotsk in 1998–2000, *J. Geophys. Res.*, 109, C09S12, doi:10.1029/2003JC001910, 2004.

3.14.4 Nitrous oxide and related substances

(1) Introduction

Nitrous oxide is a very effective heat-trapping gas in the atmosphere because it absorbs outgoing radiant heat in infrared wavelengths that are not captured by the other major greenhouse gases, such as water vapor and CO₂. The annual input of N₂O into the atmosphere is estimated to be about 16 Tg N₂O-N yr⁻¹, and the oceans are believed to contribute more than 20% of the total annual input (IPCC, 2007).

N₂O is produced by the biological processes of nitrification and denitrification (Dore et al., 1998; Knowles et al., 1981; Rysgaard et al., 1993; Svensson, 1998; Ueda et al., 1993). Depending on the redox conditions, N₂O is produced from inorganic nitrogenous compounds (NH₄ or NO₃⁻), with subsequently different isotopic fractionation factors. The isotopic signatures of N₂O confer constraints on the relative source strength, and the reaction dynamics of N₂O biological production pathways are currently under investigation. Furthermore, isotopomers of N₂O contain more easily interpretable biogeochemical information as to their sources than obtained from conventional bulk ¹⁵N and ¹⁸O measurements (Yoshida and Toyoda, 2000).

The Pacific Ocean is the largest of the world's five oceans (followed by the Atlantic Ocean, Indian Ocean, Southern Ocean, and Arctic Ocean) (CIA, www) and expected to be important for the biogeochemical and biological cycles. Thus, the study of N₂O production and nutrients dynamics are very important to examine the origins of N₂O in seawater and to estimate the inventory of N₂O from this region with respect to the troposphere.

(2) Materials and methods

Seawater samples are taken by CTD-CAROUSEL system attached Niskin samplers of 12 L at 5-22 layers and surface layer taken by plastic bucket at hydrographic stations as shown in Table 1.

Seawater samples for N₂O concentration and isotope analyses were subsampled into two glass vials: one 30 ml vial for concentration analysis and two 200 ml glass vials for isotopomer ratio analysis. The subsamples were then sterilized with saturated HgCl₂ solution (about 20 µL per 100 ml seawater). The vials were sealed with butyl-rubber septa and aluminum caps, taking care to avoid bubble formation, and then brought back to the laboratory and stored at 4°C until analysis. Dissolved and air N₂O concentrations and its isotopic compositions will be measured by GC/ECD and/or GC/IRMS.

Water sample for isotope analysis of NO₃⁻ were collected into a 50-ml syringe equipped with a DISMIC® filter (pore size: 0.45 µm). The sample was then filtrated into a polypropylene tube. The tube was stored at -20°C until analysis. Isotope ratios of NO₃⁻ will be measured by denitrifier method (Sigman et al., 2001) in which N₂O converted from nitrate is measured by using GC/IRMS.

Water sample for isotope analysis of Chlorophyll pigments were collected into a 20L light-blocking polypropylene tanks. The samples were filtered under reduced pressure and collected on two-three Whatman GF/F filters. The filters were wrapped in aluminum foil and stored at -20°C until analysis. Chlorophyll pigments were extracted and split into each pigments by HPLS. Isotope ratios of Chlorophyll pigments were measured by using EA-IRMS.

(3) Expected results

In the surface layer, N₂O concentration of water affects the sea-air flux directly (Dore et al., 1998). However the pathway of N₂O production in surface layer is still unresolved. In the surface layer, N₂O is predominantly produced by nitrification, but also by nitrifier-denitrification and denitrification if oxygen concentration is low in the water mass or particles (Maribeb and Laura, 2004). Concentrations and isotopomer ratios of N₂O together with those values of substrates for N₂O (NO₃⁻, NH₄⁺ and Chlorophyll) will reveal the pathway of N₂O production in the surface layer (especially euphotic zone).

In deeper layer, N₂O could be produced through *in situ* biological processes of settling particles or fecal pellets derived from phytoplankton or zooplankton, and N₂O maximum was indeed observed at 600-800 m depth in the North Pacific (Popp et al., 2002; Toyoda et al., 2002). However, following problems have not been resolved: (i) what the major pathway for the N₂O maximum is and (ii) whether the N₂O is produced *in situ* or transported from other area.

Although there are reports on distribution of concentration and isotopomer ratio of N₂O in the North Pacific (Toyoda et al., 2002), this study will be the first one which reveals the distribution and production pathway of N₂O by using N₂O isotopomer ratios together with those ratios of substrates for N₂O.

(8) References

- Dore, J.E., Popp, B.N., Karl, D.M. and Sansone, F.J.: A large source of atmospheric nitrous oxide from subtropical North Pacific surface water, *Nature*, 396, 63-66, 1998.
- IPCC, Climate Change 2007: The Physical Science Basis. Contribution of Working Group I to the Fourth Assessment Report of the Intergovernmental Panel on Climate Change, edited by S. Solomon et al., pp. 996, Cambridge University Press, Cambridge, United Kingdom and New York, NY, USA, 2007.
- Knowles, R., Lean, D.R.S. and Chan, Y.K.: Nitrous oxide concentrations in lakes: variations with depth and time, *Limnology and Oceanography*, 26, 855-866, 1981.
- Maribeb, C.-G. and Laura, F.: N₂O cycling at the core of the oxygen minimum zone off northern Chile, *Marine Ecology Progress Series*, 280, 1-11, 2004.
- Popp, B. N., et al.: Nitrogen and oxygen isotopomeric constraints on the origins and sea-to-air flux of N₂O in the oligotrophic subtropical North Pacific gyre, *Global Biogeochem. Cycles*, 16(4), 1064, 2002. doi: 10.1029/2001GB001806.
- Rysgaard, S., Risgaard-Petersen, N., Nielsen, L.P. and Revsbech, N.P.: Nitrification and denitrification in lake and estuarine sediments measured by the ¹⁵N dilution technique and isotope pairing, *Applied and Environmental Microbiology*, 59, 2093-2098, 1993.
- Sigman, D.M., Altabet, M.A., Michener, R.H., McCorkle, D.C., Fry, B., Holmes, R.M., 1997. Natural abundance level measurement of the nitrogen isotopic composition of oceanic nitrate: an adaptation of the ammonia diffusion method. *Marine Chemistry* 57, 227-242.
- Sigman, D. M., K. L. Casciotti, M. Andreani, C. Barford, M. Galanter, and J. K. Boehlke: A bacterial method for the nitrogen isotopic analysis of nitrate in seawater and freshwater, *Anal. Chem.*, 73, 4145-4153, 2001.
- Svensson, J.M.: Emission of N₂O, nitrification and denitrification in a eutrophic lake sediment bioturbated by *Chironomus plumosus*, *Aquatic Microbial Ecology*, 14, 289-299, 1998.

- Toyoda, S., H. Iwai, K. Koba, and N. Yoshida: Isotopomeric analysis of N₂O dissolved in a river in the Tokyo metropolitan area, *Rapid Commun. Mass Spectrom.*, 23 (6), 809-821, 2009. doi: 10.1002/rcm.3945.
- Toyoda, S., N. Yoshida, T. Miwa, Y. Matsui, H. Yamagishi, U. Tsunogai, Y. Nojiri, and N. Tsurushima: Production mechanism and global budget of N₂O inferred from its isotopomers in the western North Pacific, *Geophys. Res. Lett.*, 29 (3), 7-1-7-4, 2002.
- Ueda, S., Ogura, N. and Yoshinari, T.: Accumulation of nitrous oxide in aerobic ground water, *Water Research*, 27, 1787-1792, 1993
- www.cia.gov/cia/publications/factbook/geos/zn.html
- Yoshida, N. and Toyoda, S.: Constraining the atmospheric N₂O budget from intramolecular site preference in N₂O isotopomers, *Nature*, 405, 330-334, 2000.

3.14.5 Incubation experiments

(1) Introduction

Nitrous oxide (N₂O) is an important greenhouse gas and a key factor in stratospheric ozone destruction. Due to its long atmospheric lifetime (~120 years), N₂O has 298 and 4 times the global warming potential of CO₂ and methane respectively (IPCC, 2001). About 24% of the natural sources of atmospheric N₂O are contributed by oceans (Walter et al., 2006). N₂O is an important component of the oceanic nitrogen cycle and is essentially formed by microbial processes such as nitrification and denitrification (Codispoti et al., 2001). The future changes in climate and in the stratospheric ozone distribution depend on the evolution of N₂O emissions. Marine N₂O may change substantially as a result of the ocean acidification (OA) induced by the dissolution of anthropogenic CO₂ emissions in seawater (Beman et al., 2011; Codispoti, 2010). The reduction of seawater pH level might reduce the formation of N₂O because a drop in pH can inhibit AOB and AOA since the NH₃/NH₄⁺ equilibrium is pH sensitive (Beman et al., 2011). Thus, the study of the impact of OA on the nitrification and N₂O production rate is essential to better predict the evolution of the marine N₂O emission.

(2) Materials and methods

Seawater samples were taken by CTD-CAROUSEL system attached Niskin samplers of 12 L. Each sample was carefully sub-sampled into 100 and 200 ml glass vials and sealed with butyl-rubber septa and aluminum caps, taking care to avoid bubble formation to avoid air contamination. To evaluate the effect of OA on N₂O production rates, seawater samples were acidified by adding 0, 30 or 60 µl of HCl solution (0.5 M) using a micro-syringe. Then, 2 µL of ¹⁵NH₄Cl solution (1.8×10⁻⁷ M) was added in seawater samples (200 mL) using micro-syringe and the samples were incubated in dark at a temperature close to that at the sampling depth. After the incubation, the samples were sterilized with 0.5 mL of saturated HgCl₂ solution. Similar procedure was used to assess the effect of OA on nitrification rates. However for nitrification incubation experiments samples were not sterilized by adding a saturated HgCl₂ solution but they were filtered (0.45 µm) and frozen to stop the microbial growth. The production rate of N₂O formed by the nitrifier denitrification pathway and NO₂⁻ consumption rate by denitrification were measured by adding 2 µL of Na¹⁵NO₂ (1.4×10⁻⁷ M) in 200 ml and 100 ml respectively. After incubation, 0.5 mL of saturated HgCl₂ solution was added to the seawater samples to measure N₂O produced by nitrifier denitrification. The samples incubated

in 100 ml vials for the determination of NO_2^- consumption rate by denitrification were filtered (pore size 0.45 μm) and frozen after incubation. All samples were stored in the dark at 4°C until analysis. Dissolved N_2O concentrations and its isotopic compositions will be measured by GC-IRMS. Isotope ratios of NO_3^- will be measured by denitrifier method (Sigman et al., 2001).

(3) Expected results

In the future, nitrogen cycle might be affected directly or indirectly by OA. Recent studies have shown that a reduction of seawater pH might induce a decline of nitrification rates in shallow water masses (Beman et al. 2011; Kitidis et al., 2011). However, contrary to other studies Fulweiler et al. have found that in some cases the nitrification rates might be highest at low pH and significantly lower at high pH (Fulweiler et al., 2011). Although some studies on the effect of OA on the nitrification exist, the potential impact of OA on N_2O production processes is still poorly understood. By combining ^{15}N -isotope and N_2O isotopomer analysis, the present study will provide important information about the possible impact of OA on the nitrification rate in western north Pacific. Moreover, this study will be the first one to show the influence of decreasing pH on the oceanic N_2O production rate. These results might help to better predict the future evolution of nitrification and N_2O production rates in an acidifying ocean.

(4) References

- Beman, M.J., Chow, C.E., King, A.L., Feng, Y., Fuhrman, J.A., Andersson, A., Bates, N.R., Popp, B.N., Hutchins, D.A., 2011. Global declines in oceanic nitrification rates as a consequence of ocean acidification, *Proceedings of the National Academy of Sciences*, 108, pp. 208-213.
- Codispoti, L. A., Brandes, J. A., Christensen, J. P., Devol, A. H., Naqvi, S. W. A., Paerl, H.W., Yoshinari, T., 2001. The oceanic fixed nitrogen and nitrous oxide budgets: Moving targets as we enter the Anthropocene, *Scientia Marina*, 65, 85–105.
- Codispoti, L.A., 2010, Interesting times for marine N_2O , *Science*, 327, pp. 1339-1340.
- Fulweiler, R.W., Emery, H.E., Heiss, E.M., Berounsky, V.M., 2011. Assessing the role of pH in determining water column nitrification rates in a coastal system. *Estuaries and Coasts*, 34, 1095-1102.
- IPCC Third Assessment Report: Climate Change 2001 (TAR), Climate Change 2001: The Scientific Basis, Contribution of Working Group I to the Third Assessment Report of the Intergovernmental Panel on Climate Change, Houghton, J.T.; Ding, Y.; Griggs, D.J.; Noguer, M.; van der Linden, P.J.; Dai, X.; Maskell, K.; and Johnson, C.A., eds., 2001, Cambridge University Press, Cambridge, United Kingdom and New York, NY, USA.
- Kitidis, V. Laverock, B., McNeil, L.C., Beesley, A., Cummings, D., Tait, K., Osborn, M.A., Widdicombe, S., 2011. Impact of ocean acidification on benthic and water column ammonia oxidation. *Geophysical Research Letters*, 38
- Sigman, D. M., K. L. Casciotti, M. Andreani, C. Barford, M. Galanter, and J. K. Boehlke: A bacterial method for the nitrogen isotopic analysis of nitrate in seawater and freshwater, 2001, *Analytical Chemistry*, 73, 4145-4153.
- Walter, S., Bange, H.W., Breitenbach, U., Wallace, D.W.R., 2006, Nitrous oxide in the North Atlantic Ocean, *Biogeosciences*, 3, pp. 607-619.

4. Geophysical observation

4.1 Swath bathymetry

Takeshi MATSUMOTO (University of the Ryukyus:
Principal Investigator) (not on-board)
Masao NAKANISHI (Chiba University:
Principal Investigator) (not on-board)
Wataru TOKUNAGA (Global Ocean Development Inc., GODI)
Miki MORIOKA (GODI)
Ryo OYAMA (MIRAI crew)

(1) Introduction

R/V MIRAI is equipped with a Multi-narrow Beam Echo Sounding system (MBES), SEABEAM 3012 Upgrade Model (L3 Communications ELAC Nautik) and Sub-bottom Profiler (SBP), Bathy2010 (SyQwest). The objective of MBES is collecting continuous bathymetric data along ship's track to make a contribution to geological and geophysical investigations and global datasets.

(2) Data Acquisition

The “SEABEAM 3012 Upgrade Model” on R/V MIRAI was used for bathymetry mapping during the MR13-04 cruise from 10 July to 27 July 2013.

To get accurate sound velocity of water column for ray-path correction of acoustic multibeam, we used Surface Sound Velocimeter (SSV) data to get the sea surface (6.62m) sound velocity, and the deeper depth sound velocity profiles were calculated by temperature and salinity profiles from CTD and Argo float data by the equation in Del Grosso (1974) during the cruise.

Table 4.1-1 shows system configuration and performance of SEABEAM 3012 Upgrade Model. Table 4.1-2 shows system configuration and performance of Sub-Bottom Profiler, Bathy2010.

Table 4.1-1 System configuration and performance
SEABEAM 3012 Upgrade Model (12 kHz system)

Frequency:	12 kHz
Transmit beam width:	1.6 degree
Transmit power:	20 kW
Transmit pulse length:	2 to 20 msec.
Receive beam width:	1.8 degree
Depth range:	100 to 11,000 m
Beam spacing:	0.5 degree athwart ship
Swath width:	150 degree (max)

	120 degree to 4,500 m
	100 degree to 6,000 m
	90 degree to 11,000 m
Depth accuracy:	Within < 0.5% of depth or ± 1 m, whichever is greater, over the entire swath. (Nadir beam has greater accuracy; typically within < 0.2% of depth or ± 1 m, whichever is greater)

Table 4.1-2 System configuration and performance
Sub-bottom Profiler, Bathym2010 (3.5kHz system)

Frequency:	3.5 kHz
Transmit beam width:	23 degree
Transmit pulse length:	0.5 to 50 msec
Strata resolution:	Up to 8 cm with 300+ Meters of bottom penetration; bottom type dependant
Depth resolution:	0.1 Feet, 0.1 Meters
Depth accuracy:	± 10 cm to 100 m, $\pm 0.3\%$ to 6,000 m

(3) Preliminary Results

The results will be published after primary processing.

(4) Data Archives

Bathymetric data obtained during this cruise will be submitted to the Data Management Group (DMG) in JAMSTEC, and will be archived there.

4.2 Sea surface gravity

(1) Introduction

The local gravity is an important parameter in geophysics and geodesy. We collected gravity data at the sea surface.

(2) Parameters

Relative Gravity [CU: Counter Unit]

$$[\text{mGal}] = (\text{coef1: } 0.9946) * [\text{CU}]$$

(3) Data Acquisition

We measured relative gravity using LaCoste and Romberg air-sea gravity meter S-116 (Micro-g LaCoste, LLC) during the MR13-04 cruise from 9 July 2013 on Yokohama to 29 July 2013 on Sekinehama.

To convert the relative gravity to absolute one, we measured gravity using portable gravity meter (Scintrex gravity meter CG-5), at Yokohama and Sekinehama as the reference points.

(4) Preliminary Results

Absolute gravity table is shown in Tabel 4.2-1.

Table 4.2-1 Absolute gravity

No.	Date	U.T.C.	Port	Absolute Gravity [mGal]	Level [cm]	Draft [cm]	Gravity at Sensor * [mGal]	S-116 Gravity [mGal]
#1	09/Jul	01:23	Yokohama	979742.22	303	650	979743.47	12036.09
#2	29/Jul	03:28	Sekine	980371.94	287	620	980737.04	12665.14

*: Gravity at Sensor

$$= \text{Absolute Gravity} + \text{Sea Level} * 0.3086 / 100 + (\text{Draft} - 530) / 100 * 0.2654$$

(5) Data Archives

Surface gravity data obtained during this cruise will be submitted to the Data Management Group (DMG) in JAMSTEC, and will be archived there.

4.3 Sea Surface magnetic field

1) Three-component magnetometer

(1) Introduction

Measurements of magnetic force on the sea are required for the geophysical investigations of marine magnetic anomaly caused by magnetization in upper crustal structure. We measured geomagnetic field using a three-component magnetometer during the MR13-04 cruise from 9 July to 29 July, 2013.

(2) Principle of ship-board geomagnetic vector measurement

The relation between a magnetic-field vector observed on-board, H_{ob} , (in the ship's fixed coordinate system) and the geomagnetic field vector, F , (in the Earth's fixed coordinate system) is expressed as:

$$H_{ob} = A R P Y F + H_p \quad (a)$$

where R , P and Y are the matrices of rotation due to roll, pitch and heading of a ship, respectively. A is a 3 x 3 matrix which represents magnetic susceptibility of the ship, and H_p is a magnetic field vector produced by a permanent magnetic moment of the ship's body. Rearrangement of Eq. (a) makes

$$B H_{ob} + H_{bp} = R P Y F \quad (b)$$

where $B = A^{-1}$, and $H_{bp} = -B H_p$. The magnetic field, F , can be obtained by measuring R , P , Y and H_{ob} , if B and H_{bp} are known. Twelve constants in B and H_{bp} can be determined by measuring variation of H_{ob} with R , P and Y at a place where the geomagnetic field, F , is known.

(3) Instruments on R/V MIRAI

A shipboard three-component magnetometer system (Tierra Technica SFG1214) is equipped on-board R/V MIRAI. Three-axes flux-gate sensors with ring-cored coils are fixed on the fore mast. Outputs of the sensors are digitized by a 20-bit A/D converter (1 nT/LSB), and sampled at 8 times per second. Ship's heading, pitch, and roll are measured utilizing a Inertial Navigation System (Fiber Optical Gyro) installed for controlling attitude of a Doppler radar. Ship's position (GPS) and speed data are taken from LAN every second.

(4) Data Archives

These data obtained during this cruise will be submitted to the Data Management Group (DMG) in JAMSTEC, and will be archived there.

(5) Remarks

1. For calibration of the ship's magnetic effect, we made a "Figure eight" turn (a

- pair of clockwise and anti-clockwise rotation). The periods were follows;
- i) 09:10 - 09:40UTC 11 July around at 36-28N, 141-29E
 - ii) 10:29 - 10:57UTC 15 July around at 30-00N, 144-59E
 - iii) 08:10 - 08:37UTC 23 July around at 46-59N, 160-01E
2. The following periods, recording was stopped for data input error.
- i) 21:13 - 21:55UTC 20 July
 - ii) 22:05 - 22:14UTC 20 July

2) Cesium magnetometer

(1) Introduction

Measurement of total magnetic force on the sea is required for the geophysical investigations of marine magnetic anomaly caused by magnetization in upper crustal structure.

(2) Data Period

20:58UTC 20 July - 18:59UTC 21 July

(3) Specification

We measured total geomagnetic field using a cesium marine magnetometer (Geometrics Inc., G-882) and recorded by G-882 data logger (Cloverttech Co., Ver.1.0.0). The G-882 magnetometer uses an optically pumped Cesium-vapor atomic resonance system. The sensor fish towed 500 m behind the vessel to minimize the effects of the ship's magnetic field. Table 4.3-1 shows system configuration of MIRAI cesium magnetometer system.

Table 4.3-1 System configuration of MIRAI cesium magnetometer system.

Dynamic operating range:	20,000 to 100,000 nT
Absolute accuracy:	< ±2 nT throughout range
Setting:	Cycle rate; 0.1 sec
	Sensitivity; 0.001265 nT at a 0.1 second cycle rate
	Sampling rate; 1 sec

(4) Data Archive

Total magnetic force data obtained during this cruise was submitted to the Data Management Group (DMG) of JAMSTEC, and archived there.

4.4 Tectonic history of the mid-Cretaceous Pacific Plate

Masao NAKANISHI (Graduate School of Science, Chiba University)

Wataru TOKUNAGA (Global Ocean Development Inc.)

Miki MORIOKA (Global Ocean Development Inc.)

Ryo OYAMA (MIRAI crew)

The Pacific Plate is the largest oceanic lithospheric plate on the Earth. The Pacific Plate was born around 190 Ma, Middle Jurassic (Nakanishi et al., 1992). The tectonic history of the Pacific Plate has been exposed by many studies based on magnetic anomaly lineations. However, the tectonic history in some periods is still obscure because of lack of geophysical data. To reveal the entire tectonic history of the Pacific Plate from Middle Jurassic to the present, increase in geophysical data is indispensable.

In the seafloor around the stations KNOT and K2 there are several topographic features that bear on tectonic evolution of the mid-Cretaceous Pacific Plate. The seafloor in the survey area was formed at the Pacific-Izanagi Ridge (e.g., Mammerickx, and Sharman, 1988). They proposed a significant reorganization of the plate boundaries of the Pacific Plate in the period. To examine the reorganization, we conducted the geophysical survey in transit between KNOT and K2 sites (Figure 4.5.1a). The geomagnetic measurement was also conducted by the cesium-vapor magnetometer. Magnetic anomalies were calculated by International Geomagnetic Reference Field (International Association of Geomagnetism and Aeronomy, Working Group V-MOD, 2010).

The bathymetric survey illustrates high relief (Figure 4.5.1b). Positive free-air gravity anomalies of with an amplitude of 10-20 mGal are prominent (Figure 4.5.1c). Magnetic anomalies have 100-200 nT amplitudes except the seamount around a distance of 300 km from the KNOT site (Figure 4.5.1d). The seamount is a 2500 m in height. The gravity and magnetic anomalies over the seamount are more than 50 mGal and more than 500 nT, respectively.

References

- International Association of Geomagnetism and Aeronomy, Working Group V-MOD, International Geomagnetic Reference Field, 2010: the eleventh generation. *Geophys. J. Int.*, 83, 3, 1216-1230, December 2010. DOI: 10.1111/j.1365-246X.2010.04804.x.
- Mammerickx, J., and G. F. Sharman, 1988: Tectonic Evolution of the North Pacific During the Cretaceous Quiet Period, *J. Geophys. Res.*, 93, B4, 3009-3024, DOI:10.1029/JB093iB04p03009.
- Nakanishi, M., K. Tamaki, K. Kobayashi, A new Mesozoic isochron chart of the northwestern Pacific Ocean: Paleomagnetic and tectonic implications, *Geophys. Res. Lett.*, 19, 693-696, 1992. DOI: 10.1029/92GL00022.

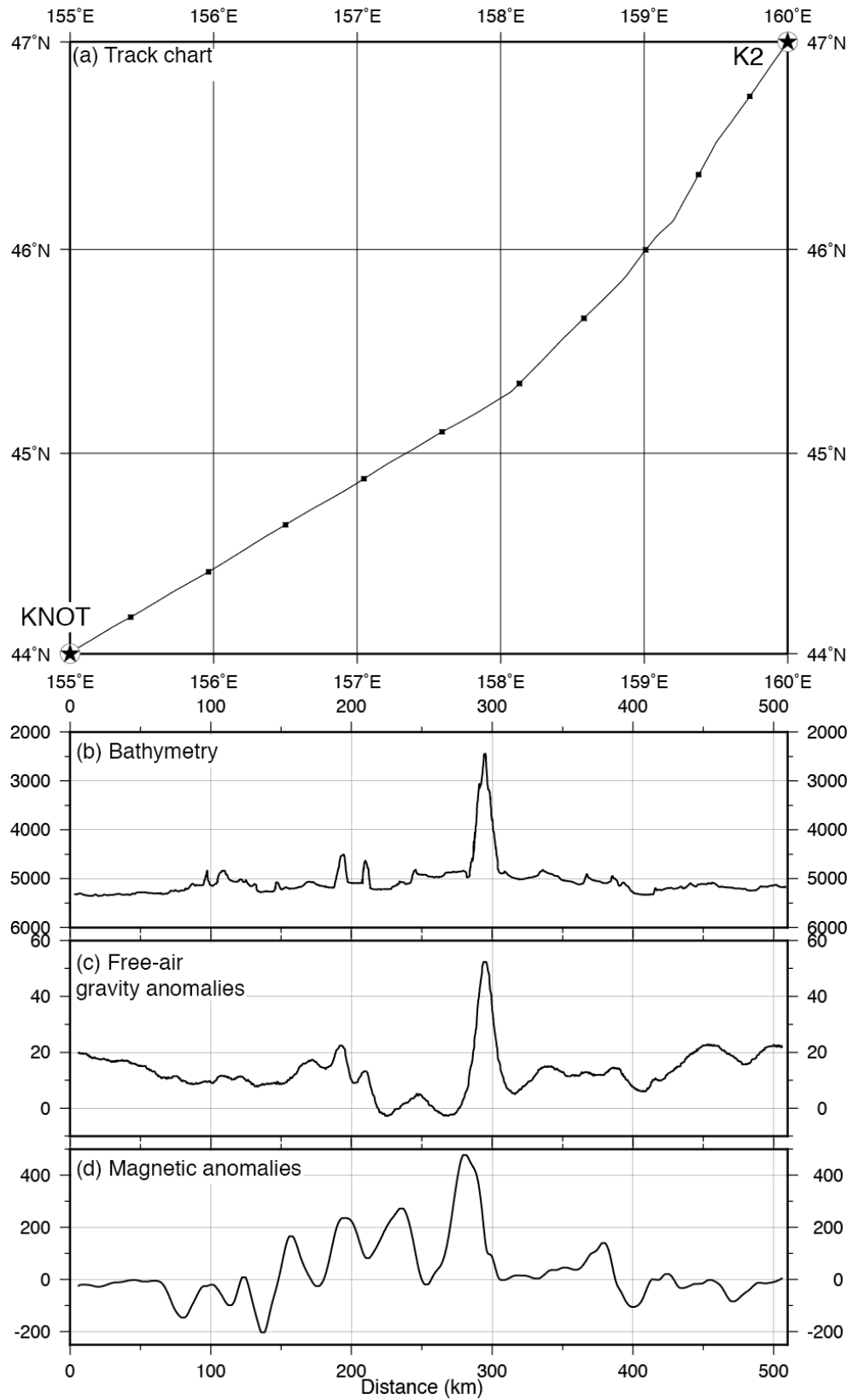


Figure 4.4.1. Track chart of the geophysical survey between KNOT and K2 sites (a) and profiles of bathymetry (b), free-air gravity anomalies (c), and magnetic anomalies (d). Stars show the KNOT and K2 sites.

5. Satellite image acquisition (MCSST from NOAA/HRPT)

Makio HONDA (JAMSTEC: Principal Investigator)
Wataru TOKUNAGA (Global Ocean Development Inc., GODI)
Miki MORIOKA (GODI)
Ryo OYAMA (MIRAI crew)

(1) Objectives

It is our objectives to collect data of sea surface temperature in a high spatial resolution mode from the Advance Very High Resolution Radiometer (AVHRR) on the NOAA polar orbiting satellites and to build a time and depth resolved primary productivity model.

(2) Methods

We receive the down link High Resolution Picture Transmission (HRPT) signal from NOAA satellites. We processed the HRPT signal with the in-flight calibration and computed the sea surface temperature by the Multi-Channel Sea Surface Temperature (MCSST) method. A daily composite map of MCSST data is processed for each day on the R/V MIRAI for the area, where the R/V MIRAI located.

We received and processed NOAA data throughout MR13-04 cruise from 10 July to 28 July, 2013.

The sea surface temperature data will be applied for the time and depth resolved primary productivity model to determine a temperature field for the model.

(3) Preliminary results

Figure 5-1 shows MCSST composite image from 10 July to 28 July, 2013.

(4) Data archives

The raw data obtained during this cruise will be submitted to the Data Management Group (DMG) in JAMSTEC.

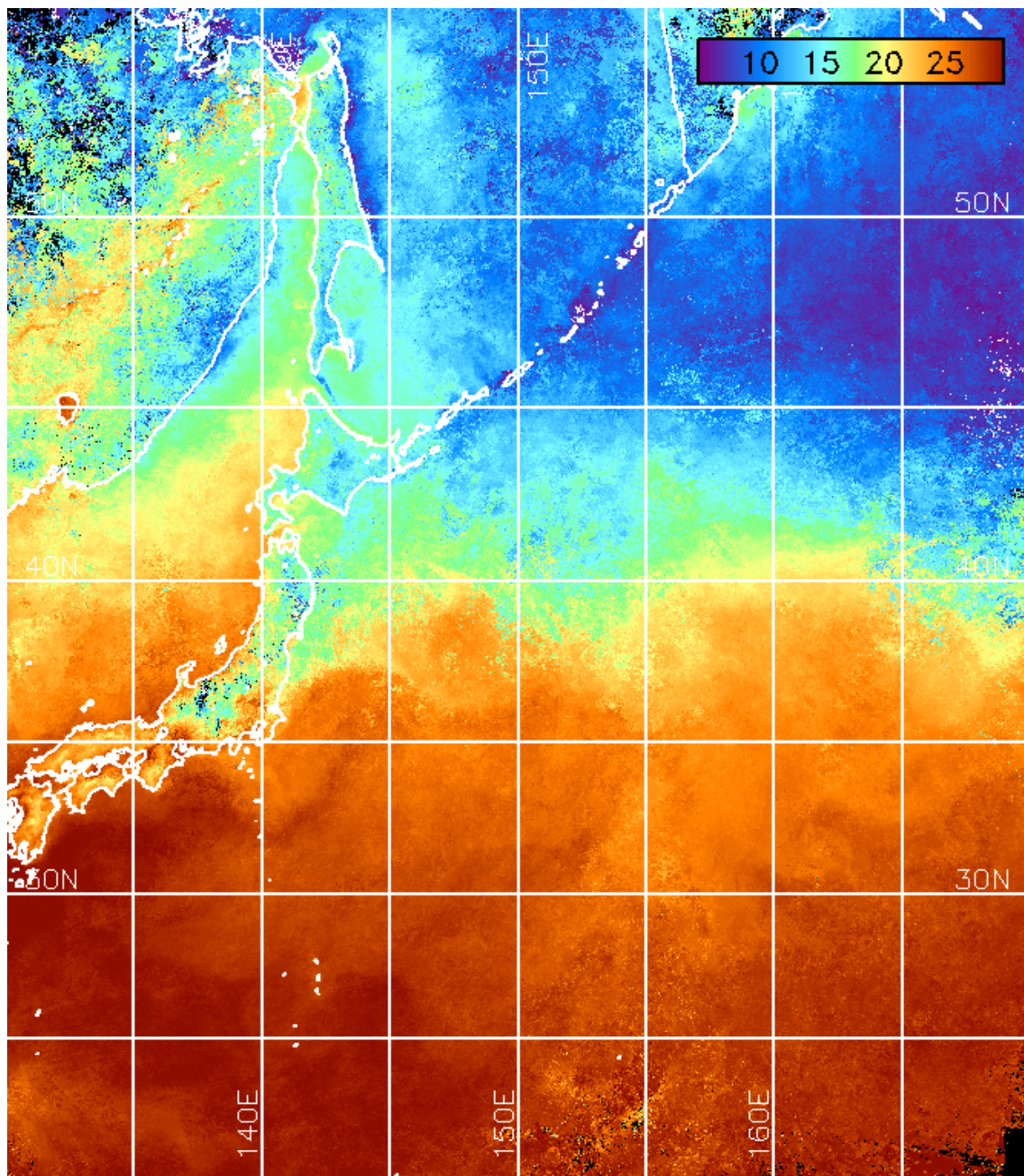


Fig.5-1 MCSST composite image from 10 July to 28 July, 2013.